USGS
science for a changing world

National Water-Quality Assessment Program

Hydrogeologic Settings and Groundwater-Flow Simulations for Regional Investigations of the Transport of Anthropogenic and Natural Contaminants to Public-Supply Wells—Investigations Begun in 2004

Professional Paper 1737–B

U.S. Department of the Interior
U.S. Geological Survey

Hydrogeologic Settings and Groundwater-Flow Simulations for Regional Investigations of the Transport of Anthropogenic and Natural Contaminants to Public-Supply Wells—Investigations Begun in 2004

Edited by Sandra M. Eberts

National Water-Quality Assessment Program

Professional Paper 1737–B

U.S. Department of the Interior
U.S. Geological Survey

U.S. Department of the Interior
KEN SALAZAR, Secretary

U.S. Geological Survey
Marcia K. McNutt, Director

U.S. Geological Survey, Reston, Virginia: 2011

Suggested citation:
Eberts, Sandra M., ed., 2011, Hydrogeologic settings and groundwater-flow simulations for regional investigations of the transport of anthropogenic and natural contaminants to public-supply wells—Investigations begun in 2004: U.S. Geological Survey Professional Paper 1737–B, 127 p.

Foreword

The U.S. Geological Survey (USGS) is committed to providing the Nation with reliable scientific information that helps to enhance and protect the overall quality of life and that facilitates effective management of water, biological, energy, and mineral resources (http://www.usgs.gov/). Information on the Nation's water resources is critical to ensuring long-term availability of water that is safe for drinking and recreation and is suitable for industry, irrigation, and fish and wildlife. Population growth and increasing demands for water make the availability of that water, measured in terms of quantity and quality, even more essential to the long-term sustainability of our communities and ecosystems.

The USGS implemented the National Water-Quality Assessment (NAWQA) Program in 1991 to support national, regional, State, and local information needs and decisions related to water-quality management and policy (http://water.usgs.gov/nawqa). The NAWQA Program is designed to answer: What is the quality of our Nation's streams and groundwater? How are conditions changing over time? How do natural features and human activities affect the quality of streams and groundwater, and where are those effects most pronounced? By combining information on water chemistry, physical characteristics, stream habitat, and aquatic life, the NAWQA Program aims to provide science-based insights for current and emerging water issues and priorities. From 1991 to 2001, the NAWQA Program completed interdisciplinary assessments and established a baseline understanding of water-quality conditions in 51 of the Nation's river basins and aquifers, referred to as Study Units (http://water.usgs.gov/nawqa/studies/study_units.html).

National and regional assessments are ongoing in the second decade (2001–2012) of the NAWQA Program as 42 of the 51 Study Units are selectively reassessed. These assessments extend the findings in the Study Units by determining water-quality status and trends at sites that have been consistently monitored for more than a decade, and filling critical gaps in characterizing the quality of surface water and groundwater. For example, increased emphasis has been placed on assessing the quality of source water and finished water associated with many of the Nation's largest community water systems. During the second decade, NAWQA is addressing five national priority topics that build an understanding of how natural features and human activities affect water quality, and establish links between sources of contaminants, the transport of those contaminants through the hydrologic system, and the potential effects of contaminants on humans and aquatic ecosystems. Included are studies on the fate of agricultural chemicals, effects of urbanization on stream ecosystems, bioaccumulation of mercury in stream ecosystems, effects of nutrient enrichment on aquatic ecosystems, and transport of contaminants to public-supply wells. In addition, national syntheses of information on pesticides, volatile organic compounds (VOCs), nutrients, trace elements, and aquatic ecology are continuing.

The USGS aims to disseminate credible, timely, and relevant science information to address practical and effective water-resource management and strategies that protect and restore water quality. We hope this NAWQA publication will provide you with insights and information to meet your needs, and will foster increased citizen awareness and involvement in the protection and restoration of our Nation's waters.

The USGS recognizes that a national assessment by a single program cannot address all water-resource issues of interest. External coordination at all levels is critical for cost-effective management, regulation, and conservation of our Nation's water resources. The NAWQA Program, therefore, depends on advice and information from other agencies—Federal, State, regional, interstate, Tribal, and local—as well as nongovernmental organizations, industry, academia, and other stakeholder groups. Your assistance and suggestions are greatly appreciated.

William H. Werkheiser
USGS Associate Director for Water

Contents

Conversion Factors Datum, and Abbreviations

Multiply	By	To obtain
	Length	
centimeter (cm)	0.3937	inch (in.)
kilometer (km)	.6214	mile (mi)
kilometer (km)	.5400	mile, nautical (nmi)
meter (m)	3.281	foot (ft)
meter (m)	1.094	yard (yd)
	Area	
square meter (m^2)	10.76	square foot (ft^2)
square meter (m^2)	.0002471	acre
hectare (ha)	2.471	acre
square kilometer (km^2)	247.1	acre
square kilometer (km^2)	.3861	square mile (mi^2)
	Volume	
liter (L)	33.82	ounce, fluid (fl. oz)
liter (L)	2.113	pint (pt)
liter (L)	1.057	quart (qt)
liter (L)	.2642	gallon (gal)
liter (L)	61.02	cubic inch (in^3)
cubic meter (m^3)	264.2	gallon (gal)
cubic meter (m^3)	.0002642	million gallons (Mgal)
cubic meter (m^3)	35.31	cubic foot (ft^3)
cubic meter (m^3)	1.308	cubic yard (yd^3)
cubic meter (m^3)	.0008107	acre-foot (acre-ft)
cubic hectometer (hm^3)	810.7	acre-foot (acre-ft)
	Flow rate	
cubic meter per second (m^3/s)	70.07	acre-foot per day (acre-ft/d)
cubic meter per second (m^3/s)	35.31	cubic foot per second (ft^3/s)
cubic meter per second (m^3/s)	22.83	million gallons per day (Mgal/d)
cubic meter per day (m^3/d)	35.31	cubic foot per day (ft^3/d)
cubic meter per year (m^3/yr)	.000811	acre-foot per year (acre-ft/yr)
Hydraulic conductivity		
meter per day (m/d)	3.281	foot per day (ft/d)
	Transmissivity	
meter squared per day (m^2/d)	10.76	foot squared per day (ft^2/d)
	Leakance	
meter per day per meter [(m/d)/m]	1	foot per day per foot [(ft/d)/ft]

Temperature in degrees Celsius (°C) may be converted to degrees Fahrenheit (°F) as follows:

°F=(1.8×°C)+32

Temperature in degrees Fahrenheit (°F) may be converted to degrees Celsius (°C) as follows:

°C=(°F-32)/1.8

Vertical coordinate information is referenced to the National Geodetic Vertical Datum of 1929 (NGVD 29) or the North American Vertical Datum of 1988 (NAVD 88)."

Horizontal coordinate information is referenced to the North American Datum of 1983 (NAD 83).

Altitude, as used in this report, refers to distance above the vertical datum.

Abbreviations for other units of measurement

microgram per liter (µg/L)

microsiemens per centimeter at 25 degrees Celsius (µS/cm at 25 °C)

milligrams per liter (mg/L)

picocuries per liter (pCi/L)

Overview of Chapter B: Additional Regional Investigations of the Transport of Anthropogenic and Natural Contaminants to Public-Supply Wells

By Sandra M. Eberts, Leon J. Kauffman, Laura M. Bexfield, and Richard J. Lindgren

Section 1 of

Hydrogeologic Settings and Groundwater-Flow Simulations for Regional Investigations of the Transport of Anthropogenic and Natural Contaminants to Public-Supply Wells—Investigations Begun in 2004

Edited by Sandra M. Eberts

National Water-Quality Assessment Program

Professional Paper 1737–B

U.S. Department of the Interior
U.S. Geological Survey

U.S. Department of the Interior
KEN SALAZAR, Secretary

U.S. Geological Survey
Marcia K. McNutt, Director

U.S. Geological Survey, Reston, Virginia: 2011

Suggested citation:
Eberts, S.M., Kauffman, L.J., Bexfield, L.M., and Lindgren, R.J., 2011, Overview of chapter B: Additional regional investigations of the transport of anthropogenic and natural contaminants to public-supply wells, section 1 *of* Eberts, S.M., ed., Hydrogeologic settings and groundwater-flow simulations for regional investigations of the transport of anthropogenic and natural contaminants to public-supply wells—Investigations begun in 2004: Reston, Va., U.S. Geological Survey Professional Paper 1737–B, pp. 1-1–1-6.

Contents

Figures

Overview of Chapter B: Additional Regional Investigations of the Transport of Anthropogenic and Natural Contaminants to Public-Supply Wells

By Sandra M. Eberts, Leon J. Kauffman, Laura M. Bexfield, and Richard J. Lindgren

Abstract

A study of the Transport of Anthropogenic and Natural Contaminants to public-supply wells (TANC study) was begun in 2001 as part of the U.S. Geological Survey National Water-Quality Assessment (NAWQA) Program. The study was designed to shed light on factors that affect the vulnerability of groundwater and, more specifically, water from public-supply wells to contamination to provide a context for the NAWQA Program's earlier finding of mixtures of contaminants at low concentrations in groundwater near the water table in urban areas across the Nation. The TANC study has included investigations at both the regional (tens to thousands of square kilometers) and local (generally less than 25 square kilometers) scales. At the regional scale, the approach to investigation involves refining conceptual models of groundwater flow in hydrologically distinct settings and then constructing or updating a groundwater-flow model with particle tracking for each setting to help quantify regional water budgets, public-supply well contributing areas (areas contributing recharge to wells and zones of contribution for wells), and traveltimes from recharge areas to selected wells. A great deal of information about each contributing area is captured from the model output, including values for 170 variables that describe physical and (or) geochemical characteristics of the contributing areas. The information is subsequently stored in a relational database. Retrospective water-quality data from monitoring, domestic, and many of the public-supply wells, as well as data from newly collected samples at selected public-supply wells, also are stored in the database and are used with the model output to help discern the more important factors affecting vulnerability in many, if not most, settings. The study began with investigations in seven regional areas, and it benefits from being conducted as part of the NAWQA Program, in which consistent methods are used so that meaningful comparisons can be made. The hydrogeologic settings and regional-scale groundwater-flow models from the initial seven regional areas are documented in Chapter A of this U.S. Geological Survey Professional Paper. Also documented in Chapter A are the methods used to collect and compile the water-quality data, determine contributing areas of the public-supply wells, and characterize the oxidation-reduction (redox) conditions in each setting. A data dictionary for the database that was designed to enable joint storage and access to water-quality data and groundwater-flow model particle-tracking output is included as Appendix 1 of Chapter A. This chapter, Chapter B, documents modifications to the study methods and presents descriptions of two regional areas that were added to the TANC study in 2004.

Introduction

Because subsurface processes and management practices differ among aquifers and public-water systems, public drinking-water-supply wells in different parts of the Nation are not equally vulnerable to contamination—even where similar contaminant sources exist. The U.S. Geological Survey's National Water-Quality Assessment Program study of the Transport of Anthropogenic and Natural Contaminants (TANC) to public-supply wells was initiated to identify why such differences exist, determine if there are similarities between different aquifer systems, examine the effects of land use, and provide a context for many of the NAWQA Program's groundwater-quality observations (Hamilton and others, 2004). By providing a general understanding of the response of wells in different systems to differing management practices, TANC study results should benefit those involved in locating wells, managing resources, and protecting groundwater quality (Eberts and others, 2005).

The TANC study investigations began in 2001 using retrospective data, a limited amount of newly collected water-quality data, and groundwater-flow models with particle tracking to evaluate factors that affect aquifer and public-supply well vulnerability to contamination at a regional scale in seven regional areas, hereafter termed "regional study areas" or simply "study areas." *Chapter A* of this U.S. Geological Survey Professional Paper presents the hydrogeologic settings—including redox and pH conditions—of the initial seven study areas and documents the accompanying regional-scale groundwater-flow models (Paschke, 2007). Chapter A also documents

study methods and the data dictionary for a relational database that was designed to store the water-quality data and public-supply well contributing area characteristics derived from the flow models and particle tracking. Since 2001, the TANC study has incorporated some additional study areas to complement the settings that were initially investigated, and minor changes have been made to the study methods.

Purpose and Scope

The purpose of this report is to document the changes made to the study methods and to present the hydrogeologic settings and regional groundwater-flow models for the two areas in which work began in 2004. This report, Chapter B, is organized into four sections: an introductory section, two study-unit specific sections with information similar to what is presented in Chapter A for the initial study areas, and an Appendix (Appendix 1 of Chapter B), which documents changes to the particle-tracking program, MODPATH (Pollock, 1994) that were necessary to accomplish the work presented herein. The combined chapters (A and B), along with the accompanying database, provide a foundation for comparative analysis of the susceptibility (characterized by the ease with which water enters and moves through an aquifer) and vulnerability (a combination of susceptibility and contaminant input, mobility, and contaminant persistence) of public-supply wells in a variety of settings. Results of these analyses are not the subject of this report, but will be reported separately.

Study Area Locations

The seven TANC study areas in which investigations began in 2001 are located in five different principal aquifers as identified by the U.S. Geological Survey (Miller, 1999) (fig. 1.1). These study areas and principal aquifers, which are described in Sections 2 thru 8 of Chapter A, are:

A2—Salt Lake Valley, Utah, in the Basin and Range basin-fill aquifers,

A3—Eagle Valley and Spanish Springs Valley, Nevada, in the Basin and Range basin-fill aquifers,

A4—San Joaquin Valley, California, in the Central Valley aquifer system,

A5—Northern Tampa Bay, Florida, in the Floridan aquifer system,

A6—Pomperaug River Basin, Connecticut, in the glacial aquifer system,

A7—Great Miami River Basin, Ohio, in the glacial aquifer system, and

A8—Eastern High Plains, Nebraska, in the High Plains aquifer.

The two study areas and associated principal aquifers that were added to the TANC study in 2004 (fig. 1.1) are:

B2—Middle Rio Grande Basin, New Mexico, in the Rio Grande aquifer system, and

B3—South-Central Texas, Texas, in the Edwards-Trinity aquifer system.

A succinct hydrogeologic description of these two study areas and the associated principal aquifers follow. Additional details for each of these two study areas are provided in Sections 2 and 3 of this chapter, Chapter B.

Rio Grande Aquifer System

The Rio Grande aquifer system is the principal aquifer in southern Colorado, central New Mexico, and western Texas (fig. 1.1) and extends approximately 181,000 square kilometers (km^2). The aquifer system consists of a network of hydraulically interconnected aquifers in basin-fill deposits located along the Rio Grande Valley and nearby valleys (Robson and Banta, 1995). Several alluvial basins of the Rio Grande aquifer system share major characteristics with the Basin and Range basin-fill aquifers of the Southwestern United States (described in *Section 1 of Chapter A*). Much of the streamflow in the northern part of the Rio Grande is from snowmelt runoff in the mountains. In the southern part of the river system, streamflow is from upstream flow, groundwater discharge, and runoff from summer thunderstorms. The arid climate of the Rio Grande Valley provides insufficient precipitation for the growth of most commercial crops; average annual precipitation at the City of Albuquerque is about 22 centimeters (cm) (Western Regional Climate Center, 2006). As a result, irrigated agriculture accounts for a substantial amount of water use within the valley (Robson and Banta, 1995).

The Middle Rio Grande Basin—a large alluvial basin of the Rio Grande aquifer system in central New Mexico—exhibits the same large thickness (hundreds to thousands of meters) of unconsolidated alluvium bounded by bedrock mountain ranges that is typical of the Basin and Range principal aquifer system. The primary mechanisms of groundwater recharge and discharge in the Middle Rio Grande Basin also are similar to those of typical Basin and Range basin-fill aquifers, with the possible exception of a substantial quantity of seepage from the dominant surface-water feature of the basin—the Rio Grande. Chemical characteristics of groundwater in the Middle Rio Grande Basin are representative of the water chemistry in Basin and Range basin-fill aquifers that are connected to adjacent basins. Concentrations of dissolved solids in groundwater within the basin range from less than 200 milligrams per liter to more than 5,000 milligrams per liter (Plummer and others, 2004).

The Middle Rio Grande regional study area is located in the northern half of the Middle Rio Grande Basin. The study area covers about 4,500 km^2, including the Albuquerque metropolitan area. The basin-fill aquifer of the Middle Rio Grande

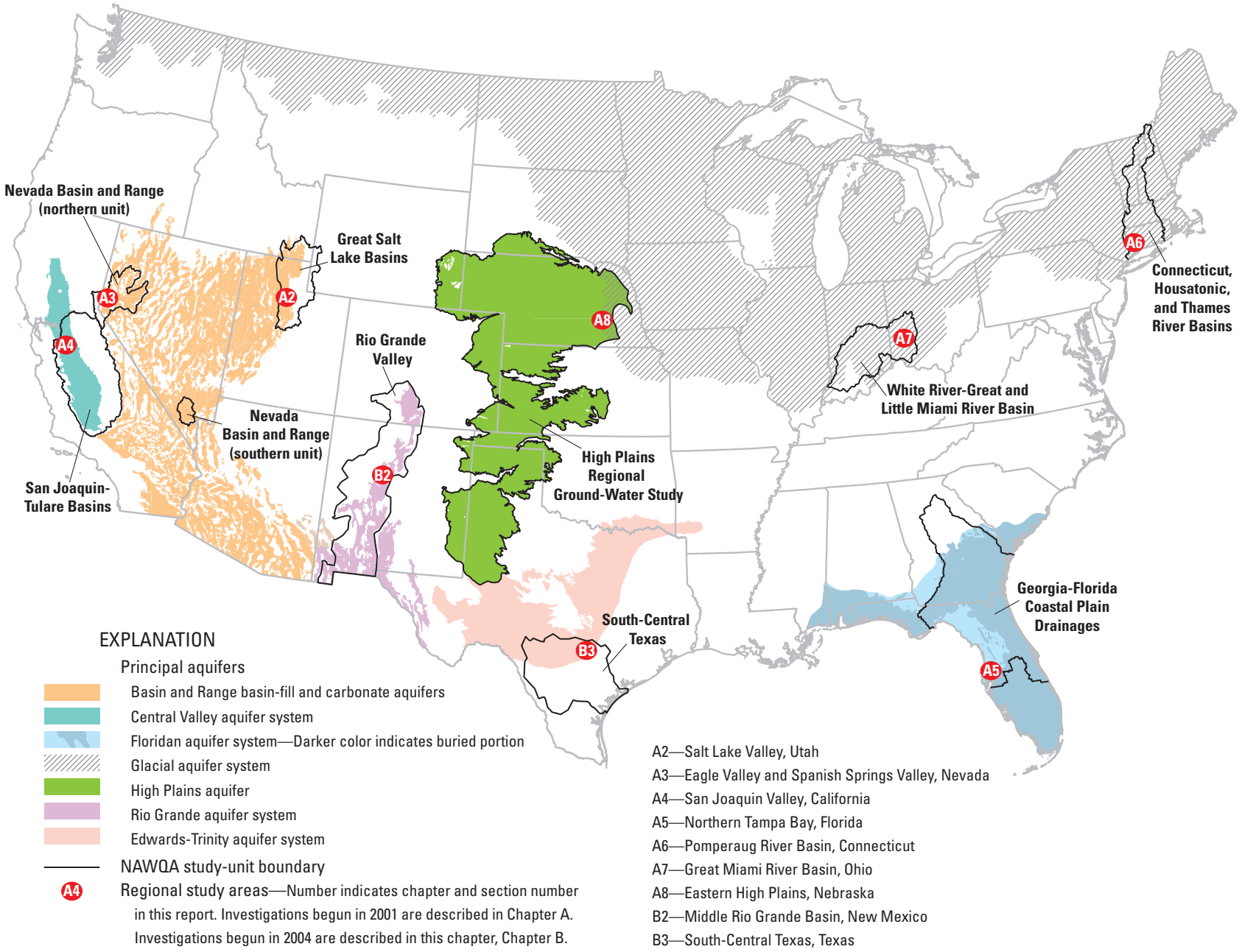

Figure 1.1. Locations of principal aquifers (Miller, 1999), National Water-Quality Assessment program study-unit boundaries, and study areas for regional investigations of the transport of anthropogenic and natural contaminants to public-supply wells begun in 2001 and 2004.

Basin and the regional study area is composed of the Tertiary to Quaternary Santa Fe Group and younger deposits, which together can reach a thickness of nearly 4,500 meters (m) and are commonly referred to as the Santa Fe Group aquifer system. The aquifer system is unconfined, with semiconfined conditions at depth. Although the depth to water is on the order of hundreds of meters throughout much of the study area, the generally shallow depth to water and intense agricultural and urban activity in the historic Rio Grande flood plain result in relatively high susceptibility and vulnerability of the aquifer to contamination in this area. Until surface-water diversions began in December 2008 to supply most water demand within the City of Albuquerque, the metropolitan area relied almost exclusively on groundwater for public supply. This change in water-supply strategy was a response to concerns about declining water levels in the aquifer (City of Albuquerque, 2003). Section 2 of this chapter presents the hydrogeologic setting, model setup, and modeling results for the Middle Rio Grande regional study area.

Edwards-Trinity Aquifer System

The Edwards-Trinity aquifer system is in carbonate and clastic rocks of Cretaceous age in a 199,000-km^2 area that extends from southeastern Oklahoma to western and south-central Texas (fig. 1.1). The aquifer system consists of three complexly interrelated aquifers—the Edwards-Trinity, the Edwards, and the Trinity aquifers. The Edwards-Trinity and the Trinity aquifers are stratigraphically equivalent in part and are hydraulically connected in some places. The Edwards aquifer overlies the Trinity aquifer and the two aquifers are hydraulically connected where no confining unit separates them. The groundwater-flow systems and permeability of the three aquifers are sufficiently different, however, to allow them to be separately mapped and described (Ryder, 1996).

The Edwards aquifer is the most transmissive of all aquifers in Texas. The carbonate rocks in the aquifer are laterally and vertically heterogeneous. Groundwater flow and aquifer properties are appreciably affected by the presence of faults and karst dissolution features. Water in such features can travel many times faster than water in the primary porosity of the rock matrix. Average annual precipitation in the area underlain by the Edwards aquifer ranges from about 56 cm in the west to about 86 cm in the east (Ryder, 1996).

The Edwards aquifer is recharged predominantly through seepage losses from surface streams that flow onto the highly permeable, fractured and faulted carbonate rocks of the Edwards aquifer outcrop (recharge zone) in the Balcones fault zone (see fig. 3.2). Discharge from the aquifer is primarily from spring flow and withdrawals by wells. Six large springs issue from the confined part of the Edwards aquifer. Comal and San Marcos Springs are the largest springs, with flow rates of 10.8 and 7.7 cubic meters per second, respectively, in 2002 (Hamilton and others, 2003).

The groundwater chemistry of the Edwards aquifer is relatively homogeneous and typical of a well-buffered carbonate aquifer system, with calcium and bicarbonate being the dominant dissolved ions. The concentration of dissolved solids in the water typically ranges from 300 to 1,200 milligrams per liter (Ryder, 1996). Widespread occurrence of low concentrations (less than 1 microgram per liter) of some anthropogenically derived compounds (for example atrazine, deethylatrazine, simazine, prometon, chloroform, and tetrachloroethylene) indicates that the aquifer is vulnerable to the effects of anthropogenic activities (Bush and others, 2000; Fahlquist and Ardis, 2004).

The South-Central Texas regional study area is the San Antonio segment of the Edwards aquifer, which overlies the fractured karstic Edwards aquifer in south-central Texas. The study area includes part of the topographically rugged Edwards Plateau and the comparatively flat Gulf Coastal Plain, which are separated by the Balcones fault zone (see fig. 3.2), and the San Antonio metropolitan area. Groundwater accounts for nearly all of the water supply in the South-Central Texas regional study area, and the Edwards aquifer is the principal source. The Edwards aquifer in the study area is unconfined within and adjacent to where it crops out at or near the land surface (recharge zone). The water table is generally greater than 30 m below the streambeds in this area. The aquifer is confined downdip of the outcrop; however, the presence of karst features and the extensive and increasing development on the recharge zone make the Edwards aquifer vulnerable to contamination. Vulnerability to contamination and the dependence of more than 1.5 million people on the aquifer for public water supply combine to make the water quality of the Edwards aquifer and the streams that recharge it a critical issue for the future of the San Antonio region. Section 3 of this chapter presents the hydrogeologic setting, model setup, and modeling results for the South-Central Texas regional study area.

Methods Update

The TANC study regional-scale investigations that began in 2001 consisted of implementing the following six tasks, which are presented in more detail in *Section 1 of Chapter A*.

1. Compilation of retrospective water-quality, well construction, water-use, and geologic data.

2. Collection of groundwater samples from public-supply wells in each study area in association with the NAWQA Source Water-Quality Assessment (SWQA) project. Sampled wells had pumping rates within the upper quartile of pumping for their respective study area.

3. Development of a steady-state regional groundwater-flow model for each study area to represent conditions for 1997–2001.

4. Use of the regional groundwater-flow models and advective particle tracking to compute the extent of the steady-state area contributing recharge and zone of contribution

for supply wells across the range of pumping rates within each modeled area.

5. Mapping of regional redox and pH conditions using the retrospective and newly collected SWQA water-quality data.

6. Development of a TANC database to store retrospective data and modeling results.

The investigations that began in 2004 implemented similar tasks with the following modifications. The collection of groundwater samples from public-supply wells was not constrained by the design of the NAWQA SWQA project, which was limited to high-production wells (Delzer and Hamilton, 2007). Rather, 15 public-supply wells from the upper quartile of pumping and 8 public-supply wells from each of the lower 3 quartiles of pumping were sampled for raw water quality in each of the 2 new study areas. The additional samples from the lower quartiles were included for the new study areas to allow for a more thorough description of the groundwater used as a drinking-water source than was possible for the initial seven study areas. Samples were analyzed for natural and anthropogenic constituents as described in Section 1 of Chapter A, with the addition of low-level analysis for halogenated volatile organic compounds (VOCs) at selected wells to serve as environmental tracers of groundwater age. Analytical methods for the age tracers are described in Busenberg and others (2006) and Shapiro and others (2004).

The areas contributing recharge and zones of contribution to supply wells in the Middle Rio Grande regional study area were simulated using a transient-state model, as opposed to a steady-state model. Consequently, the mapped areas for the Middle Rio Grande do not represent the extent of steady-state contributing areas. A modified approach was used because pumping during the past 50–60 years in the Middle Rio Grande aquifer system has changed groundwater-flow directions on a time scale that is much less than the total traveltime of most water reaching supply wells. Particles were tracked backward from each well to the areas of recharge. Then, to associate each particle with a clearly defined area and a specified volume of flow, a grid of particles was started in each cell that had been determined to be a source of water to the well and tracked forward until all particles reached a sink or until the end of the simulation time. The forward tracking was limited to particles with traveltimes less than 100 years; backward tracking alone was used for particles with longer traveltimes. The time step in which particles in a given cell were started in the forward simulation was based on the time step in which the particles began to contribute water to the well in the backwards simulation. The area associated with particles that terminated at the well during the time step representing June 2005 was mapped as the area contributing recharge to the well.

The grid-refinement approach that was used to help simulate contributing areas for wells that function as weak sinks within model cells also was adapted for use with the transient-state model of the Middle Rio Grande. A well will function as a weak sink when only some of the water entering the model cell in which it is located discharges to the well (see *Section 1 of Chapter A*). The solution to the weak sink problem is to create a highly discretized submodel (fine-grid model) for the weak sink cell so that all water entering the model cell discharges to the well. For the transient-state Middle Rio Grande model, boundary flows for the fine-grid models of the weak sink cells were set by transferring flows from each time step of the regional model to the fine-grid models cells. More specifically, regional model time steps corresponded to a stress period in the fine-grid models of the weak sink cells. Changes were made to the particle-tracking program, MODPATH (Pollock, 1994), to improve the efficiency of the weak sink program for the transient case and are documented in Appendix 1 of this chapter, Chapter B.

An additional complication arose because the MODFLOW Multi-Node-Well package (Halford and Hanson, 2002) was used in the Middle Rio Grande regional groundwater-flow model to allow for movement of water into and out of wells screened over multiple model layers based on simulated hydraulic heads. To account for this type of behavior in the fine-grid models of the weak sink cells while allowing particles to continue through a well in instances of downward leakage, the wells were simulated as follows: Well cells were defined as a stack of cells in a given row and column extending from the elevation of the top to the bottom of the screened interval of the well. The MODFLOW well package (Harbaugh, 2005) was used to set the desired pumping of the well in the top cell of the stack representing the well screen. The other cells representing the well cells were given a high vertical hydraulic conductivity (to simulate the ease of movement in the wellbore) and a reduced horizontal conductivity (to simulate the effects of well radius and formation damage near the well).

The areas contributing recharge and zones of contribution to supply wells in the South-Central Texas regional study area were estimated using a steady-state approach, similar to the initial seven study areas. However, two different models representing conditions during 2001–2003 were constructed, as opposed to a single steady-state model representing conditions during 1997–2001. Two models were constructed for this study area so that different conceptualizations of the groundwater-flow system in the South-Central Texas study area could be simulated. The first conceptualization was that of predominantly conduit flow in the aquifer. The second conceptualization was that of predominantly matrix (diffuse) flow through a network of numerous small fractures and openings. This approach was taken because the locations and interconnectedness of karst dissolution features in this study area were not known. Consequently, the simulated contributing areas for the study area were not estimated with certainty, but they provide insight into the general nature and patterns of contributing areas for public-supply wells in the area.

References Cited

Busenberg, E., Plummer, L.N., Cook, P.G., Solomon, D.K., Han, L.F., Gröning, M. and Oster, H., 2006, Sampling and analytical methods, *in*: Use of chlorofluorocarbons in hydrology, a guidebook: International Atomic Energy Agency, Vienna, p. 199–220. (Also available at *http:/www-pub.iaea.org/MTCD/publications/PDF/Pub1238_web.pdf*.)

Bush, P.W., Ardis, A.F., Fahlquist, Lynne, Ging, P.B., Hornig, C.E., and Lanning-Rush, Jennifer, 2000, Water quality in south-central Texas, Texas, 1996–98: U.S. Geological Survey Circular 1212, 32 p. (Also available at *http://pubs.usgs.gov/circ/circ1212/*.)

City of Albuquerque, 2003, San Juan-Chama Diversion Project: accessed August 2003 at *http://www.cabq.gov/waterresources/sjc.html*.

Delzer, G.C., and Hamilton, P.A., 2007, National Water-Quality Assessment Program—source water-quality assessments: U.S. Geological Survey Fact Sheet 2007–3069, 2 p. (Also available at *http://pubs.usgs.gov/fs/2007/3069/*.)

Eberts, S.M., Erwin, M.L., and Hamilton, P.A., 2005, Assessing the vulnerability of public-supply wells to contamination from urban, agricultural, and natural sources: U.S. Geological Survey Fact Sheet 2005–3022, 4 p. (Also available at *http://pubs.usgs.gov/fs/2005/3022/*.)

Fahlquist, Lynne, and Ardis, A.F., 2004, Quality of water in the Trinity and Edwards aquifers, south-central Texas, 1996−98: U.S. Geological Survey Scientific Investigations Report 2004–5201, 17 p. (Also available at *http://pubs.usgs.gov/sir/2004/5201/*.)

Halford, K.J., and Hanson, R.T., 2002, User guide for the drawdown-limited, multi-node well (MNW) package for the U.S. Geological Survey's modular three-dimensional finite-difference ground-water flow model, versions MODFLOW-96 and MODFLOW-2000: U.S. Geological Survey Open File Report 02–293, 32 p. (Also available at *http://pubs.usgs.gov/of/2002/ofr02293/text.pdf*.)

Hamilton, J.M., Johnson, S., Esquilin, R., Thompson, E.L., Luevano, G., Wiatrek, A., Mireles, J., Gloyd, T., Sterzenback, J., Hoyt, J.R., and Schindel, G., 2003, Edwards Aquifer Authority hydrogeological data report for 2002: San Antonio, Edwards Aquifer Authority, 134 p. (Also available at *http://www.edwardsaquifer.org/pdfs/reports/Hydro%20Reports/Hydro_%20Rept02.pdf*.)

Hamilton, P.A., Miller, T.L., and Myers, D.N., 2004: Water quality in the Nation's streams and aquifers—Overview of selected findings, 1991–2001: USGS Circular 1265, 20 p. (Also available at *http://pubs.usgs.gov/circ/2004/1265/*.)

Harbaugh, A.W., 2005, MODFLOW-2005, the U.S. Geological Survey modular ground-water model—the ground-water flow process: U.S. Geological Survey Techniques and Methods 6–A16 [variously paged]. (Available at *http://pubs.usgs.gov/tm/2005/tm6A16/PDF.htm*.)

Miller, J.A., 1999, Ground water atlas of the United States—Introduction and national summary: U.S. Geological Survey Hydrologic Atlas 730–A, 36 p. (Available at *http://pubs.usgs.gov/ha/ha730/ch_a/index.html*.)

Paschke, Suzanne S., ed., 2007, Hydrogeologic settings and ground-water flow simulations for regional studies of the transport of anthropogenic and natural contaminants to public-supply wells—Studies begun in 2001: U.S. Geological Survey Professional Paper 1737–A, 244 p. (Available at *http://pubs.usgs.gov/pp/2007/1737a/*.)

Plummer, L.N., Bexfield, L.M., Anderholm, S.K., Sanford, W.E, and Busenberg, E., 2004, Geochemical characterization of ground-water flow in the Santa Fe Group Aquifer System, Middle Rio Grande Basin, New Mexico: U.S. Geological Survey Water-Resources Investigations Report 03–4131, 395 p. (Also available at *http://pubs.usgs.gov/wri/wri034131/*.)

Pollock, D.W., 1994, User's guide for MODPATH/MODPATH-PLOT, version 3: A particle tracking post-processing package for MODFLOW, the U.S. Geological Survey finite-difference ground-water flow model: U.S. Geological Survey Open-File Report 94–464 [variously paged]. (Also available at *http://pubs.er.usgs.gov/publication/ofr94464*.)

Robson, S.G., and Banta, E.R., 1995, Ground water atlas of the United States—Arizona, Colorado, New Mexico, and Utah: U.S. Geological Survey Hydrologic Atlas HA 730–C, 32 p. (Available at *http://pubs.usgs.gov/ha/ha730/ch_c/index.html*.)

Ryder, P.D., 1996, Ground water atlas of the United States—Oklahoma and Texas: U.S. Geological Survey Hydrologic Atlas HA 730–E, 30 p. (Available at *http://pubs.usgs.gov/ha/ha730/ch_e/index.html*.)

Shapiro, S. D., Busenberg, E., Focazio, M. J., and Plummer, L. N., 2004, Historical trends in occurrence and atmospheric inputs of halogenated volatile organic compounds in untreated ground water used as a source of drinking water: Science of the Total Environment, v. 321, p. 201–217.

Western Regional Climate Center, 2006, Period of record monthly climate summary for Albuquerque WSFO Airport, New Mexico: accessed October 2006 at *http://www.wrcc.dri.edu/cgi-bin/cliMAIN.pl?nm0234*.

Hydrogeologic Setting and Groundwater Flow Simulation of the Middle Rio Grande Basin Regional Study Area, New Mexico

By Laura M. Bexfield, Charles E. Heywood, Leon J. Kauffman, Gordon W. Rattray, and Eric T. Vogler

Section 2 of

Hydrogeologic Settings and Groundwater-Flow Simulations for Regional Investigations of the Transport of Anthropogenic and Natural Contaminants to Public-Supply Wells—Investigations Begun in 2004

Edited by Sandra M. Eberts

Professional Paper 1737–B

U.S. Department of the Interior
U.S. Geological Survey

U.S. Department of the Interior
KEN SALAZAR, Secretary

U.S. Geological Survey
Marcia K. McNutt, Director

U.S. Geological Survey, Reston, Virginia: 2011

Suggested citation:
Bexfield, L.M., Heywood, C.E., Kauffman, L.J., Rattray, G.W., and Vogler, E.T., 2011, Hydrogeologic setting and groundwater-flow simulation of the Middle Rio Grande Basin regional study area, New Mexico, section 2 *of* Eberts, S.M., ed., Hydrologic settings and groundwater flow simulations for regional investigations of the transport of anthropogenic and natural contaminants to public-supply wells—Investigations begun in 2004: Reston, Va., U.S. Geological Survey Professional Paper 1737–B, pp. 2-1–2-61.

Contents

Figures

Tables

Hydrogeologic Setting and Groundwater Flow Simulation of the Middle Rio Grande Basin Regional Study Area, New Mexico

By Laura M. Bexfield, Charles E. Heywood, Leon J. Kauffman, Gordon W. Rattray, and Eric T. Vogler

Abstract

The transport of anthropogenic and natural contaminants to public-supply wells was evaluated in the northern part of the Middle Rio Grande Basin near Albuquerque, New Mexico, as part of the U.S. Geological Survey National Water-Quality Assessment Program. The Santa Fe Group aquifer system in the Middle Rio Grande Basin regional study area is representative of the Basin and Range basin-fill aquifers of the southwestern United States, is used extensively for public water supply, and is susceptible and vulnerable to contamination in places. Conditions within the Santa Fe Group aquifer system, which reaches a thickness of about 4,500 meters in parts of the study area, are unconfined to semiconfined. Withdrawals from public-supply wells completed in about the upper 300 meters of the aquifer system have altered the natural groundwater-flow patterns. A nine-layer, steady-state and transient groundwater-flow model of the Santa Fe Group aquifer system near Albuquerque, New Mexico, was developed by revising an existing model, and it simulates groundwater conditions through the end of 2008. The revised groundwater-flow model and advective particle-tracking simulations were used to compute areas contributing recharge and traveltimes from recharge areas for 59 public-supply wells. Model results for a full year ending October 31, 1999, indicate that recharge from river, lake, reservoir, canal, and irrigation losses provided 75 percent of the total net inflow; 48, 33 and 19 percent of the total net groundwater outflow was to drains, groundwater withdrawals, or riparian evapotranspiration, respectively. Depending on well location, particle-tracking results indicate areas contributing recharge to public-supply wells extend toward the basin margins, which are areas of mountain-front recharge and subsurface inflow, the Rio Grande, and (or) the Jemez River. Traveltimes estimated with particle tracking ranged from less than 10 years to more than 10,000 years.

Introduction

The Middle Rio Grande Basin (MRGB) regional study area for the transport of anthropogenic and natural contaminants to public-supply wells (TANC) is in the Rio Grande valley near Albuquerque, New Mexico, and is part of the Rio Grande Valley study unit of the U.S. Geological Survey National Water-Quality Assessment (NAWQA) program (fig. 2.1). The study area is in the most populous alluvial basin in the Rio Grande Valley study unit, which extends from the Rio Grande headwaters in southern Colorado to El Paso, Texas, and includes much of the Rio Grande aquifer system (fig. 2.1). The MRGB regional study area, delineated to focus data-collection efforts and investigation of the transport of anthropogenic and natural contaminants to public-supply wells in the most populous part of the MRGB, covers about the northern half of the basin, which is where most of the population resides. However, the model used by the TANC study to simulate groundwater flow within the MRGB regional study area is a revised and updated version of an existing model covering essentially the entire MRGB. The aquifer of the MRGB is one of a network of basin-fill aquifers within the Rio Grande aquifer system, and is composed of Tertiary and Quaternary deposits that together are commonly known in the MRGB as the Santa Fe Group aquifer system.

Purpose and Scope

The purpose of this Professional Paper section is to present the hydrogeologic setting of the MRGB regional study area and to document revisions and updates to an existing transient groundwater-flow model for the entire MRGB. Groundwater-flow characteristics, groundwater-withdrawal information, and water-quality data were compiled from existing data to improve the conceptual understanding of

Figure 2.1. Location of the Middle Rio Grande regional study area relative to the Rio Grande aquifer system and the Basin and Range basin-fill aquifers.

groundwater conditions in the MRGB regional study area. A nine-layer transient groundwater-flow model by McAda and Barroll (2002) of the Santa Fe Group aquifer system in the MRGB was revised and updated to simulate groundwater-flow conditions through the end of 2008. The revised groundwater-flow model and associated particle tracking were used to simulate advective groundwater-flow paths and to delineate areas contributing recharge and zones of contribution to selected public-supply wells. Groundwater traveltimes from recharge to public-supply wells, oxidation-reduction (redox) conditions along flow paths, and the presence of potential contaminant sources in areas contributing recharge were tabulated into a relational database described in Appendix 1 of Chapter A of this Professional Paper. This section, Section 2 of Chapter B, provides the foundation for future groundwater susceptibility and vulnerability analyses of the study area and comparisons among regional aquifer systems.

Study Area Description

The MRGB regional study area is located in central New Mexico near the City of Albuquerque and encompasses 4,486 square kilometers (km^2) in the northern part of the 7,922-km^2 MRGB (figs. 2.1 and 2.2). The Albuquerque metropolitan area is the most populous area in New Mexico, and it grew by more than 20 percent between 1990 and 2000, from about 589,000 to 713,000 people (U.S. Census Bureau, 2001a). Historically, groundwater has been essentially the sole source of public water supply in the metropolitan area. The groundwater-flow system in the study area is representative not only of other alluvial basins along the Rio Grande, but also of alluvial basins in the Basin and Range basin-fill aquifers of the southwestern United States (fig. 2.1; table 2.1). Both geologic sources of natural contaminants and a long history of agricultural and urban land uses in areas of intrinsic susceptibility contribute to groundwater vulnerability in the study area.

Topography and Climate

The MRGB is located primarily in the Basin and Range physiographic province (Fenneman, 1931) and is defined by the extent of Cenozoic deposits (fig. 2.2; table 2.1). The MRGB regional study area is bounded by the Jemez Mountains and the Nacimiento Uplift to the north and northwest, by the Sandia and Manzanita Mountains to the east, and by the Rio Puerco fault zone and San Juan structural basin to the west (fig. 2.2). The southern boundary was assigned to correspond with the southernmost extent of Bernalillo County, thereby defining the study area to include the two most populous counties within the basin, Bernalillo and Sandoval Counties, and the recharge areas for the groundwater used in those counties. Land-surface elevation within the study area ranges from about 1,485 meters (m) at the Rio Grande along the southern edge of the study area to more than 2,000 m along the foothills of the Sandia and Jemez Mountains. The Rio Grande and Rio Puerco are located in terraced valleys.

Most of the MRGB regional study area is categorized as having a semiarid climate, characterized by abundant sunshine, low humidity, and a high rate of evaporation that substantially exceeds the low rate of precipitation. Precipitation shows relatively large spatial variation because of the range in land-surface elevation across the area. Mean annual precipitation for 1914–2005 at Albuquerque was 21.7 centimeters per year (cm/yr) (Western Regional Climate Center, 2006a), whereas mean annual precipitation for 1953–1979 at the crest of the Sandia Mountains that border the basin to the east was 57.4 cm/yr (Western Regional Climate Center, 2006b). Most precipitation at lower elevations falls between July and October as a result of localized, high-intensity thunderstorms of short duration; winter storms of lower intensity and longer duration make a greater contribution to annual precipitation at higher elevations.

Surface-Water Hydrology

The Rio Grande is a perennial stream and is the primary surface-water feature of the MRGB regional study area, with a mean annual discharge at Albuquerque of about 37 cubic meters per second (m^3/s) for 1974–2009 (U.S. Geological Survey, Water Resources, 2010). Although the Rio Grande primarily loses water to the aquifer system as it flows through the study area from north to south, some river sections in the northern part of the study area gain water (McAda and Barroll, 2002; Plummer and others, 2004a). A system of levees and jetty jacks directs the course of the Rio Grande through the study area, and an upstream series of dams, including the dam for Cochiti Lake at the northern end of the MRGB, affects the seasonal discharge patterns of the river. From May to October, substantial quantities of water are diverted north of Albuquerque from the Rio Grande into an extensive network of irrigation canals crisscrossing the historic flood plain, also known as the Rio Grande inner valley (fig. 2.2). Riverside and interior drains maintain the water table in the inner valley at a sufficient depth below land surface to allow sustained irrigated agriculture without damaging crops.

Tributaries that contribute water to the Rio Grande within the regional study area include the Jemez River, which drains areas west of the Rio Grande and is perennial through most of the study area, and several streams and arroyos that contribute ephemeral flow to the Rio Grande only during large storm events. Many of these streams and arroyos enter the MRGB along the eastern margin, where flow may be perennial or intermittent (McAda and Barroll, 2002). The groundwater-drain system and flood-diversion channels also contribute flow to the Rio Grande.

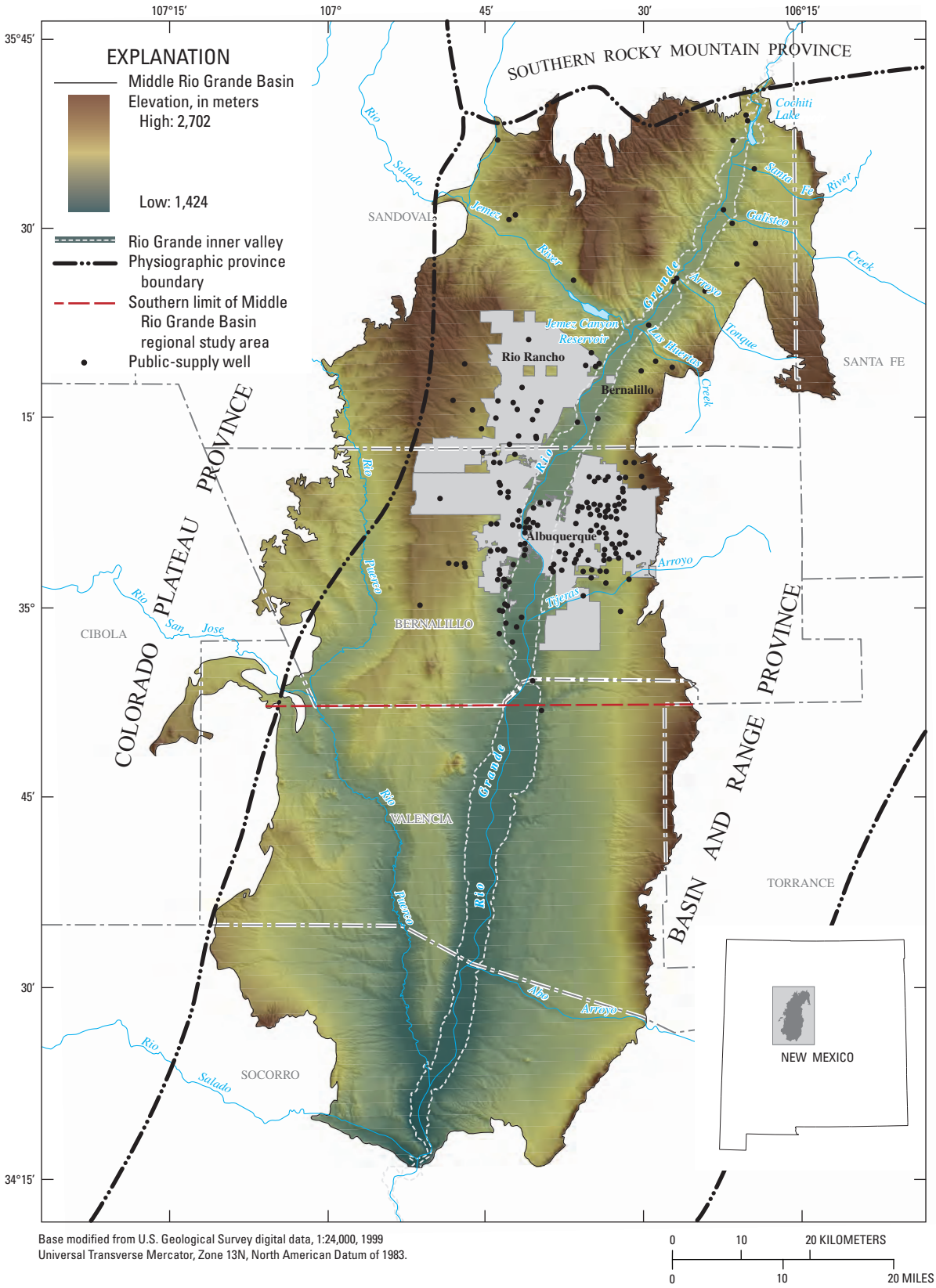

Figure 2.2. Major cultural, geographic, and hydrologic features of the Middle Rio Grande Basin and the locations of public-supply wells in the Middle Rio Grande Basin regional study area, New Mexico.

Table 2.1 Summary of hydrogeologic and groundwater-quality characteristics for the Basin and Range basin-fill aquifers and the Middle Rio Grande Basin regional study area, New Mexico.

[NAWQA, National Water-Quality Analysis; ft, feet; m, meters; in/yr, inches per year; cm/yr, centimeters per year; ºC, temperature in degrees Celsius; ºF, temperature in degrees Fahrenheit; m^3/yr, cubic meters per year; acre-ft/year, acre-feet per year; ft/day, feet per day; ft^2/day, square feet per day; m/d, meters per day; m^2/day, square meters per day; µS/cm, microsiemens per centimeter at 25 ºC; mg/L, milligrams per liter]

Characteristic	NAWQA Principal Aquifer: Basin and Range	Middle Rio Grande Basin regional study area, New Mexico
	Geography	
Topography	Altitude ranges from about 46m (150 ft) at Yuma, Arizona to over 3,048 m (10,000 ft) at the crest of some mountain ranges (Robson and Banta, 1995).	Altitude of the Rio Grande ranges from about 1,485 m (4,870 ft) at the south end of the study area to about 1,650 m (5,400 ft) at the north end. Land-surface altitude exceeds 2,000 m (6,560 ft) along foothills of the Jemez and Sandia Mountains.
Climate	Arid to semiarid climate. Precipitation ranges from 10 to 20 cm/yr (4 to 8 in/yr) in basins and 40 to 76 cm/yr (16 to 30 in/yr) in mountains (Robson and Banta, 1995).	Semiarid climate. Annual precipitation is about 22 cm (8.7 in) in the valley (Western Regional Climate Center, 2006a) and approaches 60 cm (24 in) in the Sandia Mountains (Western Regional Climate Center, 2006b). Mean monthly temperatures in the valley range from about 1.8ºC (35ºF) in January to about 25.6ºC (78ºF) in July (Western Regional Climate Center, 2006a).
Surface-water hydrology	Streams drain from surrounding mountains into basins. Basins generally slope toward a central depression with a main drainage that is dry most of the time. Many basins have playas in their lowest depressions. Groundwater discharge to streams can occur in basin depressions. (Planert and Williams, 1995)	The Rio Grande is the major stream and alternately gains and loses flow. Water from the Rio Grande is diverted into canals to supply irrigated agriculture in the flood plain. The Jemez River is a major tributary. Arroyos originating in the eastern mountains convey substantial quantities of water to the Rio Grande during storm events.
Land use	Undeveloped basins are unused, grazing, and rural residential. Developed basins are urban, suburban and agricultural.	Urban, suburban, rural residential, agricultural, and grazing.
Water use	Groundwater withdrawals from wells supply water for agricultural irrigation and municipal use. Population increases since the 1960's have increased the percentage of water being used for municipal supply.	Groundwater was essentially the sole source of public supply through 2008. Ground-water withdrawals during 2000 were about 194 million m^3/yr (157,000 acre-ft/yr) (Wilson and others, 2003). In 2000, surface-water withdrawals for agriculture nearly equaled groundwater withdrawals for public supply.
	Geology	
Surficial geology	Tertiary and Quaternary unconsolidated to moderately consolidated fluvial gravel, sand, silt and clay basin-fill deposits include alluvial fans, flood plain deposits, and playas. (Robson and Banta, 1995; Planert and Williams, 1995)	Tertiary and Quaternary unconsolidated to moderately consolidated basin-fill sediments up to about 4,500 m (15,000 ft) in thickness. Sediments include fluvial, piedmont-slope, eolian, and playa deposits. Volcanic flows and ash beds also are present.
Bedrock geology	Mountains surrounding basins are composed of Paleozoic to Tertiary bedrock formations. Tertiary volcanic and metamorphic rocks are in general impermeable. Paleozoic and Mesozoic carbonate rocks are cavernous allowing inter-basin flow in some areas. (Robson and Banta, 1995; Planert and Williams, 1995)	Most surrounding mountain ranges are composed of Precambrian plutonic and metamorphic rocks overlain by Paleozoic limestone, sandstone, and shale. Cenozoic volcanic rocks make up the Jemez Mountains.

Table 2.1 Summary of hydrogeologic and groundwater-quality characteristics for the Basin and Range basin-fill aquifers and the Middle Rio Grande Basin regional study area, New Mexico.—Continued

[NAWQA, National Water-Quality Analysis; ft, feet; m, meters; in/yr, inches per year; cm/yr, centimeters per year; ºC, temperature in degrees Celsius; ºF, temperature in degrees Fahrenheit; m^3/yr, cubic meters per year; acre-ft/year, acre-feet per year; ft/day, feet per day; ft^2/day, square feet per day; m/d, meters per day; m^2/day, square meters per day; µS/cm, microsiemens per centimeter at 25 ºC; mg/L, milligrams per liter]

Characteristic	NAWQA Principal Aquifer: Basin and Range	Middle Rio Grande Basin regional study area, New Mexico
	Groundwater hydrology	
Aquifer conditions	Unconfined basin-fill aquifers surrounded by relatively impermeable bedrock mountains and foothills. Basin groundwater-flow systems are generally isolated and not connected with other basins except in some locations where basins are hydraulically connected via cavernous carbonate bedrock.	Unconfined basin-fill aquifer surrounded by relatively impermeable uplifts. Conditions are semiconfined at depth. Groundwater flow through the central part of the basin is primarily north to south. Along basin margins, flow is directed generally toward the central part of the basin.
Hydraulic properties	Transmissivity ranges from less than 93 m^2/day (1,000 ft^2/day) to greater than 2,790 m^2/day (30,000 ft^2/day). In general, alluvial fan deposits near basin margins are more conductive than flood plain and lacustrine deposits near basin centers. (Robson and Banta, 1995; Planert and Williams, 1995)	Transmissivity estimates range from less than 65 m^2/day (700 ft^2/day) to about 7,430 m^2/day (80,000 ft^2/day) (Thorn and others, 1993). Horizontal hydraulic conductivity ranges from about $2x10^{-2}$ to $1x10^{2}$ m/day ($5x10^{-2}$ to $3x10^{2}$ ft/day), whereas vertical hydraulic conductivity ranges from about $9x10^{-5}$ to $1x10^{1}$ m/day ($3x10^{-4}$ to $4x10^{1}$ ft/day) (CH2MHill, 1999; McAda and Barroll, 2002; this report).
Groundwater budget	Recharge to basin fill deposits is from surface-water runoff in mountains where precipitation is highest. Ground-water discharges naturally as evapotranspiration to playas and stream channels in basin depressions. Groundwater withdrawal from wells is largest component of discharge from Basin and Range aquifers. (Robson and Banta, 1995)	Recharge is primarily from mountain-front processes; seepage from the Rio Grande, tributary streams and arroyos, irrigation canals, and crop irrigation; and subsurface inflow from adjacent basins. Discharge is mostly to groundwater withdrawal, groundwater evapotranspiration, drains, and streams (the Rio Grande).
Groundwater residence times	No regional information.	Modern to more than 30,000 years.
	Groundwater quality	
	Water quality varies between basins. Total dissolved solids can range from less than 500 mg/L to over 35,000 mg/L. Generally, water that has low concentrations of total dissolved solids and is oxic occurs near recharge areas of basin margins. Water with high concentrations of total dissolved solids and that is anoxic can occur with depth or near basin centers and playa lakes. (Robson and Banta, 1995; Planert and Williams, 1995)	Total dissolved solids are lowest (specific conductance less than 400 µS/cm) in water recharged along the northern and eastern mountain fronts and the Rio Grande. Calcium-bicarbonate or calcium-sodium-bicarbonate type water dominates in these areas, where pH is typically 7 to 8. Groundwater inflow from the Jemez Mountain region is sodium-bicarbonate type water and generally has pH greater than 8. Total dissolved solids are highest (specific conductance exceeding 1,000 µS/cm) where groundwater inflow or arroyo infiltration dominate recharge. Groundwater is oxic, except at shallow depths, within the Rio Grande flood plain.

Land Use

Prior to substantial urbanization of the MRGB regional study area, land outside the Rio Grande inner valley was almost exclusively rangeland. For 83 percent of the regional study area, rangeland has remained the dominant land-use type according to the National Land Cover Database (NLCD) dataset for 2001 (*http://www.mrlc.gov/*; Homer and others, 2004). In the northern part of the study area, much of this land is within American Indian reservations.

Within the inner valley—an area that is intrinsically susceptible to groundwater contamination because of depths to groundwater generally less than about 7.6 m (Anderholm, 1997)—agriculture was practiced as early as the 1700s, and grew rapidly during the mid- to late-1800s (Bartolino and Cole, 2002). Mapping of 1935 Albuquerque urban areas indicates that the city was first urbanized primarily within the inner valley (Bartolino and Cole, 2002), where industry was developed by the 1950s (U.S. Environmental Protection Agency, 2005). Population growth in the Albuquerque area since about 1940 has led to extensive urbanization of upland areas, in addition to urbanization of irrigated agricultural land in the inner valley (Bartolino and Cole, 2002). Irrigated agriculture makes up only about 3.5 percent of land in the regional study area, as shown by the 2001 NLCD dataset, probably because of urbanization and the narrow width of the inner valley. In Bernalillo County in 1992, alfalfa was the most abundant crop type based on planted acreage (Kinkel, 1995, appendix 4), and urban turf grass was the second most abundant (Bartolino and Cole, 2002). The 2001 NLCD dataset classified about11 percent of land in the regional study area as urban. In 2000, population density within the City of Albuquerque was about 960 persons per km^2, compared with less than 6 persons per km^2 for New Mexico as a whole (U.S. Census Bureau, 2006).

Water Use

Despite urbanization, irrigated agriculture remains a large water user within the MRGB regional study area. Estimates of water use in Bernalillo and Sandoval Counties (table 2.2) by Wilson and others (2003) indicate that 43.8 percent of the total surface-water and groundwater withdrawals of nearly 360,000 thousand m^3 in these two counties in 2000 was for irrigated agriculture. However, only 28.7 percent of the total water depletion, which is defined as the part of withdrawal that is lost to the local water resource for future use because of consumption, evapotranspiration, or other processes, of nearly 160,000 thousand m^3 was associated with irrigated agriculture. Almost 97 percent of the water used for irrigated agriculture was surface water, primarily diverted from the Rio Grande and delivered to areas within the inner valley. Bernalillo and Sandoval Counties extend outside the regional study area, but combined estimates of water use for these counties are expected to approximate use within the study area, where most of the population and irrigated agriculture are located.

Water use for public supply in Bernalillo and Sandoval Counties in 2000 accounted for 44.9 percent of total water withdrawals (table 2.2)—just slightly more than the use for irrigated agriculture—and about 48.9 percent of total water depletion. Essentially all the water used for public supply was groundwater (table 2.2), withdrawn primarily from the Santa Fe Group aquifer system. Most (87.6 percent) of groundwater used for public supply in 2000 was withdrawn by the City of Albuquerque (now the Albuquerque Bernalillo County Water Authority), which began diverting surface water from the Rio Grande in 2008 with the intent eventually to meet most demand; this change in water-supply strategy is largely the result of concerns about declining water levels in the aquifer (City of Albuquerque, 2003). Files of the City of Albuquerque and the Albuquerque Bernalillo County Water Authority indicate the 4 months of June through September have historically accounted for about 46 percent of annual groundwater withdrawals, and the Albuquerque Bernalillo County Water Authority plans to continue withdrawing groundwater to supplement supplies during this summer peak-demand period and during drought. Wilson and others (2003) estimated groundwater withdrawn by private domestic wells to be only about 5.3 percent of groundwater use in 2000 (table 2.2); self-supplied commercial and industrial withdrawals combined were about 7.4 percent of groundwater use.

Table 2.2 Year-2000 water-use estimates for selected counties of the Middle Rio Grande Basin, New Mexico.

Water-use category	Surface-water withdrawal (thousands of cubic meters)	Groundwater withdrawal (thousands of cubic meters)	Total withdrawal (thousands of cubic meters)	Total depletion[1] (thousands of cubic meters)
Bernalillo County				
Public water supply	82.19	145,933.11	146,015.30	64,764.36
Domestic	.00	6,874.00	6,874.00	6,874.00
Irrigated agriculture	76,392.00	4,075.42	80,467.42	22,485.14
Livestock	25.78	990.25	1,016.03	1,016.03
Commercial and industrial	.00	7,259.29	7,259.29	5,756.51
Mining and power generation	.00	1,601.34	1,601.34	1,121.62
Reservoir evaporation	.00	.00	.00	.00
County totals:	**76,499.96**	**166,733.42**	**243,233.38**	**102,017.66**
Sandoval County				
Public water supply	196.32	15,072.89	15,269.21	12,281.66
Domestic	.00	3,490.56	3,490.56	3,490.56
Irrigated agriculture	75,875.17	1,016.39	76,891.56	22,721.97
Livestock	152.98	165.99	318.97	318.97
Commercial and industrial	12.33	7,019.68	7,032.02	3,390.18
Mining and power generation	.00	540.64	540.64	432.18
Reservoir evaporation	12,791.21	.00	12,791.21	12,791.21
County totals:	**89,028.01**	**27,306.14**	**116,334.15**	**55,426.70**
Total estimated water use for Bernalillo and Sandoval Counties				
Public water supply	278.51	161,006.00	161,284.51	77,046.01
Domestic	.00	10,364.55	10,364.55	10,364.55
Irrigated agriculture	152,267.17	5,091.81	157,358.98	45,207.11
Livestock	178.76	1,156.24	1,335.00	1,335.00
Commercial and industrial	12.33	14,278.97	14,291.31	9,146.69
Mining and power generation	.00	2,141.98	2,141.98	1,553.79
Reservoir evaporation	12,791.21	.00	12,791.21	12,791.21
Total for both counties:	**165,527.97**	**194,039.56**	**359,567.53**	**157,444.36**

[1] Depletion is the part of withdrawal that is lost to the local water resource for future use because of consumption, evapotranspiration, or other processes.

Conceptual Understanding of the Groundwater System

The conceptual understanding of groundwater flow for the MRGB, and consequently of the MRGB regional study area, has been developed through investigations of the geology, hydrology, and water chemistry of the basin spanning the past 100 years. Lee (1907) conducted the first detailed reconnaissance of water resources in the Rio Grande valley. Early studies focusing on groundwater resources within the MRGB were published by Meeks (1949), Bjorklund and Maxwell (1961), and Titus (1961). The first three-dimensional groundwater-flow model of the basin was constructed by Kernodle and Scott (1986), and the first detailed study of groundwater chemistry was conducted by Anderholm (1988). Detailed investigations of the hydrogeology of the basin by Hawley and Haase (1992) and of hydrologic conditions in the basin by Thorn and others (1993) demonstrated that the extent and thickness of highly productive parts of the aquifer in the area were substantially smaller than previously believed. The need for improved knowledge of the availability of groundwater resources in the MRGB led to an intensive 6-year, multidisciplinary group of studies by Federal, State, and local agencies and universities during 1995–2001. Results of the numerous investigations included in this effort are summarized in Bartolino and Cole (2002), were incorporated into the groundwater-flow model by McAda and Barroll (2002), and are selectively discussed in the following sections.

Geology

The MRGB is located along the Rio Grande Rift, which is a generally north-south trending area of Cenozoic crustal extension, and is hydraulically connected to the Española Basin on the north and the Socorro Basin on the south. Three subbasins (fig. 2.3) that are separated by bedrock structural highs and contain alluvial fill up to about 4,500 m thick (fig. 2.4) are included within the overall MRGB (Grauch and others, 1999); the regional study area entirely encompasses the northern two subbasins. Relatively shallow benches on the east and west bound the deeper parts of the basin. In addition to major faults that juxtapose alluvium and bedrock along uplifts and benches near the basin margins, numerous other primarily north-south trending faults have caused offsets within the alluvial fill (Grauch and others, 2001; Connell, 2006) (fig. 2.3). The uplifts on the east and the Nacimiento Uplift on the northwest are composed of Precambrian plutonic and metamorphic rocks, generally overlain by Paleozoic and (or) Mesozoic sedimentary rocks (Hawley and Haase, 1992; Hawley and others, 1995). The Jemez Mountains on the north are a major Cenozoic volcanic center.

The alluvial fill of the MRGB is composed primarily of the unconsolidated to moderately consolidated Santa Fe Group deposits of late Oligocene to middle Pleistocene age, which overlie lower and middle Tertiary rocks in the central part of the basin and Mesozoic, Paleozoic, and Precambrian rocks near the basin margins (McAda and Barroll, 2002). Post-Santa Fe Group valley and basin-fill deposits of Pleistocene to Holocene age typically are in hydraulic connection with the Santa Fe Group deposits; in combination, these deposits form the Santa Fe Group aquifer system (Thorn and others, 1993). The sediments in the basin consist generally of sand, gravel, silt, and clay that were deposited in fluvial, lacustrine, or piedmont-slope environments.

Hawley and Haase (1992) defined broad lower, middle, and upper parts of the Santa Fe Group based on both the timing and environment of deposition, as described here. Sediments of the lower Santa Fe Group, which may be more than 1,000 m thick in places, were deposited about 30 to 15 million years ago in a shallow, internally drained basin. Along with piedmont-slope and eolian deposits, the lower unit includes extensive basin-floor playa deposits that have low hydraulic conductivity. The middle Santa Fe Group ranges from about 75 to 2,700 m thick and was deposited about 15 to 5 million years ago, during a time when major fluvial systems from the north, northeast, and southwest transported large quantities of sediment into the basin. In addition to piedmont-slope deposits, the middle unit consists largely of basin-floor fluvial deposits in the north and playa deposits in the south, where the fluvial systems terminated. Within the Ceja Formation, a red-brown clay layer named the Atrisco Member by Connell and others (1998), and shown on the sections in Connell (1997 and 2006) and figure 2.4, marks the top of the middle Santa Fe Group. The upper unit generally is less than about 300 m thick and was deposited about 5 to 1 million years ago during development of the ancestral Rio Grande system. The axial-channel deposits of this high-energy fluvial system include thick zones of clean sand and gravel that compose the most productive aquifer materials in the basin. Most public-supply wells in the study area are completed in the upper and (or) middle units east of the Rio Grande, and in the middle and (or) lower units west of the Rio Grande.

Post-Santa Fe Group valley-fill sediments generally are less than about 40 m thick and were deposited during the most recent (10,000- to 15,000-year) partial backfilling sequence of the Rio Grande and Rio Puerco, following earlier incision (Hawley and Haase, 1992). These sediments provide a connection between the surface-water system and the underlying Santa Fe Group deposits. Relatively young basin-fill materials also include eolian and fan deposits, along with volcanics that were emplaced during the middle to late Pleistocene.

Groundwater Occurrence and Flow

Conditions within the Santa Fe Group aquifer system of the MRGB regional study area generally are unconfined, but are semiconfined at depth. Water-level maps of predevelopment (generally pre-1960) conditions in the study area (Meeks, 1949; Bjorklund and Maxwell, 1961; Titus, 1961; Bexfield

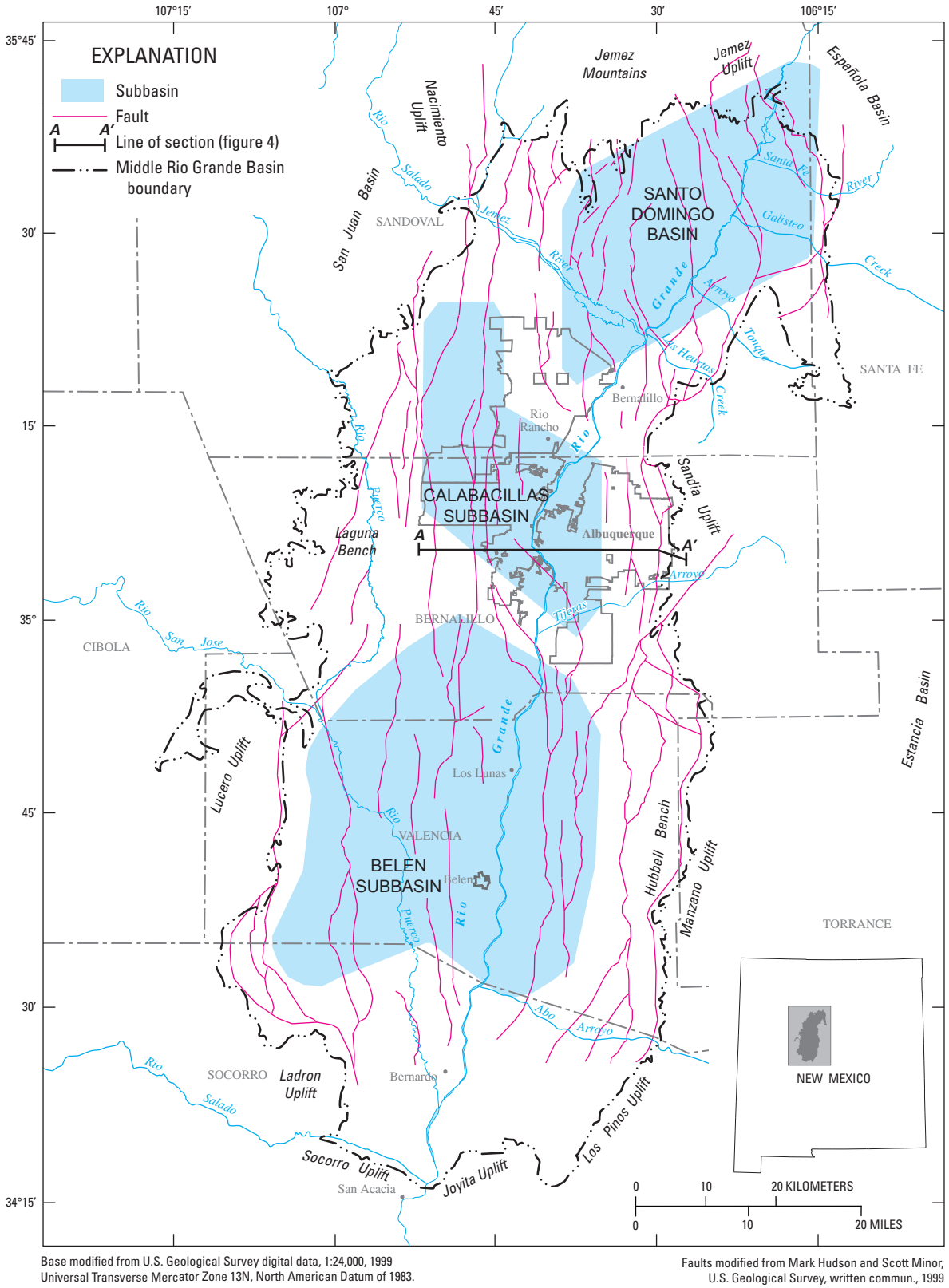

Base modified from U.S. Geological Survey digital data, 1:24,000, 1999
Universal Transverse Mercator Zone 13N, North American Datum of 1983.

Faults modified from Mark Hudson and Scott Minor, U.S. Geological Survey, written commun., 1999

Figure 2.3. Major structural features in the Middle Rio Grande Basin, New Mexico.

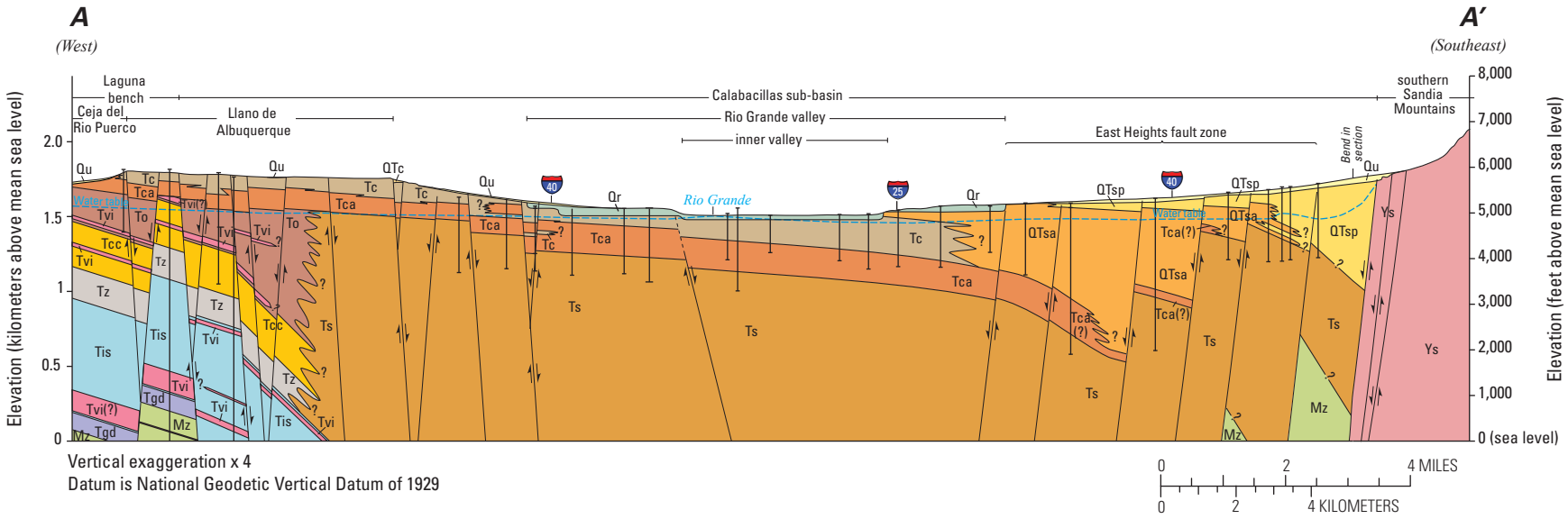

EXPLANATION

Post-Santa Fe Group deposits

- **Qu** — Pleistocene and Holocene sediments, undivided
- **Qr** — Rio Grande fluvial deposits, undivided (modern-middle Pleistocene)

Santa Fe Group deposits

- **Ts** — Rio Grande fluvial deposits, undivided lower and middle subgroups (upper Oligocene-upper Miocene)
- **QTsa** — Sierra Ladrones Formation, axial-fluvial member (Pliocene-lower Pleistocene)
- **QTsp** — Sierra Ladrones Formation, upper piedmont member (Pliocene-lower Pleistocene)
- **Tc** — Ceja Formation, undivided (Pliocene-lower Pleistocene(?))
- **QTc** — Calabacillas Formation (upper Pliocene(?))
- **Tca** — Ceja Formation, Atrisco Member (Pliocene)
- **To** — Arroyo Ojito Formation, undivided (middle-upper Miocene)
- **Tcc** — Cerro Conejo Formation (middle Miocene)
- **Tz** — Zia Formation, undivided (upper Oligocene-lower Miocene)

Pre-Santa Fe Group deposits

- **Tis** — Unit of Isleta well #2 (upper Eocene-Oligocene) sandstone, mudstone, and interbedded volcanic rocks described by Lozinsky (1994) in subsurface
- **Tvi** — Interbedded volcanic rocks of Tertiary age.
- **Tgd** — Diamond Tail and Galisteo Formations, undivided.
- **Mz** — Mesozoic sedimentary rocks, undivided.

Crystalline rocks

- **Ys** — Sandia granite.
- Fault—Arrows indicate direction of movement.
- Contact—Queried where uncertain.
- Deep well in geologic cross section.

Figure 2.4. Geologic section through Albuquerque, New Mexico (modified from Connell, 1997). See figure 2.3 for section location. Formations and member names usage from the New Mexico Bureau of Geology and Mineral Resources (Connell, 1997).

and Anderholm, 2000) indicate that the principal direction of groundwater flow was north to south through the center of basin, with greater components of east-to-west flow near the basin margins (fig. 2.5). This general flow pattern reflects not only sedimentation patterns in the basin, but also the areal distribution of groundwater recharge and discharge (fig. 2.6). Mountain-front processes (shallow subsurface groundwater inflow and infiltration through mountain stream channels) contribute recharge along the northern and eastern basin margins, where deep subsurface inflow through mountain blocks also occurs. The San Juan Basin contributes subsurface groundwater inflow along the western margin of the MRGB. Along most of its length, the Rio Grande leaks water to the aquifer system, as do some tributary streams and arroyos. Before the arrival of irrigated agriculture and a substantial population, most discharge occurred through riparian evapotranspiration (fig. 2.6*A*) (McAda and Barroll, 2002), defined for this study as evapotranspiration from the water table in riparian areas along the Rio Grande inner valley and the Jemez River. Since development of irrigated agriculture and urbanized areas, water also recharges the aquifer system through seepage from irrigation canals, irrigated agricultural fields, and septic systems (fig. 2.6*B*); although not specifically addressed by previous groundwater budgets for the MRGB, irrigated urban landscaping and leaky sewer and (or) water-distribution lines also are likely to contribute recharge in some areas. Water now also discharges from the system through groundwater drains (riverside and interior) and groundwater withdrawals for public supply.

Predevelopment water-level maps indicate the presence of depressions—or "water-level troughs"—in the water-level surface both east and west of the Rio Grande (fig. 2.5). Highly permeable channel gravels west of the Rio Grande in the far north part of the basin (Smith and Kuhle, 1998) and east of the Rio Grande near Albuquerque (Hawley and Haase, 1992) support the hypothesis of high permeability pathways as the most probable explanation for the groundwater troughs in these areas (McAda and Barroll, 2002). Kernodle and others (1995) also hypothesized the presence of a relatively thick sequence of permeable material in the area of the trough west of the Rio Grande near Albuquerque, but detailed lithologic information subsequently obtained from wells in the area generally do not appear to support this hypothesis (Hawley, 1996; Stone and others, 1998; Tiedeman and others, 1998). Based on groundwater chemistry, Plummer and others (2004a, b, c) hypothesized that this trough may be a transient feature that reflects changes in the quantity and spatial distribution of recharge through time. The transient paleohydrologic model of Sanford and others (2004a, b) indicates that recharge quantities probably have changed through time and that low rates of recharge along basin margins have contributed to trough formation. Horizontal anisotropy and faults acting as flow barriers also have been proposed as factors contributing to the existence of the trough west of Albuquerque (McAda and Barroll, 2002).

Large and extensive water-level declines from sustained groundwater withdrawals in urbanized areas have substantially altered the direction of groundwater flow in the regional study area, particularly in and around Albuquerque (Bexfield and Anderholm, 2002a) (fig. 2.7). Water-level declines since predevelopment in the production zone (the depth interval from which most supply-well withdrawals occur—typically from less than about 60 m to 275 m or more below the water table) have exceeded 30 m across broad areas east of the Rio Grande and 20 m across smaller areas west of the Rio Grande. Consequently, groundwater now flows into the major pumping centers from all directions (fig. 2.7). Also, water-level declines in the aquifer have induced additional inflow from the surface-water system compared with predevelopment conditions.

Water-level data from deep piezometer nests across the Albuquerque area indicate that vertical gradients generally are downward in the Rio Grande inner valley and areas to the west, and upward in areas east of the inner valley, except in close proximity to the mountain front (Bexfield and Anderholm, 2002b). These deep nests typically include three piezometers with relatively short screened intervals (on the order of a few meters) located near the water table (shallow), the middle of the production zone (middle), and the bottom of the production zone (deep). Using data from continuous water-level monitors for 1997–1999, Bexfield and Anderholm (2002b) found that water levels in the middle and deep zones tend to respond in a similar manner to seasonal changes in groundwater withdrawals (fig. 2.8), with seasonal water-level variations in individual piezometers ranging from less than 0.3 m to more than 6 m. Water levels at the water table (where the storage coefficient is largest) change the least from seasonal changes in groundwater withdrawals. For the Garfield Park nest in the Rio Grande inner valley, the water table shows seasonal variations apparently associated with seepage of irrigation water through canals and (or) turf areas. In some nests, the time lag between water-level changes in different zones was shorter than in other nests, indicating a better hydraulic connection (Bexfield and Anderholm, 2002b). Vertical gradients between individual zones in the nests generally were smallest east of the inner valley, and they ranged in magnitude from about 0.002 (upward) to 0.080 (downward) overall. In most nests, water levels appeared to be declining at an annual rate of about 0.3 m or less (Bexfield and Anderholm, 2002b).

Aquifer Hydraulic Properties

Horizontal hydraulic conductivities for the Santa Fe Group aquifer system have mostly been estimated from aquifer-test data in long-screened wells (Thorn and others, 1993) and slug-test data in piezometers (Thomas and Thorn, 2000). For the upper Santa Fe Group, estimates generally range from about 1.2 to 46 meters per day (m/d) (Thorn and others, 1993), although smaller conductivities have been estimated for discrete fine-grained zones (Thomas and Thorn, 2000). Estimates at the higher end of the range for the upper Santa Fe Group typically come from wells located east of the Rio Grande that are completed in axial-channel deposits of the ancestral river. For the middle and lower parts of the Santa

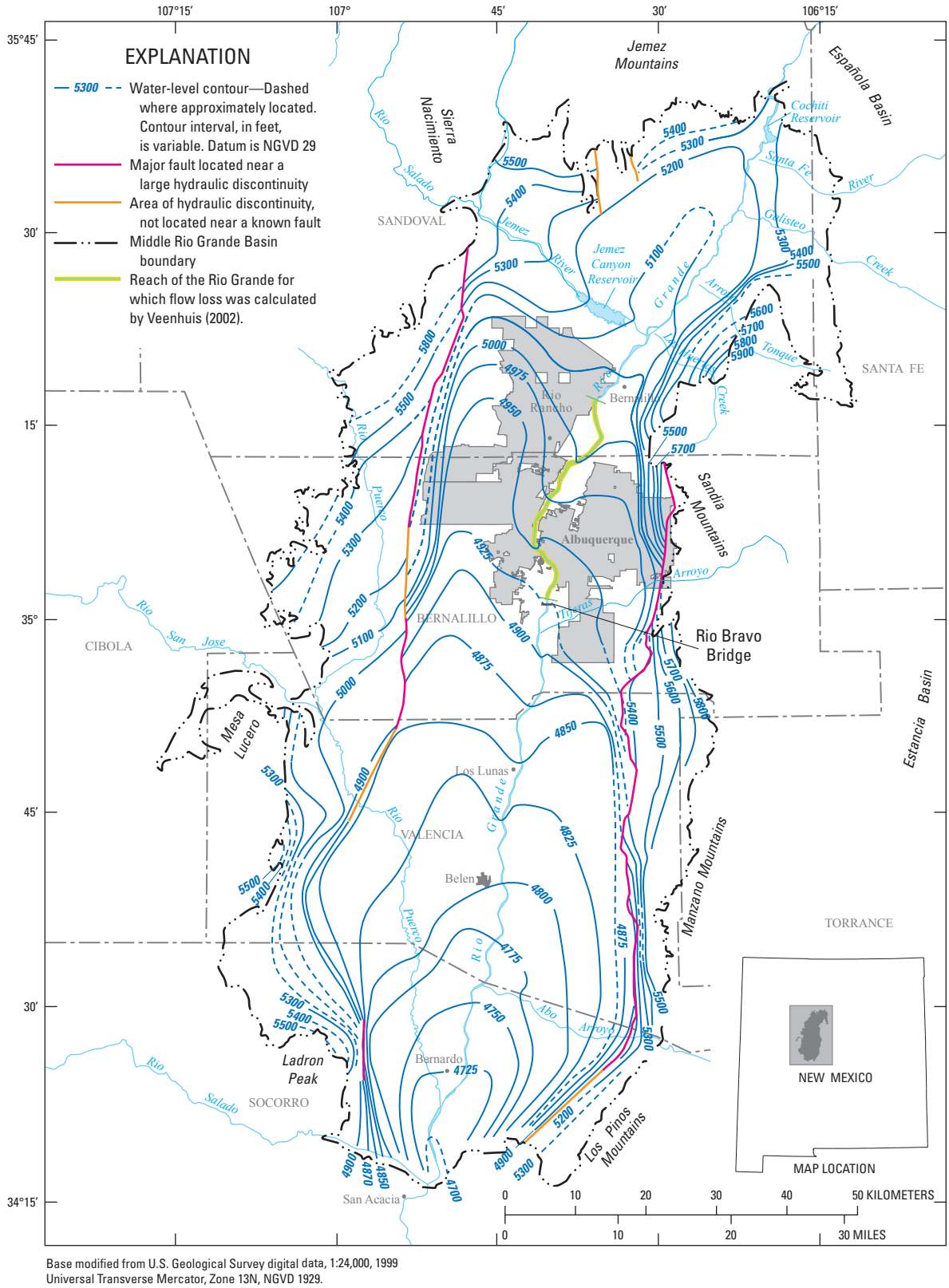

Base modified from U.S. Geological Survey digital data, 1:24,000, 1999
Universal Transverse Mercator, Zone 13N, NGVD 1929.

Figure 2.5. Groundwater levels that represent predevelopment conditions, Middle Rio Grande Basin, New Mexico (modified from Bexfield and Anderholm, 2000). The unit of measurement for contour interval (feet) and the use of the National Geodetic Vertical Datum of 1929 have been retained from the source illustration (Bexfield and Anderholm, 2000).

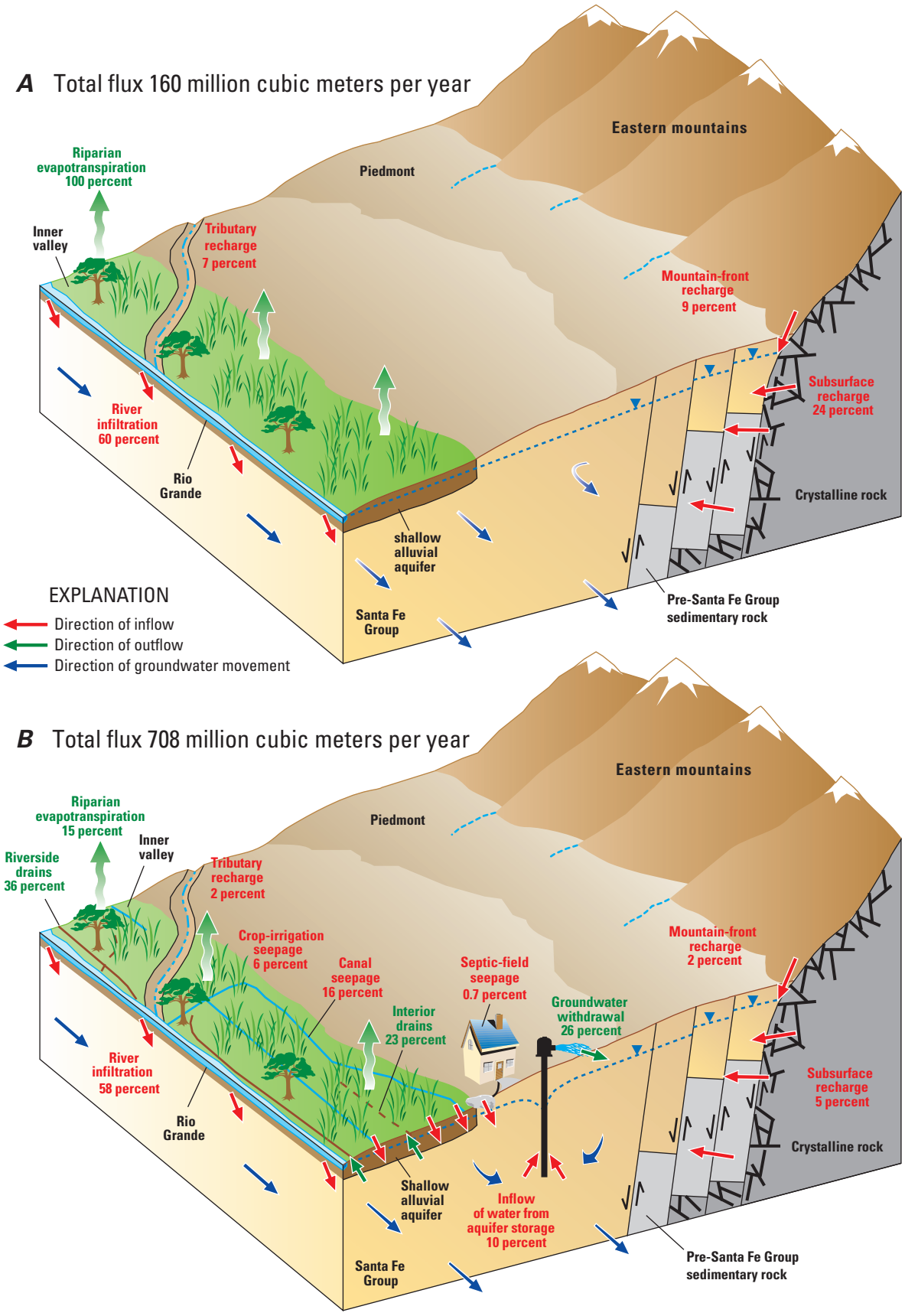

Figure 2.6. Conceptual diagram of regional groundwater flow and budget components near Albuquerque, New Mexico under *A*, predevelopment and *B*, modern conditions. Details of the water budget are provided in table 2.3.

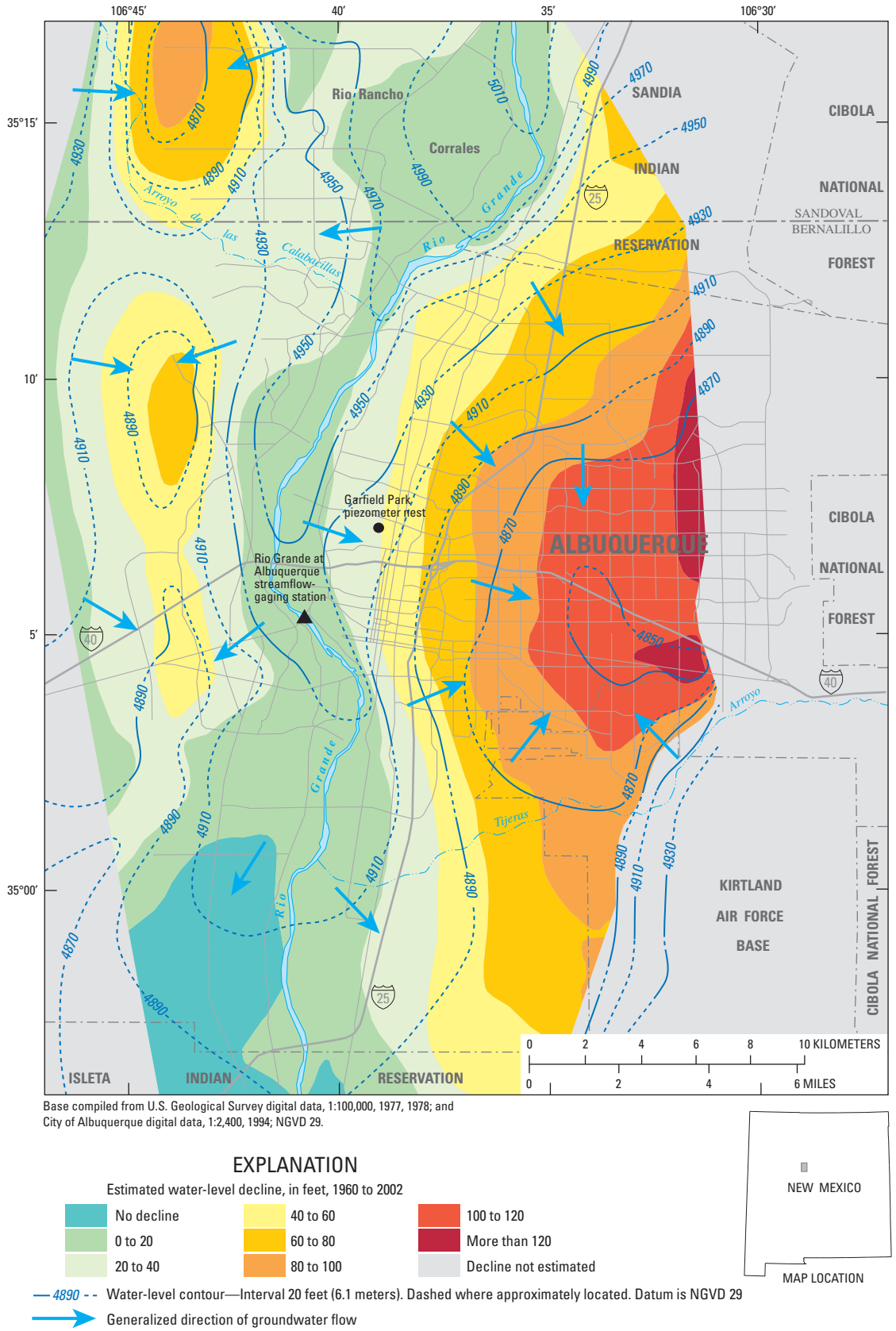

Figure 2.7. Water levels representing 1999–2002 conditions in the production zone in the Albuquerque area, New Mexico, and estimated water-level declines, 1960–2002 (modified from Bexfield and Anderholm, 2002a). The unit of measurement for estimated water-level decline (feet) and the use of the National Geodetic Vertical Datum of 1929 have been retained from the source illustration (Bexfield and Anderholm, 2002a).

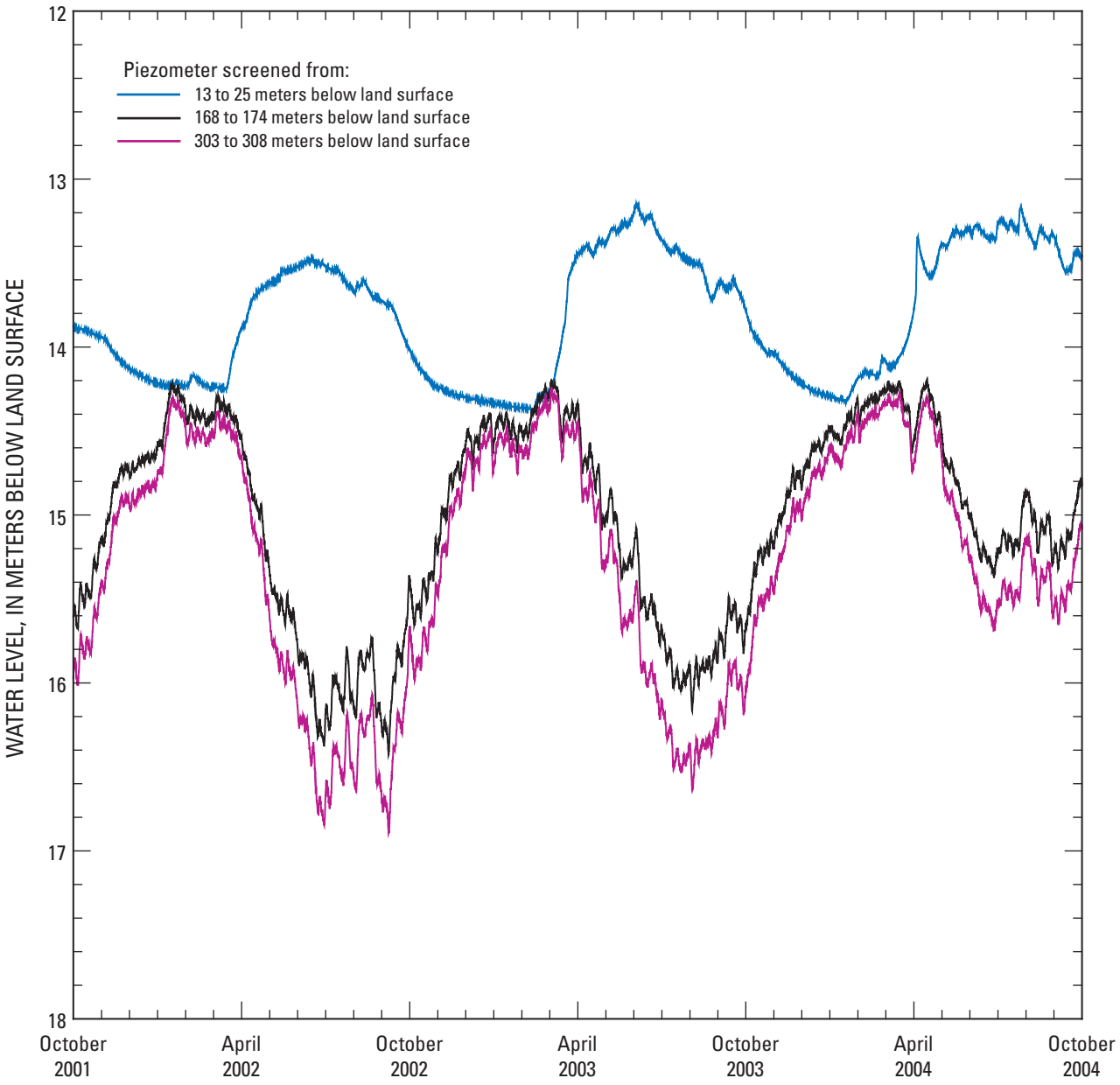

Figure 2.8. Water levels in piezometers in the Garfield Park piezometer nest located in the Rio Grande inner valley, Albuquerque, New Mexico. The location of the piezometer nest is shown on figure 2.7.

Fe Group, estimated hydraulic conductivities tend to be about 3.4 m/d or smaller (McAda and Barroll, 2002). Studies of the post-Santa Fe Group alluvium along the Rio Grande resulted in a wide range of hydraulic-conductivity determinations, from less than 0.1 m/d for silty clays to more than 100 m/d for coarse materials (McAda and Barroll, 2002). For a model simulation of an aquifer test in a public-supply well located in the inner valley in the Albuquerque area, McAda (2001) found a hydraulic conductivity of about 14 m/d to be appropriate for the river alluvium.

No specific yield data were found for the Santa Fe Group aquifer system (Kernodle and others, 1995), but specific yields of about 0.15 to 0.20 have been used in groundwater-flow models in the MRGB, because these values are considered to be in a range typical of basin fill (McAda and Barroll, 2002). Using data from an extensometer in the Albuquerque area, Heywood (1998; 2001) calculated the elastic specific storage of Santa Fe Group sediments to be 6 x 10^{-7} per m, equal to that used in models by Kernodle and others (1995) and McAda and Barroll (2002). Unpublished USGS bulk-density and moisture-content data for saturated sediments collected at various depths from a borehole in the upper Santa Fe Group indicate 0.3 to 0.4 as a reasonable range of porosity.

Table 2.3. Model-computed net annual groundwater budgets for steady-state conditions and year ending October 31, 1999, from the McAda and Barroll (2002) groundwater-flow model, Middle Rio Grande Basin, New Mexico.

[m^3/yr; cubic meters per year; —, not applicable]

Water-budget component	Steady state				Year ending October 31, 1999			
	Specified net flow (10^6 m^3/yr)	Computed net flow (10^6 m^3/yr)	Total net flow (10^6 m^3/yr)	Percentage of net inflow or outflow	Specified net flow (10^6 m^3/yr)	Computed net flow (10^6 m^3/yr)	Net flow rate (10^6 m^3/yr)	Percentage of net inflow or outflow
Model inflow (recharge)								
Mountain-front recharge	15	—	15	9	15	—	15	2
Tributary recharge	11	—	11	7	11	—	11	2
Subsurface inflow	38	—	38	24	38	—	38	5
Canal seepage	0	—	0	0	111	—	111	16
Crop-irrigation seepage	0	—	0	0	43	—	43	6
Rio Grande and Cochiti Lake[1]	—	78	78	49	—	390	390	55
Jemez River and Jemez Canyon Reservoir[1]	—	18	18	11	—	21	21	3
Septic-field seepage	0	—	0	0	5	—	5	1
Aquifer storage[2]	—	0	0	0	—	74	74	10
Total inflow[3]	**—**	**—**	**160**	**100**	**—**	**—**	**708**	**100**
Model outflow (discharge)								
Riverside drains	—	0	0	0	—	256	256	36
Interior drains	—	0	0	0	—	164	164	23
Groundwater withdrawal[4]	0	—	0	0	185	—	185	26
Riparian evapotranspiration	—	159	159	100	—	104	104	15
Total outflow[3]	**—**	**—**	**159**	**100**	**—**	**—**	**709**	**100**

[1] Cochiti Lake and Jemez Canyon Reservoir were not present during steady-state conditions.

[2] Net inflow of water from aquifer storage reflects loss of water from aquifer storage to the groundwater system (that is, a decline in aquifer storage).

[3] Due to flow rate rounding, budget discrepancies in the table differ from the corresponding model output. Model-computed volumetric budget discrepancies are 0.02 percent for the steady-state stress period and 0.07 percent for the stress period ending October 31, 1999.

[4] Includes withdrawals for domestic, municipal, commercial, and industrial uses.

Patterns in faulting and sedimentation in the MRGB led McAda and Barroll (2002) to use horizontal-anisotropy ratios (defined as ratios of hydraulic conductivity along model columns to hydraulic conductivity along model rows) of 1:1, 2:1, and 5:1 in selected areas of their model of the basin. McAda and Barroll (2002) state that vertical anisotropy ratios (defined as ratios of horizontal hydraulic conductivity to vertical hydraulic conductivity) used in models of the basin have ranged between about 80:1 and 1,000:1; as a result of calibration, the ratio used throughout their model was 150:1. Using detailed profiles of temperature with depth, Reiter (2001) estimated a vertical (downward) specific discharge of about 0.12 meters per year (m/yr) in the 157-m deep Rio Bravo Park well located adjacent to the Rio Grande near the southern part of Albuquerque. Water-level data for two depths at the Rio Bravo Park location (about 6.7 and 157 m) (DeWees, 2003) indicate a downward vertical gradient of about 0.011. By use of these data and the estimated horizontal hydraulic conductivity of 2.4 m/d at corresponding depths in this area (McAda and Barroll, 2002), a vertical hydraulic conductivity of about 0.03 m/d and vertical anisotropy ratio of 80:1 was estimated for this site.

Water Budget

Conceptual water budgets have been developed for the MRGB in association with previous groundwater-flow models. Because the McAda and Barroll (2002) model incorporated the latest estimates of various budget components resulting from the 1995–2001 intensive multidisciplinary group of studies of hydrogeology in the basin (Cole, 2001b), this model budget (table 2.3) provides the basis for most of the discussion in this section.

As a result of high evaporation rates and generally large depths to groundwater, areal recharge to the Santa Fe Group aquifer system of the MRGB from precipitation is believed to be minor (Anderholm, 1988). Instead, groundwater recharge occurs primarily along surface-water features and basin margins. Using the chloride-balance method, Anderholm (2001) calculated mountain-front recharge along the entire eastern margin of the basin to total about 14 x 10^6 cubic meters per year (m^3/yr), although other methods have indicated this value might be as high as about 47 x 10^6 m^3/yr (Anderholm, 2001). The McAda and Barroll (2002) model uses a value totaling 15 x 10^6 m^3/yr along all basin margins (table 2.3), including areas along the Jemez Mountains on the north and Ladron Peak on the southwest, where mountain-front recharge has not been quantified. Subsurface recharge occurring as groundwater inflow from adjacent basins has been estimated through groundwater-flow modeling, using supporting evidence from studies of hydrogeology (Smith and Khule, 1998; Grant, 1999) and groundwater ages (Sanford and others, 2004a, b). McAda and Barroll (2002) use a total of 38 x 10^6 m^3/yr of subsurface recharge for the basin.

Within the MRGB, most recharge to the aquifer system occurs as seepage of surface water along the Rio Grande and the Jemez River, as well as (in modern times) along features of their associated irrigation systems (table 2.3). By comparison, tributary recharge is small along the Rio Puerco in the west, the Rio Salado in the south, and streams and arroyos entering the basin from the east (which generally do not contain persistent flow more than a few hundred meters from the mountain front). Based partly on streamflow losses estimated by Thomas and others (2000) for the Santa Fe River in the northeast, tributary recharge in the McAda and Barroll (2002) model totals 11 x 10^6 m^3/yr. Even prior to large-scale declines in groundwater levels associated with withdrawals for public supply, the Rio Grande, which is in hydraulic connection with the Santa Fe Group aquifer system along its entire length through the basin, is thought to have lost water to the aquifer system. The McAda and Barroll (2002) model simulates the net magnitude of these losses under steady-state conditions to be 78 x 10^6 m^3/yr. Along the Jemez River, which is in hydraulic connection with the aquifer system through most of its length within the basin, these net losses are simulated to be 18 x 10^6 m^3/yr under steady-state conditions and only slightly higher (21 x 10^6 m^3/yr) in modern times, including after commencement of Jemez Reservoir operation in 1979.

Seepage of water to the aquifer system in the Rio Grande inner valley has increased since urbanization and the development of large-scale irrigation systems in the MRGB, as simulated by the water budget of McAda and Barroll (2002) for the year starting on November 1, 1998, and ending on October 31, 1999 (table 2.3). The model simulates seepage from irrigation canals, including some along the Jemez River, as contributing 111 x 10^6 m^3/yr of water to the aquifer system. By applying an estimated average recharge rate of 0.15 m/yr to all agricultural cropland along the Rio Grande and Jemez River, recharge through crop-irrigation seepage is estimated to total 43 x 10^6 m^3/yr. Because of declines in groundwater levels and commencement of Cochiti Lake operations in 1973, seepage along the Rio Grande is simulated to be 390 x 10^6 m^3/yr, or five times the seepage simulated under steady-state conditions. Another source of recharge resulting from urbanization is septic-field seepage, which occurs both within and outside the Rio Grande inner valley and is estimated by McAda and Barroll (2002) to total about 5 x 10^6 m^3/yr for the year ending on October 31, 1999, based on census data and an estimated seepage rate of 0.23 cubic meters per day (m^3/d) per person. Leakage of water from sewer and (or) water-distribution pipes is a potential source of recharge from urbanization, but it was not included in the McAda and Barroll (2002) model.

Under steady-state conditions, groundwater discharged from the aquifer system primarily through evapotranspiration from riparian vegetation and wetlands in the Rio Grande inner valley (Kernodle and others, 1995). Groundwater withdrawals for public supply and construction of an extensive groundwater drainage system in the inner valley have lowered the water table and resulted in reduced riparian evapotranspiration to 104 x 10^6 m^3/yr for the year ending on October 31, 1999, in comparison to 159 x 10^6 m^3/yr under steady-state conditions, as simulated by McAda and Barroll (2002). The largest component of outflow from the aquifer system currently is discharge to the groundwater drain system, which the McAda and Barroll (2002) model simulated to total 420 x 10^6 m^3/yr (table 2.3), with slightly more than 60 percent of this discharge being to the riverside drains, as opposed to interior drains located farther from the Rio Grande. Much of the groundwater discharging to the drain system is water that infiltrated from the Rio Grande or seeped from irrigation canals and irrigated fields (McAda and Barroll, 2002). Groundwater likely also discharges directly to the Rio Grande in some reaches, particularly in the northern part of the basin (Trainer and others, 2000; McAda and Barroll, 2002), and it leaves the MRGB in relatively small quantities as underflow at the southern end (Sanford and others, 2004b). Groundwater withdrawals currently are a major component of the water budget (26 percent of total discharges), discharging an estimated 185 x 10^6 m^3/yr from the aquifer system during the year ending on October 31, 1999 (table 2.3), and resulting in the simulated removal of 74 x 10^6 m^3/yr from aquifer storage during the same year.

Groundwater Age

The age of most groundwater in the Santa Fe Group aquifer system of the MRGB, as estimated using carbon-14 (^{14}C), is on the order of thousands of years (fig. 2.9) (Plummer and others, 2004a, b, c). Groundwater less than 2,000 years in age typically is found only near known areas of recharge—primarily basin margins and surface-water features. Chlorofluorocarbons and tritium—indicators of the presence of young (post-1950s) recharge—were most common at relatively shallow depths within the Rio Grande inner valley (Plummer and others, 2004a). However, chlorofluorocarbons and tritium

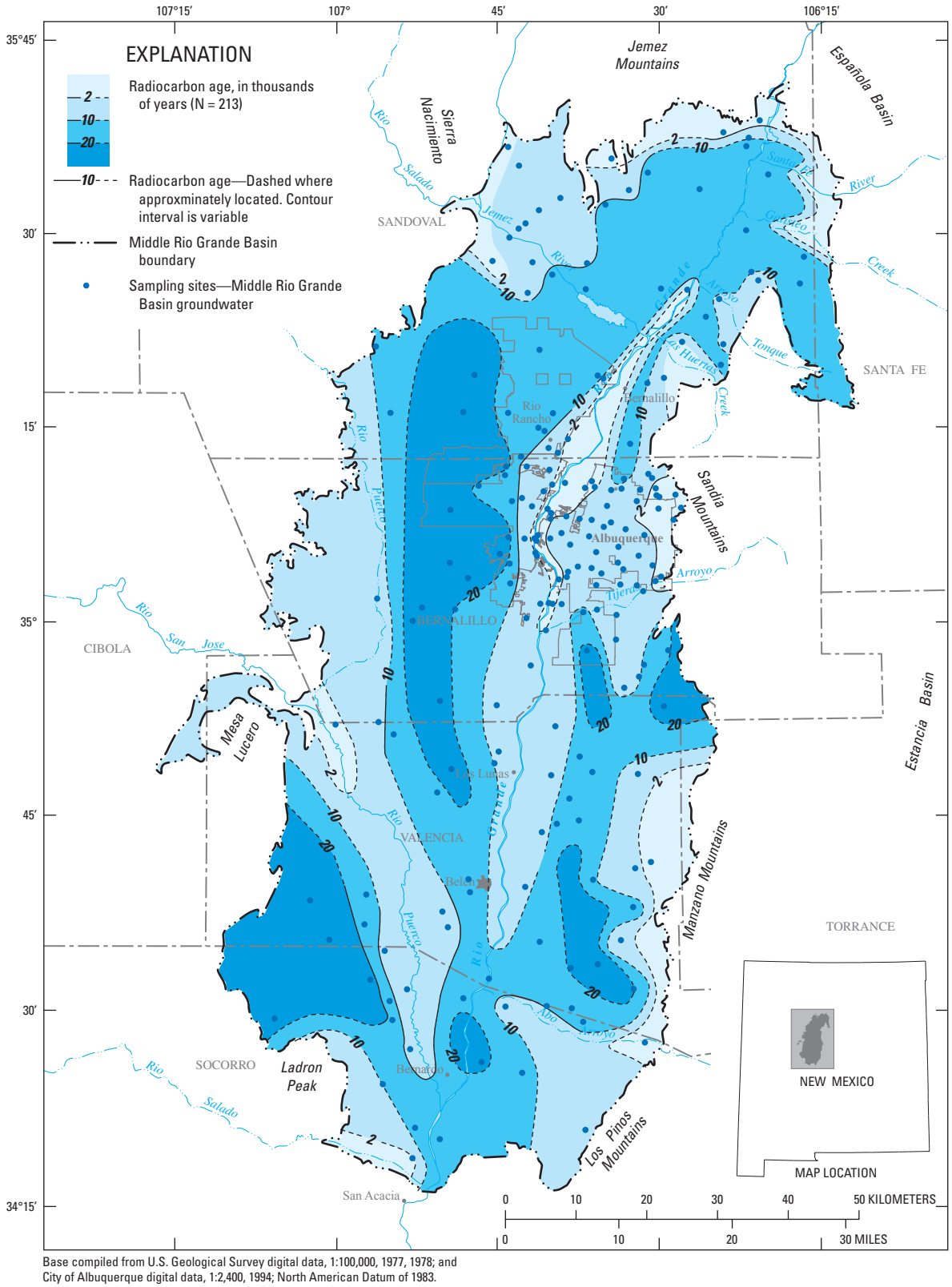

Base compiled from U.S. Geological Survey digital data, 1:100,000, 1977, 1978; and City of Albuquerque digital data, 1:2,400, 1994; North American Datum of 1983.

Figure 2.9. Estimated ages of groundwater in the Santa Fe Group aquifer system, Middle Rio Grande Basin, New Mexico (modified from Plummer and others, 2004a).

were detected in some samples from the water table beneath upland areas, indicating the potential presence of recharge sources in these areas that have not been well characterized. Spatial patterns in groundwater ages indicate that the residence time of much of the groundwater in the basin exceeds 10,000 years (fig. 2.9), thereby illustrating that water flux through the basin is relatively small given the basin's size. Simulation of paleorecharge conditions in the basin using a transient groundwater-flow model calibrated to ^{14}C activities (Sanford and others, 2004a, b) indicates that flux might have been as much as 10 times larger during the last glacial maximum, which occurred approximately 21,500 years ago.

Groundwater Quality

Because sediments of the Santa Fe Group aquifer system are relatively unreactive, groundwater quality in the MRGB regional study area is determined primarily by the source of recharge rather than by processes occurring within the aquifer (Plummer and others, 2004a). Studies by Anderholm (1988), Logan (1990), Bexfield and Anderholm (2002b), and Plummer and others (2004a, b) have illustrated spatial patterns in water chemistry across the Albuquerque area and (or) the MRGB. Based primarily on hydrochemical patterns in data from hundreds of wells of various types (public supply, monitoring, domestic, and other), Plummer and others (2004a, b) delineated individual hydrochemical zones throughout the MRGB (fig. 2.10 and table 2.4), each with relatively homogeneous groundwater chemistry that is distinct from other zones. These zones represent individual sources of recharge to the basin and are used to facilitate this discussion of water chemistry within the MRGB regional study area. To further enhance this discussion, groundwater chemistry data collected for the TANC study (as described in Section 1 of this chapter, Chapter B, and Section 1 of Chapter A) were incorporated, as were data obtained from various sources for additional wells within the regional study area that were sampled between 2000 and 2004.

Groundwater along the Jemez and Sandia mountain fronts has some of the smallest dissolved-solids concentrations found in the MRGB. The Northern Mountain Front and Eastern Mountain Front zones of Plummer and others (2004a, b), which delineate areas where relatively high-elevation mountain-front recharge processes dominate, include most of the wells located along these mountain fronts and groundwater in those zones has specific-conductance values that commonly are less than 400 microsiemens per centimeter at 25 degrees Celsius (µS/cm) (table 2.4). Groundwater in these zones typically is of the calcium-bicarbonate type, although sodium is the dominant cation in places. The groundwater generally has pH between 7 and 8 and is well oxidized as indicated by dissolved-oxygen concentrations (fig. 2.11). In the Northwestern zone, which delineates groundwater believed to have recharged at relatively low elevations along the Jemez mountain front (Plummer and others, 2004a), dissolved-solids concentrations, sodium concentrations, and pH values typically are slightly higher than those found in the Northern Mountain Front zone. Similar to the Northern and Eastern Mountain Front zones, groundwater of the Northwestern zone also is generally well oxidized, with the exception of a relatively small area in the far northwestern corner (fig. 2.11*A*). In fact, in most areas of the MRGB, groundwater continues to be well oxidized even far from sources of recharge and at depths of nearly 100 m, probably because of a general paucity of organic carbon in aquifer materials (Plummer and others, 2004a).

Groundwater in the Central zone (fig. 2.10), representing recharge from the Rio Grande and its associated irrigation system, has relatively small dissolved-solids concentrations, indicated by specific-conductance of generally less than 600 µS/cm (table 2.4). Bicarbonate is the dominant anion in groundwater of this zone; the cation content is dominated by calcium and (or) sodium. The pH generally is between 7 and 8, but exceeds 8 in places—particularly at depth—likely in association with cation exchange on clays that allows increased dissolution of calcium carbonate where present (Plummer and others, 2004a). Unlike the oxidized redox conditions observed for groundwater in most of the basin, conditions at shallow depths within the Central zone tend to be manganese or iron reducing (fig. 2.11), probably reflecting greater organic-carbon content for sediments within the Rio Grande inner valley. At some sites in the Central zone, elevated dissolved-solids concentrations, indicated by specific-conductance values greater than 800 µS/cm, at shallow depths might be indicative of recent recharge of irrigation water, septic-tank effluent, or other sources associated with anthropogenic activity.

The West-Central zone extends southward from the Jemez Mountain area through much of the western half of the MRGB (fig. 2.10) and extends at depth beneath adjacent hydrochemical zones to the east. The West-Central zone represents groundwater inflow that entered at depth along the northern margin the basin. Dissolved-solids concentrations are moderate throughout much of this zone, where specific-conductance values generally are less than 600 µS/cm (table 2.4), despite estimates of groundwater age on the order of tens of thousands of years (fig. 2.9). Most groundwater in the zone is of the sodium-bicarbonate type, although sulfate is the dominant anion in places. The groundwater is generally well oxidized (fig. 2.11); pH exceeds 8 over broad areas, and approach or exceed 9 in places. Groundwater of the West-Central zone commonly has arsenic concentrations greater than the U.S. Environmental Protection Agency drinking-water standard of 10 micrograms per liter (U.S. Environmental Protection Agency, 2006). The elevated arsenic concentrations in this zone generally are associated with silicic volcanism in the Jemez Mountains and with desorption from metal oxides, especially in areas where pH exceeds about 8.5 (Bexfield and Plummer, 2003; Plummer and others, 2004a). Elevated arsenic concentrations in groundwater in other areas of the MRGB typically are associated with deep mineralized water that appears to upwell along major structural features, also resulting in elevated concentrations of chloride and other elements (Bexfield and Plummer, 2003; Plummer and others, 2004a).

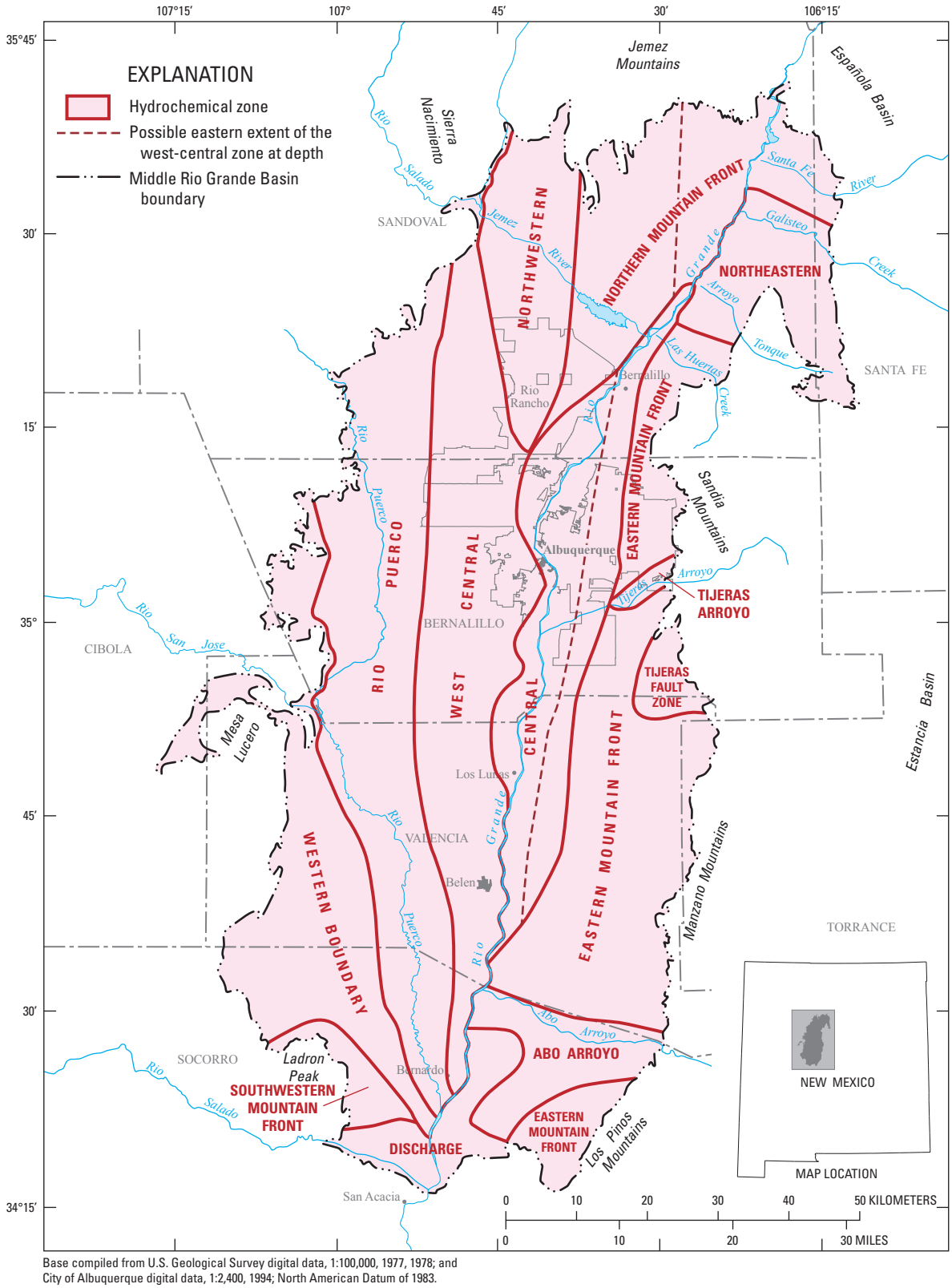

Base compiled from U.S. Geological Survey digital data, 1:100,000, 1977, 1978; and City of Albuquerque digital data, 1:2,400, 1994; North American Datum of 1983.

Figure 2.10. Hydrochemical zones in the Middle Rio Grande Basin, New Mexico (modified from Plummer and others, 2004a).

Table 2.4. Median values of selected water-quality parameters by hydrochemical zone, Middle Rio Grande Basin, New Mexico.

[—, no data; µS/cm, microsiemens per centimeter at 25 degrees Celsius; deg. C, degrees Celsius; mg/L, milligrams per liter; µg/L, micrograms per liter; pmC, percent modern carbon]

Hydrochemical zone	Specific conductance (µS/cm)	Field pH	Water temperature (deg. C)	Dissolved oxygen (mg/L)	Calcium (mg/L)	Magnesium (mg/L)	Sodium (mg/L)	Potassium (mg/L)
Northern Mountain Front	340	7.49	18.9	5.12	38.5	6.1	20.0	4.9
Northwestern	400	7.84	20.6	6.68	33.9	4.2	49.9	5.7
West Central	535	8.22	23.8	3.00	12.0	2.5	103	4.2
Western Boundary	4,572	7.70	22.0	4.09	135	56.4	589	15.2
Rio Puerco	2,731	7.50	20.0	3.73	135	42.7	290	10.4
Southwestern Mountain Front	462	8.11	19.1	4.43	52.6	13.5	27.8	2.5
Abo Arroyo	1,055	7.45	20.7	6.23	92.5	34.4	49.2	3.1
Eastern Mountain Front	382	7.67	22.0	5.16	45.0	5.1	29.2	2.2
Tijeras Fault Zone	1,406	7.42	18.5	4.66	171	36.0	95.0	6.1
Tijeras Arroyo	677	7.39	16.1	6.97	89.4	24.5	29.3	3.8
Northeastern	1,221	7.50	19.4	6.44	141	29.5	81.8	4.8
Central	436	7.74	18.1	0.12	42.9	8.0	31.0	6.4
Discharge	1,771	7.70	20.6	0.08	93.0	31.0	190	10.5

Hydrochemical zone	Barium (mg/L)	Boron (mg/L)	Chromium (µg/L)	Copper (µg/L)	Iron (mg/L)	Lead (µg/L)	Lithium (mg/L)	Manganese (mg/L)
Northern Mountain Front	0.062	0.043	1.2	0.8	0.060	0.20	0.058	0.005
Northwestern	0.056	0.118	2.0	0.4	0.030	0.10	0.068	0.002
West Central	0.032	0.239	5.7	0.5	0.028	0.11	0.045	0.002
Western Boundary	0.014	0.900	10.6	3.0	0.213	0.12	0.251	0.041
Rio Puerco	0.014	0.291	3.0	3.4	0.130	0.10	0.253	0.015
Southwestern Mountain Front	0.045	0.094	1.9	9.3	0.030	0.41	0.041	0.007
Abo Arroyo	0.017	0.130	4.4	2.0	0.105	0.10	0.031	0.004
Eastern Mountain Front	0.084	0.050	1.0	1.7	0.031	0.27	0.020	0.003
Tijeras Fault Zone	0.046	0.347	1.7	4.3	0.111	0.34	0.227	0.023
Tijeras Arroyo	0.057	0.060	1.1	1.0	0.050	0.10	0.017	0.005
Northeastern	0.018	0.215	3.2	3.7	0.170	0.11	0.040	0.004
Central	0.083	0.085	1.0	0.8	0.041	0.10	0.040	0.015
Discharge	0.030	0.630	10.2	1.7	0.080	0.15	0.326	0.010

Table 2.4. Median values of selected water-quality parameters by hydrochemical zone, Middle Rio Grande Basin, New Mexico.—Continued

[—, no data; µS/cm, microsiemens per centimeter at 25 degrees Celsius; deg. C, degrees Celsius; mg/L, milligrams per liter; µg/L, micrograms per liter; pmC, percent modern carbon]

Hydrochemical zone	Alkalinity (mg/L as sodium bicarbonate)	Sulfate (mg/L)	Chloride (mg/L)	Fluoride (mg/L)	Bromide (mg/L)	Silica (mg/L)	Nitrate (mg/L as N)	Aluminum (µg/L)	Arsenic (µg/L)
Northern Mountain Front	137	19.5	5.6	0.35	0.08	53.3	0.56	—	3.2
Northwestern	160	44.8	8.5	0.61	0.07	30.1	2.44	—	9.8
West Central	174	92.0	13.4	0.99	0.11	34.5	1.24	6.76	23.2
Western Boundary	300	793	820	1.64	0.38	22.5	0.86	5.00	1.8
Rio Puerco	190	1,080	185.8	0.63	0.64	21.8	0.88	5.00	1.0
Southwestern Mountain Front	202	53.0	15.0	1.02	0.21	17.6	1.12	3.31	0.2
Abo Arroyo	148	346	25.9	0.90	0.17	24.0	1.40	4.14	5.2
Eastern Mountain Front	157	31.0	10.5	0.60	0.17	28.4	0.31	5.56	2.0
Tijeras Fault Zone	599	100	139	1.27	0.69	18.9	1.09	5.22	2.2
Tijeras Arroyo	240	115	56.6	0.60	0.35	19.5	3.79	4.09	1.0
Northeastern	208	390	22.7	0.51	0.19	38.5	0.64	4.34	2.7
Central	158	66.0	16.6	0.44	0.09	47.0	0.08	6.00	5.4
Discharge	157	290	280	1.40	0.47	39.0	0.42	4.50	9.9

Hydrochemical zone	Molybdenum (µg/L)	Strontium (mg/L)	Uranium (µg/L	Vanadium (µg/L)	Zinc (µg/L)	Delta deuterium (δD) (per mil)	Delta oxygen-18 ($\delta^{18}O$) (per mil)	Delta carbon-13 ($\delta^{13}C$) (per mil)	Carbon-14 (^{14}C) (pmC)
Northern Mountain Front	1.7	0.31	1.0	6.4	258.	-77.7	-10.9	-8.50	33.4
Northwestern	3.4	0.57	2.7	15.6	9.0	-64.7	- 8.73	-6.93	29.6
West Central	8.2	0.20	3.7	27.9	5.0	-96.7	-12.7	-7.18	8.80
Western Boundary	9.9	2.09	4.4	5.7	118	-64.4	- 9.12	-4.70	6.19
Rio Puerco	7.0	3.92	6.0	3.4	117	-61.6	- 8.51	-7.65	36.4
Southwestern Mountain Front	3.0	0.86	0.9	1.0	252	-53.5	- 7.74	-5.76	40.0
Abo Arroyo	3.4	1.48	5.4	9.5	8.1	-65.2	- 9.05	-6.72	24.1
Eastern Mountain Front	2.0	0.32	3.6	7.5	6.7	-81.0	-11.4	-8.70	47.2
Tijeras Fault Zone	3.7	1.11	7.3	6.3	61.5	-74.2	-10.3	-0.98	9.70
Tijeras Arroyo	1.9	0.47	3.7	3.0	4.5	-75.7	-10.3	-6.80	72.8
Northeastern	6.7	1.72	8.5	3.8	99.5	-68.6	- 9.72	-6.40	28.5
Central	5.0	0.40	3.6	9.3	5.0	-95.4	-12.8	-8.87	61.0
Discharge	10.3	3.02	3.9	7.1	16.2	-90.8	-12.1	-7.00	10.8

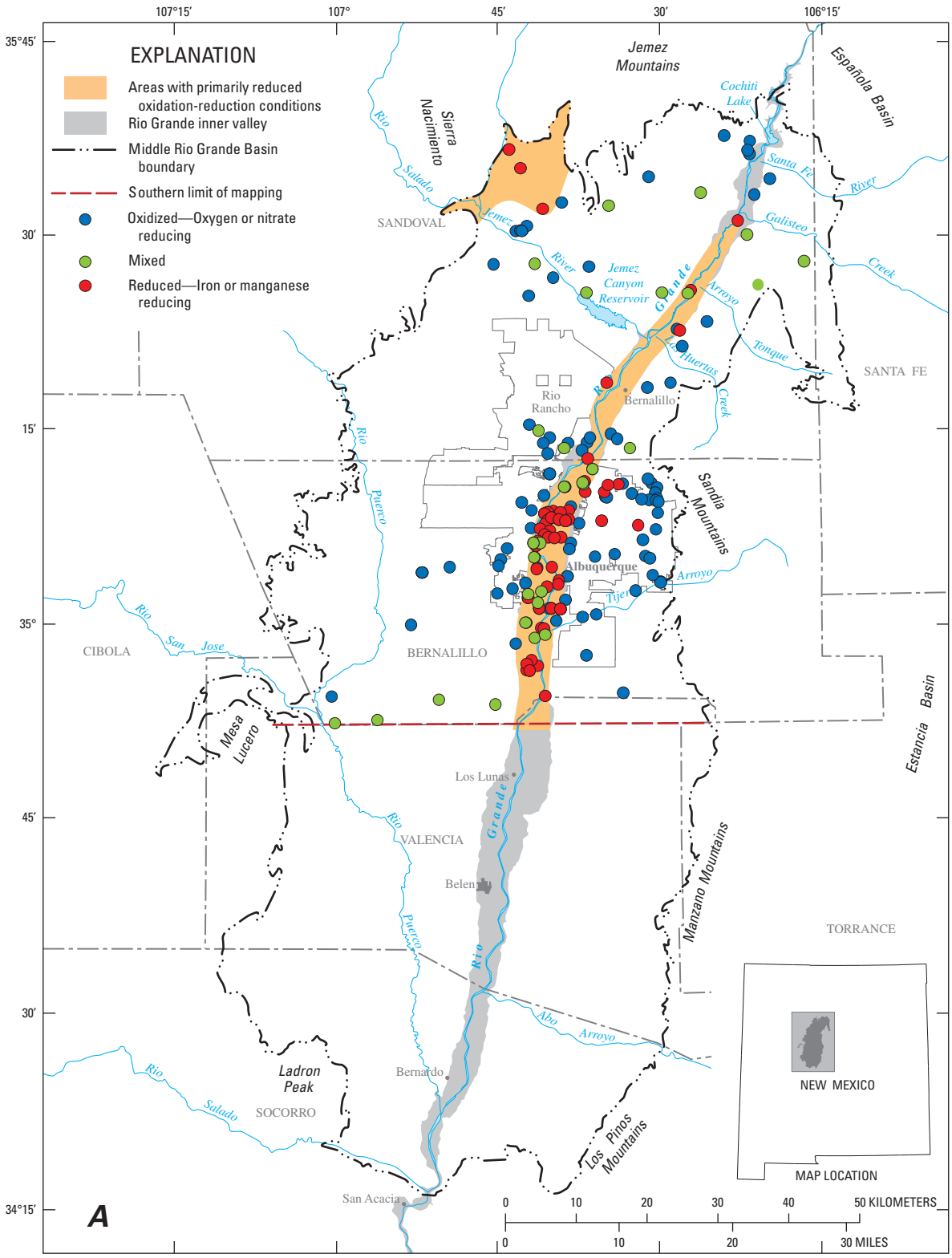

Base modified from U.S. Geological Survey digital data, 1:24,000, 1999
Universal Transverse Mercator Zone 13N, North American Datum of 1983.

Figure 2.11*A*. Oxidation-reduction conditions for the upper 90 meters of the aquifer, Middle Rio Grande Basin regional study area, New Mexico.

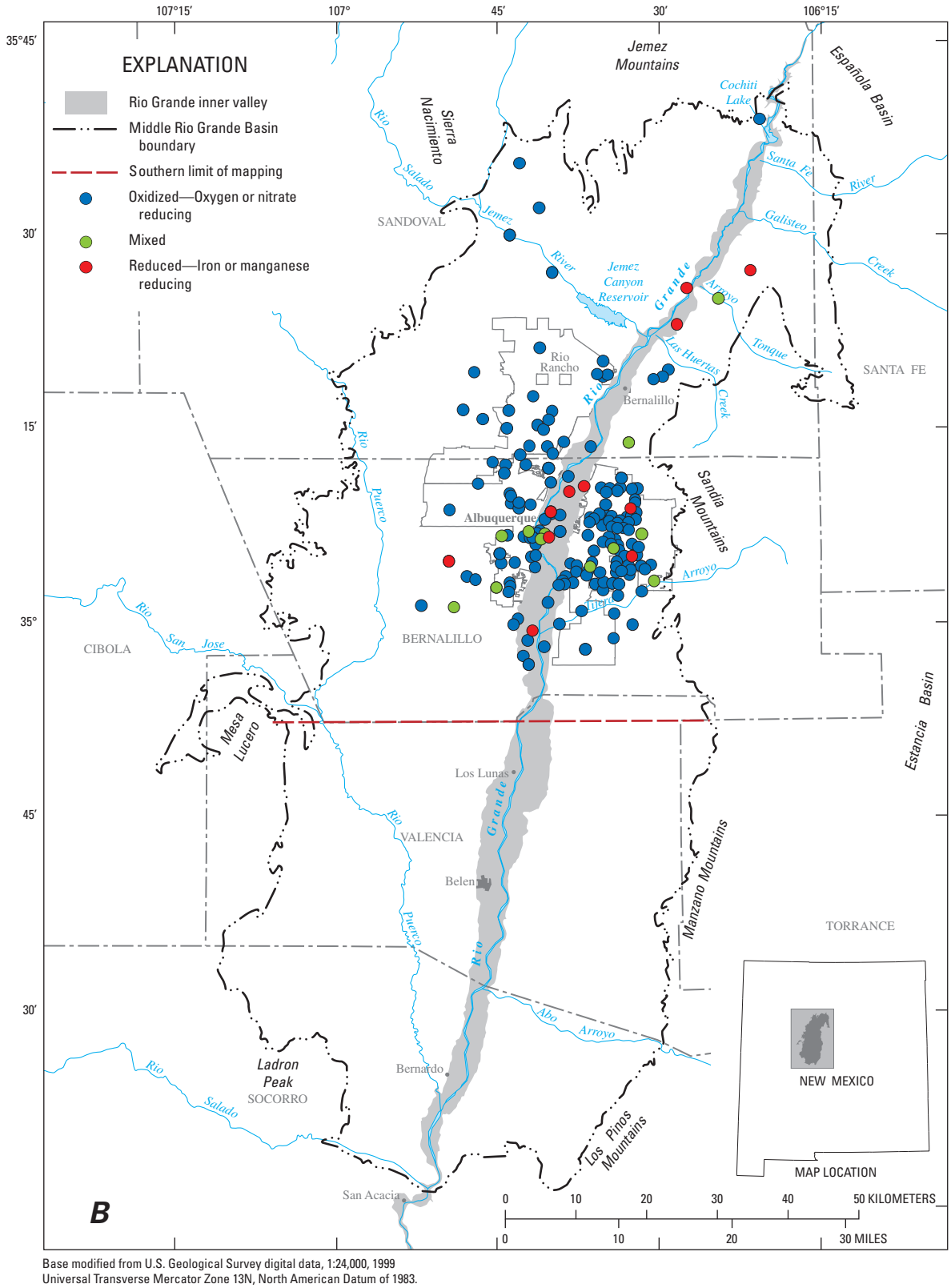

Base modified from U.S. Geological Survey digital data, 1:24,000, 1999
Universal Transverse Mercator Zone 13N, North American Datum of 1983.

Figure 2.11*B*. Oxidation-reduction conditions for the deeper parts of the aquifer, Middle Rio Grande Basin regional study area, New Mexico.

The MRGB regional study area also includes part or all of five other hydrochemical zones defined by Plummer and others (2004a, b): the Western Boundary, Rio Puerco, Northeastern, Tijeras Fault Zone, and Tijeras Arroyo zones. These zones are dominated by groundwater inflow along basin margins or major fault systems and (or) by arroyo recharge. With the exception of the Tijeras Arroyo zone, groundwater in these zones has relatively large dissolved-solids concentrations, indicated by specific-conductance values generally greater than 1,000 µS/cm (table 2.4), and is not typically used for public water supply. Groundwater in the Tijeras Arroyo zone is partly characterized by elevated concentrations of nitrate, calcium, magnesium, sulfate, and chloride relative to the Eastern Mountain Front zone. Similar to the Eastern Mountain Front zone, groundwater in the Tijeras Arroyo zone is well oxidized and has pH between 7 and 8 (fig. 2.11).

Groundwater-Flow Simulations

A MODFLOW (Harbaugh, 2005) model was constructed and calibrated to simulate groundwater flow in a 6,077-km^2 area of the MRGB (fig. 2.12*A*). This model (subsequently referred to as the "revised model") simulates conditions in a different area than the previously defined MRGB regional study area, because it is based on the groundwater-flow model documented by McAda and Barroll (2002), which simulated conditions through March 2000. Relative to the McAda and Barroll (2002) model, the revised model incorporates 8.8 additional years of groundwater withdrawal data (through December, 2008), finer horizontal spatial discretization, leakage from the water-distribution and sewer systems in the greater Albuquerque metropolitan area, and simulation of reported withdrawals with the Multi-Node Well (MNW1) Package (Halford and Hanson, 2002). Model-input files were constructed for compatibility with MODFLOW-2005 (Harbaugh, 2005), and some parameter values were adjusted by model calibration with PEST (Doherty, 2005). Changes to most conceptual aspects of the McAda and Barroll (2002) model, such as the hydrogeologic framework and boundary-condition specifications, were minimized.

Conditions prior to 1900 are represented by a steady-state stress period, which provides the initial conditions for subsequent transient stress periods simulating 109 years, from 1900 through December 31, 2008. Time discretization is similar to that used in the McAda and Barroll (2002) model. Stress periods simulating time from 1900 to 1974 and 1975 through 1989, are 5 and 1 years long, respectively. Seasonal stress periods used after January 1, 1990, simulate both irrigation seasons that extend from March 16 through October 31 and winter seasons that extend from November 1 through March 15. Significant changes to surface-water features, such as the construction of riverside drains on either side of the Rio Grande, Cochiti Lake, and Jemez Canyon Reservoir, are simulated at representative stress periods by changes to boundary-condition specifications with the River and Drain Packages of MODFLOW (Harbaugh, 2005). The riverside and interior drain cell locations changed during the course of the transient simulation.

Modeled Area and Spatial Discretization

The model domain, which includes the metropolitan area of Albuquerque, is somewhat smaller than the MRGB and is bounded on the eastern and western sides by normal faults that are thought to form distinct hydrologic boundaries (Kernodle and others, 1995) (fig. 2.3). The northern and southern boundaries correspond to the MRGB boundaries located at Cochiti Lake and San Acacia (fig. 2.12*A*), respectively. The model domain incorporates the Cenozoic Rio Grande Rift deposits, which range in thickness from 4 m on the basin margins to approximately 4,600 m and 5,300 m in the deepest parts of the Belen and Calabacillas subbasins, respectively, and includes the Santa Fe Group aquifer system.

The revised model grid is comprised of 9 layers, each containing 312 rows and 160 columns of finite-difference cells that have uniform horizontal dimensions of 0.5 by 0.5 km, which is finer than the 1.0- by 1.0-km cell dimensions of the McAda and Barroll (2002) model. There are a maximum of 24,305 active cells per layer, with the most active cells located in layer 1 and a progressive decrease to 18,944 active cells in layer 9. The simulated direction of anisotropy is aligned with the model grid, corresponding to the general north-south strike of major faults in the basin (Mark Hudson and Scott Minor, U.S. Geological Survey, written commun., 1999). The top four layers are convertible from confined to unconfined conditions.

Although nine model layers (fig. 2.13) represent the Santa Fe Group aquifer system within the MRGB, they do not represent particular lithologic units, with the exception of layers 1 and 2, which represent post-Santa-Fe-Group alluvium within the Rio Grande inner valley. The bases of model layers 1 through 7 tilt upward from south to north, such that they each maintain a consistent depth beneath the Rio Grande. The thickness of model layers 1 through 5 increases with distance perpendicular from the Rio Grande, as do the model-layer-bottom elevations of layers 1 through 4. The thickness of the unsaturated zone in model layer 1 increases away from the Rio Grande to a maximum of 585 m. For simulated steady-state hydraulic heads, the saturated thickness in layer 1 is up to 14 m thick. The steady-state saturated thickness of layers 2, 3, 4, and 5 ranges between 15–23, 30–47, 65–103, and 118–184 m, respectively. The base of layer 5 is at an elevation 244 m below the Rio Grande, and it maintains that elevation perpendicular to the trend of the river except where basement rock is at a higher elevation near the basin perimeter. Layers 6 and 7 have constant thicknesses of 183 and 305 m, respectively. The top of layer 8 is at an elevation 732 m below the Rio Grande, except near the basin perimeter, where the base rises, and ranges in thickness from 18 to 1,175 m. The thickness of layer 9 ranges from 153 to 2,350 m. Cells in layers 1–9 are active where the base of the cell is higher than the base of the Santa Fe Group basin fill.

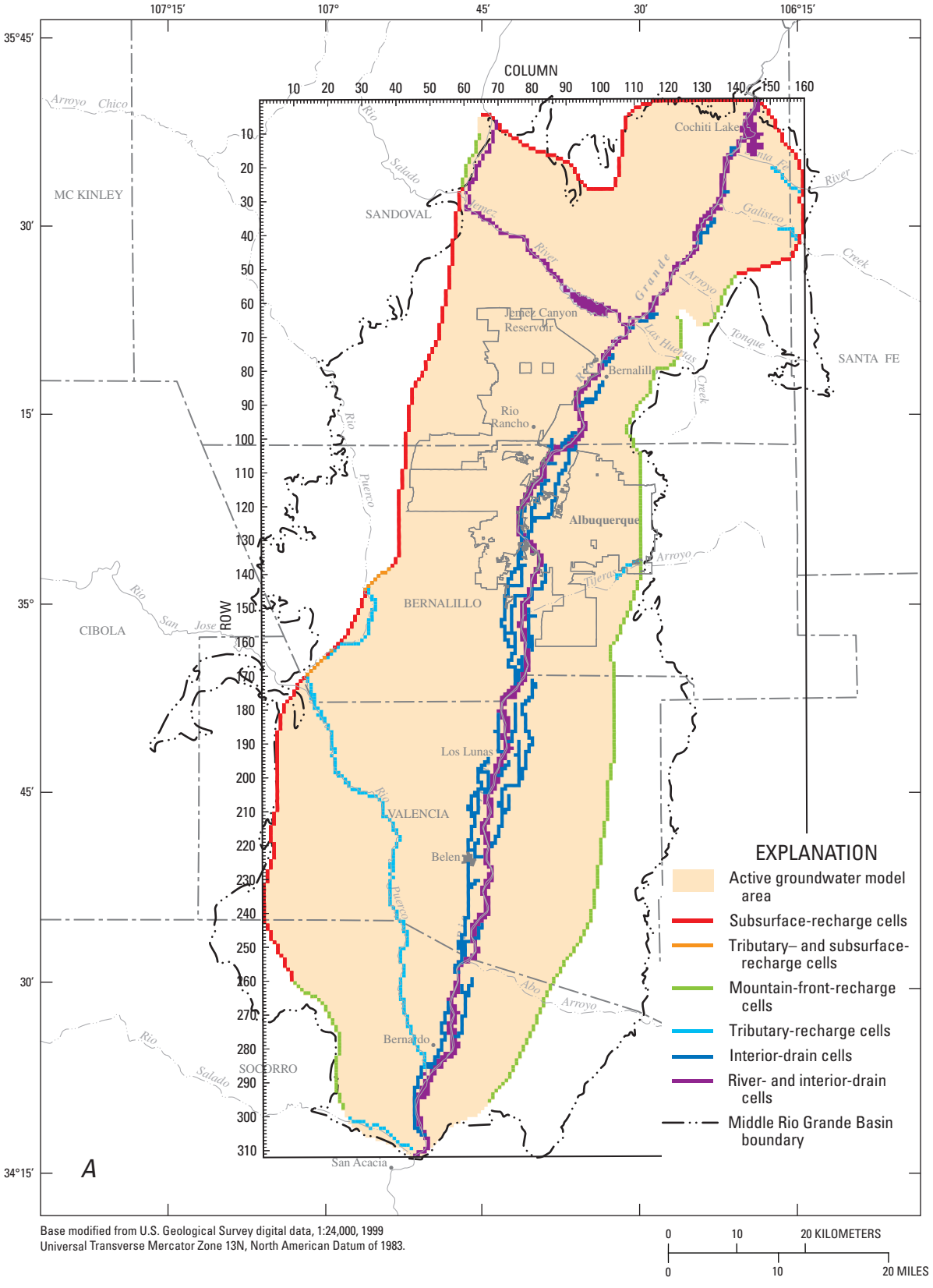

Figure 2.12*A*. Revised groundwater-flow model showing groundwater-flow model domain and selected boundary conditions, Middle Rio Grande Basin, New Mexico. With the exception of subsurface recharge, applied to model layers 1–3, boundary conditions are applied to the uppermost active model finite-difference cell. For all deeper layers and where no boundary condition is shown, the lateral boundary is no-flow. Depicted drain-boundary locations (*A*) are those simulated for the period from Nov. 1, 1991, through the end of the simulation in 2008.

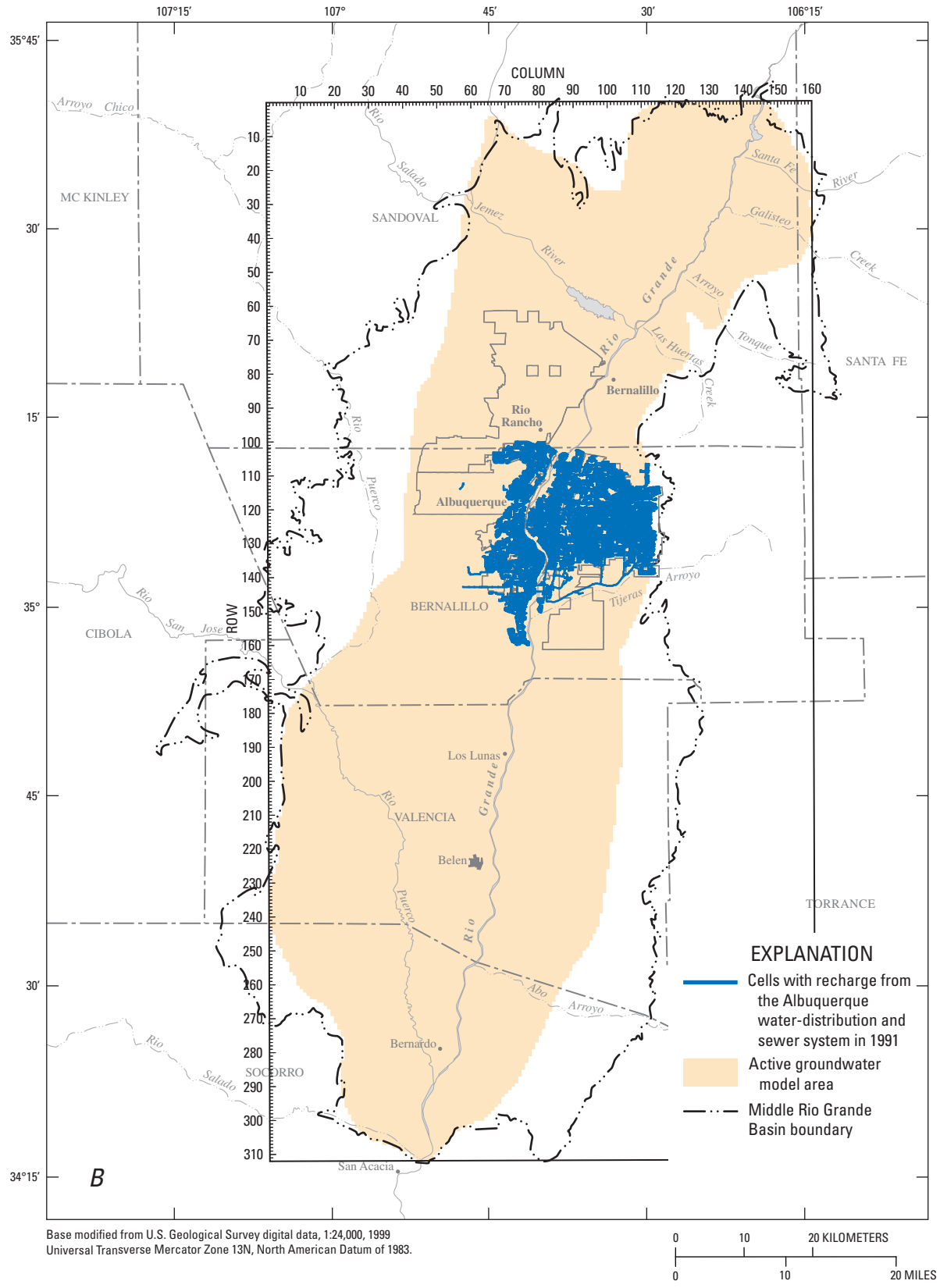

Figure 2.12*B*. Revised groundwater-flow model showing water-distribution and sewer system, Middle Rio Grande Basin, New Mexico. With the exception of subsurface recharge, applied to model layers 1–3, boundary conditions are applied to the uppermost active model finite-difference cell. For all deeper layers and where no boundary condition is shown, the lateral boundary is no-flow. Depicted drain-boundary locations (*A*) are those simulated for the period from Nov. 1, 1991, through the end of the simulation in 2008.

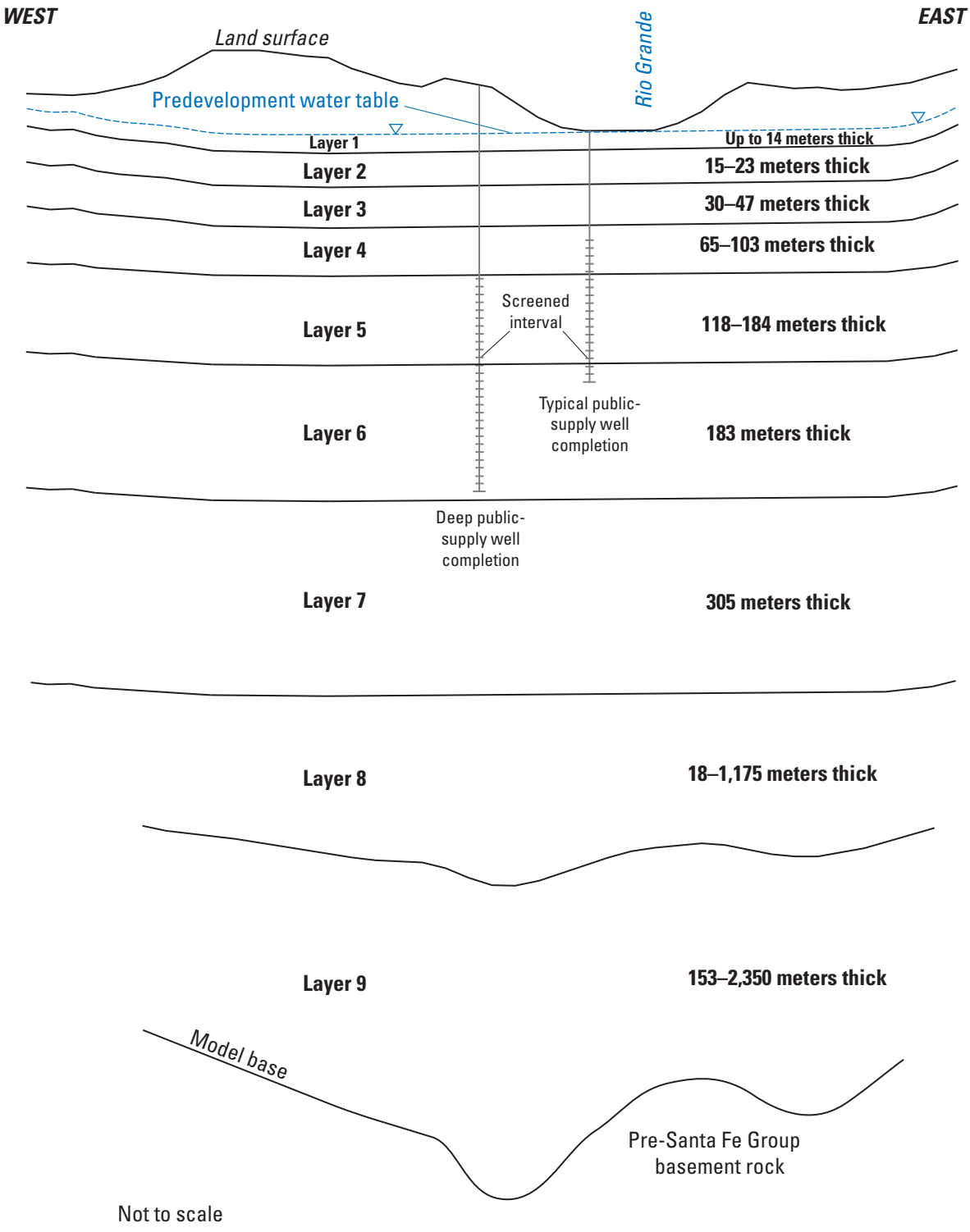

Figure 2.13. Configuration of layers in the revised groundwater-flow model, Middle Rio Grande Basin, New Mexico (modified from McAda and Barroll, 2002).

Simulation-Code Modifications

Modifications to the Well Package, which were previously documented by McAda and Barroll (2002), and that reassign specified flows in cells that dry out to successively deeper model layers, were made to the MODFLOW-2005 version of the source code. A version of the executable code that runs under Windows® operating systems was compiled with double precision, which reduced mass-balance errors during simulation time steps when cells dry out. Use of the NOCV-CORRECTION option in the Layer Property Flow Package (Harbaugh, 2005) was required for model convergence.

Boundary Conditions and Model Stresses

The top of the groundwater model corresponds to the land surface. The bottom of the groundwater model is a no-flow boundary that corresponds to the base of the Santa Fe Group aquifer system. The perimeter of the model domain is simulated with specified-flow boundary conditions. Other features within the model domain are simulated with either specified-flow or head-dependent-flow boundary conditions, as described below.

Specified-Flow Boundaries

Flows representing mountain-front and tributary recharge, seepages from canals, irrigated areas, and septic systems, and leakage from the sewer/water collection/distribution systems for the greater Albuquerque metropolitan area were specified into the uppermost active finite-difference cells in each model layer (figs. 2.12*A* and *B*). Flows representing subsurface underflow from outside the perimeter of the model domain and domestic groundwater withdrawals from within the MRGB were specified as described below.

Subsurface, Mountain-Front, and Tributary Recharge

Specified flows to layers 1 through 3 along most of the western and northern model boundaries simulate underflow (subsurface recharge) into the basin based on information described in McAda and Barroll (2002), the total of which was 37 x 10^6 m^3/yr (table 2.5).

A total of 15 x 10^6 m^3/yr of mountain front recharge was specified into the uppermost active model layer along the northern, eastern, and southwestern boundaries of the model (table 2.5) as described in McAda and Barroll (2002). Recharge rates calculated by Anderholm (2001) along the Sandia, Manzanita, Manzano, and Los Pinos Mountains are included in the total value.

The total of 11.1 x 10^6 m^3/yr (table 2.5) of tributary recharge estimated by McAda and Barroll (2002) was specified with the Recharge Package (Harbaugh, 2005). Simulated recharge from tributaries along the southern and western model boundaries, which correspond to the Rio Salado and Rio Puerco, respectively, accounts for 3.0 x 10^6 m^3/yr of this total. In the northeastern part of the MRGB, specified recharge from Galisteo Creek and the Santa Fe River was 2.2 x 10^6 and 4.3 x 10^6 m^3/yr, respectively. On the eastern side of the MRGB, a portion (0.9 x 10^6 m^3/yr) of the total recharge calculated by Anderholm (2001) in the area of Tijeras Arroyo has been simulated as tributary recharge, and the remainder has been simulated as mountain-front recharge. Recharge specified from the Rio Puerco was 0.7 x 10^6 m^3/yr.

Seepage

Canal seepage was simulated within the Rio Grande inner valley for a network that also includes laterals, feeder canals, and ditches. A Geographic Information System (GIS) database (R.A. Durall, U.S. Geological Survey, written commun., 2001) that contains width and depth data was used to define the canal network. Where data were unavailable, characteristics were based on average conditions for the same feature class. Canal seepage was not explicitly specified prior to 1930 due to a lack of data, but it was considered part of the specified crop-irrigation seepage. Because canals were both constructed and abandoned between 1900 and 2000, the locations of specified canal seepage change between stress periods. Canal seepage was not simulated for the 4.5-month long stress periods after 1989 because canals were not operated during the winter. Using the method and equation described in McAda and Barroll (2002), recharge specified into the aquifer from canal seepage for the year ending on October 31, 1999, was calculated to be 115 x 10^6 m^3/yr (table 2.5).

Specification of the spatial distribution of crop-irrigation seepage was based upon GIS data of land use in the Rio Grande inner valley for 1935 (National Biological Service, undated) and for 1955, 1975, and 1992 (Bureau of Reclamation, undated). Specification of crop-irrigation seepage along the Jemez River Valley was based upon the Bureau of Reclamation data from 1955 and 1975. McAda and Barroll (2002) calculated an average recharge rate (weighted by crop types) of 0.21 m/yr for 1991 and 1993 that was reduced to 0.15 m/yr to account for the rotation of crops and fallow land (McAda and Barroll, 2002). The specified crop-irrigation flux rate was the product of 0.15 m/yr with the fraction of cropland area in a model cell. Because crop irrigation occurs mainly during the irrigation season, it was not included in winter-season stress periods, simulated after 1989. Total specified recharge from crop-irrigation seepage for the year ending on October 31, 1999, was 41 x 10^6 m^3/yr (table 2.5).

Septic-field seepage originates from septic tanks and leach fields in populated areas that are not connected to sewage collection systems. Specification of septic-field seepage with the Recharge Package for stress periods after 1960 was based on population density. Prior to 1960, most of the population in unsewered areas lived in the Rio Grande inner valley, where septic-return flows were considered to be volumetrically insignificant compared with other components of the Rio Grande surface-water system. Population density was determined using U.S. Census Bureau tract data from 1970

Table 2.5. Model-computed net annual groundwater budgets for steady-state conditions and year ending October 31, 1999, for the revised groundwater-flow model , Middle Rio Grande Basin, New Mexico.

[m^3/yr; cubic meters per year; —, not applicable]

Water-budget component	Steady state				Year ending October 31, 1999			
	Specified net flow (106 m^3/yr)	Computed net flow (106 m^3/yr)	Total net flow (106 m^3/yr)	Percentage of net inflow or outflow	Specified net flow (106 m^3/yr)	Computed net flow (106 m^3/yr)	Net flow rate (106 m^3/yr)	Percentage of net inflow or outflow
Model inflow (recharge)								
Mountain-front recharge	15	—	15	10	15	—	15	3
Tributary recharge	11	—	11	7	11	—	11	2
Subsurface inflow	37	—	37	25	37	—	37	6
Canal seepage	0	—	0	0	115	—	115	20
Crop-irrigation seepage	0	—	0	0	41	—	41	7
Rio Grande and Cochiti Lake[1]	—	74	74	49	—	264	264	45
Jemez River and Jemez Canyon Reservoir[1]	—	14	14	9	—	16	16	3
Septic-field seepage	0	—	0	0	3	—	3	1
Sewer- and distribution-system leakage	0	—	0	0	14	—	14	2
Aquifer storage[2]	—	0	0	0	—	67	67	11
Total inflow[3]	—	—	**151**	**100**	—	—	**583**	**100**
Model outflow (discharge)								
Riverside drains	—	0	0	0	—	148	148	25
Interior drains	—	0	0	0	—	132	132	23
Groundwater withdrawal[4]	0	—	0	0	191	—	191	33
Riparian evapotranspiration	—	152	152	100	—	112	112	19
Total outflow[3]	—	—	**152**	**100**	—	—	**583**	**100**

[1] Cochiti Lake and Jemez Canyon Reservoir were not present during steady-state conditions.

[2] Net inflow of water from aquifer storage reflects loss of water from aquifer storage to the groundwater system (that is, a decline in aquifer storage).

[3] Due to flow rate rounding, budget discrepancies in the table differ from the corresponding model output. Model-computed volumetric budget discrepancies are 0.2 percent for the steady-state stress period and 0.07 percent for the stress period ending October 31, 1999.

[4] Includes withdrawals for domestic, municipal, commercial, and industrial uses.

through 2000 (U.S. Census Bureau, 1970; 1980; 1990; 2001b). The amount of septic-field seepage applied to a model cell was calculated as the product of the population in the cell with the rate of septic-field seepage per person (McAda and Barroll, 2002). Assuming that 90 to 95 percent of indoor water use was not consumed (McAda and Barroll, 2002), and that average indoor water use is approximately 0.24 m^3 per person per day (Wilson, 1992), the average seepage rate was 0.23 m^3 per person per day. Specified recharge from septic field seepage for the year ending on October 31, 1999, totaled 3 x 10^6 m^3/yr.

Water-level drawdowns simulated by the McAda and Barroll (2002) model were greater than drawdowns observed under Albuquerque east of the Rio Grande. McAda and Barroll (2002) noted that water-distribution and sewer system leakages, which were not simulated in their model, should decrease water-level drawdowns. Water-distribution-system losses, which were primarily attributed to leakage, metering inaccuracies, and unauthorized consumption during the years 2004 to 2007, ranged from 9.9 percent to 15.4 percent (City of Albuquerque, 2009). Because the quantity of leakage from the Albuquerque water-distribution and sewer systems has been uncertain, leakage was assumed to be 10 percent of the City of Albuquerque annual groundwater withdrawals for each stress period of this simulation. GIS databases of the extent of the Albuquerque Metropolitan area in the years 1935, 1951, 1973, and 1991 (Feller and Hester, 2001) were intersected with GIS databases of the City of Albuquerque water-distribution and sewage-pipe systems to generate geospatial data of the areas susceptible to pipe leakage at those times. Although the spatial distributions of water-pipe leaks (New Mexico Environmental Finance Center, 2006) and sewer-pipe leaks (Camp Dresser & McKee, 1998) have been correlated with material pipe types, the leaky-pipe recharge flux was homogeneously specified over areas designated as susceptible to pipe leakage in each stress period (fig. 2.12*B*). Simulated recharge to the aquifer from sewer and water collection/distribution losses for the year ending on October 31, 1999, was 14 x 10^6 m^3/yr.

Domestic Groundwater Withdrawals

Withdrawals of groundwater from domestic wells were simulated with a modified version of the Well Package beginning with the 1960–64 stress period. Domestic-well withdrawals were assigned to model cells based on population densities from U.S. Census Bureau tract data from 1970, 1980, 1990, and 2000 (U.S. Census Bureau, 1970; 1980; 1990; 2001b). A per-person withdrawal rate of 0.38 m^3 per day (for indoor and outdoor purposes) was used based on a study by Wilson (1992). The total domestic-well withdrawal from a model cell was calculated as the product of this rate times the population density times the cell area. Because domestic-well-construction data were lacking, layer assignments for domestic wells were based on the steady-state water table depth: layer 1 for water-table depths of less than 15.24 m, layer 2 for depths 15.24 to 91.44 m, and layer 3 for depths greater than 91.44 m. The modified version of the Well Package transfers withdrawals in cells that become dry to the next lower active cell, thereby preventing exclusion of domestic-well withdrawals when the water table declines below the bottom of the specified model layer. Specified domestic-well withdrawals for the year ending on October 31, 1999, totaled 8.2 x 10^6 m^3/yr.

Head-Dependent-Flow Boundaries

Reported groundwater withdrawals, the Rio Grande and Jemez River, riverside and interior drains, Jemez Canyon Reservoir and Cochiti Lake, and evapotranspiration were simulated as head-dependent-flow boundaries (fig. 2.12*A*).

Reported Groundwater Withdrawals

Reported withdrawals of groundwater from production wells serving municipal, commercial, and industrial purposes were simulated with the Multi-Node Well Package (Halford and Hanson, 2002). For each stress period, the total withdrawal from each well was specified based on monthly or annual withdrawal reports that were adjusted to the stress period timing. The simulated layer-by-layer distribution of the total withdrawal specified for the well depends largely on the specified hydraulic conductivities in each of the finite-difference cells penetrated by the well-screen interval and on differences in simulated head between the withdrawal well and the heads in each of those cells. Although hydraulic heads in production wells are also affected by turbulent-flow head losses near the well and flow through drilling-damaged formation, gravel pack, or the well screen, these effects were not directly simulated.

Groundwater-withdrawal records were obtained from the New Mexico Office of the State Engineer, the City of Albuquerque, and Bjorklund and Maxwell (1961). Because groundwater- withdrawal data prior to the 1960s were limited, many earlier withdrawal rates for the City of Albuquerque, the University of New Mexico, Kirtland Air Force Base, and two local power-plant supply wells were extrapolated from later records (Kernodle and others, 1995). For wells not operated by these entities, withdrawals were specified only in years for which records were available. Consequently, model-simulated withdrawals may under-represent actual withdrawals.

Rivers

Seepage between the Rio Grande and the underlying Santa Fe Group aquifer system was simulated with the River Package (Harbaugh, 2005). The simulated conductance between a river boundary and an underlying finite-difference cell is the product of the riverbed hydraulic conductivity with the riverbed area in the model cell, divided by the riverbed thickness. McAda and Barroll (2002) estimated a riverbed hydraulic conductivity of 0.03 m per day by calibration of simulated river seepage to an independent flow loss calculation for the Rio Grande and riverside drains (Veenhuis, 2002). The riverbed area varies depending on the geometry of the Rio

Grande within individual model cells, and riverbed thickness was assumed to be 0.3 m (Kernodle and others, 1995).

Riverbed areas within each model cell were calculated using the National Biological Service GIS databases for 1935 and 1989 (Roelle and Hagenbuck, 1994), which provided information about perennially and seasonally flooded areas. The specified riverbed areas for the revised model differ from the McAda and Barroll (2002) model because they include exposed sandbars. McAda and Barroll (2002) used measurements of historically low flows in October and high flows in May to estimate average conditions from 1900 through 1989. The Rio Grande stage during this time period was determined from USGS topographic maps. For the seasonal stress periods beginning in 1990, riverbed area within each model cell was adjusted based on average seasonal flow conditions at USGS streamflow-gaging station 08330000 (fig. 2.7). McAda and Barroll (2002) calculated percentages of seasonally flooded areas to add to perennially flooded areas to yield riverbed areas for each model cell at various times. They also derived a relation between river-stage change and the ratio of perennially to seasonally flooded channel areas that was used to specify the stage for each model cell during post-1989 stress periods in the revised model.

Like the Rio Grande, the Jemez River is in hydraulic connection with the aquifer system and was simulated with the River Package. Unlike the Rio Grande, however, only limited descriptive information was available for the Jemez River. The riverbed hydraulic conductance was specified as the product of the length of the river in a model cell and a parameter that incorporated river-bed width, thickness, and hydraulic conductivity. This parameter was specified as 75 and 25 m/d for the upper and lower reaches of the river, respectively. According to McAda and Barroll (2002): "The upper reach has a steeper gradient and a higher flow energy than the lower reach, resulting in a greater proportion of coarse material in the riverbed; therefore the upper reach was assumed to have a relatively larger riverbed hydraulic conductivity than the lower reach."

Drains

McAda and Barroll (2002) classified drains in the Rio Grande valley into two types: "riverside drains" and "interior drains." Beginning in the late 1920s, riverside drains were constructed on either side of the Rio Grande in the MRGB to mitigate water logging of agricultural land near the Rio Grande, and to enable water to be returned to the Rio Grande. Riverside drains can either gain or lose water, depending upon the drain stage and drain-bed altitude with respect to the water table, and were therefore simulated with the River Package. A GIS database (R.A. Durall, U.S. Geological Survey, written commun., 2001) was used to specify the locations, areas, and bed elevations of the drains. Following McAda and Barroll (2002), all drain-bed conductances were calculated by assuming the existence of "drain beds" with a hydraulic conductivity of 0.3 m/d and a thickness of 0.3 m. Riverside drains simulated 148 x 10^6 m^3/yr of net outflow from the aquifer during the year ending on October 31, 1999.

Interior drains were also installed during the late 1920s and early 1930s to intercept canal and crop-irrigation seepage in the inner valley. Water captured by interior drains from the shallow part of the aquifer system is discharged to the riverside drains. Because interior drains are thought to only intercept and convey water, they were simulated using the Drain Package (Harbaugh, 2005). Drain stages were specified for each cell as the land surface elevation at the center of the cell minus the average drain-stage depth below land surface. Interior drains simulated a net outflow of 132 x 10^6 m^3/yr from the aquifer during the year ending on October 31, 1999.

Lakes and Reservoirs

The Jemez Canyon Reservoir was constructed along the lower reach of the Jemez River above its confluence with the Rio Grande to trap sediment. Prior to 1979, the reservoir stored water for short periods that were not simulated. For simulation stress periods beginning in 1979 and continuing through October 2000, after which the reservoir was completely drained, the reservoir was simulated with the River Package. Average annual stages were used for all stress periods; no attempt was made to simulate seasonal changes in reservoir stage. The reservoir bottom area was estimated for each stage using USGS 30-meter 1:24,000 Digital Elevation Models (DEMs). Because information on the hydraulic conductivity of the reservoir bed was not available, McAda and Barroll (2002) estimated the reservoir bed hydraulic conductance during model calibration. Their factor of 0.0015 per day (representing hydraulic conductivity divided by bed thickness) was applied to the reservoir area for 1979–1984; this value was reduced to 0.001 per day for 1985–2001 to account for the accumulation of fine-grained sediment. Simulated combined seepage from Jemez Canyon Reservoir and the Jemez River to the aquifer was 16 x 10^6 m^3/yr during the year ending on October 31, 1999; for steady state, simulated recharge from the Jemez River alone was 14 x 10^6 m^3/yr.

Cochiti Lake is located along the upper reach of the Rio Grande, and it began storing water in November 1973. Because the model uses a 5-year stress period for 1970–1974, simulation of Cochiti Lake with the River Package commences with the model stress period that begins in 1975. McAda and Barroll (2002) adjusted the Cochiti Lake bed hydraulic conductance to calibrate simulated seepage to measurement-based seepage estimates. Their factors, which represent hydraulic conductivity divided by bed thickness and range from 0.001 to 0.0027 per day, were applied to the reservoir area for simulated annual-average reservoir stages obtained from USGS Water-Data Reports for New Mexico (various years). The steep topography near Cochiti Lake required USGS 10-meter DEMs for lake-bed-area calculations. Simulated combined seepage from Cochiti Lake and the Rio Grande to the aquifer was 264 x 10^6 m^3/yr during the

year ending on October 31, 1999; for steady state, simulated recharge from the Rio Grande alone was 74 x 10^6 m^3/yr.

Riparian Evapotranspiration

Evapotranspiration from the riparian corridors that border the Rio Grande and Jemez River was simulated with the Evapotranspiration Segments Package (Banta, 2000). Simulated evapotranspiration rates decrease in linear segments from 1.5 m/yr where the water table is at land surface, to 0.6 m/yr where the water table is 2.7 m below land surface, to 0.2 m/yr where the water table is 4.9 m below land surface, and finally to zero where the water table is 9.1 m below land surface. The depths delineating these linear segments and associated rates correspond to the rooting depths of salt cedar (Bureau of Reclamation, 1973), willow (Robinson, 1958), and cottonwood trees (Robinson, 1958), respectively. The 1935 Rio Grande riparian corridor delineation (National Biological Service GIS data, undated) was used to specify evapotranspiration areas for stress periods from 1900 through 1944. Additional GIS data for Rio Grande riparian corridor delineations for 1955, 1975, and 1992 (Bureau of Reclamation, undated) were used for the remaining simulated periods. To specify riparian evapotranspiration areas along the Jemez River, stress periods from 1900 to 1964 utilized 1955 land-use data, and stress periods after 1965 utilized 1975 land-use data. Simulated evapotranspiration from the area under Jemez Canyon Reservoir was discontinued for stress periods after the reservoir was filled. For seasonal stress periods after 1989, evapotranspiration was simulated only during the summer stress periods. Simulated outflow from the aquifer due to riparian evapotranspiration was 152 x 10^6 m^3/yr for the steady-state stress period and 112 x 10^6 m^3/yr for the stress periods representing the year ending on October 31, 1999.

Aquifer Hydraulic Properties

McAda and Barroll (2002) based their distribution of zones of simulated hydraulic conductivity upon a three-dimensional digital geologic model of the hydrostratigraphic units (Cole, 2001a), with modifications based on findings of Hawley and Haase (1992), Hawley and others (1995), Connell and others (1998), and Smith and Kuhle (1998). Based partly on further work by Connell (2006), this zone distribution was modified in model layer 4 to simulate higher hydraulic conductivities in an area previously zoned for silt. The hydraulic-property parameter values documented by McAda and Barroll (2002) were used as starting values for model calibration by nonlinear regression with PEST (Doherty, 2005), and they are tabulated with the corresponding calibrated parameter values in table 2.6. Parameters representing aquifer storage properties and various recharge fluxes were not modified in the PEST calibration. The calibrated horizontal hydraulic conductivities specified in the revised model range from 0.02 to 15.5 m/d in the east-west direction along model rows (fig. 2.14 *A*1–*A*9). Horizontal anisotropy, which is expressed as the ratio of north-south to east-west hydraulic conductivity, in model layers 3 through 8 ranges from 5:1 along a naturally occurring groundwater trough (Meeks, 1949; Bjorklund and Maxwell, 1961; Bexfield and Anderholm, 2000) located in the west-central portion of the MRGB (fig. 2.14*B*1) to 1.5:1 throughout most of the central portion of the MRGB, and is isotropic in the northern and peripheral areas of the MRGB. The pattern of horizontal anisotropy for model layers 1 and 2 is similar, but isotropic in the post-Santa Fe Group alluvium within the Rio Grande inner valley (fig. 2.14*B*2). Horizontal hydraulic conductivity in model layer 9 is isotropic. The finite-difference model grid is aligned with an assumed north-south principal direction of anisotropy that corresponds to the north-south orientation of major faults in the basin, some of which are thought to impede groundwater flow. Major faults that McAda and Barroll (2002) determined were likely to act as "significant flow barriers" were simulated to vertically penetrate all nine model layers with the Horizontal Flow Barrier (HFB) package (figs. 2.14*B*1 and 2.14*B*2).

Vertical hydraulic conductivity is represented as a fraction of the horizontal hydraulic conductivity in two zones in model layers 1 and 2; one zone represents axial-river and alluvium deposits in the inner valley, where the ratio of horizontal to vertical hydraulic conductivity is 1.06:1, and the second zone represents the remainder of the model domain, outside of the inner valley, where the ratio of horizontal to vertical hydraulic conductivity ratio is 132:1) (fig. 2.14*C*). The vertical anisotropy ratio of 132:1 was also used throughout layers 3–9 and is similar to that simulated by other models of the MRGB (McAda and Barroll, 2002; McAda, 2001; Tiedeman and others, 1998); however, the vertical anisotropy representing the axial-river and alluvium deposits in the inner valley is significantly lower than the values used in previous models.

Specific storage was specified at 6.6 x 10^{-6} per meter based on water-level-change and associated extensometric-strain measurements (Heywood, 2001, 1998). Specific yield was specified at 0.20 for all zones representing different lithologies in the model, as was done by McAda and Barroll (2002).

Table 2.6. Parameter values and sensitivities in the revised groundwater-flow model of the Middle Rio Grande Basin near Albuquerque, New Mexico.

[Calibrated values of parameters with names shown in italic type did not differ from initial values]

Parameter description	Parameter name	Relative sensitivity	Calibrated value	Initial value	Composite sensitivity
Horizontal hydraulic conductivity of medium sand	Ksdm	0.172	0.43	0.46	0.403
Horizontal hydraulic conductivity of axial channel deposits	K*axial*1	.141	9.14	9.14	.015
Horizontal hydraulic conductivity of Santo Domingo subbasin	Ksdmc	.141	2.23	2.44	.064
Horizontal hydraulic conductivity of buffer area around axial channel deposits	Kaxial2	.131	2.96	4.57	.044
Horizontal hydraulic conductivity of eolian sand deposits	Ksdeo	.073	1.52	2.44	.048
Horizontal hydraulic conductivity of inner valley alluvium	Kalluv	.068	12.50	13.72	.005
Horizontal hydraulic conductivity of fine-medium sand deposits	K*sdfm*	.050	.02	.02	3.297
Horizontal hydraulic conductivity of silty deposits	Ksilts	.050	2.13	.61	.023
Horizontal hydraulic conductivity of sediment in new zone	Kdirt	.049	15.54	.61	.003
Horizontal hydraulic conductivity of piedmont sediments	Kpdmt	.042	3.66	.15	.011
Horizontal hydraulic conductivity of western Santo Domingo subbasin and south	K*sdmcwest*	.040	2.44	2.44	.016
Horizontal hydraulic conductivity of NW part of Santo Domingo subbasin	K*nw*	.026	.15	.15	.169
Horizontal hydraulic conductivity of coarse sand and gravel deposits	Kcgsv	.013	3.66	.15	.004
Horizontal hydraulic conductivity of intrusives	K*intr*	.005	.30	.30	.017
Horizontal hydraulic conductivity of volcanics	K*volc*	.003	2.44	2.44	.001
Anisotropy of horizontal hydraulic conductivity	HANIyes	.942	1.52	2	.620
Isotropy of horizontal hydraulic conductivity in areas defined as horizontally isotropic	*HANIno*	.543	1	1	.543
Anisotropy of horizontal hydraulic conductivity in "trough area"	*HANItrf*	.188	5	5	.038
Ratio of horizontal to vertical hydraulic conductivity	VANI2	.711	132	150	.005
Ratio of horizontal to vertical hydraulic conductivity	VANI1	.010	1.06	150	.009

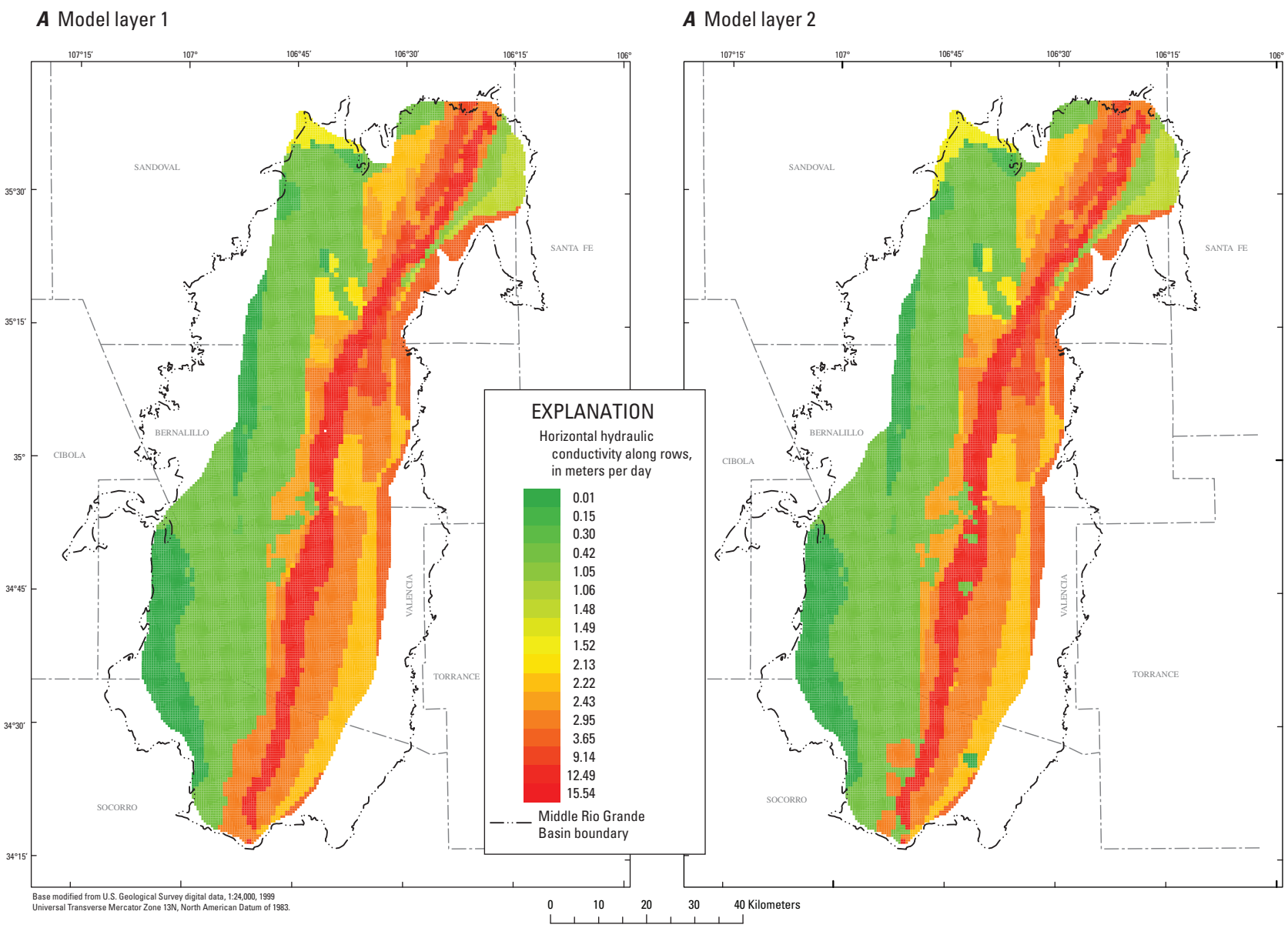

Figure 2.14*A1–A2*. Distribution of simulated horizontal hydraulic conductivity in the east-west direction for model layers 1–9, Middle Rio Grande Basin, New Mexico.

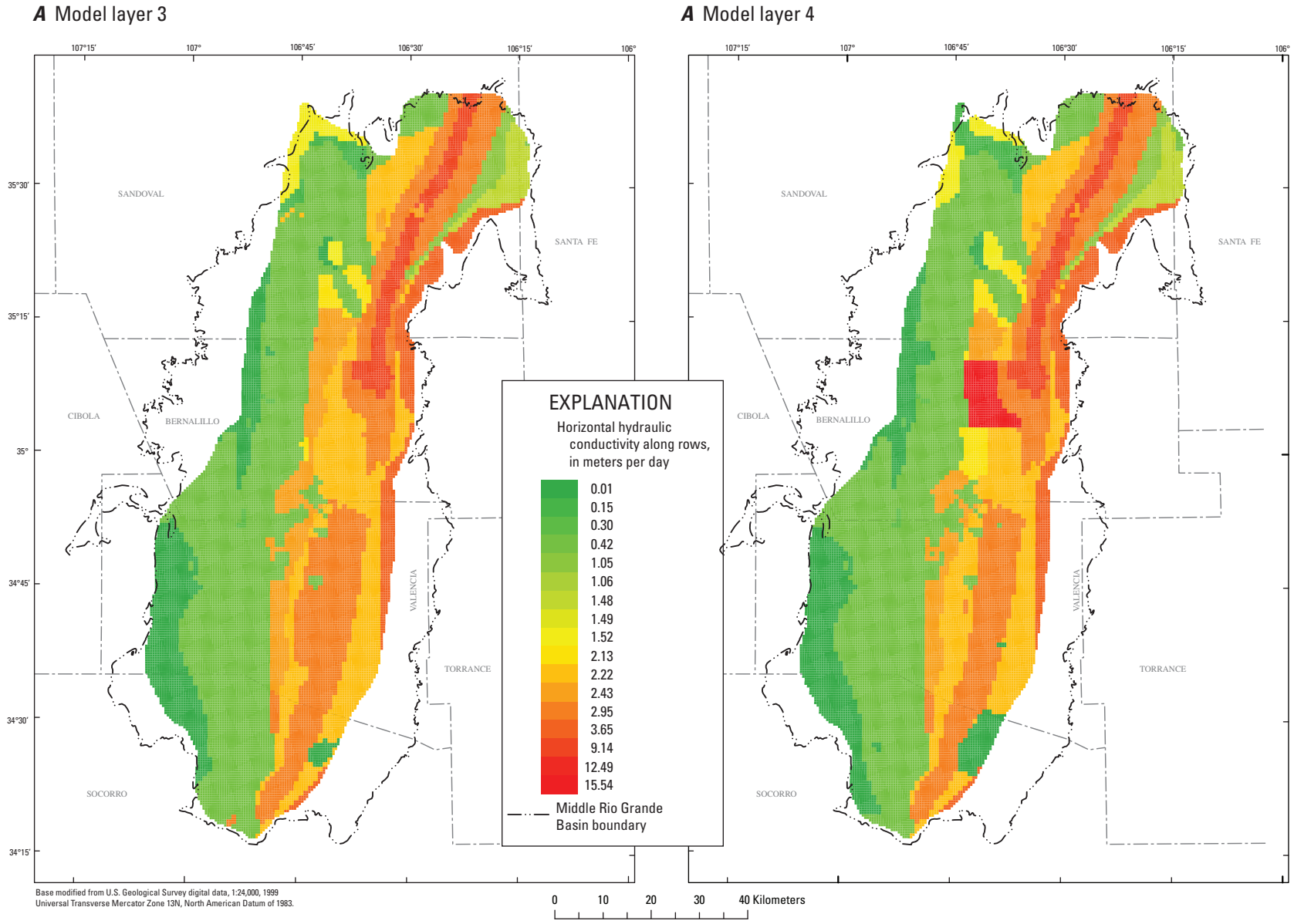

Figure 2.14*A3–A4.* Distribution of simulated horizontal hydraulic conductivity in the east-west direction for model layers 1–9, Middle Rio Grande Basin, New Mexico.

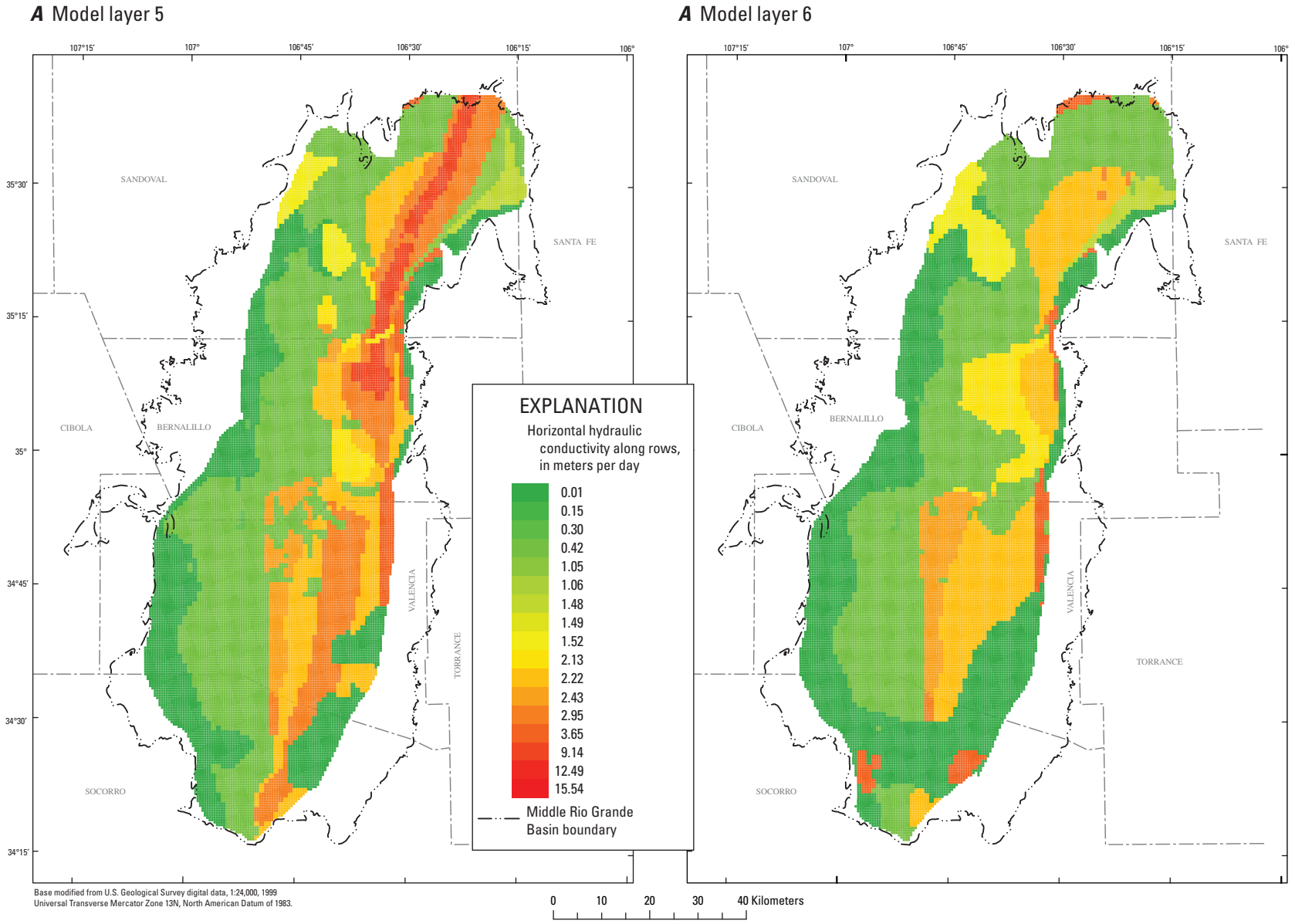

Figure 2.14*A5–A6*. DDistribution of simulated horizontal hydraulic conductivity in the east-west direction for model layers 1–9, Middle Rio Grande Basin, New Mexico.

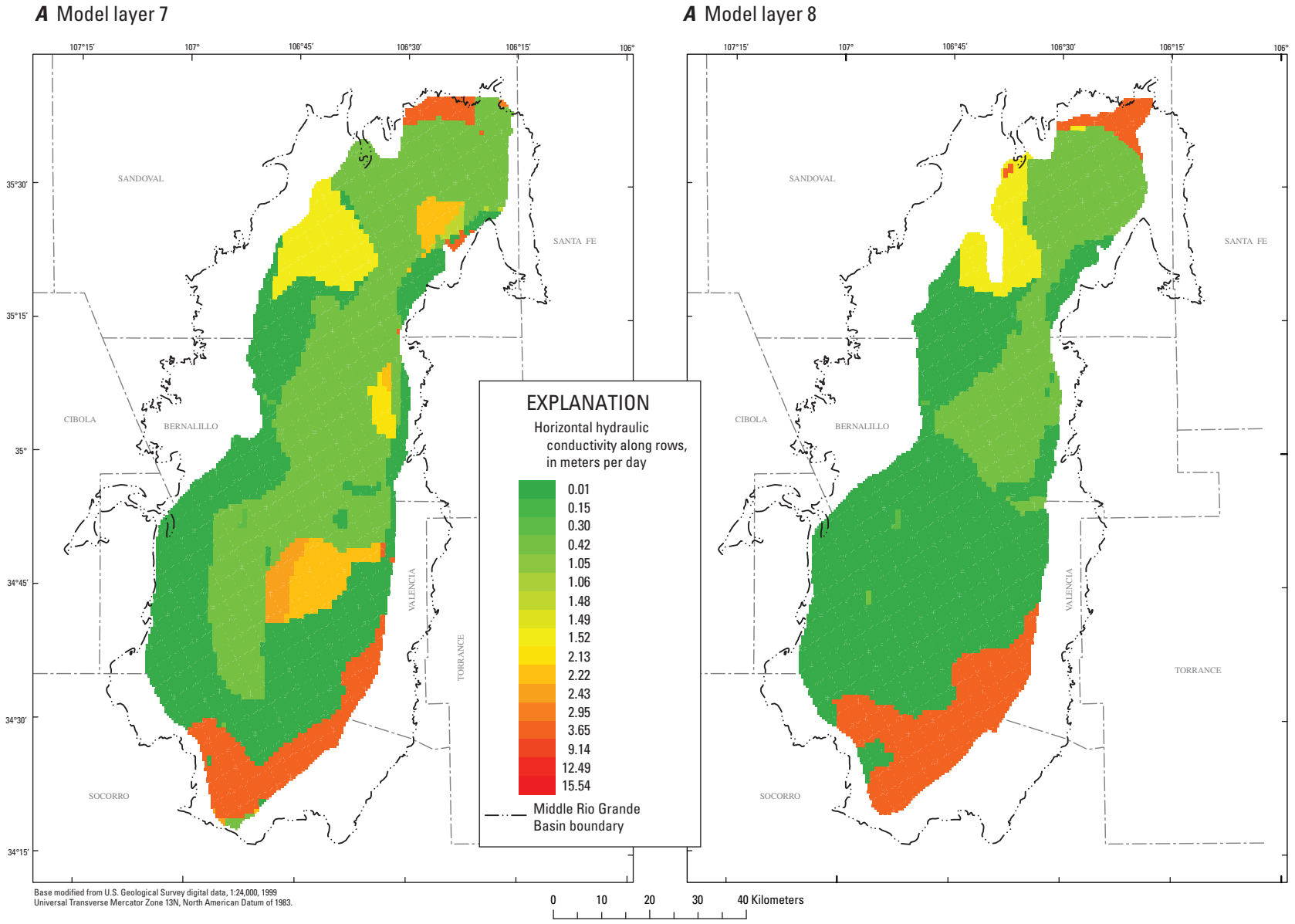

Figure 2.14*A7–A8*. Distribution of simulated horizontal hydraulic conductivity in the east-west direction for model layers 1–9, Middle Rio Grande Basin, New Mexico.

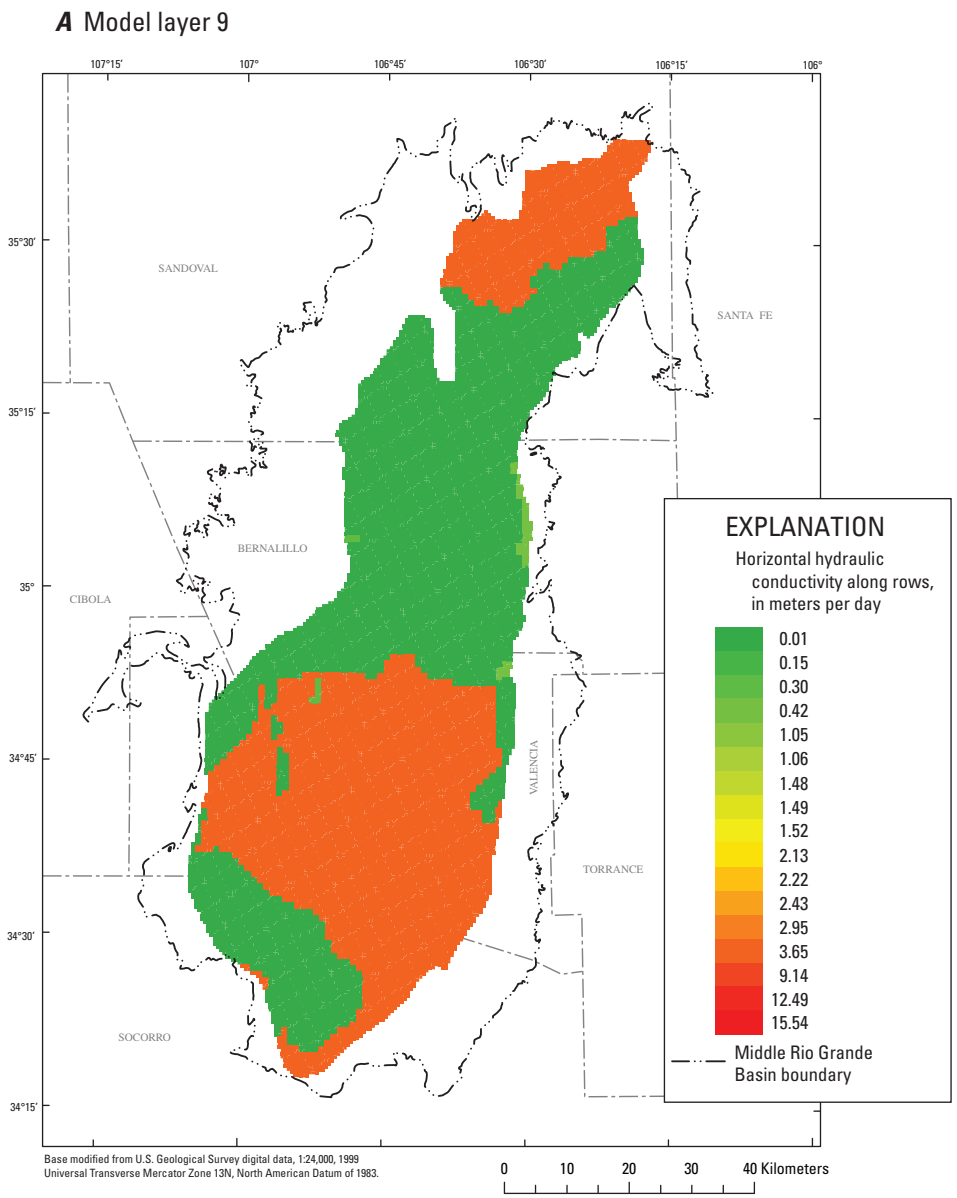

Figure 2.14*A9*. Distribution of simulated horizontal hydraulic conductivity in the east-west direction for model layers 1–9, Middle Rio Grande Basin, New Mexico.

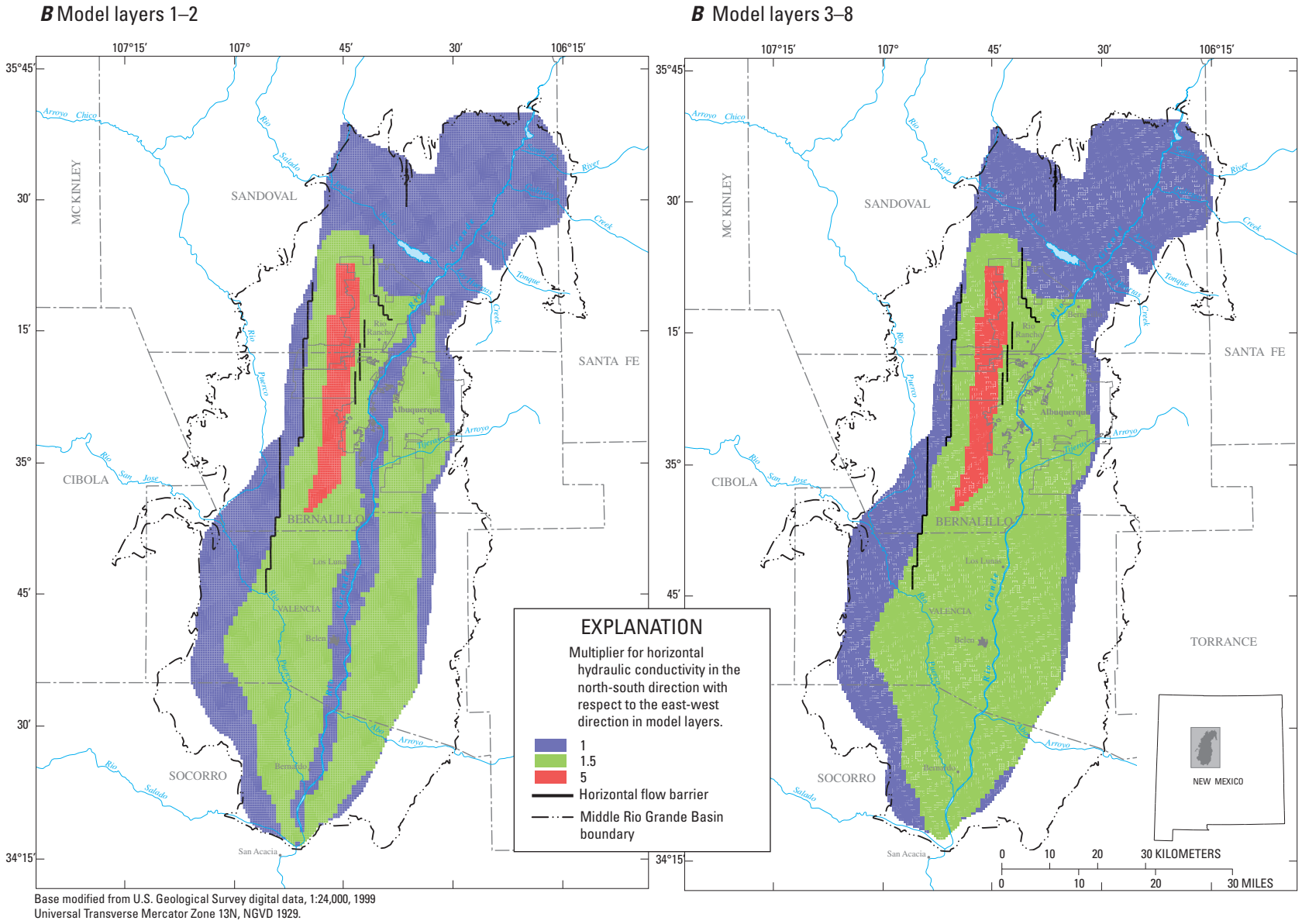

Figure 2.14*B*. Ssimulated horizontal anisotropy for layers 1–2 and 3–8, Middle Rio Grande Basin, New Mexico.

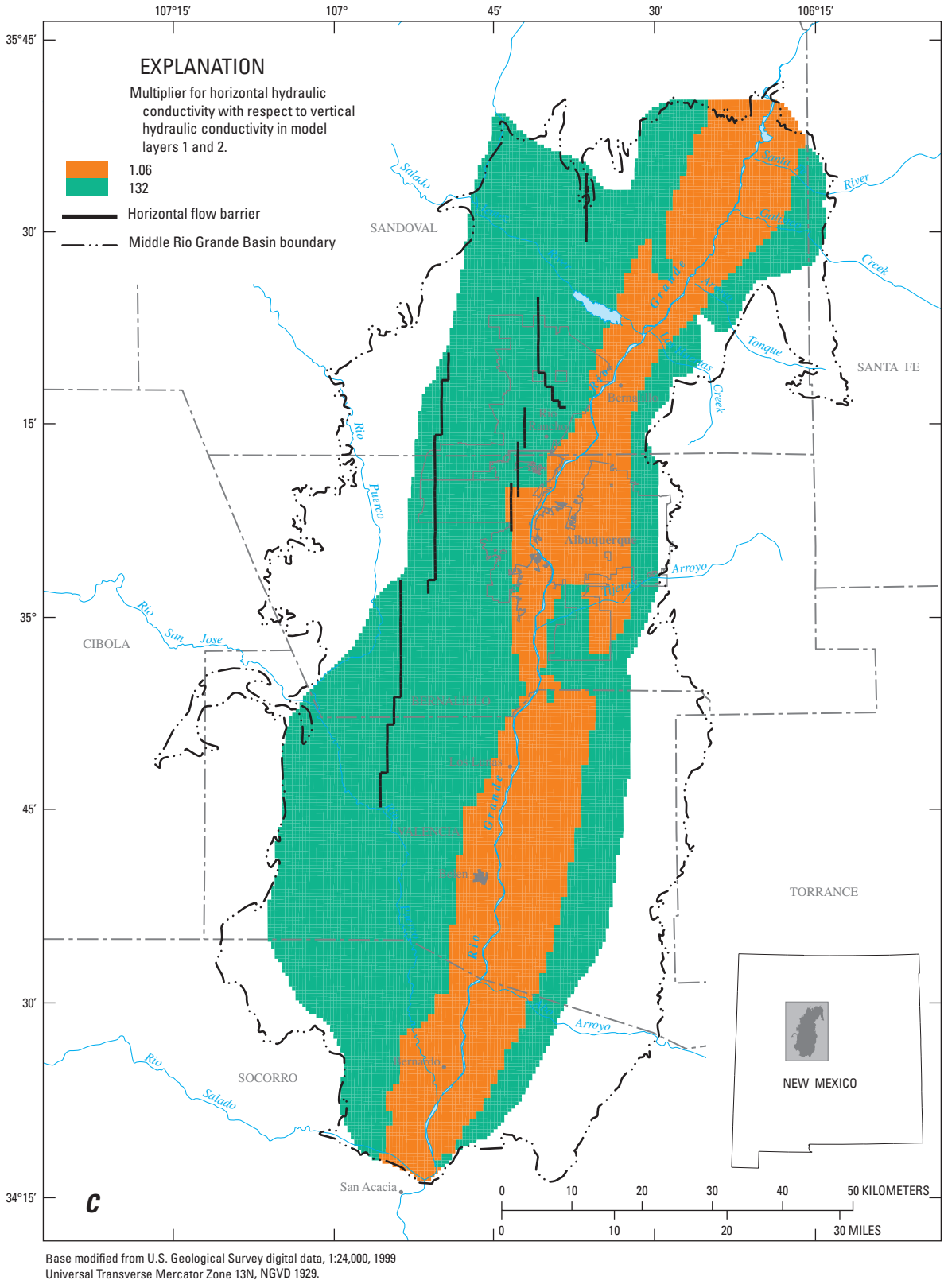

Base modified from U.S. Geological Survey digital data, 1:24,000, 1999
Universal Transverse Mercator Zone 13N, NGVD 1929.

Figure 2.14*C*. Simulated vertical anisotropy for layers 1–2 of the revised groundwater-flow model, Middle Rio Grande Basin, New Mexico.

Model Evaluation

McAda and Barroll (2002) used a trial-and-error approach to calibrate their MRGB model to 344 reconstructed predevelopment hydraulic heads (Bexfield and Anderholm, 2000), 984 measured hydraulic heads, estimated seepage loss from Cochiti Lake, and a flow-loss measurement (Veenhuis, 2002) along the reach of the Rio Grande between Bernalillo and the Rio Bravo Bridge south of Albuquerque. In addition to head observations utilized by McAda and Barroll (2002), 490 additional head observations (DeWees, 2006) were utilized for calibration of the revised MRGB model by nonlinear regression with PEST. The values of parameters representing horizontal and vertical hydraulic conductivities were estimated by minimizing the objective function:

$$\sum_{i=1}^{N}\left(\omega_i h_i - \omega_i h'_i\right)^2$$

where h is the measured head for observation i, h'_i is the simulated-equivalent head to observation i, ω_i is the weight applied to observation i and its simulated equivalent, and N is the number of head observations used in the regression, which is 1,818. The head-observation weights (ω_i) utilized by McAda and Barroll (2002), applied as the inverse of the estimated variance in the measurements, were also used for the PEST calibration. Parameter adjustment during PEST calibration caused additional finite-difference cells to "go dry," which occasionally prevented computation of simulated-equivalent heads at observed locations and times by the Head-Observation Package of MODFLOW. To allow the PEST calibration to proceed under these circumstances, it was necessary to substitute alternative heads for these observations utilizing the program SIM ADJUST (Poeter and Hill, 2008).

PEST computes a "composite sensitivity" (Doherty, 2005) of each model parameter with respect to all the weighted simulated heads ($\omega_i \ h'_i$). The relative composite sensitivities of parameters included in the regression were calculated by multiplying the composite sensitivities computed at the final parameter values with their corresponding final parameter value, and are summarized in table 2.6.

The head observations common to both the McAda and Barroll (2002) model and the revised model were used to compare overall fit between the two models. For each model, the sum-of-squared unweighted residuals (SSE) were calculated for this observation subset using the equation:

$$SSE = \sum_{i=1}^{N}\left(h_i - h'_i\right)^2$$

where N is the number of head observations common to both models, which is 1,328. The *SSE* of the revised model is about 82 percent of the *SSE* of McAda and Barroll (2002) model, indicating a slightly improved overall fit for the revised model.

Simulated Hydraulic Heads

Steady-state hydraulic heads simulated with the revised model of the MRGB generally are within 10 m of reconstructed predevelopment hydraulic heads (Bexfield and Anderholm, 2000) in the vicinity of Albuquerque, along the Rio Grande, and in the southern part of the basin. Eighty-nine percent of the simulated transient hydraulic heads are within 10 m of the measured heads, and the smallest residuals occur in the area described above for the steady-state observations. The largest residuals occur near the lateral model boundaries in the same locations as large residuals discussed by McAda and Barroll (2002) and likely are due to structural-model error, which may include the possible existence of nonsimulated "perched" conditions, uncertainty of recharge, and heterogeneity of hydraulic conductivity in various forms, including faults. Bexfield and Anderholm (2000) also discussed possible causes of observed "hydraulic discontinuities" located near major faults in these areas.

Simulated heads in the area of the water-level trough noted by McAda and Barroll (2002) are as much as 48 m higher than reconstructed steady-state (Bexfield and Anderholm, 2000) heads and water levels measured at observation wells (fig. 2.15). The similar residual magnitude and construction of both models suggests that this misfit is due to similar, yet unknown, structural-model error as discussed by McAda and Barroll (2002).

The locations of 20 observation wells for which McAda and Barroll (2002) also simulated hydrographs are shown in figure 2.15*B*. Hydrographs simulated with the revised model (figure 2.16) are very similar to those presented by McAda and Barroll (2002), but an improved fit to the observed heads is apparent for five of the wells. For example, heads simulated for the Tierra Mirage observation well (fig. 2.16*C*) northeast of Albuquerque are lower and closer to observed heads than those simulated with the McAda and Barroll (2002) model. Heads simulated for four observation wells (figures 2.16*I–L*) in the Albuquerque area better represent drawdown than corresponding heads simulated by the McAda and Barroll (2002) model, which increasingly under predict head through the period of record. The higher hydraulic heads simulated for these observation wells in the revised model probably result from larger simulated vertical hydraulic conductivity and (or) simulated recharge from the water-distribution system in the Albuquerque area.

Residuals of model-simulated hydraulic heads (calculated as measured minus simulated head) are plotted against their corresponding measured values for both the steady-state and all transient stress periods in figure 2.17. Measured hydraulic heads of approximately 1,625 m have the largest residuals, which, as described above, are located south of Albuquerque along the western and eastern model boundaries (fig. 2.15). A histogram of the residual magnitudes (fig. 2.18) illustrates that most are less than 5 m. The largest negative and positive residuals are -48 and 155 m, respectively, with a median of -1.18 m, and a mean of -0.76 m. This negative model bias reflects

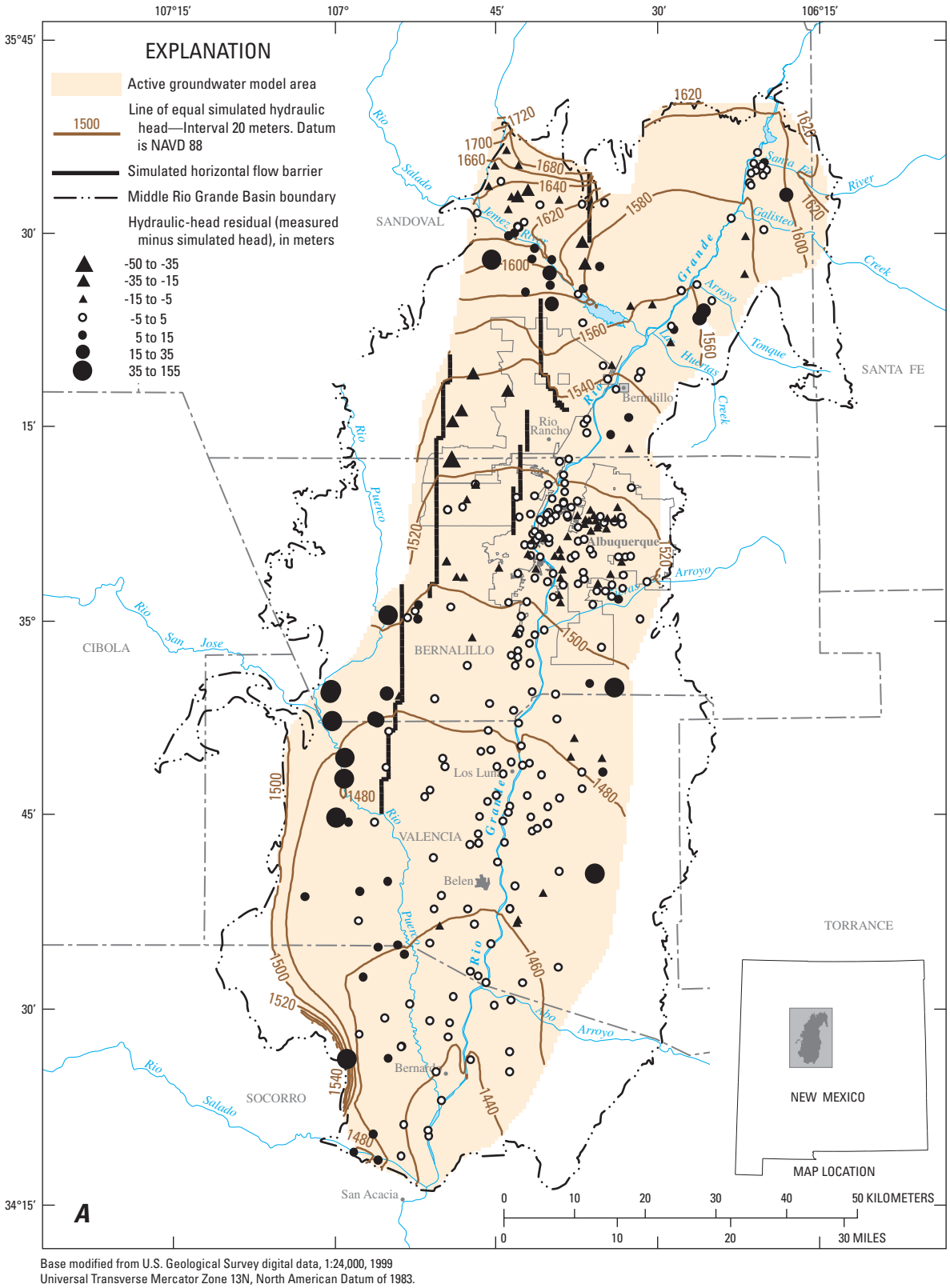

Base modified from U.S. Geological Survey digital data, 1:24,000, 1999
Universal Transverse Mercator Zone 13N, North American Datum of 1983.

Figure 2.15*A*. Simulated steady-state water table and hydraulic-head residual at each steady-state observation well, Middle Rio Grande Basin, New Mexico.

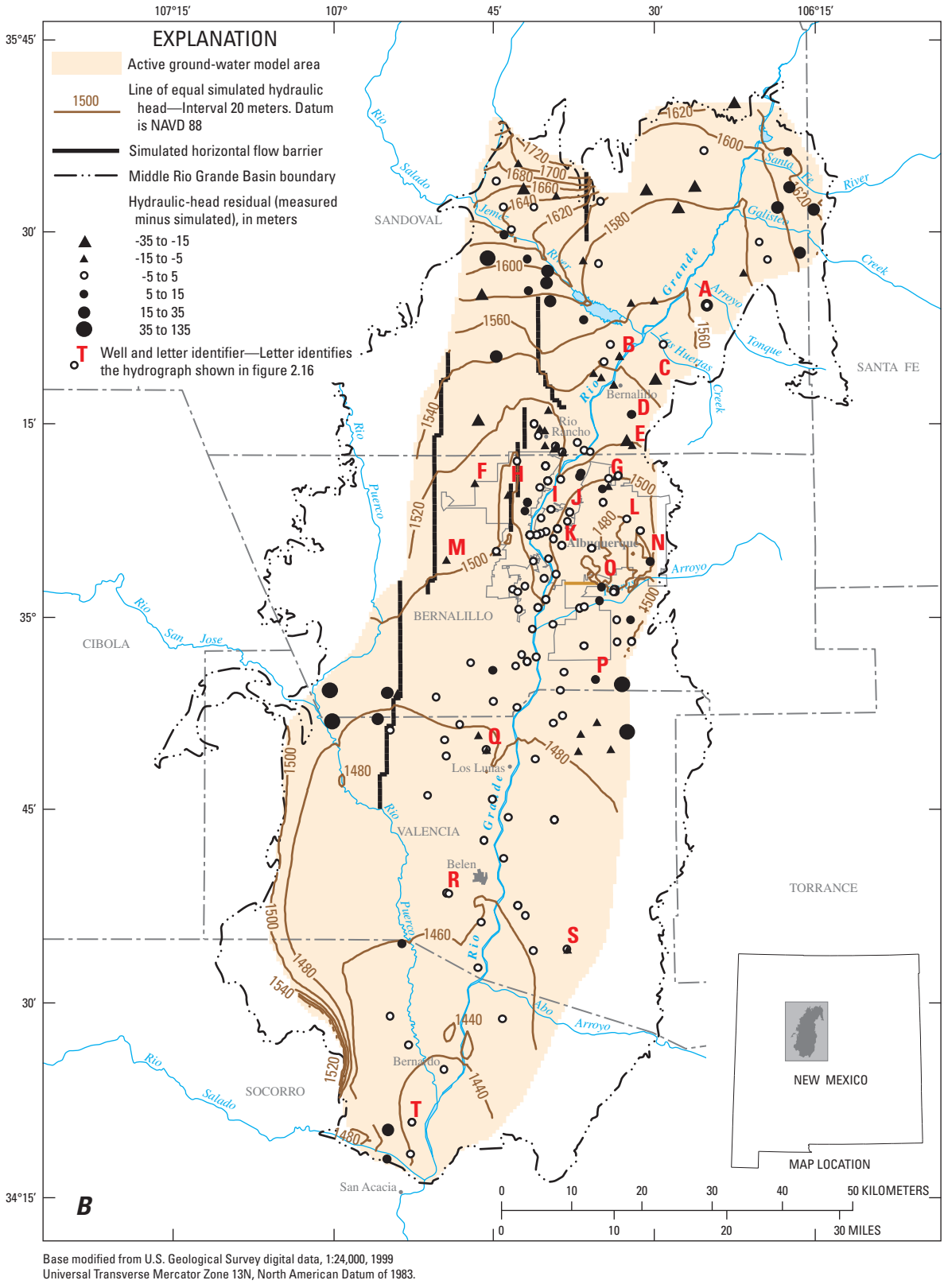

Base modified from U.S. Geological Survey digital data, 1:24,000, 1999
Universal Transverse Mercator Zone 13N, North American Datum of 1983.

Figure 2.15*B*. Simulated March 2008 water table and maximum hydraulic-head residual for the period 1900-2008 at each transient observation well for the revised groundwater-flow model, Middle Rio Grande Basin, New Mexico.

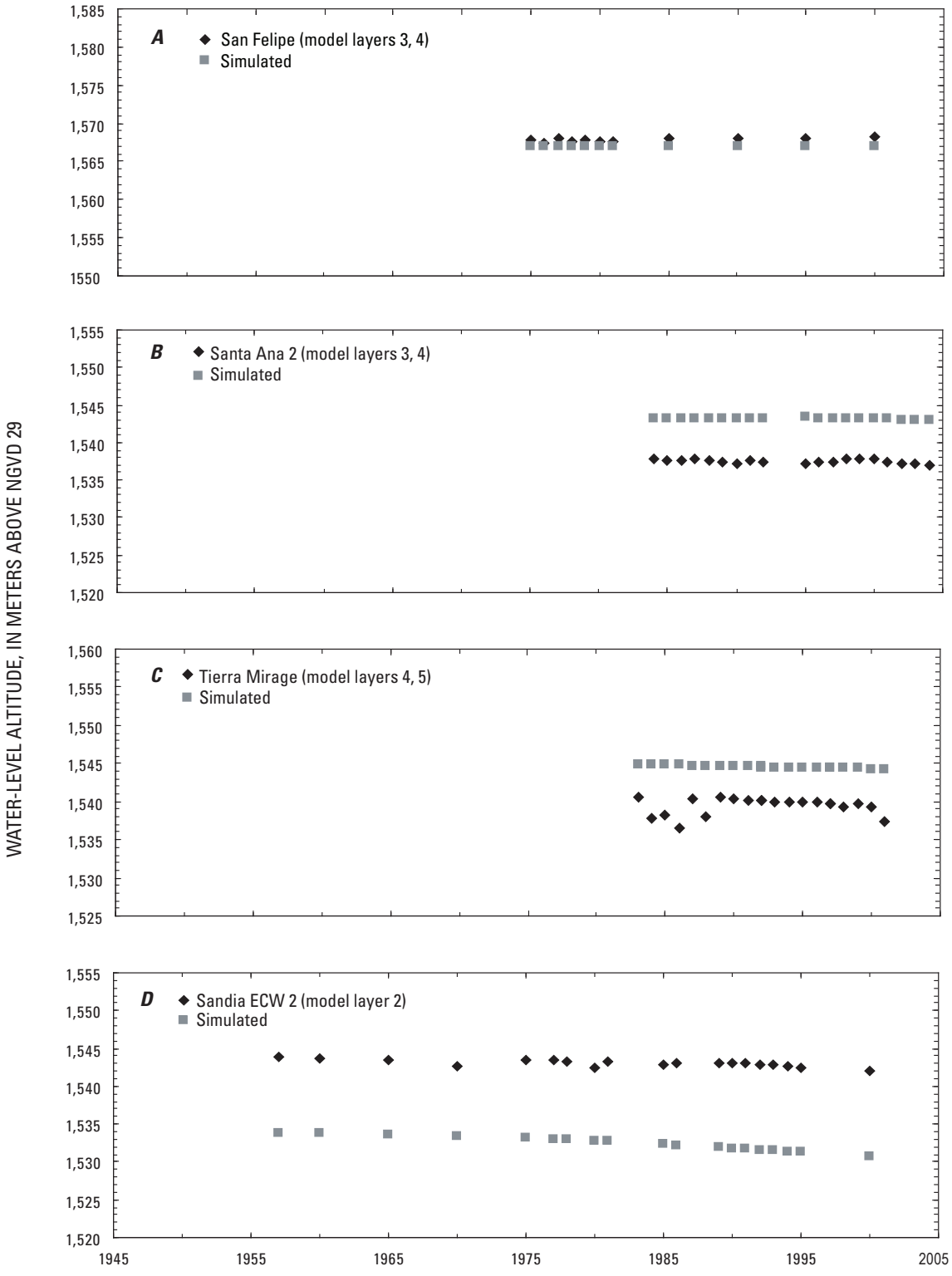

Figure 2.16*A*–*D*. Measured and simulated hydraulic heads for selected wells in the revised groundwater-flow model, Middle Rio Grande Basin, New Mexico. Well locations are shown in figure 2.15*B*. *A*, San Felipe, model layers 3 and 4; *B*, Santa Ana 2, model layers 3 and 4; *C*, Tierra Mirage, model layers 4 and 5; *D*, Sandia ECW 2, model layer 2.

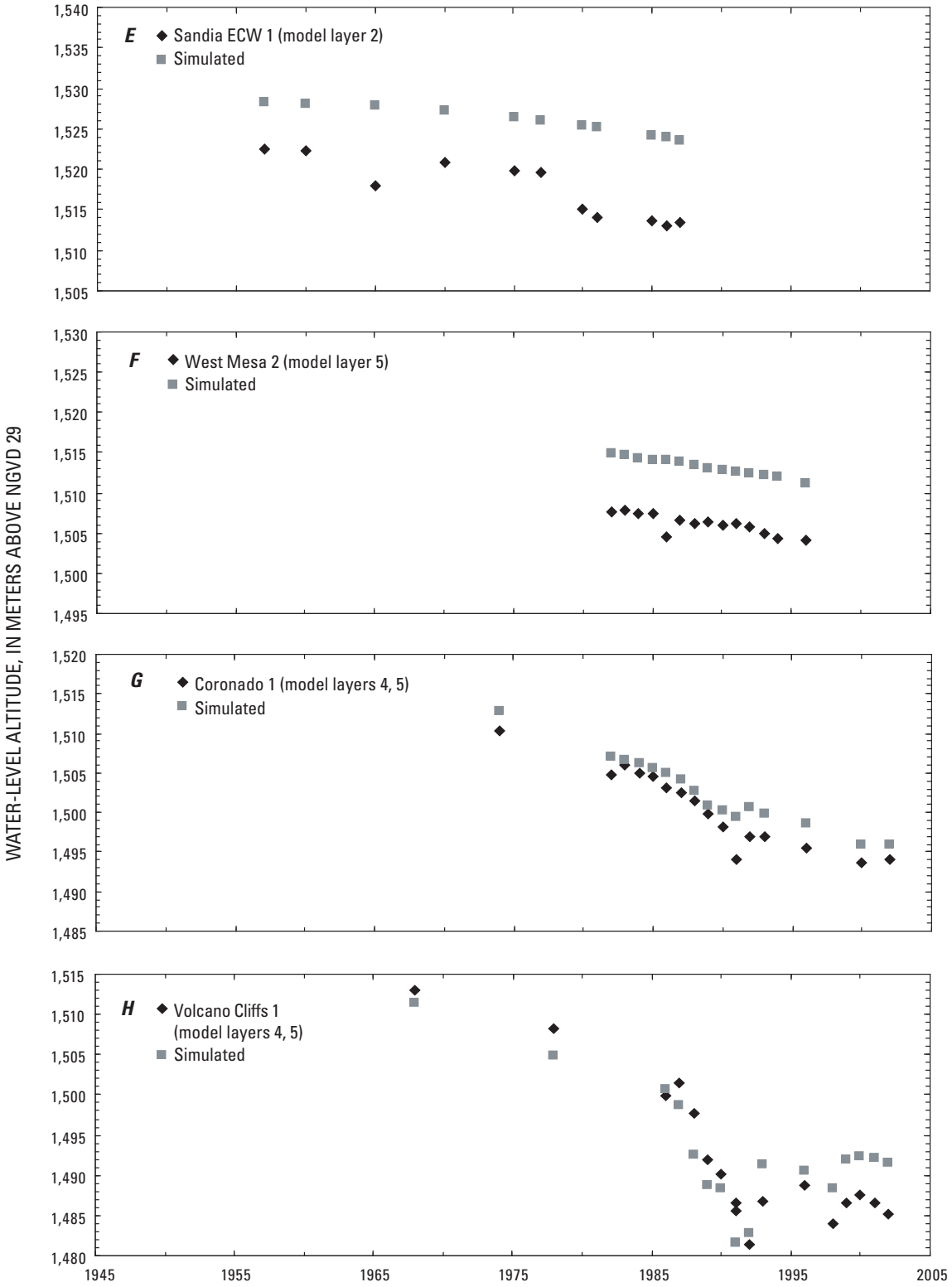

Figure 2.16*E–H*. Measured and simulated hydraulic heads for selected wells in the revised groundwater-flow model, Middle Rio Grande Basin, New Mexico. Well locations are shown in figure 2.15*B*. *E*, Sandia ECW 1, model layer 2; *F*, West Mesa 2, model layer 5; *G*, Coronado 1, model layers 4 and 5; *H*, Volcano Cliffs 1, model layers 4 and 5.

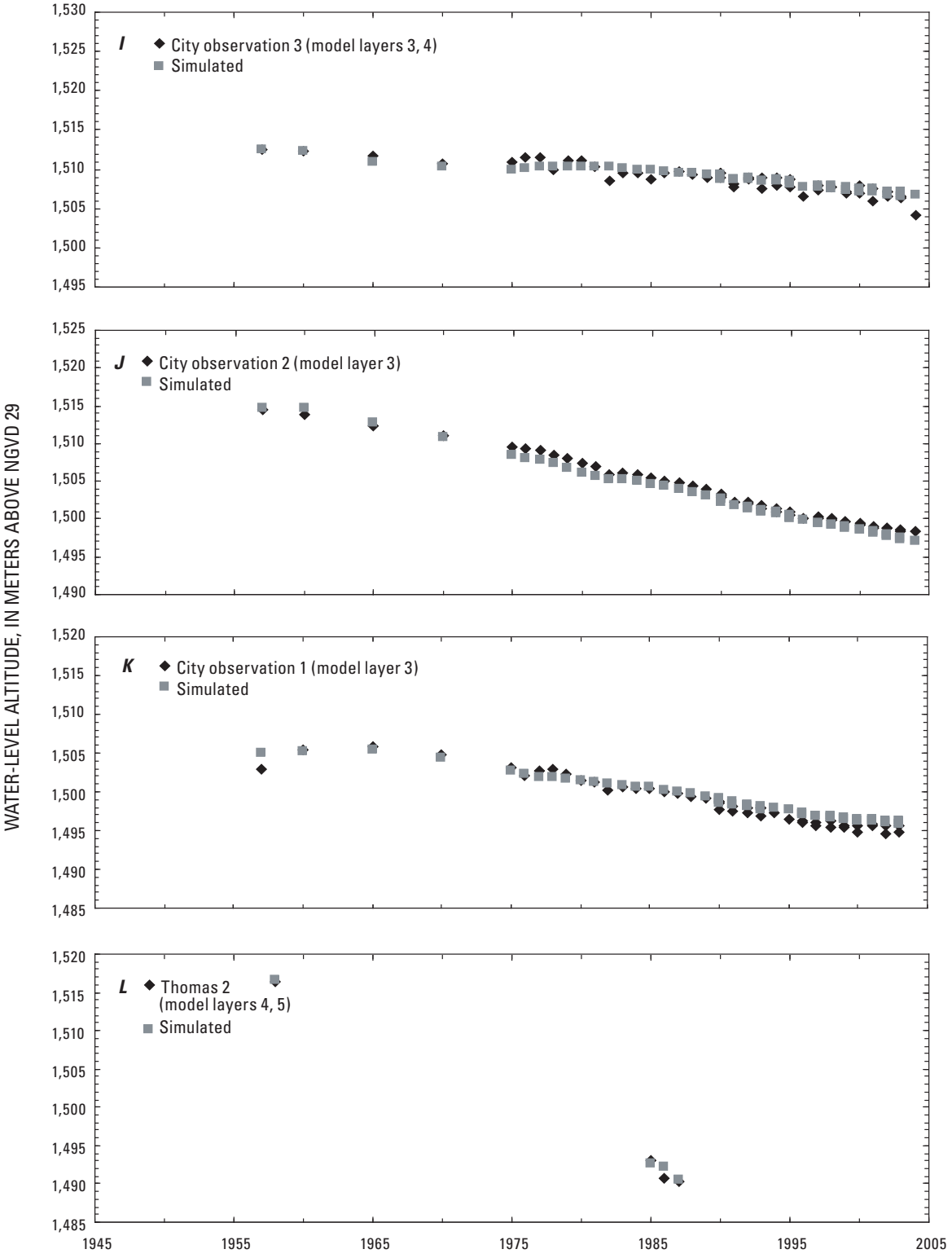

Figure 2.16*I–L*. Measured and simulated hydraulic heads for selected wells in the revised groundwater-flow model, Middle Rio Grande Basin, New Mexico. Well locations are shown in figure 2.15*B*. *I*, City Observation 3, model layers 3 and 4; *J*, City Observation 2, model layer 3; *K*, City Observation 1, model layer 3; *L*, Thomas 2, model layers 4 and 5.

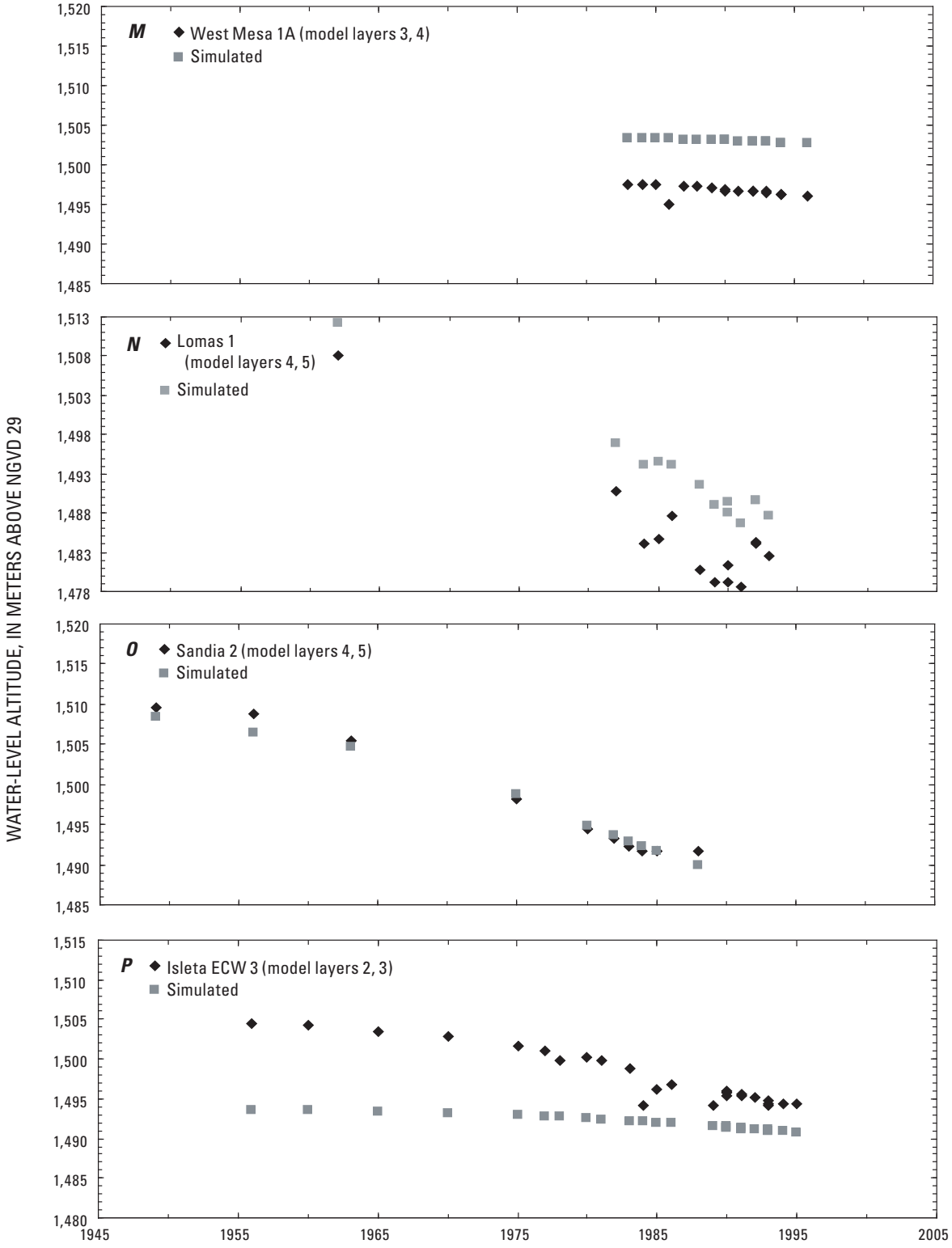

Figure 2.16*M–P*. Measured and simulated hydraulic heads for selected wells in the revised groundwater-flow model, Middle Rio Grande Basin, New Mexico. Well locations are shown in figure 2.15*B*. *M*, West Mesa 1A, model layers 3 and 4; *N*, Lomas 1, model layers 4 and 5; *O*, Sandia 2, model layers 4 and 5; *P*, Isleta ECW 3, model layers 2 and 3.

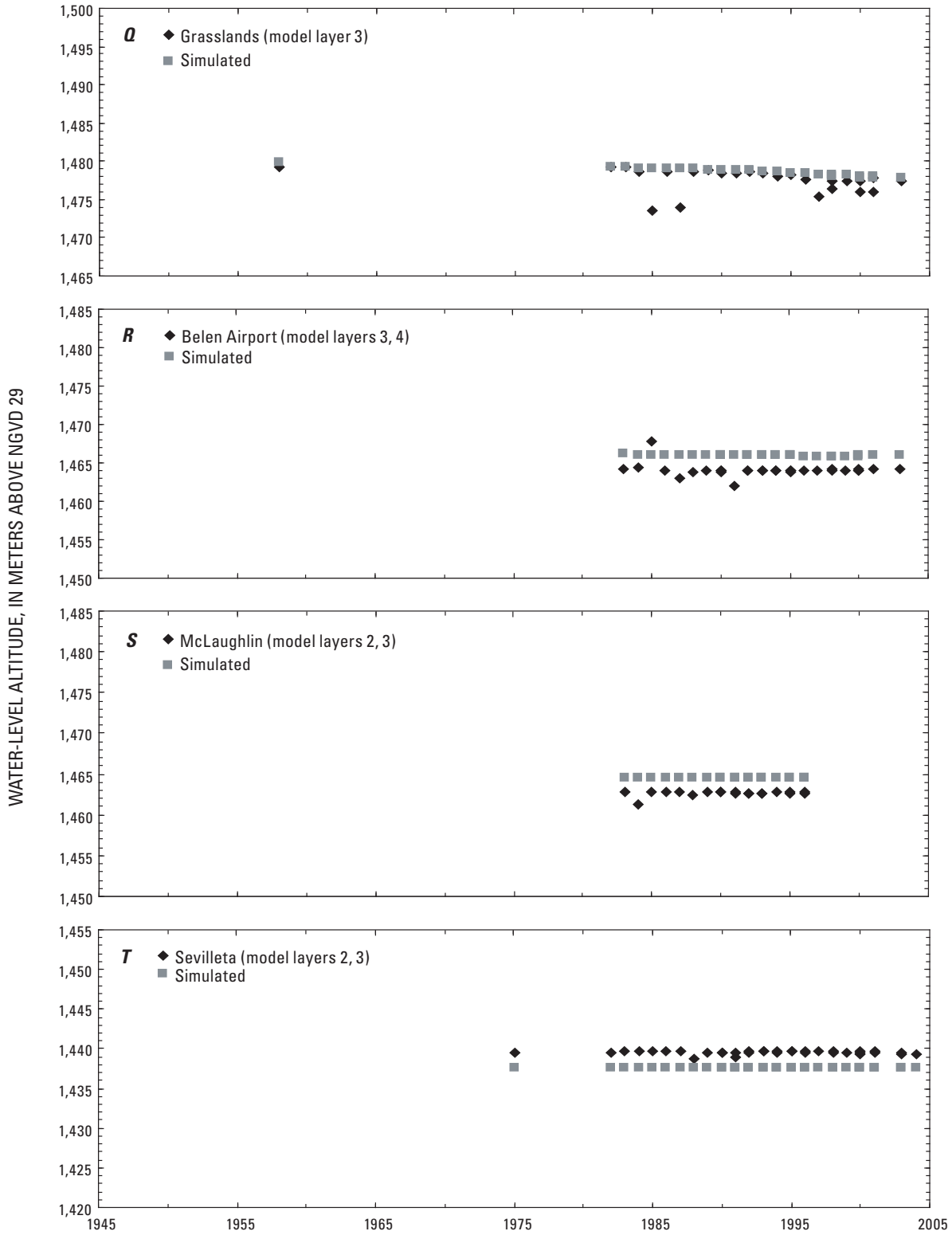

Figure 2.16*Q*–*T*. Measured and simulated hydraulic heads for selected wells in the revised groundwater-flow model, Middle Rio Grande Basin, New Mexico. Well locations are shown in figure 2.15*B*. *Q*, Grasslands, model layer 3; *R*, Belen Airport, model layers 3 and 4; *S*, McLauglin, model layers 2 and 3; *T*, Sevilleta, model layers 2 and 3.

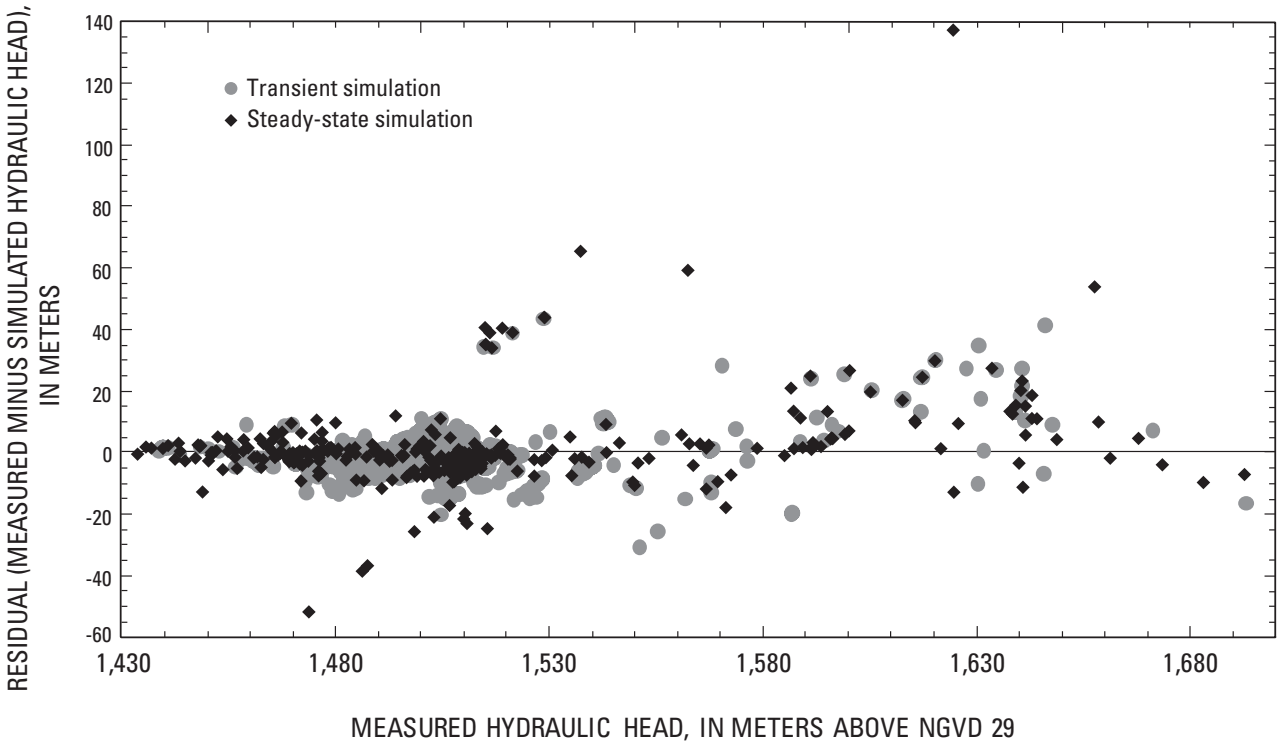

Figure 2.17 Comparison of residuals and measured hydraulic heads, steady-state and transient simulations of the revised groundwater-flow model, Middle Rio Grande Basin, New Mexico.

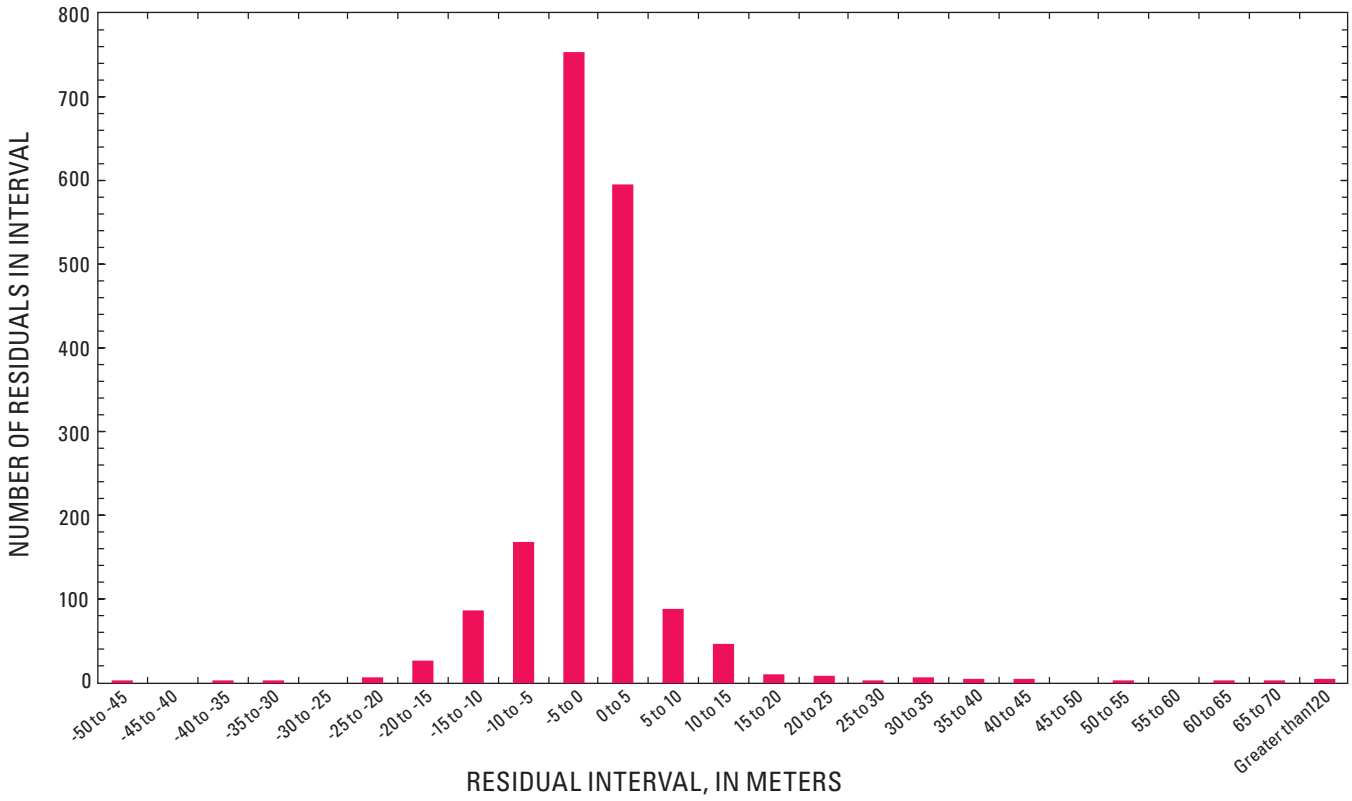

Figure 2.18 Hydraulic-head residuals from the steady-state and transient stress periods of the revised groundwater-flow model, Middle Rio Grande Basin, New Mexico. Residuals are calculated as measured minus observed heads.

structural model error possibly due to under representation of groundwater withdrawals (noted in the "Reported Groundwater Withdrawals" section), as well as error in the specification of the magnitude and spatial distribution of recharge, hydraulic conductivity, and aquifer storage properties.

Although simulated transient hydraulic-heads are within 5 m of historical measurements throughout most of the model domain (fig. 2.15*B*), measured heads are substantially higher than simulated heads near the basin margins, particularly to the west. (Likely causes of this model error are discussed above.)

Model-Computed Water Budgets

Net simulated inflow and outflow for the revised MRGB model was calculated by subtracting river leakage out of the groundwater system from the total inflows and outflows so that comparisons could be made with the original MRGB model (McAda and Barroll. 2002). The net inflow and outflow simulated with the revised MRGB model for the steady-state stress period representing predevelopment conditions was 152 x 10^6 m^3/yr (table 2.5), with a numerical discrepancy of 0.2 percent. Recharge from the Rio Grande and Jemez River account for 58 percent of the total net inflow, and subsurface, mountain-front, and tributary recharge account for the remaining 42 percent of the net inflow. The simulated net outflow is accounted for entirely by riparian evapotranspiration. Steady-state simulated river inflows and outflows totaled 106.4 x 10^6 and 18.3 x 10^6 m^3/yr, respectively.

The average net inflow and outflow simulated with the revised MRGB model for the two transient stress periods representing the year ending October 31, 1999, was 583 x 10^6 m^3/yr (table 2.5), with a numerical discrepancy of 0.07 percent. The nearly four-fold simulated increase in total net inflow and outflow from 1900 (steady state) to 1999 resulted from development of surface-water and groundwater resources. By 1999, recharge from river, lake, reservoir, canal, and irrigation accounted for 75 percent of the total net inflow, whereas subsurface, mountain-front, and tributary recharge accounted for 11 percent. The remaining net inflow (14 percent) was simulated from septic-field seepage, leakage from sewer and water-distribution systems, and aquifer storage depletion. Outflow to drains, groundwater withdrawals, and riparian evapotranspiration account for 48, 33, and 19 percent, respectively, of the total net outflow. Although outflow to rivers was also simulated during the transient stress periods, this quantity was less than simulated inflow from rivers and is therefore not apparent in the *net* total.

For the year ending October 31, 1999, the simulated net inflow from the Rio Grande and outflow to drains for the revised MRGB model (table 2.5) are smaller by 126 x 10^6 m^3/yr and 140 x 10^6 m^3/yr, respectively, than the flows simulated with the McAda and Barroll (2002) model (table 2.3). In contrast to this difference over the entire model domain, the seepage simulated from the Rio Grande in the sub-domain of the revised model between Bernalillo and the Rio Bravo Bridge south of Albuquerque (fig. 2.5) is greater than both the seepage simulated by the McAda and Barroll (2002) model and the flow loss of 2.05 x10^5 m^3/d measured by Veenhuis (2002). Whereas the river inflow simulated by the McAda and Barroll (2002) model along this reach model was 27 percent less than the Veenhuis (2002) observation, the inflow simulated by the revised model was 20 percent greater than the observation. This difference in simulated inflow results from the refined discretization of the revised model, which typically separates river and drain boundaries that coexisted in the same 1-km finite-difference cells in the McAda and Barroll (2002) model into separate 0.5-km cells. This additional simulated inflow from the river causes increased simulated outflow to nearby drains. The difference in simulated flow between layer 1 cells that contain river boundaries and underlying layer 2 cells in this reach of the Rio Grande (from Bernalillo to the Rio Bravo Bridge) south of Albuquerque is negligible (less than 0.1 percent) between the two models.

Areas Contributing Recharge to Public-Supply Wells

The revised MRGB model was used to estimate traveltime distributions, areas contributing recharge, and zones of contribution under transient conditions for 59 public-supply wells in the greater Albuquerque area using the MODPATH (Pollock, 1994) particle-tracking post processor and methods outlined in Section 1 of this professional paper chapter. The model-computed areas contributing recharge are based on advective groundwater flow and do not account for mechanical dispersion. Advection-dispersion transport simulations would likely yield larger areas contributing recharge than advective particle-tracking simulations because the effects of dispersion caused by aquifer heterogeneity would be included.

In addition to heads and cell-to-cell flows from the groundwater-flow model, the MODPATH simulation requires effective porosity to calculate groundwater-flow velocities. For particle tracking based on a steady-state groundwater-flow model, the effective porosity affects only the simulated traveltime. In contrast, for particle tracking based on a transient groundwater-flow model, both the location of flow paths and the traveltime are affected by the value chosen for effective porosity.

To examine the effects of effective porosity on traveltimes and on the areas contributing recharge, particle tracking was performed using four values of effective porosity for layer 1: 0.02, 0.08, 0.2 and 0.35. The effective porosity was assumed to decrease with depth. For the lower two values of effective porosity, the value was decreased by 0.001 for each layer. For the higher two values of effective porosity, the value was decreased by 0.01 for each layer. No measurements of effective porosity are known to exist for the Santa Fe Group aquifer system. The effective porosity for a sand aquifer is probably closest to 0.35; however, use of a range of values accounts for groundwater-velocity variations resulting from

hydraulic-conductivity variations on a scale that cannot be incorporated in a regional-scale model.

Figure 2.19 shows the median simulated distribution of traveltimes of water to the 59 wells for the four simulated effective porosities. Particles were tracked backwards from the wells from a starting time of June 2005. The median simulated distribution of traveltimes was computed by using the median of the percentage of water in the wells with a traveltime less than the given year for each yearly increment based on all the simulated areas contributing recharge, and will be referred to hereafter as the distribution for the "typical" well. The distribution of these traveltimes for the typical well ranged from less than 10 years to more than 10,000 years; the shortest traveltimes coincide with the smallest effective porosity. Traveltimes of 100 years or less were observed for about 95 percent of the water entering the typical well when an effective porosity of 0.02 was simulated and 25 percent for an effective porosity of 0.08. For simulated effective porosities of 0.2 and 0.35, nearly all traveltimes to the typical well exceeded 400 years. These results indicate that for most public-supply wells in the greater Albuquerque area that contain tracers of young recharge, such as trichlorotrifluoroethane (CFC-113), either some percentage of the zones of contribution to these wells have effective porosities in the range of around 0.10 or smaller or the tracers arrive at these wells through some other fast pathways that are not adequately represented in the model.

The simulated traveltime distributions for water entering the public-supply wells were used with input histories of CFC-113 and ^{14}C to compute the concentrations of these tracers at the wells where there were corresponding measurements (37 wells for CFC-113, 13 wells for ^{14}C). To compute the concentrations of the CFC-113, the traveltime for each particle associated with a well was subtracted from the year when the well was sampled, and then that resulting year was matched against the input history for CFC-113. For ^{14}C, the initial activity was considered to be a value of 100 percent

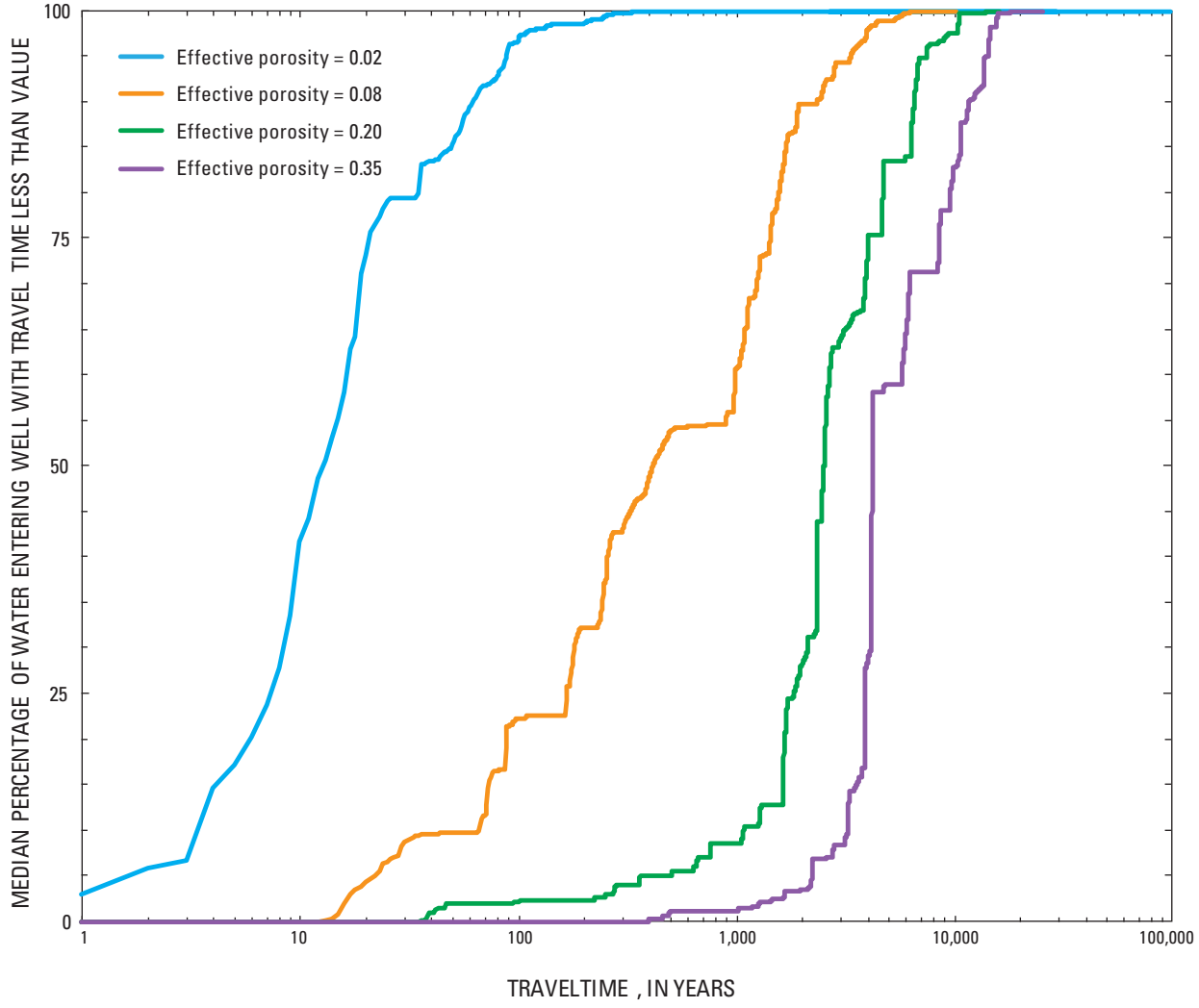

Figure 2.19. Median simulated distributions of traveltimes of groundwater to 59 public-supply wells under transient conditions with the revised groundwater-flow model, Middle Rio Grande Basin, New Mexico.

modern carbon. This value was decayed based on an exponential decay rate corresponding to a half life of 5,730 years and the traveltime of each particle, and the resulting concentration also was expressed as percent modern carbon. A volume-weighted average of the individual tracer concentrations for all of the particles was computed as the concentration that would be measured in the well.

Figure 2.20 shows box plots of the measured tracer concentrations (^{14}C data from Plummer and others [2004a] and CFC-113 data from Plummer and others [2004a] and from wells sampled for the TANC study, as described in Section 1 of this professional paper chapter), as well as the simulated concentrations based on the four different effective porosities. The distribution for the measured CFC-113 concentrations is most similar to the distribution of simulated values using the effective porosity of 0.08. The percent modern carbon values of ^{14}C, in contrast, are best matched by an effective porosity of 0.35. The results of these comparisons indicate that no single effective porosity is sufficient to match the measured data. Different effective porosities yield different groundwater velocities and, in reality, there are likely a wide range of groundwater velocities in the aquifer due to variation in hydraulic conductivity and effective porosity that cannot be adequately represented in a regional model such as the one presented here. Most flow paths probably have a groundwater velocity best represented by an effective porosity near 0.35, although some flow paths through the system likely have groundwater velocities represented by an effective porosity as low as 0.02. The composite of different velocities is reflected in the wells where tracers introduced into the atmosphere since the 1940s are detected, although the age implied by ^{14}C is thousands of years.

By comparing figures 2.21*A–D*, one can see that the size of the zone of contribution and the size of the area contributing recharge where traveltime to the well is less than 100 years decrease with increasing effective porosities. Although most flow and recharge occurs through contribution zones and recharge areas delineated with the larger effective porosities, the larger contribution zones and recharge areas for traveltimes less than 100 years shown with an effective porosity of 0.02 are important in showing areas that might be able to contribute flow and anthropogenic contaminants relatively quickly to public-supply wells.

The simulated directions of flow and areas contributing recharge to wells vary based on the position of a well in the valley. The wells to the west of the Rio Grande generally have flow paths from the northwest with the main source of water being the Jemez River. This result is in contrast to previous investigations that determined the Jemez River was primarily a gaining stream (Craig, 1992) and that "infiltration from the Jemez River appears to be limited primarily to a relatively narrow and shallow area located directly along the river" (Plummer and others, 2004a). The wells on the east side, but close to the Rio Grande, generally have flow paths flowing from the northwest, north, and northeast with sources of water mainly from the Jemez River, Rio Grande, and subsurface flow along the northern boundary. The wells in the far east of the valley generally have flow paths from the northeast with the main source of water being mountain-front recharge along the eastern side of the valley. An example of the pathlines representing each of these general flow patterns is shown in figure 2.21*B* in blue, green, and brown, respectively. The traveltimes of less than 100 years are generally from areas where either urban recharge or seepage from the Rio Grande is occurring.

Limitations and Appropriate Use of the Model

The revised groundwater-flow model for the MRGB was designed to evaluate the water budget under both steady-state and modern conditions from1900 to 2008, approximately delineate areas contributing recharge to public-supply wells, and support future local data-collection and modeling efforts. Like any numerical groundwater model, the revised MRGB model is a simplified representation of the physical system, and it is intended to simulate the general characteristics of that system rather than detailed local attributes. In particular, the model of the MRGB was designed to be suitable for regional-scale, rather than local-scale, applications. In addition, the model calibration is nonunique, meaning that a different combination of model parameter values could produce a similar simulated hydraulic-head distribution. Limitations inherent to the model, assumptions and simplifications made during model development, and errors in the conceptual model of the physical characteristics of the system all constrain the appropriate use of the model.

Detailed simulation of shallow groundwater flow between the Rio Grande, various canals, and drains within the Rio Grande inner valley may be limited by the 500-m finite-difference-cell spacing. Although the simulated interaction between these features is improved over the 1,000-m finite-difference-cell spacing of the McAda and Barroll (2002) model, in which boundary conditions representing these features are often collocated in the same finite-difference cell, a finer spatial discretization would likely be necessary to adequately simulate flow between the Rio Grande and individual canals and drains.

Model-computed areas contributing recharge and traveltimes through zones of contribution to public-supply wells have multiple sources of uncertainty. For example, error in the model's representation of the hydrologic system in the northern part of the MRGB might contribute to the simulation of infiltration from the Jemez River into the aquifer system, which is contrary to the interpretation of some previous investigations (Craig, 1992; Plummer and others, 2004a). If this simulated source of water from the Jemez River is not representative of actual conditions, the simulated zones of contribution from the northwest to wells on the west side of the Rio Grande may be in error. Other substantial sources of uncertainty are related to the long flow paths and residence times of groundwater in the MRGB. The groundwater-flow model was designed to simulate the regional groundwater system during the time period from 1900 to 2008, which is when

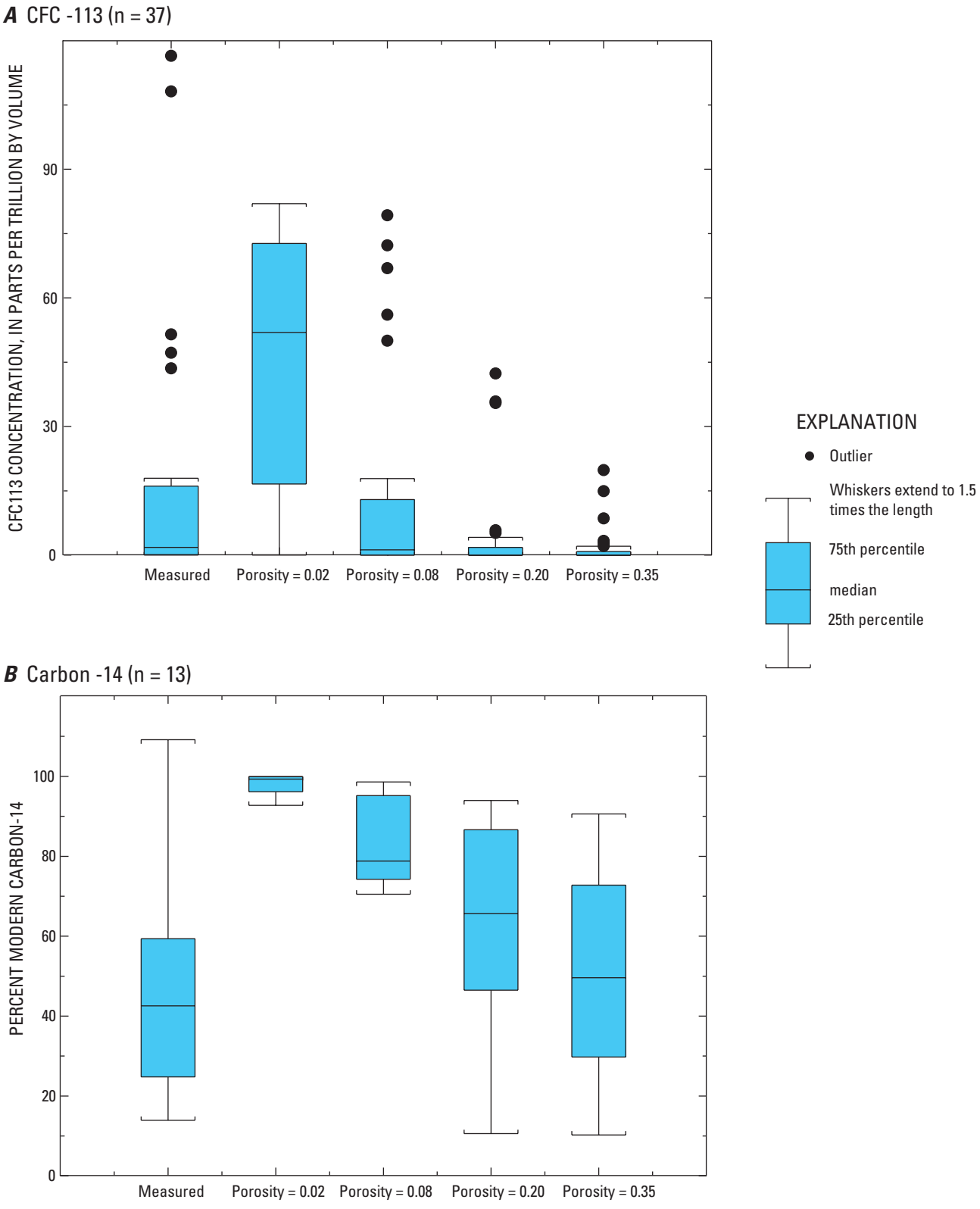

Figure 2.20. Distributions of measured and simulated *A*, trichlorotrifluoroethane (CFC-113) concentrations and *B*, carbon-14 values in public-supply wells simulated under transient conditions with the revised groundwater-flow model, Middle Rio Grande Basin, New Mexico. (Measured carbon-14 data from Plummer and others , 2004a, and CFC-113 data from Plummer and others, 2004a, and from wells sampled for the Transport of Anthropogenic and Natural Contaminants study, as described in Section 1 of this professional paper chapter)

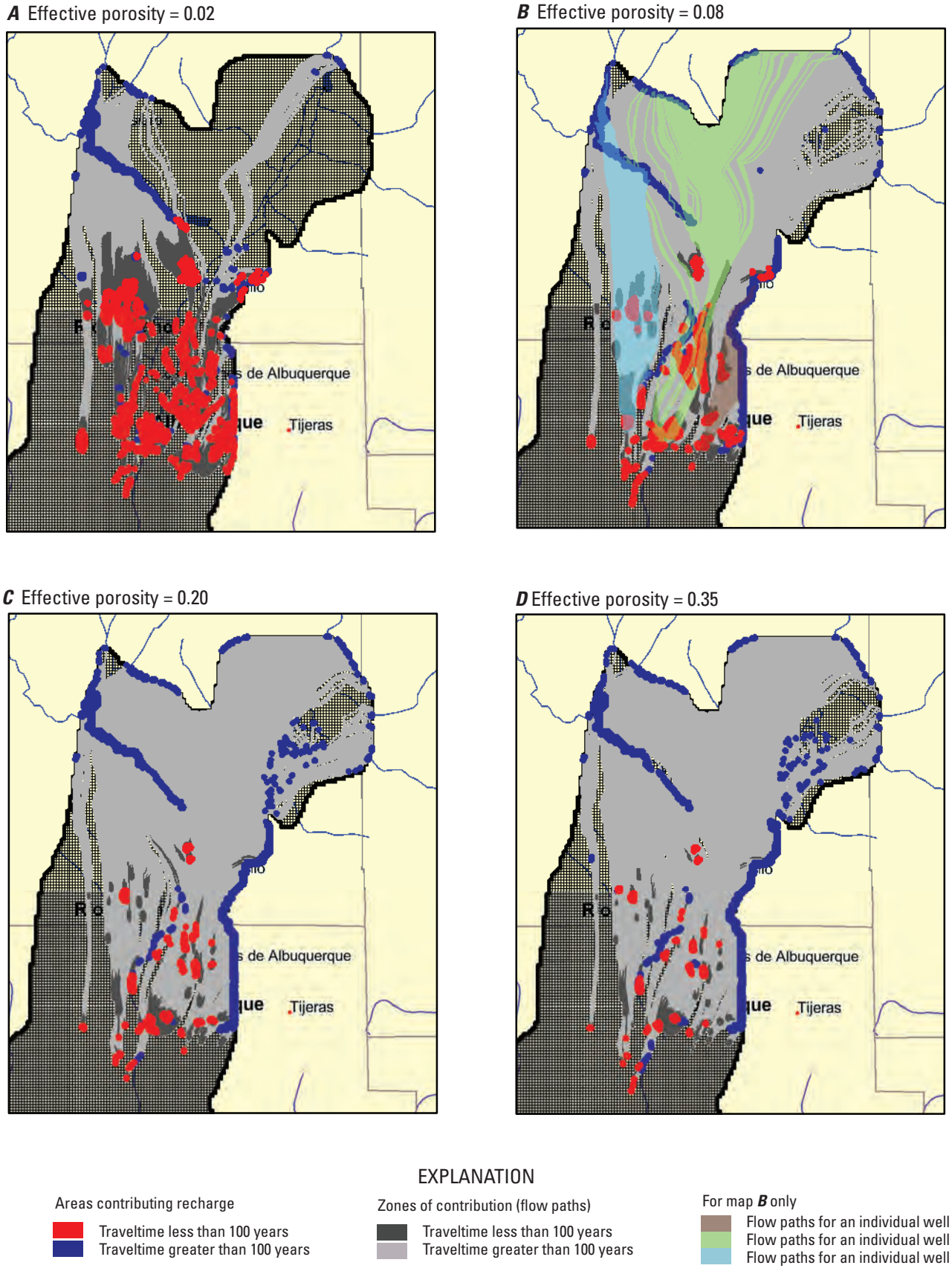

Figure 2.21. Areas contributing recharge and zones of contribution to 59 public-supply wells for effective porosities of *A*, 0.02, *B*, 0.08, *C*, 0.2, and *D*, 0.35 in the revised groundwater-flow model, regional study area, Middle Rio Grande Basin, New Mexico.

observations of important hydrologic characteristics—such as position of the Rio Grande and groundwater levels —were available or could be estimated. In contrast, as discussed in the "Groundwater Age" section, estimated residence times of groundwater to wells throughout most of the basin are thousands to tens of thousands of years. These long residence times are partly the result of recharge occurring primarily along basin margins and surface-water features, which can be located tens of kilometers from the public-supply wells to which the recharge contributes.

The comparison of simulated and measured tracer concentrations indicates the limitation of the model to correctly simulate the actual mix of traveltimes to wells, given the parameterization of effective porosity and hydraulic conductivity used in the model. The traveltime distribution for any given well should be considered to be some combination of the traveltime distributions from the various values of effective porosity used. However, the exact proportion of each is uncertain, depending on the actual heterogeneity of the aquifer materials existing in the zone of contribution to the wells.

Although inherent sources of uncertainty affect the accuracy of the areas contributing recharge and traveltimes through zones of contribution simulated with the revised MRGB model for groundwater that recharged the aquifer at any time, estimates of these characteristics for groundwater likely to have recharged more than about 100 years ago are especially uncertain. Backward particle tracking was conducted using the steady-state stress period (during which simulated hydrologic conditions are constant) to simulate all times prior to 1900. However, these simulated steady-state conditions could differ considerably from actual historical conditions. In particular, several thousands of years ago factors that could have resulted in substantially different groundwater-flow characteristics than those simulated include climatic changes that altered the quantity and distribution of recharge, which would cause changes to the hydraulic-head distribution and, consequently, both flow directions and velocities. Evidence that such climatic changes have occurred is provided by Plummer and others (2004a), who also used chemical and isotopic data to infer groundwater source areas, flowpaths, and traveltimes that in some cases differ considerably from those simulated with the model.

Although the simulation of contributing areas and traveltimes with the MRGB groundwater-flow model is limited by inherent uncertainty, the simulated results are useful, particularly for order-of-magnitude comparisons with other TANC study areas. For example, knowledge that, unlike most other TANC study areas, a substantial percentage of water contributed to wells in the MRGB regional study area was recharged more than 100 years ago (prior to most human development) provides valuable information for assessing relative vulnerability of the wells in the different study areas to contamination.

The revised MRGB groundwater-flow model, which uses previously specified boundary conditions and newly calibrated aquifer hydraulic conductivities, provides a representation of groundwater flow conditions for 1900 to 2008. The model is suitable for evaluating regional water budgets and groundwater-flow paths in the study area from 1900 to 2008, but has limited utility in determining flow characteristics prior to this time period and may not be suitable for long-term predictive simulations. This regional model provides a tool to evaluate aquifer vulnerability at a regional scale, to facilitate order-of-magnitude comparisons of groundwater traveltime between regional aquifer systems, and to guide future detailed investigations in the study area.

References Cited

Anderholm, S.K., 1988, Ground-water geochemistry of the Albuquerque-Belen Basin, Central New Mexico: U.S. Geological Survey Water-Resources Investigations Report 86–4094, 110 p.

Anderholm, S.K., 1997, Water-quality assessment of the Rio Grande valley, Colorado, New Mexico, and Texas—shallow ground-water quality and land use in the Albuquerque area, central New Mexico, 1993: U.S. Geological Survey Water-Resources Investigations Report 97–4067, 73 p.

Anderholm, S.K., 2001, Mountain-front recharge along the east side of the Albuquerque Basin, Central New Mexico (revised): U.S. Geological Survey Water-Resources Investigations Report 00–4010, 36 p.

Banta, E.R., 2000, MODFLOW-2000, the U.S. Geological Survey modular ground-water model—documentation of packages for simulating evapotranspiration with a segmented function (ETS1) and drains with return flow (DRT1): U.S. Geological Survey Open-File Report 00–466, 127 p.

Bartolino, J.R., and Cole, J.C., 2002, Ground-water resources of the Middle Rio Grande Basin, New Mexico: U.S. Geological Survey Circular 1222, 132 p.

Bexfield, L.M., and Anderholm, S.K., 2000, Predevelopment water-level map of the Santa Fe Group aquifer system in the Middle Rio Grande Basin between Cochiti Lake and San Acacia, New Mexico: U.S. Geological Survey Water-Resources Investigations Report 00–4249, 1 sheet.

Bexfield, L.M., and Anderholm, S.K., 2002a, Estimated water-level declines in the Santa Fe Group aquifer system in the Albuquerque area, central New Mexico, predevelopment to 2002: U.S. Geological Survey Water-Resources Investigations Report 02–4233, 1 sheet.

Bexfield, L.M., and Anderholm, S.K., 2002b, Spatial patterns and temporal variability in water quality from City of Albuquerque drinking-water supply wells and piezometer nests, with implications for the ground-water flow system: U.S. Geological Survey Water-Resources Investigations Report 01–4244, 101 p.

Bexfield, L.M., and Plummer, L.N., 2003, Chapter 11—Occurrence of arsenic in ground water of the Middle Rio Grande Basin, central New Mexico, *in* Welch, A.H., and Stollenwerk, K.G., eds., Arsenic in ground water—Geochemistry and occurrence: Boston, Kluwer Academic Publishers, p. 295–327.

Bjorklund, L.J., and Maxwell, B.W., 1961, Availability of ground water in the Albuquerque area, Bernalillo and Sandoval Counties, New Mexico: New Mexico State Engineer Technical Report 21, 117 p.

Bureau of Reclamation, 1973, Progress report—Phreatophyte investigations—Bernardo evapotranspirometers: Albuquerque, Middle Rio Grande Project Office, 50 p.

Camp Dresser & McKee, 1998, City of Albuquerque Water Conservation Program Evaluation: Sanitary Sewer Exfiltration Analysis: consulting report to the City of Albuquerque [variously paged].

CH2MHill, 1999, City of Albuquerque Public Works Department water resources strategy implementation, diversion options task 2.1.1.1.3, Hydrogeologic field investigation report: Consultant's report prepared for the City of Albuquerque Public Works Department: [variously paged].

City of Albuquerque, 2003, San Juan-Chama Diversion Project: accessed August 2003 at *http://www.cabq.gov/waterresources/sjc.html.*

City of Albuquerque, 2009, Distribution system water loss: accessed May 2009 at *http://www.cabq.gov/progress/public-infrastructure/dcc-17/indicator-17-2.*

Cole, J.C., 2001a, 3-D geologic modeling of regional hydrostratigraphic units in the Albuquerque segment of the Rio Grande Rift, *in* Cole, J.C., ed., U.S. Geological Survey Middle Rio Grande Basin Study—Proceedings of the Fourth Annual Workshop, Albuquerque, New Mexico, February 15–16, 2000: U.S. Geological Survey Open-File Report 00–488, p. 26–28.

Cole, J.C., ed., 2001b, U.S. Geological Survey Middle Rio Grande Basin Study—Proceedings of the Fourth Annual Workshop, Albuquerque, New Mexico, February 15–16, 2000: U.S. Geological Survey Open-File Report 00–488, 57 p.

Connell, S.D., 1997, Geology of Alameda quadrangle, Bernalillo and Sandoval Counties, New Mexico: Socorro, New Mexico Bureau of Mines and Mineral Resources Open-File Digital Map Series OF–DM–10, last modified September 16, 1999, 1 sheet.

Connell, S.D., 2006, Preliminary geologic map of the Albuquerque-Rio Rancho metropolitan area and vicinity, Bernalillo and Sandoval Counties, New Mexico: New Mexico Bureau of Geology and Mineral Resources Open-File Report 496, 2 pls.

Connell, S.D., Allen, B.D., and Hawley, J.W., 1998, Subsurface stratigraphy of the Santa Fe Group from borehole geophysical logs, Albuquerque area, New Mexico: New Mexico Geology, v. 20, no. 1, p. 2–7.

Craig, S.D., 1992, Water Resources on the Pueblos of Jemez, Zia, and Santa Anna, Sandoval County, New Mexico: U.S. Geological Survey Water-Resources Investigations Report 89–4091, 122 p., 4 pls.

DeWees, R.K., 2003, Water-level data for the Albuquerque Basin and adjacent areas, Central New Mexico, period of record through 2002: U.S. Geological Survey Open-File Report 03–321, 41 p.

DeWees, R.K., 2006, Water-level data for the Albuquerque Basin and adjacent areas, Central New Mexico, period of record through 2004: U.S. Geological Survey Open-File Report 2006–1281, 40 p.

Doherty, John, 2005, PEST: model-independent parameter estimation, user manual (5th ed.): Watermark Numerical Computing, Corinda, Australia, 336 p.

Feller, Mark R., and Hester, David J., 2001, SLEUTH Urban Landscape Change 2050 Calibration and Prediction datasets covering (16) 1:24,000-scale quadrangles within the Albuquerque, New Mexico Metropolitan Statistical Area, distributed to the New Mexico Bureau of Geology and Mineral Resources.

Fenneman, N.M., 1931, Physiography of the Western United States: New York, McGraw-Hill, 534 p.

Grant, P.R., Jr., 1999, Subsurface geology and related hydrologic conditions, Santa Fe Embayment and contiguous areas, New Mexico, *in* Pazzaglia, F.J., and Lucas S.G., eds., Albuquerque Geology, New Mexico Geological Society Fiftieth Annual Field Conference, September 22–25, 1999: Socorro, New Mexico Geological Society, p. 425–435.

Grauch, V.J.S., Gillespie, C.L., and Keller, G.R., 1999, Discussion of new gravity maps for the Albuquerque Basin area, *in* Pazzaglia, F.J., and Lucas, S.G., eds., Albuquerque Geology, New Mexico Geological Society Fiftieth Annual Field Conference, September 22–25, 1999: Socorro, New Mexico Geological Society, p. 119–124.

Grauch, V.J.S., Hudson, M.R., Minor, S.A., 2001, Aeromagnetic expression of faults that offset basin fill, Albuquerque Basin, New Mexico: Geophysics, v. 66, no. 3, p. 707–720.

Halford, K.J and Hanson, R.T., 2002, User guide for the drawdown-limited Multi-Node Well (MNW) package for the U.S. Geological Survey's modular three-dimensional finite-difference ground-water flow model, versions MODFLOW-96 and MODFLOW-2000: U.S. Geological Survey Open-File Report 02–293, 33 p.

Harbaugh, A.W., 2005, MODFLOW-2005, the U.S. Geological Survey modular ground-water model—the Ground-Water Flow Process: U.S. Geological Survey Techniques and Methods 6–A16 [variously paged].

Hawley, J.W., 1996, Hydrogeologic framework of potential recharge areas in the Albuquerque Basin, central New Mexico: New Mexico Bureau of Mines and Mineral Resources Open-File Report 402D, chap. 1, 68 p.

Hawley, J.W., and Haase, C.S., 1992, Hydrogeologic framework of the northern Albuquerque Basin: Socorro, New Mexico Bureau of Mines and Mineral Resources Open-File Report 387 [variously paged].

Hawley, J.W., and Haase, C.S., and Lozinsky, R.P., 1995, An underground view of the Albuquerque Basin, *in* Ortega-Klett, C.T., ed., The water future of Albuquerque and the Middle Rio Grande Basin: Proceedings of the 39th Annual New Mexico Water Conference, November 3–4, 1994: New Mexico Water Resources Research Institute WRRI Report no. 290, p. 37–55.

Heywood, C.E., 1998, Piezometric-extensometric estimations of specific storage in the Albuquerque Basin, New Mexico, *in* Borchers, J.E., ed., Land subsidence case studies and current research: Proceedings of the Dr. Joseph F. Poland Symposium, Special Publication No. 8, Association of Engineering Geologists, Sacramento Section and Association of Engineering Geologists Subsidence Committee: Belmont, Calif., Star Publishing Company, p. 435–440.

Heywood, C.E., 2001, Piezometric-extensometric test results, *in* Thorn, C.R., Analytical results of a long-term aquifer test conducted near the Rio Grande, Albuquerque, New Mexico: U.S. Geological Survey Water-Resources Investigations Report 00–4291, p. 8–11.

Homer, C. Huang, C., Yang, L., B. Wylie B., and Coan, M., 2004, Development of a 2001 National Landcover Database for the United States: Photogrammetric Engineering and Remote Sensing, v. 70, no. 7, July 2004, p. 829–840, accessed Sept. 14, 2010, at *http://www.mrlc.gov/*.

Kernodle, J.M., McAda, D.P., and Thorn, C.R., 1995, Simulation of ground-water flow in the Albuquerque Basin, central New Mexico, 1901–1994, with projections to 2020: U.S. Geological Survey Water-Resources Investigations Report 94–4251, 114 p.

Kernodle, J.M., and Scott, W.B., 1986, Three-dimensional model simulation of steady-state ground-water flow in the Albuquerque-Belen Basin, New Mexico: U.S. Geological Survey Water-Resources Investigations Report 84–4353, 58 p.

Kinkel, B., 1995, Estimates of consumptive use requirements for irrigated agriculture and riparian vegetation, v. I: Bureau of Reclamation Albuquerque Area Office, Middle Rio Grande Water Assessment Supporting Document no. 6, 31 p.

Lee, W.T., 1907, Water resources of the Rio Grande valley and their development: U.S. Geological Survey Water-Supply Paper 188, 59 p.

Logan, L.M., 1990, Geochemistry of the Albuquerque municipal area, Albuquerque, New Mexico: Socorro, New Mexico Institute of Mining and Technology, Independent study, 234 p.

Lozinsky, R.P., 1994, Cenozoic stratigraphy, sandstone petrology, and depositional history of the Albuquerque basin, central New Mexico: Geological Society of American Special Paper 291, p. 73–82.

McAda, D.P., 2001, Simulation of a long-term aquifer test conducted near the Rio Grande, Albuquerque, New Mexico: U.S. Geological Survey Water-Resources Investigations Report 99–4260, 66 p.

McAda, D.P., and Barroll, Peggy, 2002, Simulation of groundwater flow in the Middle Rio Grande Basin between Cochiti and San Acacia, New Mexico: U.S. Geological Survey Water-Resources Investigations Report 02–4200, 81 p.

Meeks, T.O., 1949, The occurrence of ground water in the Tijeras Soil Conservation District, Bernalillo County, New Mexico: U.S. Department of Agriculture Regional Bulletin 109, Geological Series I, Soil Conservation Service Region 6 [variously paged].

New Mexico Environmental Finance Center, 2006, Review of leak and repair data, phase 1 report prepared for the Albuquerque Bernalillo County Water Utility Authority: 91 p.

Planert, Michael, and Williams, J.S., 1995, Ground water atlas of the United States—California and Nevada: U.S. Geological Survey Hydrologic Atlas 730–B, 28 p. (Also available at *http://pubs.usgs.gov/ha/ha730/ch_b/index.html.)*

Plummer, L.N., Bexfield, L.M., Anderholm, S.K., Sanford, W.E., and Busenberg, Eurybiades, 2004a, Geochemical characterization of ground-water flow in the Santa Fe Group aquifer system, Middle Rio Grande Basin, New Mexico: U.S. Geological Survey Water-Resources Investigations Report 03–4131, 395 p.

Plummer, L.N., Bexfield, L.M., Anderholm, S.K., Sanford, W.E., and Busenberg, Eurybiades, 2004b, Hydrochemical tracers in the Middle Rio Grande Basin, USA—1. Conceptualization of groundwater flow: Hydrogeology Journal, v. 12, no. 4, p.359–388.

Plummer, L.N., Sanford, W.E., Bexfield, L.M., Anderholm, S.K., and Busenberg, Eurybiades, 2004c, Using chemical data and aquifer simulation to characterize recharge and groundwater flow in the Middle Rio Grande Basin, New Mexico, *in* Hogan, J.F., Phillips, F.M., and Scanlon, B.R., eds., Groundwater recharge in a desert environment—the Southwestern United States, Water Science and Applications Series, v. 9: Washington, D.C., American Geophysical Union, p. 185–216.

Poeter, Eileen P., and Mary C. Hill, 2008, SIM_ADJUST—A computer code that adjusts simulated equivalents for observations or predictions: International Ground Water Modeling Center Report GWMI 2008–01, 28 p.

Pollock, D.W., 1994, User's Guide for MODPATH/MODPATH-PLOT, version 3: A particle tracking post-processing package for MODFLOW, the U.S. Geological Survey finite-difference ground-water flow model: U.S. Geological Survey Open-File Report 94–464 [variously paged]. (Also available at *http://pubs.er.usgs.gov/publication/ofr94464*.)

Reiter, M., 2001, Using precision temperature logs to estimate horizontal and vertical groundwater flow components: Water Resources Research, v. 37, no. 3, p. 663–674.

Robinson, T.W., 1958, Phreatophytes: U.S. Geological Survey Water-Supply Paper 1423, 84 p.

Robson, S.G., and Banta, E.R., 1995, Ground water atlas of the United States—Arizona, Colorado, New Mexico, and Utah: U.S. Geological Survey Hydrologic Atlas 730–C, 32 p. (Also available at *http://pubs.usgs.gov/ha/ha730/ch_c/index.html.)*

Roelle, J.E., and Hagenbuck, W.W., 1994, Surface cover maps of the Rio Grande floodplain from Velarde to Elephant Butte Reservoir, New Mexico: U.S. Geological Survey, Fort Collins, Colo., 57 p.

Sanford, W.E., Plummer, L.N., McAda, D.P., Bexfield, L.M., and Anderholm, S.K., 2004a, Hydrochemical tracers in the Middle Rio Grande Basin, USA—2. Calibration of a groundwater-flow model: Hydrogeology Journal, v. 12, no. 4, p. 389–407.

Sanford, W.E., Plummer, L.N., McAda, D.P., Bexfield, L.M., and Anderholm, S.K., 2004b, Use of environmental tracers to estimate parameters for a predevelopment- ground-water-flow model of the Middle Rio Grande Basin, New Mexico: U.S. Geological Survey Water-Resources Investigations Report 03–4286, 102 p.

Smith, G.A., and Kuhle, A.J., 1998, Hydrostratigraphic implications of new geological mapping in the Santo Domingo Basin, New Mexico: New Mexico Geology, v. 20, no. 1, p. 21–27.

Stone, B.D., Allen, B.D., Mikolas, M., Hawley, J.W., Haneberg, W.C., Johnson, P.S., Allred, B, and Thorn, C.R., 1998, Preliminary lithostratigraphy, interpreted geophysical logs, and hydrogeologic characteristics of the 98th Street core hole, Albuquerque, New Mexico: U.S. Geological Survey Open-File Report 98–210, 82 p.

Thomas, C.L., Stewart, A.E., and Constantz, J., 2000, Determination of infiltration and percolation rates along a reach of the Santa Fe River near La Bajada, New Mexico: U.S. Geological Survey Water-Resources Investigations Report 00–4141, 65 p.

Thorn, C.R., McAda, D.P., and Kernodle, J.M., 1993, Geohydrologic framework and hydrologic conditions in the Albuquerque Basin, central New Mexico: U.S. Geological Survey Water-Resources Investigations Report 93–4149, 106 p.

Thomas, C.L., and Thorn, C.R., 2000, Use of air-pressurized slug tests to estimate hydraulic conductivity at selected piezometers completed in the Santa Fe Group aquifer system, Albuquerque area, New Mexico: U.S. Geological Survey Water-Resources Investigations Report 00–4253, 19 p.

Tiedeman, C.R., Kernodle, J.R., and McAda, D.P., 1998, Application of nonlinear-regression methods to a ground-water flow model of the Albuquerque Basin, New Mexico: U.S. Geological Survey Water-Resources Investigations Report 98–4172, 90 p.

Titus, F.B., 1961, Ground-water geology of the Rio Grande trough in north-central New Mexico, *with sections on* the Jemez Caldera and Lucero Uplift, *in* Northrop, S.A., ed., Guidebook of the Albuquerque country: New Mexico Geological Society, 12th Field Conference, p. 186–192.

Trainer, F.W., Rogers, R.J., and Sorey, M.L., 2000, Geothermal hydrology of Valles Caldera and the southwestern Jemez Mountains, New Mexico: U.S. Geological Survey Water-Resources Investigations Report 00–4067, 115 p.

U.S. Census Bureau, 1970, Master reference file for 1970 census.

U.S. Census Bureau, 1980, Master reference file for 1980 census.

U.S. Census Bureau, 1990, Master reference file for 1990 census.

U.S. Census Bureau, 2001a, Ranking tables in metropolitan areas—Population in 2000 and population change from 1990 to 2000 (PHC–T–3): accessed October 2006 at *http://www.census.gov/population/www/cen2000/phc-t3.html*

U.S. Census Bureau, 2001b, Redistricting Census 2000 TIGER/Line files, accessed May 2006 at *http://rgisbeta.unm.edu/browsedata*

U.S. Census Bureau, 2006, GCT–PH1. Population, housing units, area, and density: 2000 for New Mexico: accessed October 2006 at *http://factfinder.census.gov/servlet/GCTTable?_bm=y&-context=gct&-ds_name=DEC_2000_SF1_U&-mt_name=DEC_2000_SF1_U_GCTPH1_ST7&-CONTEXT=gct&-tree_id=4001&-geo_id=04000US35&-format=ST-7|ST-7S&-_lang=en*

U.S. Environmental Protection Agency, 2005, South Valley, New Mexico: EPA ID# NMD 980745558: accessed October 2006 at *http://www.epa.gov/earth1r6/6sf/pdffiles/southval.pdf.*

U.S. Environmental Protection Agency, 2006, National primary drinking water regulations:, accessed December 2006 at *http://www.epa.gov/safewater/contaminants/index.html*

U.S. Geological Survey, Water Resources, 2010, National Water Information System, USGS surface water annual statistics for New Mexico, 1974–2009: U.S. Geological Survey database, accessed October 28, 2010, at URL *http://waterdata.usgs.gov/nm/nwis/annual/?referred_module=sw&site_no=08330000&por_08330000_3=558903,00060,3,1942,2009&start_dt=1974&end_dt=2009&year_type=W&format=html_table&date_format=YYYY-MM-DD&rdb_compression=file&submitted_form=parameter_selection_list*

Veenhuis, J.E., 2002, Summary of flow loss between selected cross sections on the Rio Grande in and near Albuquerque, New Mexico: U.S. Geological Survey Water-Resources Investigations Report 93–4213, 17 p.

Western Regional Climate Center, 2006a, Period of record monthly climate summary for Albuquerque WSFO Airport, New Mexico: accessed October 2006 at *http://www.wrcc.dri.edu/cgi-bin/cliMAIN.pl?nm0234*

Western Regional Climate Center, 2006b, Period of record monthly climate summary for Sandia Crest, New Mexico: accessed October 2006 at *http://www.wrcc.dri.edu/cgi-bin/cliMAIN.pl?nm8011*

Wilson, B.C., 1992, Water use by categories in New Mexico counties and river basins, and irrigated acreage in 1990: New Mexico State Engineer Technical Report 47, 141 p.

Wilson, B.C., Lucero, A.A., Romero, J.T., and Romero, P.J., 2003, Water use by categories in New Mexico counties and river basins, and irrigated acreage in 2000: New Mexico State Engineer Office Technical Report 51, 164 p.

Hydrogeologic Setting and Groundwater-Flow Simulations of the South-Central Texas Regional Study Area, Texas

By Richard J. Lindgren, Natalie A. Houston, MaryLynn Musgrove, Lynne S. Fahlquist, and Leon J. Kauffman

Section 3 of

Hydrogeologic Settings and Groundwater-Flow Simulations for Regional Investigations of the Transport of Anthropogenic and Natural Contaminants to Public-Supply Wells—Investigations Begun in 2004

Edited by Sandra M. Eberts

Professional Paper 1737–B

U.S. Department of the Interior
U.S. Geological Survey

U.S. Department of the Interior
KEN SALAZAR, Secretary

U.S. Geological Survey
Marcia K. McNutt, Director

U.S. Geological Survey, Reston, Virginia: 2011

Suggested citation:
Lindgren, R.J., Houston, N.A., Musgrove, M., Fahlquist, L.S., and Kauffman, L.J., 2011, Hydrogeologic setting and groundwater-flow simulations of the South-Central Texas regional study area, Texas, section 3 *of* Eberts, S.M., ed., Hydrologic settings and groundwater-flow simulations for regional investigations of the transport of anthropogenic and natural contaminants to public-supply wells—Investigations begun in 2004: Reston, Va., U.S. Geological Survey Professional Paper 1737–B, pp. 3-1–3-51.

Contents

Figures

Tables

Hydrogeologic Setting and Groundwater-Flow Simulations of the South-Central Texas Regional Study Area, Texas

By Richard J. Lindgren, Natalie A. Houston, MaryLynn Musgrove, Lynne S. Fahlquist, and Leon J. Kauffman

Abstract

The transport of anthropogenic and natural contaminants to public-supply wells was evaluated for part of the Edwards aquifer in south-central Texas as part of the U.S. Geological Survey National Water-Quality Assessment Program. The Edwards aquifer in the South-Central Texas regional study area is used extensively for public-water supply, is a source of water to major springs, and is susceptible and vulnerable to contamination. The Edwards aquifer is part of an aquifer system developed in thick and regionally extensive Lower Cretaceous carbonates that underlie large areas of Texas. The carbonates in the Edwards aquifer are laterally and vertically heterogeneous. Groundwater flow and aquifer properties of the Edwards aquifer in the study area are appreciably affected by the presence of faults and karst dissolution features.

Existing one-layer, steady-state and transient groundwater-flow models of the Edwards aquifer in the study area were modified to include a finer model grid and one additional layer. The original Edwards aquifer models had been calibrated for two hydraulic conductivity distributions, one representing predominantly conduit flow in the aquifer and the other representing predominantly matrix (diffuse) flow through a network of numerous small fractures and openings. The conduit-flow and diffuse-flow rediscretized regional Edwards aquifer models were recalibrated for steady-state conditions during 2001, a representative year for the recent time period, and transient conditions during 2000–03. The calibrated rediscretized regional Edwards aquifer models and advective particle-tracking simulations were used to compute groundwater-flow paths, areas contributing recharge, and traveltimes from recharge areas for public-supply wells.

Model results from the steady-state simulation indicate recharge from precipitation, about 96 percent of inflow, provides most of the groundwater inflow. The steady-state simulation indicates that about 54 percent of groundwater discharge is to springflow and about 46 percent is to withdrawals by wells. Particle-tracking results indicate minimum computed traveltimes to public-supply wells varied from less than one to 987 years and maximum computed traveltimes ranged from 9 to 5,263 years. The average computed traveltime of 276 years to public-supply wells was greater for the conduit-flow rediscretized regional Edwards aquifer model than the 191 years computed for the diffuse-flow rediscretized regional Edwards aquifer model. For the conduit-flow rediscretized regional Edwards aquifer model, on average, only about 1.3 percent of the flow to a public-supply well was less than 10 years old, about 17 percent of the flow to a public-supply well was less than 50 years old, and about 52 percent of the flow to a public-supply well was less than 200 years old. The corresponding percentages for the diffuse-flow rediscretized regional Edwards aquifer model were greater, 1.9, 24, and 67 percent, respectively. The computed traveltimes are probably much longer than actual traveltimes in the aquifer, because the regional groundwater-flow models do not accurately represent flow through local karst dissolution features.

Introduction

The South-Central Texas regional study area for the transport of anthropogenic and natural contaminants to public-supply wells (TANC) is within the Edwards-Trinity aquifer system (fig. 3.1). The study area overlies the fractured karstic Edwards aquifer in south-central Texas and includes the San Antonio metropolitan area (fig. 3.2). The South-Central Texas regional study area coincides with the San Antonio and Barton Springs segments of the Edwards aquifer (fig. 3.2). The Edwards-Trinity aquifer system underlies a portion of the South-Central Texas study unit of the U.S. Geological Survey (USGS), National Water-Quality Assessment, and much of west-central and south-central Texas. Vulnerability to contamination and the dependence of more than 1.5 million people on the aquifer for public water supply combine to make the water quality of the Edwards aquifer and the streams that recharge it a critical issue for the future of the Greater San Antonio Area, as well as the larger San Antonio region, which for the purposes of this report approximately coincides with the extent of the San Antonio and Barton Springs segments of the Edwards aquifer.

Base from U.S. Geological Survey digital data, Albers equal-area projection, standard parallels 29° 30' North and 45° 30' North, central meridian 100° West, North American Datum of 1983

EXPLANATION

- South-Central Texas regional study area
- Edwards-Trinity aquifer system
- National Water-Quality Analysis study unit—South-Central Texas

Figure 3.1. Location of the South-Central Texas regional study area within the Edwards-Trinity aquifer system.

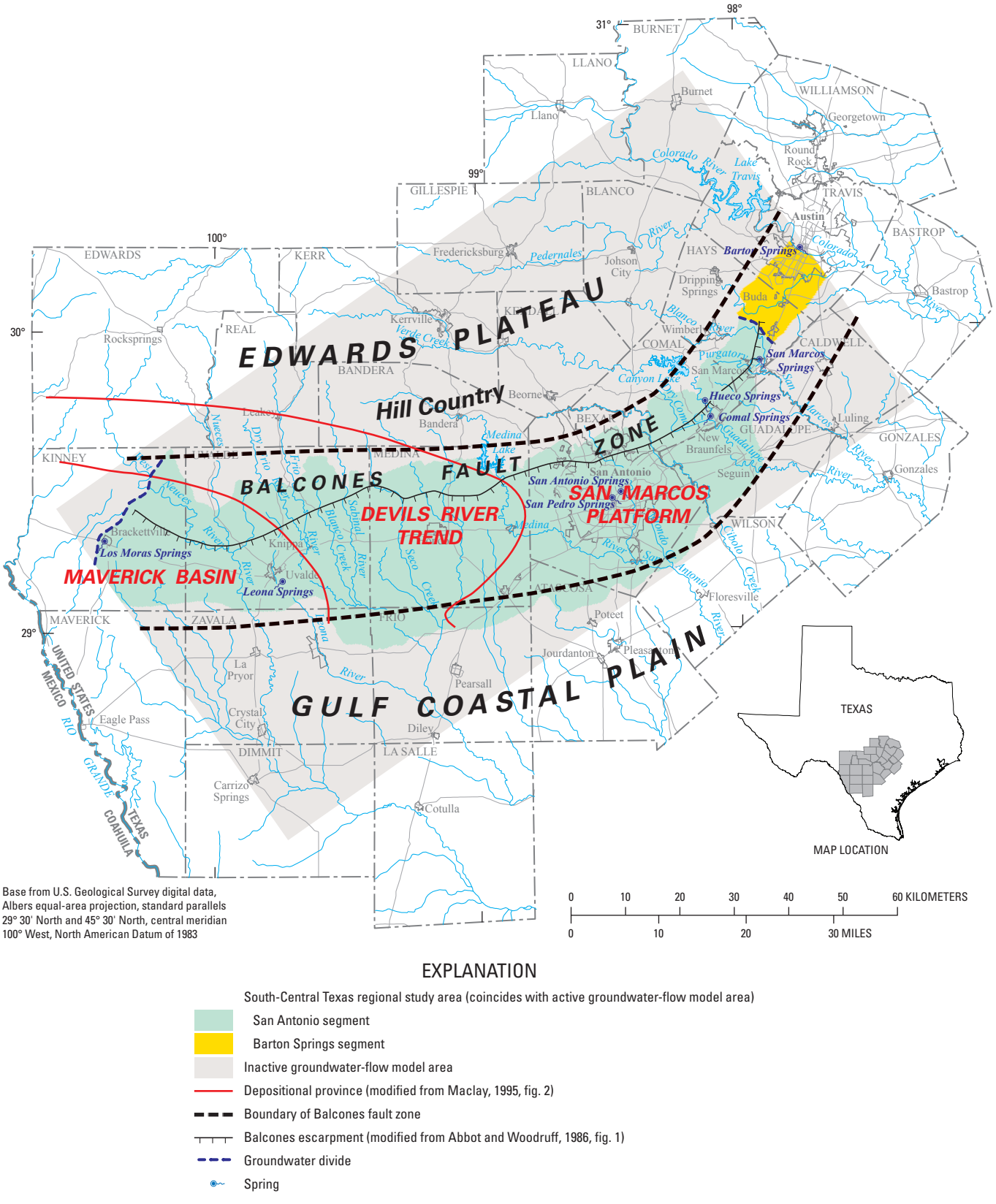

Figure 3.2. Locations of the groundwater-flow model area for the South-Central Texas regional study, Edwards aquifer segments, and physiographic regions, major groundwater divides and Balcones fault zone, and depositional provinces, San Antonio region, Texas.

Purpose and Scope

The purpose of this Professional Paper section is to present the hydrogeologic setting of the South-Central Texas regional study area. The section also documents the revision and recalibration of regional groundwater-flow models for the study area for steady-state and transient conditions. Groundwater-flow characteristics, pumping-well information, and water-quality data were compiled from existing data to develop a conceptual understanding of groundwater conditions in the study area. Two existing groundwater-flow models of the area with two different horizontal hydraulic-conductivity distributions (Lindgren and others, 2004; Lindgren, 2006) were modified to include a finer model grid and one additional model layer. The models were recalibrated for average conditions during 2001 for the steady-state calibration and were recalibrated for the time period from 2000 to 2003 for the transient calibration. The year 2001 was assumed to be representative of average conditions for the time period from 2000 to 2003, which was the time period selected for data compilation and modeling exercises to facilitate future comparisons between varying TANC regional study areas. The updated groundwater-flow models and associated particle tracking were used to simulate advective groundwater-flow paths and to delineate areas contributing recharge to selected public-supply wells. Groundwater traveltimes from recharge to public-supply wells, oxidation-reduction (redox) conditions along flow paths, and the presence of potential contaminant sources in areas contributing recharge were tabulated into a relational database described in Appendix 1 of Chapter A of this Professional Paper. This section, Section 3 of Chapter B, provides the foundation for future groundwater susceptibility and vulnerability analyses of the study area and comparisons among regional aquifer systems.

Study Area Description

The South-Central Texas regional study area was selected for study because the Edwards aquifer is used extensively for public-water supply and is susceptible and vulnerable to contamination. The aquifer was the first to be designated as a sole source aquifer, defined by the U.S. Environmental Protection Agency (USEPA) as an aquifer that supplies 50 percent or more of the drinking water of an area. The South-Central Texas regional study area also includes a range of hydrogeologic features, including karst features, and land-use conditions within the San Antonio and Barton Springs segments of the Edwards aquifer in south-central Texas (fig. 3.2, table 3.1).

Topography and Climate

The South-Central Texas regional study area includes part of the topographically rugged Edwards Plateau, the eastern part of which locally is called the “Hill Country,” and the comparatively flat Gulf Coastal Plain, which are separated by the Balcones escarpment (fig. 3.2). The Balcones escarpment, a surface manifestation of the Balcones fault zone, is a physiographic feature that also separates the Trinity aquifer in the Hill Country from the Edwards aquifer. Land surface altitude ranges from about 137 meters (m) in the eastern part of the study area near the Colorado River to about 594 m in the northwestern part of the study area in the Edwards aquifer recharge zone; topographic relief locally changes dramatically, by hundreds of meters.

The climate in the South-Central Texas regional study area is semiarid in the western part to subtropical humid in the eastern part (Larkin and Bomar, 1983). Average annual rainfall varies from 56 cm at Brackettville in the west to 86 cm at Austin in the east. Months- to years-long droughts that strain water supplies and produce widespread crop failure commonly are followed by wet periods that include torrential rains and flash floods (Bomar, 1994). Storms can produce rapid runoff and recharge to the Edwards aquifer. After many months of drought, in October 1998 more than 381 millimeters of rain fell in a 2-day period on the karstic, unconfined part of the Edwards aquifer (the recharge zone), and even higher rainfall rates were observed in some areas (Slade and Persky, 1999). Groundwater levels in some monitoring wells rose more than 30 m during a 2-week period in response to this storm.

Surface-Water Hydrology

Karst features such as sinkholes, solution enlargement along fractures and bedding planes, caves, and springs are prevalent in the South-Central Texas regional study area. In the recharge zone (outcrop) (fig. 3.3), karst landforms include large shallow, internally drained depressions that are typically tens to hundreds of meters across; depressions of holes in creek bottoms; and small upland features such as sinkholes and solution-enlarged fractures (Hovorka and others, 2004). In addition, more than 400 caves have been inventoried in the Edwards aquifer outcrop (Veni, 1988; Elliott and Veni, 1994).

The South-Central Texas regional study area encompasses the upper parts of the Nueces, San Antonio, and Guadalupe River Basins, as well as part of the Colorado River Basin for the Barton Springs segment (fig. 3.3). Surface water and groundwater in the South-Central Texas regional study area are uniquely interrelated. Springs and seeps discharge

Table 3.1. Summary of hydrogeologic and groundwater-quality characteristics for the Edwards-Trinity aquifer system and the South-Central Texas regional study area, San Antonio region, Texas.

[km, kilometers; m, meters; ºC, degrees Celsius; mm, millimeters; mm/yr, millimeters per year; m/d, meters per day; m^2/d, meters squared per day; m^3/s, cubic meters per second; m^3/d, cubic meters per day; hm^3, cubic hectometers; hm^3/yr, cubic hectometers per year; mg/L, milligrams per liter]

Characteristic	Edwards-Trinity Aquifer System	South-Central Texas regional study area
	Geography	
Topography	Much of the area is characterized by flat to rolling, largely rocky plains that are dissected in places to form steep-walled canyons. Relief locally is tens of meters. Transition from Edwards Plateau to the west and nearly level to gently rolling Gulf Coastal Plain to the east, separated by Balcones escarpment (fig.3.2). Land surface altitude ranges from 1,787 m in west Texas to 64 m in west Arkansas. Karst landforms prevalent in outcrop (recharge zone) (National Hydrography Dataset Plus, 2007).	Topographically rugged and picturesque Edwards Plateau and rolling to hilly Gulf Coastal Plain separated by Balcones escarpment (fig. 3.2); relief locally is hundreds of meters. Land surface altitude ranges from about 137 m in east to 594 m in west. Karst landforms prevalent in outcrop (recharge zone).
Climate	Semiarid in west to subtropical humid in east; average annual precipitation ranges from 279 mm in west Texas to 1,448 mm in western Arkansas. Average annual high temperature ranges from 39.4ºC to 29.4ºC in west Texas. Average annual low temperature ranges from -2.8ºC in west Texas to 5ºC southwest of San Antonio (U.S. Department of Agriculture, 2007).	Semiarid in west to subtropical humid in east; Precipitation 551 mm/yr in west to 851 mm/yr in east.
Surface-water hydrology	In the Edwards plateau region, springs and seeps contribute baseflow to streams that drain the plateau. Major streams that cross the area flow southward and southeastward toward the Gulf Coast. In the southern part of the aquifer system, most of the streams lose their baseflow to the fractured, karstic Edwards formation in the Balcones fault zone (Ryder, 1996).	Includes upper parts of the Nueces, San Antonio, and Guadalupe River Basins, as well as part of the Colorado River Basin for the Barton Springs segment. Most streams lose all of their base flow as recharge to the Edwards aquifer in the Edwards aquifer recharge zone. Comal and San Marcos Springs are the largest springs, with discharges of 10.8 and 7.7 m3/s, respectively (Hamilton and others, 2003).
Land use	Forest and rangeland (81 percent), agriculture (11), urban (6), and water, wetlands, strip mines, and barren (2) (Homer and others, 2004). Major urban cities include San Antonio, Austin, and Dallas-Fort Worth metropolitan areas.	Forest and rangeland (73 percent), agriculture (13), urban (12), and water, wetlands, strip mines, and barren (2) (Homer and others, 2004).
Water use	Total water use in 2000 was estimated to be 2.80 m3/d, of which irrigation was 1.07, public-supply was 1.55, and self-supplied industrial was 0.18. Of the total, 2.76 m3/d was used in Texas, 0.015 in Oklahoma, and 0.025 in Arkansas (Maupin and Barber, 2005).	In 2003, water use from the Edwards aquifer in Atascosa, Bexar, Comal, Hays, Kinney, Medina, Travis and Uvalde Counties was estimated to be 460.7 hm3 (Texas Water Development Board, 2008). Municipal withdrawals accounted for about 70 percent and irrigation accounts for 27 percent; the remaining 3 percent included manufacturing, steam electric, mining and livestock.

Table 3.1. Summary of hydrogeologic and groundwater-quality characteristics for the Edwards-Trinity aquifer system and the South-Central Texas regional study area, San Antonio region, Texas.—Continued

[km, kilometers; m, meters; ºC, degrees Celsius; mm, millimeters; mm/yr, millimeters per year; m/d, meters per day; m^2/d, meters squared per day; m^3/s, cubic meters per second; m^3/d, cubic meters per day; hm^3, cubic hectometers; hm^3/yr, cubic hectometers per year; mg/L, milligrams per liter]

Characteristic	Edwards-Trinity Aquifer System	South-Central Texas regional study area
	Geology	
Surficial deposits	Limestone and dolostone in outcrop area (recharge zone); limestone, chalk, shale, clay, and gravel in confined zone.	Limestone and dolostone in outcrop area (recharge zone); limestone, chalk, shale, clay, and gravel in confined zone.
Bedrock geologic units	Cretaceous, generally carbonate in the upper part and clastic sandstone in the lower part, relatively flat lying to north and west, more steeply dipping toward the coast. Rocks are exposed in updip areas, and dip and thicken east- and southward below overlying confining units (Ryder, 1996; Renken, 1998).	Carbonate sequence from 0 m (at updip boundary of outcrop area (recharge zone)) to 335 m (in western part of confined zone) thick; fractured with many dissolution features, especially in outcrop areas (recharge zone).
	Groundwater hydrology	
Aquifer conditions	Unconfined in outcrop area (recharge zone); confined downdip of outcrop area.	Unconfined in outcrop area (recharge zone); confined downdip of outcrop area (recharge zone).
Hydraulic properties	Transmissivity=18,580-185,800 m^2/d Storage coefficient=$1x10^{-5}$ to $1x10^{-4}$ Specific yield= average 0.02–0.04 (Ryder 1996).	Transmissivity=39,947 to 204,380 m^2/d Horizontal hydraulic conductivity= $3.05x10^{-4}$ to $3.05x10^{4}$ m/d Storage coefficient=$1x10^{-5}$ to $8x10^{-4}$ (San Antonio segment); Specific storage=$3.28x10^{-6}$ to $9.51x10^{-2}$ m^{-1} (Barton Springs segment); Specific yield=0.005 to 0.20; porosity =0.04 to 0.42 (Hovorka and others, 1996; Hovorka and others, 1998; Maclay and Land, 1988; Maclay and Rettman, 1973; Maclay and Small, 1984; Senger and Kreitler, 1984; Sieh, 1975; Slade and others, 1985; Scanlon and others, 2002).
Water budget	Recharge is generally as precipitation that falls on aquifer outcrop areas and as seepage from streams and ponds where the head gradient is downward. Discharge is by evapotranspiration, spring discharge, diffuse lateral or upward leakage into shallower aquifers, and withdrawals from wells. Much of the natural discharge from the aquifer is as spring flows along the southeastern edge of the Edwards Plateau where erosion has cut the rocks of the Edwards Group down to the water table (Ryder, 1996).	For the San Antonio segment, recharge from seepage losses from streams and infiltration of rainfall 862.2 hm^3/yr; subsurface inflow from Trinity aquifer about 2 to 9 percent of total recharge. Discharge to springs about 53 percent or 459.2 hm^3/yr; withdrawals by wells about 43 percent or 370.8 hm^3/yr; unknown amount discharges to Leona River floodplain and subsequently leaves study area (Hamilton and others, 2003). For the Barton segment, recharge from seepage losses from streams and infiltration of rainfall 53.6 hm^3/yr; subsurface inflow from Trinity aquifer minimal. Discharge to springs about 91 percent or 49.0 hm^3/yr; withdrawals by wells about 9 percent or 4.6 hm^3/yr (Scanlon and others, 2001).

Table 3.1. Summary of hydrogeologic and groundwater-quality characteristics for the Edwards-Trinity aquifer system and the South-Central Texas regional study area, San Antonio region, Texas.—Continued

[km, kilometers; m, meters; ºC, degrees Celsius; mm, millimeters; mm/yr, millimeters per year; m/d, meters per day; m^2/d, meters squared per day; m^3/s, cubic meters per second; m^3/d, cubic meters per day; hm^3, cubic hectometers; hm^3/yr, cubic hectometers per year; mg/L, milligrams per liter]

Characteristic	Edwards-Trinity Aquifer System	South-Central Texas regional study area
	Groundwater hydrology—Continued	
Groundwater residence times	Unknown	As short as a few days for rapid-response system (conduits) (Tomasko and others, 2001; Worthington, 2004). Generally less than 200 years (Leon Kauffman, U.S. Geological Survey, written commun., 2008). MODPATH results inconclusive because of karst terrain.
Lengths of groundwater travel paths	Unknown	Generally less than 160 km; median of about 40 km (Leon Kauffman, U.S. Geological Survey, written commun., 2008). Generally shorter in the Barton segment.
	Groundwater quality	
Water chemistry (dissolved solids, pH, reduction-oxidation conditions, major water types)	Dissolved solids range from 280 to 1500 mg/L in the freshwater part, increasing in concentration from the recharge area to downdip area. Saline water exists downdip of the freshwater zone.	Dissolved solids range from 280 to 560 mg/L with a median of 380 mg/L; pH ranges from 6.5 to 7.4 with a median of 7.0; reduction-oxidation conditions are predominantly oxidizing; Calcium and bicarbonate are dominant dissolved ions (Marylynn Musgrove, USGS, written commun., 2007).
Major contaminants (natural and anthropogenic)	Nitrate; radon; pesticides including atrazine and deethylatrazine; volatile organic compounds including trichloromethane, bromodichloromethane, chlorodibromomethane, perchloroethylene, and solvents (Bush and others, 2000; Fahlquist and Ardis, 2004).	Nitrate; radon; pesticides including atrazine and deethylatrazine; volatile organic compounds including trichloromethane, bromodichloromethane, chlorodibromomethane, perchloroethylene, and solvents (Bush and others, 2000; Fahlquist and Ardis, 2004).

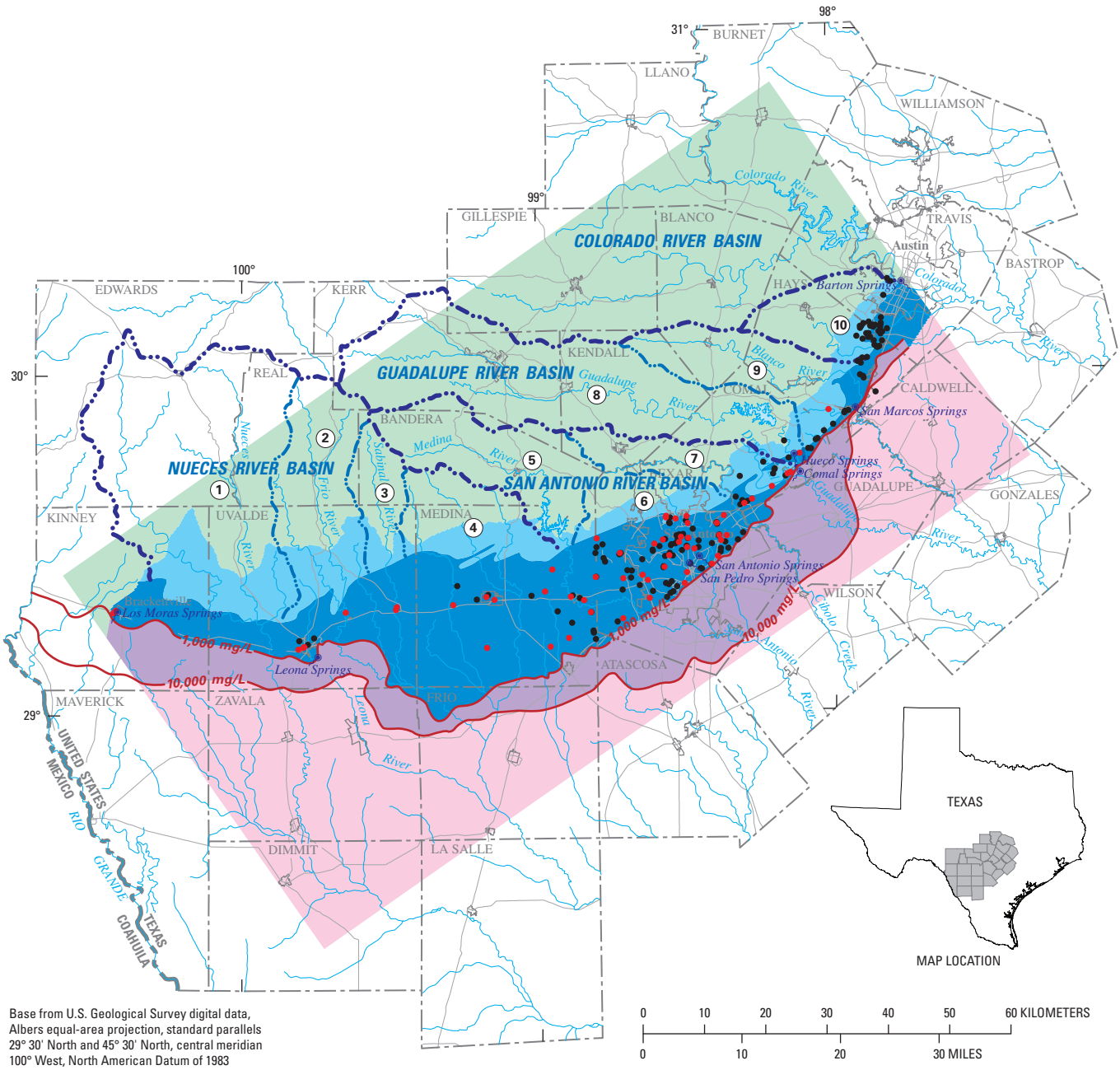

EXPLANATION

South-Central Texas regional study area (coincides with active groundwater-flow model area) and adjacent hydrogeologic zones

- Recharge zone (outcrop) (modified from Puente, 1978)
- Freshwater zone
- Freshwater/saline-water transition zone

Inactive groundwater-flow model area hydrogeologic zones

- Catchment zone
- Saline zone
- Line of equal dissolved solids concentration, in milligrams per liter (A.L. Schultz, consultant, written commun., 2000)

Catchment area

- Major river basin boundary
- Stream basin or contributing area boundary
- Public supply well sampled by NAWQA
- Public supply well
- Spring

Stream basin or contributing area

1. Nueces-West Nueces River Basin
2. Frio-Dry Frio River Basin
3. Sabinal River Basin
4. Area between Sabinal and Medina River Basins (includes Hondo and Seco Creeks)
5. Medina River Basin
6. Area between Medina River Basin and Cibolo-Dry Comal Creek Basins (includes Saludo Creek)
7. Cibolo and Dry Comal Creek Basins
8. Guadalupe River Basin (includes Guadelupe River and Verde Creek)
9. Blanco River Basin (includes Blanco River andPurgatory Creek)
10. Barton Springs segment contributing area (includes Barton, Williamson, Slaughter, Bear, and Onion Creeks)

Figure 3.3. Hydrogeologic zones and catchment area (upper parts of stream basins that contribute recharge) of the Edwards aquifer and locations of public-supply wells, San Antonio region, Texas.

along impermeable zones of the Trinity aquifer in the deeply incised stream channels of the Edwards Plateau (fig. 3.2). These springs provide base flow to streams that flow southward and eastward from the plateau. As they flow across the highly permeable, fractured and faulted carbonate rocks of the Edwards aquifer in the Balcones fault zone, most streams lose all of their base flow as recharge to the Edwards aquifer in the Edwards aquifer recharge zone (fig. 3.4). Six large springs (from west to east Los Moras, San Pedro, San Antonio, Comal, San Marcos, and Barton), important to the local recreational economy as well as to downstream users, issue from the confined part of the Edwards aquifer. Two additional springs, Leona Springs and Hueco Springs, occur in the study area, but all or part of their discharge is derived from sources other than the confined part of the Edwards aquifer. Comal and San Marcos Springs are the largest springs, with total discharges of 339.0 and 241.7 cubic hectometers (hm^3), respectively, in 2002, which translates to flow rates of 10.8 and 7.7 cubic meters per second (m^3/s), respectively (Hamilton and others, 2003). The springs of the Edwards aquifer provide unique habitat for about 90 plant and animal species, about one-half of which are subterranean and include such organisms as blind shrimp, salamanders, and catfish (Bush and others, 2000). Some species have been federally listed as endangered or threatened.

Over most semiarid regions of the Edwards Plateau and Hill Country, soil development is poor and generally less than 0.3 m thick. In the Edwards Plateau, soils tend to be calcareous stony clays vegetated by desert shrubs in the west and juniper, oak, and mesquite in the east. The Hill Country soils and vegetation are similar to those of the Edwards Plateau. In the northeastern part of the Balcones fault zone, soils are calcareous clay, clayey loam, and sandy loam with some prairie vegetation. West of San Antonio in the southwestern part of the Balcones fault zone, vegetation is predominantly juniper, oak, and mesquite (Kier and others, 1977).

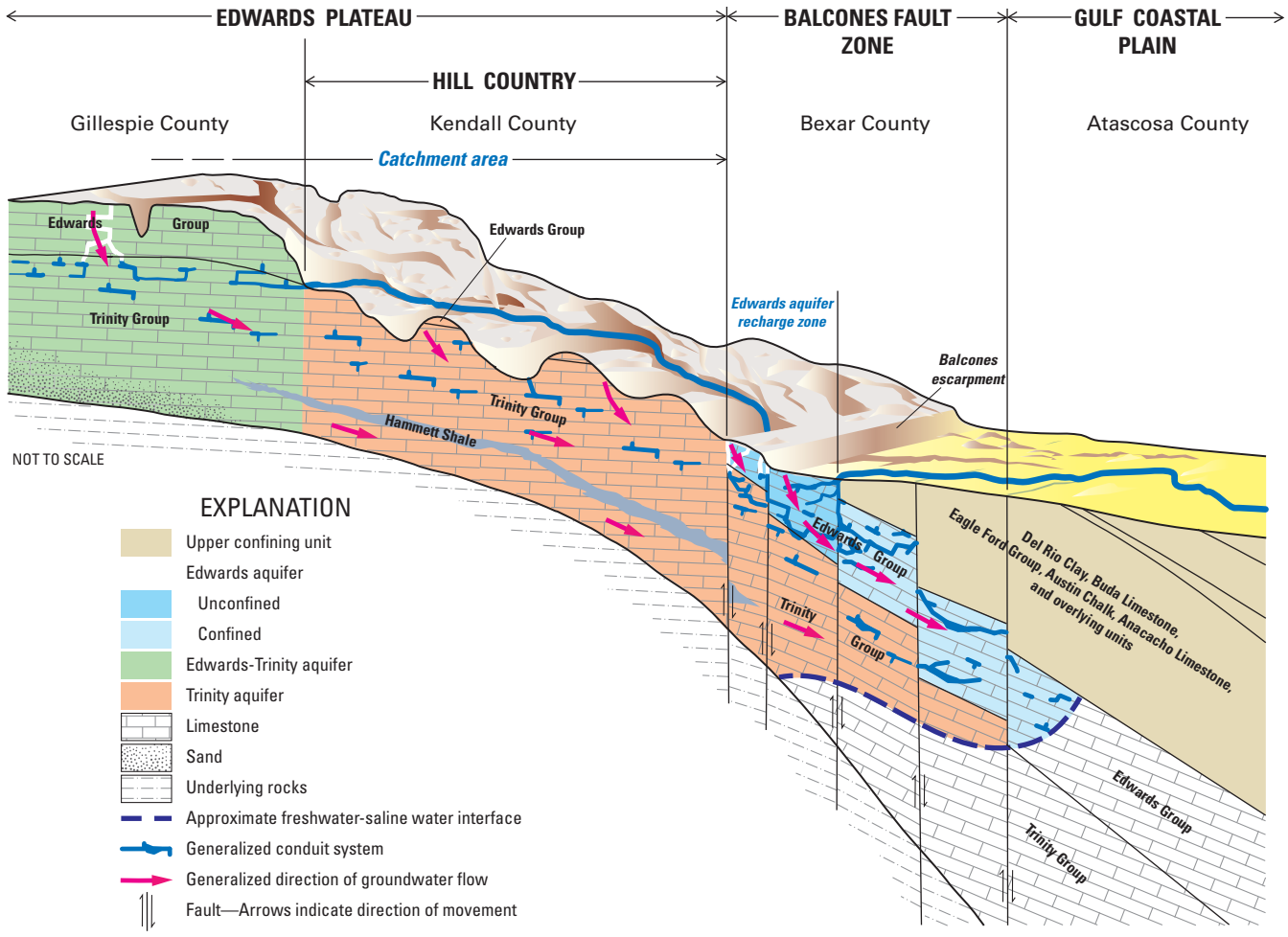

Figure 3.4. Diagrammatic north-northwest-to-south-southeast section showing hydrogeologic framework and generalized groundwater-flow directions, Edwards Plateau to Gulf Coastal Plain, San Antonio region, Texas.

Land Use

Land use in the South-Central Texas regional study area correlates with physiography. The rugged, thin-soiled terrain of the Edwards Plateau is largely undeveloped and rangeland predominates. The flatter, thicker-soiled terrain of the Gulf Coastal Plain is better suited to growing crops—primarily hay, sorghum, wheat, corn, and oats. In 2001, land use (Homer and others, 2004) in the South-Central Texas regional study area was quantified as 13 percent agriculture; 12 percent urban; 73 percent forest, shrub, and grassland; and 2 percent was water, wetlands, strip mines, or barren land. San Antonio is the principal urban area and includes much of Bexar County in the central part of the South-Central Texas regional study area (fig. 3.2).

Water Use

Groundwater accounts for nearly all of the water supply in the South-Central Texas regional study area, and the Edwards aquifer, one of the most productive aquifers in the world, is the principal source. Withdrawals from the Edwards aquifer meet the water-supply needs of more than 1.5 million people in the San Antonio region and support farming and ranching west of San Antonio. In 2003, water use from the Edwards aquifer in Atascosa, Bexar, Comal, Hays, Kinney, Medina, Travis and Uvalde Counties was estimated to be 460.7 hm^3 (Texas Water Development Board, 2008). Municipal withdrawals accounted for about 70 percent and irrigation accounts for 27 percent of water use; the remaining 3 percent included manufacturing, steam electric, mining, and livestock. An estimate for domestic use was not available. Bexar and Uvalde Counties are the largest producers of groundwater from the Edwards aquifer in the South-Central Texas regional study area; use in Bexar County is mostly municipal, and use in Uvalde County is mostly irrigation.

Conceptual Understanding of the Groundwater System

The Edwards aquifer is part of an aquifer system developed in thick and regionally extensive Lower Cretaceous carbonates that underlie large areas of Texas. The conceptualization of the Edwards aquifer includes a description of the geologic and hydrologic setting within which the aquifer functions. Groundwater flow and aquifer properties are appreciably affected by the presence of faults and karst dissolution features. The Balcones fault zone is a system of high-angle normal faults with net displacement toward the Gulf of Mexico and constitutes the principal structural deformation affecting aquifer development. Karst features in the Edwards aquifer include caves and solution-enlarged fractures (conduits). The Edwards aquifer is recharged predominantly through seepage losses from surface streams that flow onto the outcrop of the aquifer. Discharge from the aquifer is primarily from withdrawals by wells and springflow.

Hydrogeology

The Cretaceous strata of south-central Texas regionally include two aquifers, the Edwards aquifer in the Balcones fault zone and the Trinity aquifer in the Hill Country (fig. 3.4). The correlation chart (table 3.2) summarizes the relation among time-stratigraphic, rock-stratigraphic, and hydrogeologic units. The upper zone of the Trinity aquifer generally has lower permeability than the Edwards aquifer and, because of shaley interbeds, has a much lower vertical than horizontal permeability (Mace and others, 2000). Conventionally, the lower boundary of the Edwards aquifer is defined as the top of the Glen Rose Limestone (table 3.2). Cross-formational interconnection across the boundary between the two aquifers regionally is probable, however. Both units are karstic limestones, and large caves that cross the contact are interpreted as evidence that cross-formational flow occurs through karst systems in at least parts of the San Antonio segment of the Edwards aquifer (Veni, 1988; Vauter, 1992).

The carbonates in the Edwards aquifer are laterally and vertically heterogeneous. Maclay and Small (1976, table 1) defined eight “hydrostratigraphic” units within the Kainer, Person, and Georgetown Formations that compose the Edwards aquifer in the San Marcos platform of the Balcones fault zone (table 3.2). Groschen (1996) indicated that aquifer subdivisions III, VI, and VII transmit most of the groundwater within the San Antonio region. However, high-permeability dissolution features have been observed in all of the hydrostratigraphic units. The Edwards aquifer contains carbonates that have numerous intervals of intercrystalline high porosity, as well as petrophysical properties that make the carbonates subject to development of karst conduits (Hovorka and others, 1998). The Georgetown Formation, commonly included within the Edwards aquifer (table 3.2), consists of stratigraphically distinct limestone that overlies and is generally of lower porosity and permeability than the Edwards Group. The thick and regionally extensive shale of the Del Rio Clay directly overlies and confines the Edwards aquifer.

The altitude of the top of the Edwards aquifer ranges from about 305 m above NGVD 29 near the recharge zone in the western part of the San Antonio segment to about 1,219 m below NGVD 29 near the downdip limit of the aquifer in Frio County. The aquifer thickness ranges from 0 m at the updip boundary of the oucrop area (recharge zone) to about 335 m in the confined part of the aquifer in Kinney County (fig. 3.5).

Fractures, solution-enlarged fractures, and caves make up 1 to 3 percent of the outcrop area in the San Antonio segment of the Edwards aquifer (Hovorka and others, 1998). More than 400 caves have been inventoried in the Edwards aquifer outcrop (Veni, 1988; Elliott and Veni, 1994). Maclay and Small (1984) hypothesized that solution channels within the Edwards

Table 3.2. Correlation of Cretaceous stratigraphic units and hydrogeologic units, and relative permeabilities in the rediscretized regional Edwards aquifer models area, San Antonio region, Texas (modified from Maclay, 1995, fig. 11).

[The descriptors "very small," "moderate," and "large" refer to the relative permeability of stratigraphic units, and arrows indicate an interval of uniform relative permeability, by depth, in a stratigraphic unit.]

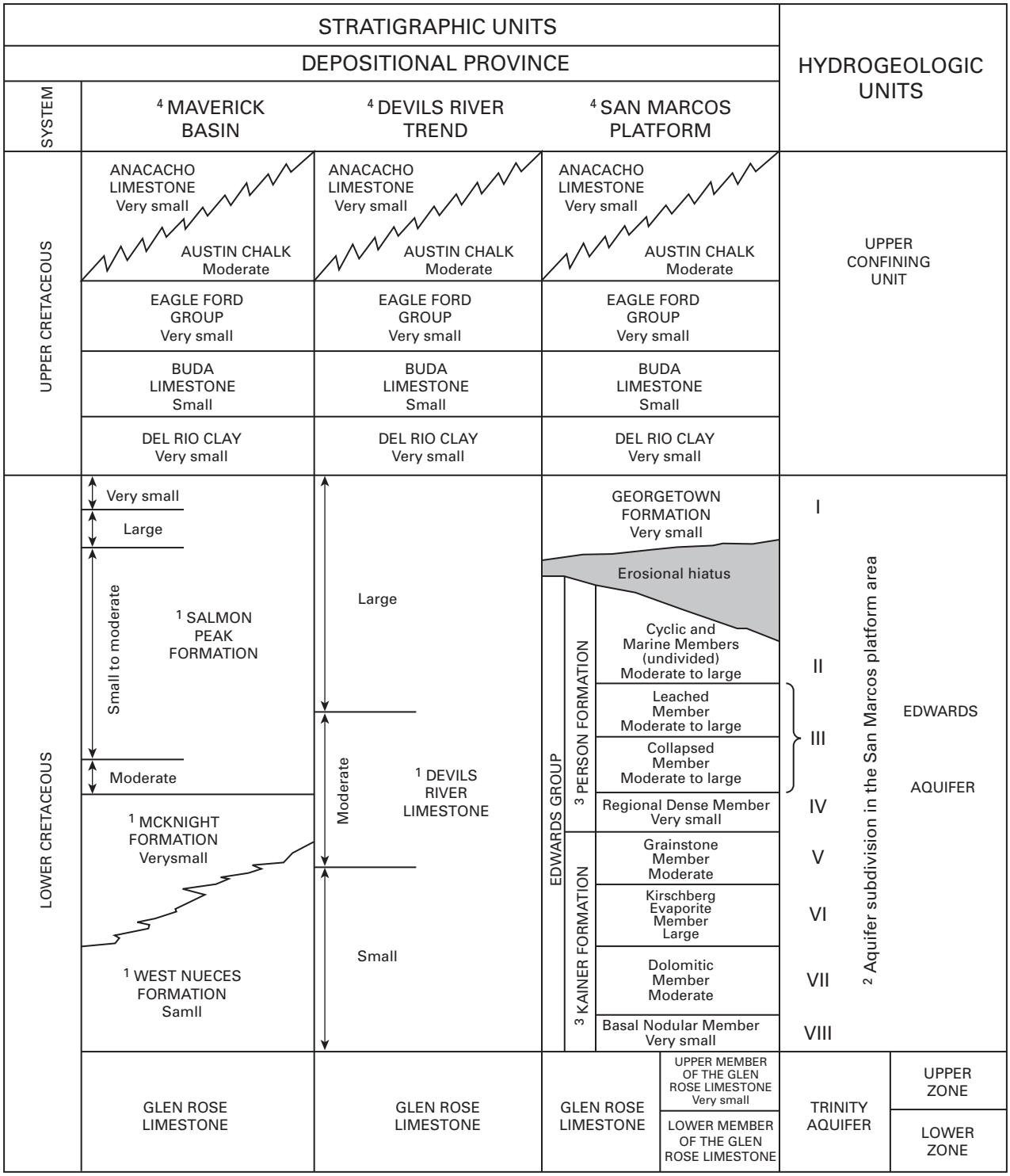

1 Lozo and Smith (1964).
2 Maclay and Small (1984).
3 Modified from Rose (1972).
4 Location shown in figure 3.2.

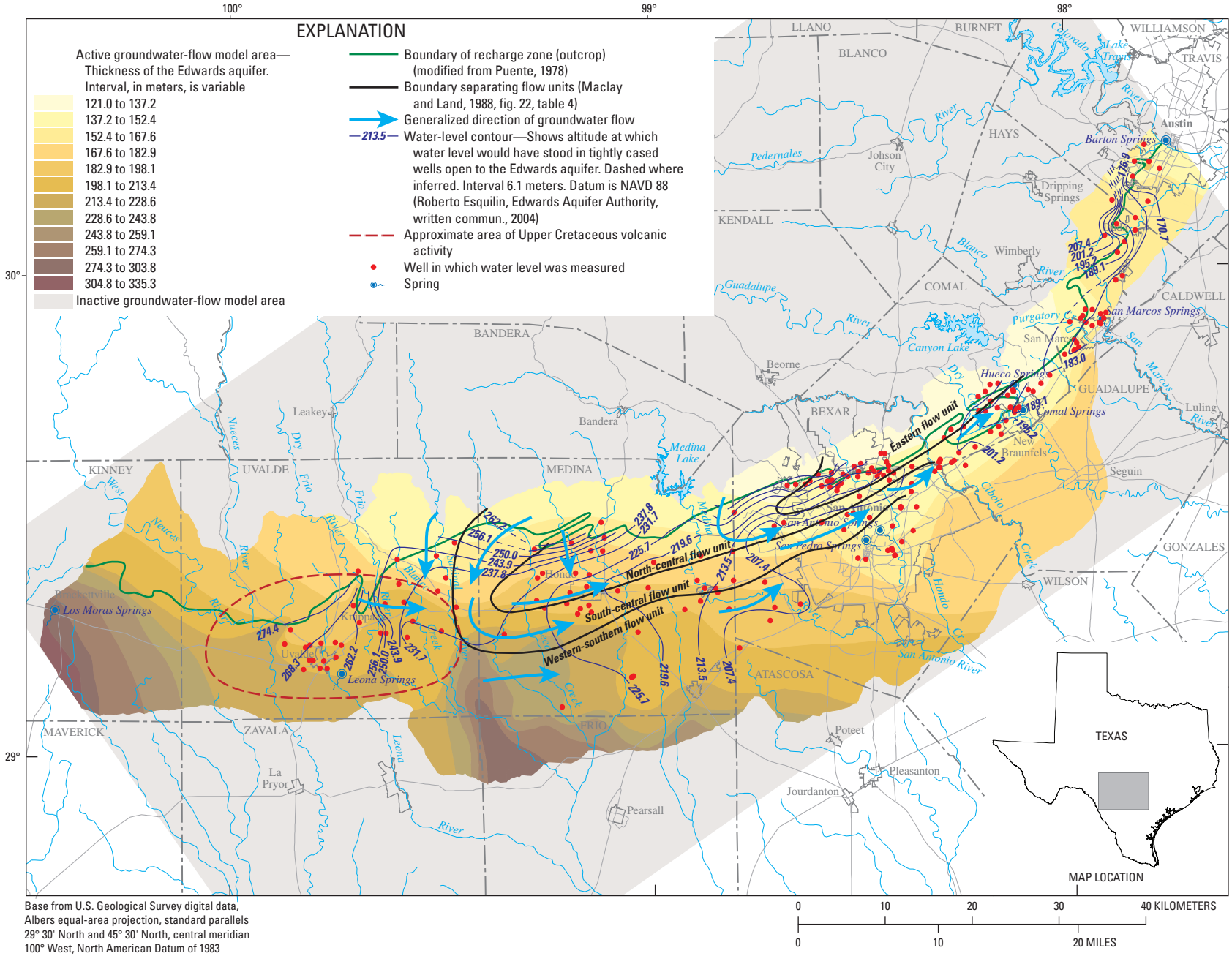

Figure 3.5. Thickness and potentiometric surface and inferred regional groundwater-flow pattern in the Edwards aquifer, October 27–November 2, 2001, South-Central Texas regional study area, San Antonio region, Texas.

aquifer might be oriented parallel to the courses of streams recharging the Edwards aquifer and that vertical solution channels are well developed below segments of stream courses in the recharge zone. Worthington (2004) conceptualized a dendritic pattern of conduit connection from the recharge zone to the confined zone. A regionally extensive system of high-permeability zones is defined by broad troughs in the potentiometric surface, which indicate the potential for development or the presence of conduits, in the confined zone of the Edwards aquifer. A wide trough extends westward from central Bexar County to western Medina County and also further westward to Uvalde County (Hovorka and others, 2004, figs. 7, 8, 9, and 10). Relatively high porosity and permeability in the deepest parts of the aquifer near the freshwater/saline-water interface, anomalously high well yields, and sharp chemical gradients indicate that flow might be focused in this area (Maclay and Small, 1984; Hovorka and others, 1998). Large-scale structural troughs, grabens and synclines, with increased flow occur in the Edwards aquifer, and conduit development in these is favored. Worthington (2004, fig. 17) identified nine major structural troughs in the San Antonio segment of the Edwards aquifer. The locations of conduits in the Edwards aquifer were inferred by Worthington (2004, fig. 21) and Hovorka and others (2004).

The principal evidence of flow through karst is the heterogeneous and rapidly responsive nature of water-level variation. Using data from single storms, Worthington (2004) demonstrated two distinct responses in the Edwards aquifer, corresponding to conduit flow and matrix and small fracture flow. Wells close together can have different responses to a single recharge pulse (Johnson and others, 2002). The response of springs to rainfall is rapid. The maximum lag between rainfall and peak springflow was 11 days or less at Comal Springs and 9 days or less at San Marcos Springs following an intense storm October 17–19, 1998, centered in Comal County (Tomasko and others, 2001). In addition, tracer testing in the San Antonio segment of the Edwards aquifer has shown rapid flow (velocities of 180 to 800 meters per day (m/d) over distances of 0.8 to 4.0 kilometers (km)) from wells to the nearby high-flow springs (Ogden and others, 1986; Rothermel and others, 1987; Schindel and others, 2002).

Groundwater Occurrence and Flow

The northern Edwards aquifer boundary is defined by the updip limit of contiguous, outcropping rocks of the Edwards Group, Georgetown Formation, and their westward stratigraphic equivalents (Edwards rocks) and the southern boundary by the 10,000-milligrams per liter (mg/L) dissolved-solids concentration line, which is the downdip boundary of the freshwater/saline-water transition zone (fig. 3.3). The San Antonio segment of the aquifer (fig. 3.2) contains the most productive and transmissive parts of the aquifer. The San Antonio segment of the aquifer discharges primarily to Comal and San Marcos Springs, whereas the Barton Springs segment discharges primarily to Barton Springs (fig. 3.2).The Edwards aquifer is unconfined adjacent to and in the recharge zone (outcrop), where recharge occurs (fig. 3.3). The water table is at depths generally greater than 30 m below the streambeds. The Edwards aquifer is confined in downdip parts of the Balcones fault zone, including the freshwater zone and the freshwater/saline-water transition zone (fig. 3.3).

The groundwater-flow system of the Edwards aquifer in the San Antonio region includes (1) the catchment area in the Edwards Plateau, where the rocks of the Edwards-Trinity and Trinity aquifers are exposed and receive direct recharge to the water table; (2) the recharge zone, where streams lose flow directly into the unconfined Edwards aquifer and the aquifer receives direct recharge to the water table; and (3) the confined zone, which comprises the freshwater zone and the freshwater/saline-water transition zone (figs. 3.3 and 3.4). Water that enters the catchment area and recharge zone moves from unconfined to confined parts of the aquifer through generally southeasterly flow paths (fig. 3.5). In the confined zone, the water moves under low hydraulic gradients through fractured, highly transmissive, cavernous strata toward the east and northeast, where it is discharged through springs and wells. The freshwater zone and the freshwater/saline-water transition zone are hydraulically interconnected, but the aquifer transmits water in the freshwater zone at a much greater rate than in the transition zone (Schultz, 1992). Geochemical interpretation of water compositions (Clement, 1989; Oetting, 1995) documents slow movement of freshwater into the transition zone.

Conduits are major contributors to flow in the Edwards aquifer (Hovorka and others, 2004; Worthington, 2004). The multimodal permeability distribution of the Edwards aquifer (Hovorka and others, 1998) implies that the fastest-moving water, in fractures and conduits, can travel many times faster than the largest volume of water, in the matrix. Based on comparisons between mean matrix permeability and mean hydraulic conductivities estimated from aquifer tests, the contribution of matrix permeability to regional-scale hydraulic conductivity likely is minor, and most Edwards aquifer water flows through fractures and conduits (Hovorka and others, 1998). The absence of major known saline-water discharge areas might limit flow and conduit development in the freshwater/saline-water transition zone.

Faults can either increase or decrease total transmissivity (Hovorka and others, 1998). Some of the abundant, interconnected fractures in intensely fractured zones adjacent to faults have been enlarged, and they might focus flow parallel to faults. Where calcite cement fills breccia, cross-fault flow might be decreased. Stratigraphic offset of permeable zones along faults might also decrease the cross-fault flow (Maclay and Small, 1983, 1984). Holt (1959) observed nearly 30 m of head difference across faults in northern Medina County, and George (1952) reported head differences of 1.8 to 7.9 m across segments of major faults in unconfined, less-transmissive parts of the aquifer in Comal County. Maclay (1995) and Groschen (1996) characterized flow in the Edwards aquifer as being

controlled laterally by barrier faults that locally compartmentalize the aquifer, especially toward the eastern part of the San Antonio segment. Maclay and Land (1988) hypothesized that large-throw faults in Medina County act as barriers and divert flow to the west before flow is redirected back toward the east (fig. 3.5). Water entering the recharge zone flows on relay ramps—transfer zone accommodating deformation between normal fault segments with similar dip directions (Peacock and Sanderson, 1994)—to the west and southwest before resuming the eastward regional flow direction.

Aquifer Hydraulic Properties

The hydraulic properties of primary interest include permeability, hydraulic conductivity, transmissivity, anisotropy, and storativity. Qualitative estimates of relative permeability for stratigraphic and hydrogeologic units are shown in table 3.2. Matrix, fracture, and conduit permeability occur in the Edwards aquifer. The carbonate matrix of the Edwards aquifer is very permeable; however, in many intervals, the very high permeabilities resulting from conduits and fractures dwarf the matrix contribution. Outcrops, which are at the highest altitudes, show abundant dissolution features and additional karst features that have developed in near-surface settings; however, matrix porosity and permeability of outcrop rocks are low relative to those in the aquifer. Geochemical processes that favor dissolution might account for greater development of conduit and matrix permeability in the deeper, downdip parts of the aquifer (Hovorka and others, 1998).

Transmissivity and hydraulic conductivity of the Edwards aquifer each vary over several orders of magnitude. On the basis of numerical modeling results, Maclay and Land (1988) estimated transmissivities of more than 399,470 meters squared per day (m^2/d) in Comal County near Comal Springs in the freshwater confined zone of the aquifer; their smallest estimated transmissivity was 12 m^2/d in the freshwater/saline-water transition zone. The transmissivity for most of the freshwater zone of the confined aquifer ranges from 39,947 to 204,380 m^2/d and in the recharge area generally is less than 39,947 m^2/d (Maclay and Land, 1988). Hovorka and others (1998) reported that transmissivity ranges from $9.29x10^{-3}$ to $9.29x10^5$ m^2/d, and hydraulic conductivity ranges from $3.05x10^{-4}$ to $3.05x10^4$ m/d, on the basis of specific-capacity and other aquifer tests. Painter and others (2002) estimated hydraulic conductivity for the Edwards aquifer in the San Antonio region ranging from 0.3 to 2,239 m/d, based on a combination of spatial statistical methods and model calibration for hydraulic conductivity using a Bayesian updating procedure (Woodbury and Ulrych, 1998, 2000).

Hovorka and others (1998, table 10) reported mean hydraulic conductivities, computed from specific capacity, for the recharge zone (outcrop) and confined zone of the San Antonio segment of the Edwards aquifer of 0.085 and 10.4 m/d, respectively, and 3.4 m/d for the aquifer as a whole. A mean of 0.03 m/d was reported for the hydraulic conductivity of the matrix. Structurally influenced cave systems contribute the highest hydraulic conductivities (3.05 to $3.05x10^5$ m/d), solution-enhanced fractures and stratigraphicallycontrolled karst features contribute intermediate values, and the porous carbonate matrix contributes hydraulic conductivities of $3.05x10^{-4}$ to 3.05 m/d (Hovorka and others, 1998).

The quantitative magnitude of anisotropy of the Edwards aquifer is largely unknown. Factors that might influence anisotropy in the aquifer include the presence of barrier faults with large vertical displacements and the development of conduits. Water circulation might cause focused dissolution and the development of conduits along the main flow paths in carbonate aquifers. Because faults are most abundant across northern Medina, central Bexar, southern Comal, southern Hays, and central Travis Counties (Maclay and Small, 1984, fig. 3; Baker and others, 1986, fig. 2), the strongest anisotropy exists east of Uvalde County. The ratio of anisotropy, which is the ratio of y-direction transmissivity to x-direction transmissivity, derived from past digital-model analysis ranges from 0:1 to 1:1 (Maclay and Land, 1988). The regional maximum directional transmissivity is generally aligned from the west-southwest to the east-northeast, parallel with structural features and prevailing groundwater flow paths.

The amount and distribution of water in the Edwards aquifer are related to the development of porosity and the storage characteristics of the aquifer. Hovorka and others (1996) estimated that Edwards aquifer porosity varies vertically from lows of 4 to 12 percent to highs of 20 to 42 percent, and the average for the entire aquifer is 18 percent. The effective porosity generally ranges from 2 to 14 percent (Maclay and Small, 1976); 6 percent is considered to be average (Maclay, 1995). Reported estimates of specific yield for the San Antonio segment of the Edwards aquifer range from 0.025 to 0.20, and reported estimates of storage coefficient range from $1x10^{-5}$ to $8x10^{-4}$ (Maclay and Rettman, 1973; Sieh, 1975; Klemt and others, 1979; Maclay and Small, 1984; Maclay and Land, 1988; Hovorka and others, 1993). Reported estimates of specific yield for the Barton Springs segment range from 0.005 to 0.06, and reported specific storage ranges from $3.28x10^{-6}$ to $9.51x10^{-2}$ m^{-1} (Brune and Duffin, 1983; Senger and Kreitler, 1984; Slade and others, 1985; Scanlon and others, 2002).

Water Budget

Water-level fluctuations reflect changes in the amount of water in storage in the Edwards aquifer. The aquifer is dynamic, and water levels generally respond to temporal and spatial variations in recharge and groundwater withdrawals. During periods of drought, water levels decline but recover rapidly in response to recharge. Although recurring droughts and floods have caused appreciable short-term fluctuations in water levels, long-term hydrographs from about 80 years of record indicate no net decline—or rise—of water levels in the San Antonio area.

The total amount of stored water in the Edwards aquifer represents the long-term accumulation of the volumetric difference between recharge and discharge. Hovorka and others (1996) estimated the total amount of water-filled pore space within the San Antonio segment of the Edwards aquifer to be 213,420.6 hm^3. Of this, 193,682.3 hm^3 of water is stored in the confined zone and 19,738.3 hm^3 is stored in the unconfined zone. Maclay (1989) estimated that 30,841.1 to 67,850.5 hm^3 of water in the Edwards aquifer is circulating in pore space or drainable by gravity.

Estimates for the major sources of water to and discharges from the San Antonio segment of the Edwards aquifer are shown in table 3.3. Similar estimates for the Barton Springs segment of the aquifer are incomplete and not readily available. Estimated average annual flow rates are given for 1993–2002, a relatively wet period, and for 1934–2002. Recharge from leakage through streambeds and infiltration of precipitation in interstream areas was about 14 percent greater during 1993–2002 compared to the long-term average for 1934–2002. Total discharge was also greater during 1993–2002than the 1934–2002 long-term average, due to greater springflowresulting from greater recharge and greater withdrawals resulting from increased demands for groundwater. The sources of water to and discharges from the Edwards aquifer in the South-Central Texas regional study area are discussed in more detail in the following sections of the report.

Recharge

The Edwards aquifer is recharged through (1) seepage losses from surface streams that drain the Hill Country, where the streams flow onto the outcrop of the Edwards aquifer; (2) infiltration of rainfall on the outcrop; (3) subsurface inflow across the updip margin of the Balcones fault zone, where the Trinity aquifer is laterally adjacent to the downfaulted Edwards aquifer (LBG-Guyton Associates, 1995); and (4) movement of water from the Trinity aquifer, where it underlies the Edwards aquifer, into the Edwards aquifer (fig. 3.4). The primary source of recharge is seepage from streams crossing the outcrop; hence, the outcrop is synonymous with the recharge zone. The headwater stream basins compose the catchment area and recharge zone (fig. 3.3). All of the base flow and some of the storm runoff of streams crossing the recharge zone, other than the Guadalupe River, infiltrate to the unconfined aquifer and are losing streams. Reported percentages of the total recharge that occurs as infiltration in interstream areas, rather than in streambeds, are (1) 15 percent for the Barton Springs segment of the Edwards aquifer (Slade and others, 1985; Scanlon and others, 2002) and (2) 20 percent (Klemt and others, 1979; Thorkildsen and McElhaney, 1992) and 40 percent (Maclay and Land, 1988) for the San Antonio segment.

Estimates of the combined recharge to the San Antonio segment of the Edwards aquifer from stream seepage and infiltration of rainfall range from a low of 53.9 hm^3 during 1956 to a high of 3,066.8 hm^3 during 1992 (Hamilton and others, 2003). The long-term (1934–2002) mean annual recharge to the Edwards aquifer is 862.2 hm^3 (median 688.1 hm^3) and for 1993–2002, is 979.6 hm^3 (median 710.9 hm^3) (Hamilton and others, 2003). Monthly rates of recharge for the San Antonio segment of the Edwards aquifer from seepage losses from streams and infiltration of rainfall in the recharge zone are computed from records of streamflow-gaging stations near upstream and downstream limits of the recharge area and from estimated runoff in the recharge area (Puente, 1978; Slattery, 2004). Recent unpublished work indicates that 50 to 60

Table 3.3. Estimated water budget components for the San Antonio segment of the Edwards aquifer for 1993–2002 and 1934–2002, San Antonio region, Texas.

[Recharge includes leakage from streams through streambeds and infiltration of precipitation in interstream areas. Estimates of recharge, withdrawals (pumpage), and springflow are from Hamilton and others (2003). Estimates of inflow from Trinity aquifer are from Mace and others (2000). hm3/yr, cubic hectometers per year]

Budget component	Source			
	1993–2002		1934–2002	
	Flow rate (hm^3/yr)	Percentage of total sources or discharges	Flow rate (hm^3/yr)	Percentage of total sources or discharges
Recharge	980	93	862	92
Inflow from Trinity aquifer	79	7	79	8
Total sources	1,059	100	941	100
Discharge				
Withdrawals (pumpage)	512	49	375	45
Springflow	535	51	459	55
Total discharges	1,046	100	835	100

percent of the stream channel for Cibolo Creek between the streamflow-gaging stations, which was used to estimate the leakage from Cibolo Creek to the Edwards aquifer, lies within the Trinity aquifer outcrop area (Darwin Ockerman, U.S. Geological Survey, written commun., 2002).

The Edwards aquifer in much of the Balcones fault zone is juxtaposed against the Trinity aquifer both at the surface and at depth, and the Trinity aquifer likely discharges directly into the Edwards aquifer. The volume of flow from the Trinity aquifer into the Edwards aquifer can only be estimated. The available estimates vary. Woodruff and Abbott (1986) reported that recharge from Trinity aquifer inflow is 6 percent of total recharge, or about 50.6 hectometers per year (hm^3/yr) on average, to the Edwards aquifer. LBG-Guyton Associates (1995) estimated an approximate range of Trinity aquifer underflow to the Edwards aquifer in the San Antonio region, excluding the Cibolo Creek contribution, of about 3.3 to 14.1 hm^3/yr, representing about 2 percent of total average annual recharge to the Edwards aquifer. A flow of about 79.0 hm^3/yr from the upper and middle zones of the Trinity aquifer in the direction of the Edwards aquifer, representing about 9 percent of the average estimated annual recharge to the Edwards aquifer, was simulated by Mace and others (2000).

Discharge

Most discharge from the Edwards aquifer occurs as (1) withdrawals by industrial, irrigation, and public-supply wells, and (2) springflow. Groundwater withdrawals by wells have increased with increasing population. From 1934 through 2002, the lowest estimated annual pumpage (withdrawals) was 125.7 hm^3 in 1934 and the highest was 669.1 hm^3 in 1989 (Hamilton and others, 2003). Springflow from the San Antonio segment averaged 459.2 hm^3/yr (median 463.6 hm^3/yr) for 1934–2002 (Hamilton and others, 2003). Total annual springflow from the Edwards aquifer has varied as much as an order of magnitude over the period of record. Springflow totaled 86.1 hm^3 in 1956 during the 1950s drought and reached a record high of 990.4 hm^3 in 1992 (Hamilton and others, 2003). Water also discharges from the Edwards aquifer to the Leona River floodplain in south-central Uvalde County. Green (2004) estimated that as much as 123.4 hm^3/yr is discharged from the Edwards aquifer to the Leona River floodplain, about 13 percent of which becomes surface flow in the Leona River and about 87 percent becomes subsurface flow in the sand and gravel deposits. Part of the subsurface flow ultimately discharges to Leona Springs.

Thousands of water wells tap the Edwards aquifer in the San Antonio region. Annual discharge by wells increased steadily at an average annual rate of about 5.6 hm^3/yr, more than tripling between 1939 and 2000. Municipal, irrigation, and industrial water use make up more than 95 percent of annual withdrawals from the Edwards aquifer in each county except for Comal County, where mining by rock quarries also accounts for appreciable withdrawals. In Bexar, Hays, Kinney, and Travis Counties, municipal water withdrawals account for more than 85 percent of annual withdrawals. Irrigation accounts for more than 60 percent of withdrawals in Uvalde County and more than 80 percent in Medina County. Bexar and Uvalde Counties are the largest producers of groundwater from the Edwards aquifer in the San Antonio region. Pumpage is concentrated in the confined part of the Edwards aquifer, and the largest withdrawals are in and around San Antonio. Yields of more than 3.5 cubic meters per minute (m^3/min) are common for wells in the confined freshwater zone of the Edwards aquifer. The density of wells in the unconfined recharge zone of the aquifer is substantially less than that in the confined zone, and typically the yields are smaller.

Springs and seeps are the major natural discharge outlets for the Edwards aquifer, accounting for nearly all natural discharge from the aquifer. Comal and San Marcos Springs are the largest springs, with total discharges of 339.0 and 241.7 hm^3, respectively, in 2002, which translates to flow rates of 10.76 and 7.67 cubic meters per second (m^3/s), respectively (Hamilton and others, 2003). Groschen (1996) postulated that the locations of most major springs in the Edwards aquifer are structurally controlled. Groundwater flow is diverted along barrier faults, with vertical openings at a few places along faults where springs can emerge. Faults that intersect the aquifer at depth provide a pathway for water to rise to the land surface. Leona Springs consists of a number of seeps emerging from permeable gravel of the Leona Formation within the channel of the Leona River in Uvalde County. The average annual discharge estimated by the USGS for Leona Springs was about 16.0 hm^3 (0.51 m^3/s) for 1939–2000. However, the discharge from Leona Springs estimated by the USGS might appreciably underestimate the actual discharge because of unmeasured discharge from the Edwards aquifer to the overlying Leona gravels (Green, 2004).

Increases in pumpage upgradient from the springs have, at times, appreciably reduced the discharge at Comal Springs. The only period of zero flow at Comal Springs was from June 13, 1956, to November 4, 1956, near the end of the severe drought of the 1950s. Maclay (1995) concluded that most of the San Marcos Springs discharge might be derived from water entering the aquifer in the Cibolo Creek and Dry Comal Creek, Guadalupe River, and Blanco River Basins (fig. 3.2). Hueco Springs is the only large spring in the Edwards aquifer outcrop area—its 1945–73 average annual flow was about 1.0 m^3/s—and it is believed to have a much smaller contributing area than any of the other major springs. An unknown percentage of the Hueco Springs flow might be derived from the Trinity aquifer (LBG-Guyton Associates, 1995). Increased pumpage, primarily from wells in San Antonio, has resulted in frequent periods of zero discharge from San Antonio and San Pedro Springs (Brune, 1975). San Antonio Springs has a larger discharge capacity and higher spring orifice altitude than San Pedro Springs.

Groundwater Quality

The groundwater chemistry of the Edwards aquifer in the San Antonio segment is relatively homogeneous and typical of a well-buffered carbonate aquifer system. Water-chemistry data collected for the USGS NAWQA Program during 1996–2006 include results from domestic, public, monitoring, and other wells located in both unconfined (recharge zone) and confined parts of the aquifer. Calcium and bicarbonate are the dominant dissolved ions, reflecting the carbonate lithology of the aquifer. Dissolved-solids concentrations of the unconfined and confined parts of the aquifer are similar, with a median value of 380 milligrams per liter (mg/L) and a range from 280 mg/L to 560 mg/L. The pH values range from 6.5 to 7.4 standard units, with a median of 7.0.

Oxidation-reduction (redox) conditions in the Edwards aquifer are characterized by predominantly oxidizing conditions. A few isolated wells that have higher dissolved-solids concentrations, or less oxidizing conditions, may be influenced by water from the underlying Trinity aquifer or saline water in the Edwards aquifer. Oxygen-reducing conditions generally occur upgradient of the 1,000 mg/L dissolved-solids concentration line, which is the updip boundary of the freshwater/saline-water transition zone (fig. 3.6). Variably-reducing conditions typically occur downgradient of this boundary.

The water chemistry of groundwater samples from the unconfined part of the Edwards aquifer is not significantly different from that of samples from the confined part of the aquifer, including spring samples. Nonetheless, as groundwater-residence times increase along flow paths from shallow unconfined parts of the aquifer to deep confined parts, geochemical evolution processes may affect the proportions of dissolved ions. Water samples from wells completed in the confined part of the aquifer generally have slightly lower bicarbonate, calcium, and dissolved oxygen and slightly higher sodium, sulfate, chloride, and strontium concentrations compared to water samples from wells completed in the unconfined part.

The USGS defined a national background threshold of 2.0 mg/L as nitrogen for nitrate (U.S. Geological Survey, 1999). Samples with nitrate concentrations greater than 2.0 mg/L as nitrogen might contain nitrogen derived from anthropogenic sources, for example, from human or industrial waste, fertilizer use, or livestock operations. Nitrate concentrations in water samples collected for the USGS NAWQA Program during 1996–2006 ranged from nondetection, defined as less than 0.05mg/L, to 8.23 mg/L, with a median of 1.68 mg/L. Nitrate nitrogen concentrations did not exceed the public drinking-water standard of 10 mg/L (U.S. Environmental Protection Agency, 2006).

Radon activities in water samples from the unconfined Edwards aquifer ranged from 80 to 776 picocuries per liter (pCi/L), and radon in 10 samples exceeded a proposed public drinking-water standard of 300 pCi/L. The source of radon in the Edwards aquifer is unknown (Bush and others, 2000).

Most water samples from the Edwards aquifer contained tritium (^{3}H) at concentrations indicating that the water was derived from recharge within the last decade, including five water samples from springs that issue from the confined part of the Edwards aquifer (Fahlquist and Ardis, 2004).

Organic compounds have been found throughout the Edwards aquifer, mostly at very low concentrations of much less than 1 microgram per liter (µg/L) (Musgrove and others, 2010). Pesticide compounds were widely measured in water samples from the Edwards aquifer collected for the USGS NAWQA Program during 1996–2006, albeit at very low concentrations (much less than 1 µg/L). Atrazine and its breakdown product deethylatrazine were the most frequently detected compounds; they were detected in greater than 50 percent of the wells, similar to the results observed for other USGS NAWQA major aquifer studies across the Nation (Bush and others, 2000; U.S. Geological Survey, 1999; Fahlquist and Ardis, 2004). Frequency of detection and range of concentration were 55 percent and less than 0.001 to 0.132 µg/L, respectively, for atrazine and 68 percent and less than 0.002 to 0.053 µg/L, respectively, for deethylatrazine. Other pesticide compounds also were detected, but less frequently. Some water samples from the Edwards aquifer contained more than one pesticide compound. Moran and others (2002) reported that the most commonly detected volatile organic carbon compounds (VOCs) in USGS NAWQA major aquifer studies across the Nation, regardless of well type, are trihalomethanes (THMs) and solvents. Similar results were observed for NAWQA samples collected from the Edwards aquifer. Most VOCs were measured at small concentrations, which were much less than 1 µg/L; however, some were measured at concentrations greater than 1 µg/L. The most frequently detected VOCs in water samples from the Edwards aquifer, which were detected in greater than 50 percent of water samples, were trichloromethane (chloroform), and tetrachloroethene (PCE). Frequency of detection and range of concentration were 66 percent and less than 0.024 to 5.88 µg/L, respectively, for trichloromethane and 43 percent and less than 0.027 to 0.95 µg/L, respectively, for tetrachloroethene.

Groundwater-Flow Simulations

Existing numerical models of groundwater flow developed in MODFLOW-2000 (Harbaugh and others, 2000) for the Edwards aquifer (Lindgren and others, 2004; Lindgren, 2006) (hereinafter, the original Edwards aquifer models) were modified to simulate groundwater flow in the South-Central Texas regional study area. The original Edwards aquifer models were calibrated for steady-state and transient conditions. The steady-state calibration period was 1939–46, representing average conditions for a near-predevelopment interval when irrigation development was minimal. The transient calibration period, which includes changes in groundwater storage over time, was 1947–2000, including 648 monthly stress periods.

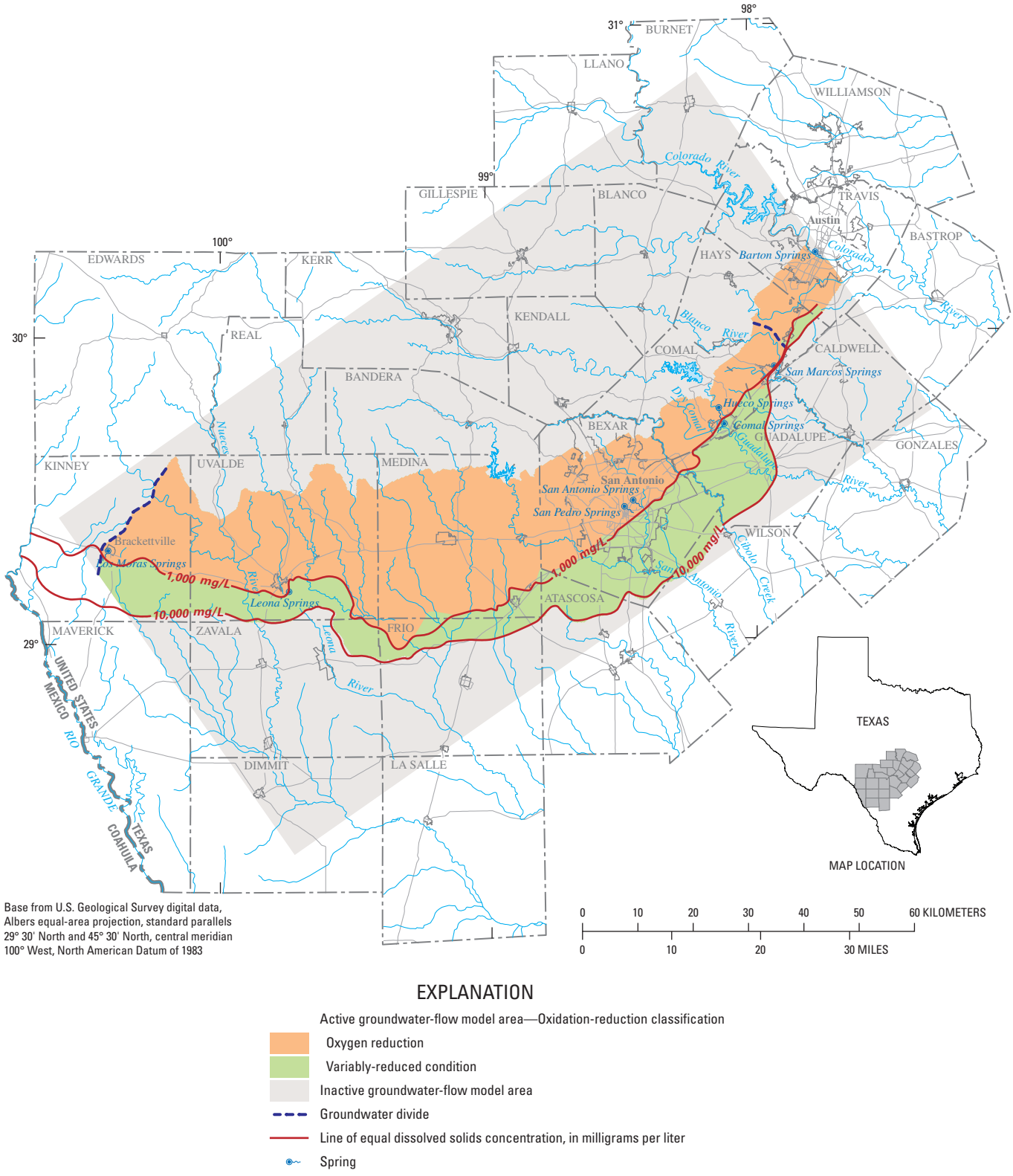

Figure 3.6. Oxidation-reduction classification zones for the Edwards aquifer in the South-Central Texas regional study area, San Antonio region, Texas.

The original Edwards aquifer models were calibrated for two hydraulic-conductivity distributions. A numerical groundwater-flow model (hereinafter, the conduit-flow Edwards aquifer model) of the karstic Edwards aquifer in south-central Texas was developed for a study conducted during 2000–03 on the basis of a conceptualization emphasizing conduit development and conduit flow (Lindgren and others, 2004). Uncertainties regarding the degree to which conduits pervade the Edwards aquifer and influence groundwater flow, as well as other uncertainties inherent in simulating conduits, raised the question of whether or not a model based on the conduit-flow conceptualization was the optimum model for the Edwards aquifer. Accordingly, a model with an alternative hydraulic-conductivity distribution without conduits was developed in a study conducted during 2004–05 (Lindgren, 2006). The hydraulic-conductivity distribution for the modified Edwards aquifer model (hereinafter, the diffuse-flow Edwards aquifer model) is based primarily on a conceptualization in which flow in the aquifer predominantly is through a network of numerous small fractures and openings.

The original Edwards aquifer models were modified for the South-Central Texas regional study to a finer discretization, both horizontally and vertically, and updated to include the 2001–2003 time period. The rediscretized Edwards aquifer models (hereinafter, the rediscretized regional Edwards aquifer models) were calibrated using two different hydraulic-conductivity distributions, based on conduit flow or diffuse flow, as for the original Edwards aquifer models. The two rediscretized regional Edwards aquifer models are hereinafter referred to as the conduit-flow rediscretized regional Edwards aquifer model and the diffuse-flow rediscretized regional Edwards aquifer model. The initial boundary conditions and hydraulic properties used in the rediscretized regional Edwards aquifer models were the same as those used in the original Edwards aquifer models, but they were adjusted to conform to the smaller grid size in the rediscretized regional Edwards aquifer models.

Model Area and Spatial Discretization

The uniformly spaced finite-difference grid used to spatially discretize the model area for the rediscretized regional Edwards aquifer models has 740 rows and 1,400 columns and is rotated 35 degrees counterclockwise from horizontal (fig. 3.7). The dimensions of the grid cells are uniformly 201.2 m along rows and columns, half the dimensions of those for the original Edwards aquifer models (Lindgren and others, 2004; Lindgren, 2006). Two model layers were used to represent the multiple hydrogeologic zones that comprise the Edwards aquifer, compared to the one model layer for the original Edwards aquifer models. Model layer 1 represents the hydrostratigrahic units of the Edwards aquifer above the Regional Dense Member (table 3.2). Model layer 2 represents the hydrostratigrahic units of the Edwards aquifer below, and including, the Regional Dense Member (table 3.2). The layer thickness for model layer 1 ranges from 0 to 218.2 m and for model layer 2 ranges from 2.74 to 358.1 m. The Edwards aquifer was not discretized more finely in the vertical dimension because of a lack of hydrogeologic data sufficient to spatially define additional individual zones within the aquifer. The extent of layer 2 for the rediscretized regional Edwards aquifer models is the same as the extent of the single layer for the original Edwards aquifer models (Lindgren and others, 2004, fig. 2). The extent of layer 1 for the rediscretized regional Edwards aquifer model (fig. 3.7) coincides approximately with the areas where the hydrostratigraphic units of the Edwards aquifer above the Regional Dense Member are present.

Boundary Conditions

The boundary conditions for model layers 1 and 2 of the rediscretized regional Edwards aquifer models (fig. 3.7) are generally the same as for the original Edwards aquifer models (Lindgren and others, 2004, fig. 18). The interested reader is referred to Lindgren and others (2004) and Lindgren (2006) for further discussion of boundary conditions in the original Edwards aquifer models. The MODFLOW well package was used to simulate a constant flux through the northern model boundary and the northern part of the western model boundary for layer 2 for all stress periods. The northern boundary for layer 1 of the rediscretized regional Edwards aquifer models corresponds approximately with the physical limits of the hydrostratigraphic units that the layer represents; therefore, a no-flow boundary condition was imposed.

The eastern model boundary and the southern part of the western model boundary for layers 1 and 2 of the rediscretized regional Edwards aquifer models were assigned a no-flow boundary condition (fig. 3.7). The northern part of the eastern model boundary is defined by the location of the Colorado River, which is a regional sink for the Edwards aquifer. The southern part of the western model boundary coincides with the location of a groundwater divide near Brackettville in Kinney County (LBG-Guyton Associates, 1995). A no-flow boundary condition was also imposed for layers 1 and 2 for the southern model boundary coinciding with the 10,000-mg/L dissolved solids concentration line, assuming minimal down-dip flow of freshwater from the Edwards aquifer.

Aquifer Structure

Model aquifer structure considerations include assigning top and bottom altitudes of the Edwards aquifer to model cells and the simulation of faults and conduits. The altitude of the top of model layer 1 for the rediscretized regional Edwards aquifer models is the same as the altitude of the top of the single model layer simulated in the original Edwards aquifer models (Lindgren and others, 2004; Lindgren, 2006). However, model layer 1 is absent in the rediscretized regional Edwards aquifer models in areas where the hydrostratigrahic units above the Regional Dense Member are absent. These areas where model layer 1 is absent are limited to the Edwards aquifer outcrop area (recharge zone). The altitude of the

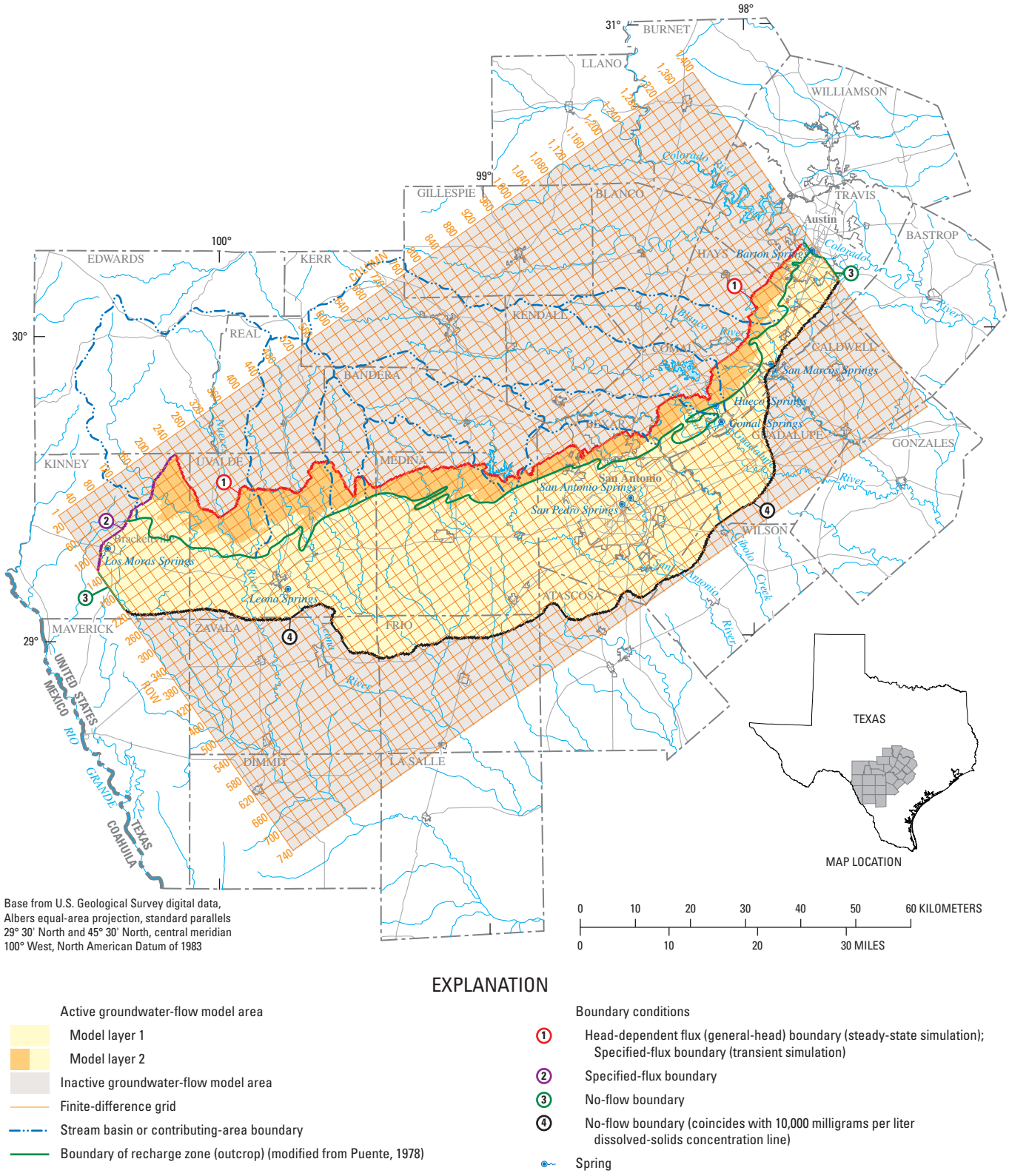

EXPLANATION

Active groundwater-flow model area
- Model layer 1
- Model layer 2

Inactive groundwater-flow model area

Finite-difference grid

Stream basin or contributing-area boundary

Boundary of recharge zone (outcrop) (modified from Puente, 1978)

Boundary conditions
- (1) Head-dependent flux (general-head) boundary (steady-state simulation); Specified-flux boundary (transient simulation)
- (2) Specified-flux boundary
- (3) No-flow boundary
- (4) No-flow boundary (coincides with 10,000 milligrams per liter dissolved-solids concentration line)
- Spring

Figure 3.7. Model grid, extent of model layers, and boundary conditions for the rediscretized regional Edwards aquifer models, San Antonio region, Texas.

bottom of model layer 1 coincides with the altitude of the top of the Regional Dense Member. The altitude of the top of model layer 2 for the rediscretized regional Edwards aquifer models coincides with the land-surface altitude in those areas where model layer 1 is absent. The altitude of the bottom of model layer 2 coincides with the altitude of the top of the Glen Rose Limestone, except where it is modified in the recharge zone (Lindgren and others, 2004).

The anisotropy of the Edwards aquifer is largely unknown, except for that attributable to the presence of faults. The anisotropic effects of faults were incorporated in the original and the rediscretized regional Edwards aquifer models by using the MODFLOW Horizontal Flow Barrier package (Harbaugh and others, 2000). Conduits are simulated in the conduit-flow Edwards aquifer models (original and rediscretized regional models) by narrow (0.40-km wide), initially continuously connected zones with large hydraulic-conductivity values. The locations of conduit zones in the conduit-flow Edwards aquifer model were assigned on the basis of the conduit locations inferred by Worthington (2004) (Lindgren and others, 2004, fig. 7) and modified during model calibration (Lindgren and others, 2004, fig. 7). The interested reader is referred to Lindgren and others (2004) for further discussion of the simulation of faults and conduits.

Aquifer Hydraulic Properties

The aquifer hydraulic properties specified in the Edwards aquifer models (original and rediscretized regional models) are hydraulic conductivity and storativity. The horizontal hydraulic-conductivity distribution for the conduit-flow Edwards aquifer model (Lindgren and others, 2004) includes two components. The first component is the hydraulic-conductivity distribution developed by Painter and others (2002), with values ranging from 0.3 to 2,239 m/d. An approach based on nonparametric geostatistics, stochastic simulation, and numerical flow simulation was used to upscale and interpolate hydraulic-conductivity estimates to the Edwards aquifer model grid. The second component is the network of conduits, as mapped by Worthington (2004, fig. 21) (Lindgren and others, 2004, fig. 7). For the Barton Springs segment of the aquifer, the hydraulic-conductivity distribution from Scanlon and others (2002), rather than that of Painter and others (2002), was used.

The horizontal hydraulic-conductivity distribution for the diffuse-flow Edwards aquifer model (Lindgren, 2006) is based primarily on a diffuse-flow conceptualization of groundwater flow. The preliminary diffuse-flow hydraulic-conductivity distribution included a total of 24 zones—8 for the recharge zone, 15 for the confined freshwater zone, and 1 for the freshwater/saline-water transition zone. The initial model simulation results for the diffuse-flow Edwards aquifer model indicated that the simulated springflows for Comal and San Marcos Springs were much lower than the measured springflows, and further upscaling of hydraulic conductivity was required to simulate the high measured springflows. The required upscaling of the hydraulic conductivity was accomplished by the insertion of broad high hydraulic conductivity (HHC) zones within the model domain. The widths of the delineated HHC zones vary from as narrow as 1.2 km near the freshwater/saline-water interface and San Marcos Springs to as wide as approximately 8 to 16 km.

The initial hydraulic-conductivity distributions for the conduit-flow rediscretized regional Edwards aquifer model and the diffuse-flow rediscretized regional Edwards aquifer model were the same as for the conduit-flow Edwards aquifer model and the diffuse-flow Edwards aquifer model, respectively. The initial horizontal hydraulic-conductivity distributions for layers 1 and 2 in the rediscretized regional Edwards aquifer models (conduit-flow and diffuse-flow) were the same.

Because the rediscretized regional Edwards aquifer models include two model layers, vertical hydraulic conductivity also needed to be specified. Isotropic conditions were assumed, with the vertical hydraulic conductivity for each model cell being the same as the horizontal hydraulic conductivity. Although hydrogeologic units with differing relative permeabilities ranging from very small to large comprise the Edwards aquifer (table 3.2), (1) vertical variations in hydraulic conductivity in the aquifer indicate that the entire aquifer is highly permeable as well as highly variable (Hovorka and others, 1998) and (2) the Regional Dense Member, which has a very small permeability (table 3.2), is generally not considered a regional confining unit. Unrestricted vertical flow and mixing in the aquifer is also indicated by the relatively uniform quality and temperature of water throughout the aquifer (Maclay, 1995). A sensitivity analysis done for vertical hydraulic conductivity indicated that reducing vertical hydraulic conductivity by factors of 0.1, 0.01, and 0.001 for the steady-state simulations had minimal effects on the residuals for hydraulic heads for the rediscretized regional Edwards aquifer models (conduit-flow and diffuse-flow models). The reductions in the mean absolute error of the residuals for hydraulic heads resulting from the variations in vertical hydraulic conductivity were less than 0.03 m. The changes in the residuals for springflows were generally less than 6 percent, except for as much as 23 percent for Comal Springs for the diffuse-flow model, as much as 27 percent for San Marcos Springs for the conduit-flow model, and as much as 46 percent for San Antonio Springs for both models. A reduction in the vertical hydraulic conductivity resulted in both increases and decreases in the residuals for springflows. For the conduit-flow model, reducing the vertical hydraulic conductivity resulted in a decrease in the residuals for all of the springs except San Antonio Springs. For the diffuse-flow model, reducing the vertical hydraulic conductivity resulted in a decrease in the residuals for San Marcos and Leona Springs and an increase in the residuals for Comal, San Antonio, and San Pedro Springs.

The initial storativity values were varied during model calibration for the conduit-flow Edwards aquifer model, resulting in a zonation of values (Lindgren and others, 2004). The storativity distribution for the diffuse-flow Edwards aquifer model and for the rediscretized regional Edwards aquifer models (conduit-flow and diffuse-flow models) are the same

as the final calibrated storativity distribution for the conduit-flow Edwards aquifer model (Lindgren and others, 2004). The storativity distribution for model layers 1 and 2 of the rediscretized regional Edwards aquifer models is the same. The interested reader is referred to Lindgren and others (2004) and Lindgren (2006) for further discussion of the simulation of hydraulic properties in the original Edwards aquifer models.

Model Stresses

Stresses include recharge to and discharge from the Edwards aquifer. Recharge to the Edwards aquifer occurs primarily by seepage from streams to the aquifer in the recharge zone. Discharge from the Edwards aquifer includes withdrawals by wells and springflow.

Recharge

Recharge to the Edwards aquifer occurs primarily by seepage from streams to the aquifer in the recharge zone (fig. 3.3). Additional recharge is from infiltration of rainfall in the interstream areas of the recharge zone. Recharge in the San Antonio segment of the aquifer by seepage from streams and infiltration of rainfall was assigned to eight major recharging streams and their interstream areas (hereinafter referred to as recharge subzones) in the recharge zone (fig. 3.8), on the basis of monthly recharge rates to the Edwards aquifer for 2000–2003 computed by the USGS and published, as annual totals, by the Edwards Aquifer Authority (EAA). Recharge rates for the Guadalupe River recharge subzone, not computed by the USGS, were calculated as the average of the recharge rates for the adjacent Cibolo Creek and Dry Comal Creek and Blanco River recharge subzones. Annual and monthly recharge rates for six recharge basins in the Barton Springs segment of the aquifer (fig. 3.8) were estimated using the methods described by Barrett and Charbeneau (1996) and Scanlon and others (2002). Recharge rates for the Colorado River recharge subzone were assumed to be the same as for the adjacent Barton Creek subzone. Monthly recharge rates for the recharge subzones simulated in the rediscretized regional Edwards aquifer models (conduit-flow and diffuse-flow models) are shown in table 3.4. For both the San Antonio and Barton Springs segments of the Edwards aquifer, 85 percent of the recharge was applied to streambed cells and the remaining 15 percent was applied to the interstream cells. A specified-flux boundary, simulated using the MODFLOW recharge package, was used to represent recharge to the aquifer in the recharge zone in the original and rediscretized regional Edwards aquifer models. No recharge was applied to cells outside the recharge zone.

Discharge

Discharge from the Edwards aquifer includes withdrawals by wells and springflow. Withdrawals by wells for 2000–03 were compiled and distributed spatially and temporally within the model grid for the rediscretized regional Edwards aquifer models (conduit-flow and diffuse-flow models). The vertical assignment of pumpage to a layer was done based on the percentage of the screened interval in each of the two layers. Withdrawals were separated into four categories based on water use: municipal, irrigation, industrial, which includes manufacturing, mining, and power generation, and livestock. Municipal withdrawals were provided (1) by well by EAA, Bexar Metropolitan Water District, and Fort Clark Municipal Utility District and (2) by entry point by the San Antonio Water System (SAWS) for each of their 36 well fields. Irrigation, industrial, and livestock withdrawals were provided by well for most of the model area, with the exception of Kinney County, where irrigation withdrawals were spatially distributed for the land-use categories of row crops, small grains, and orchard/vineyards. Industrial and livestock withdrawals for Kinney County are minimal and were not simulated in the models. All municipal and irrigation withdrawals for the years 2000 through 2003 were distributed to stress periods (months) based on factors developed for the original Edwards aquifer model (Lindgren and others, 2004). All industrial and livestock withdrawals were distributed to stress periods (months) based on factors provided by the reporting agency or developed by the Texas Water Development Board.

Discharge from the Edwards aquifer also includes springflow. Comal, San Marcos, Leona, San Antonio, and San Pedro Springs were simulated in the original and the rediscretized regional (layer 1) Edwards aquifer models and used for model calibration (fig. 3.7). The springs were simulated in the models using the MODFLOW drain package (Harbaugh and others, 2000). The MODFLOW drain package simulates the effects of features that remove water from the aquifer at a rate proportional to (1) the difference between the hydraulic head in the aquifer and the drain elevation and (2) the hydraulic conductance. The hydraulic conductance depends on the characteristics of the convergent flow pattern toward the drain, as well as on the characteristics of the drain itself and its immediate environment (Harbaugh and others, 2000). Conductance was adjusted during model calibration for the original Edwards aquifer model to match measured values of discharge to simulated values (Lindgren and others, 2004).

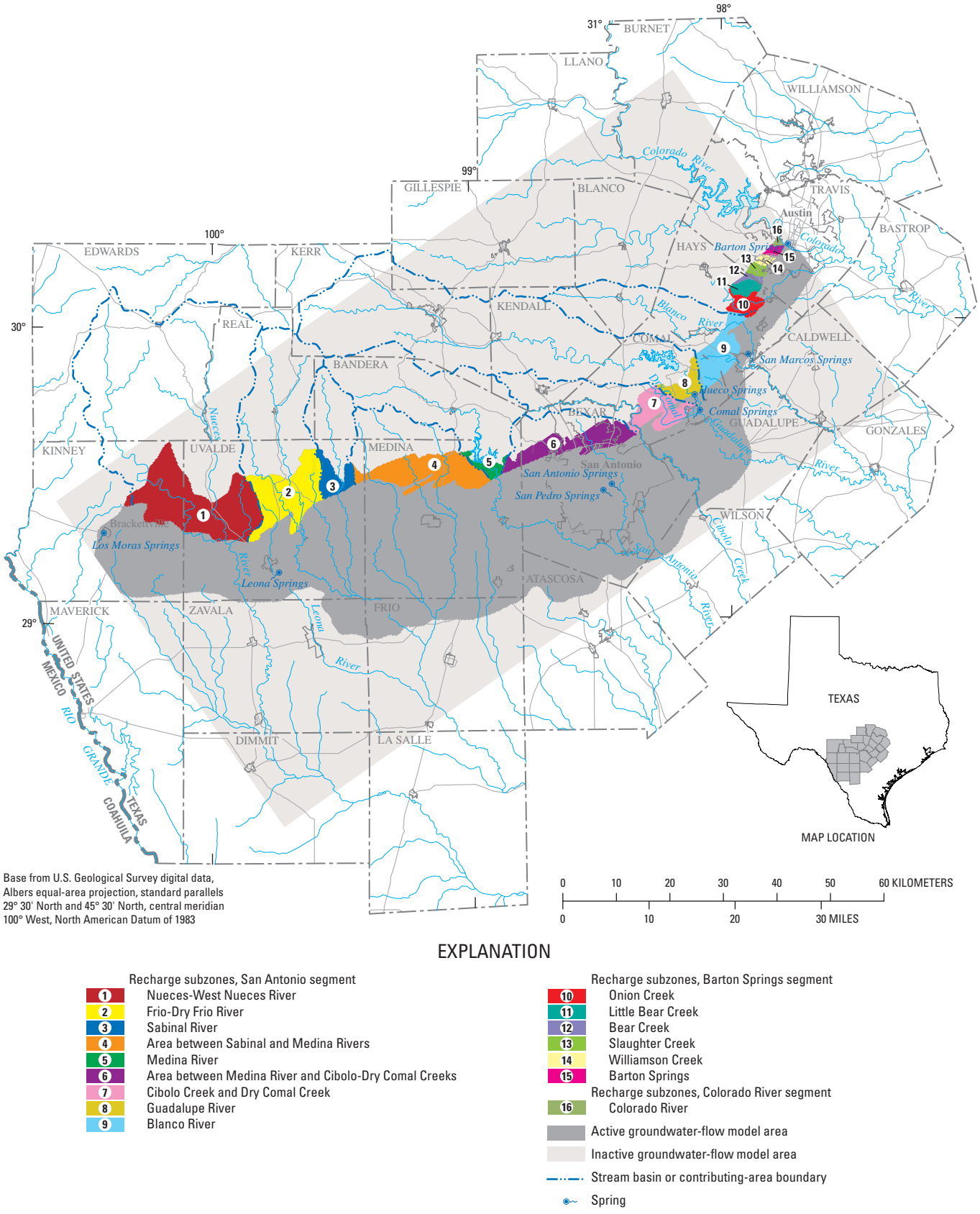

Figure 3.8. Simulated subzones of the recharge zone of the Edwards aquifer in the South-Central Texas regional study area, San Antonio region, Texas.

Table 3.4. Estimated recharge rates, by recharge subzone, in the rediscretized regional Edwards aquifer models area, 2000—2003, San Antonio region, Texas.

[Monthly recharge rates have been estimated by the U.S. Geological Survey for the San Antonio segment of the Edwards aquifer since 1934. For the Guadalupe River Basin, recharge is assumed to be negligible and is not estimated by the U.S. Geological Survey. Monthly recharge rates for the Barton Springs segment of the Edwards aquifer for 2000-2003 were estimated using the methods described by Barrett and Charbeneau (1996) and Scanlon and others (2002). The Barton Springs segment other than Onion Creek includes the Little Bear Creek, Bear Creek, Slaughter Creek, Williamson Creek, and Barton Creek recharge basins]

	Estimated recharge rate (cubic meters per month)									
	Recharge subzone									
	San Antonio segment								Barton Springs segment	
Month-Year	Nueces-West Nueces River	Frio-Dry Frio River	Sabinal River	Area between Sabinal and Medina River	Medina River	Area between Medina River and Cibolo Creek	Cibolo Creek and Dry Comal Creek	Blanco River	Onion Creek	Barton Springs segment other than Onion Creek
January-00	3,108,341	4,090,296	422,855	635,760	5,515,626	717,009	396,835	1,503,290	1,035,934	1,266,142
February-00	3,326,852	3,828,719	416,566	591,494	5,023,402	719,641	581,080	1,619,181	839,464	1,026,011
March-00	3,456,589	3,799,355	403,548	475,256	5,798,131	1,079,651	850,361	1,802,104	968,876	1,184,182
April-00	3,107,460	2,655,413	304,888	290,819	5,551,402	744,379	651,944	1,678,744	881,007	1,076,786
May-00	2,561,451	2,214,916	165,780	360,878	5,061,645	503,578	573,994	3,151,378	921,473	1,126,244
June-00	14,547,044	9,618,531	2,185,168	1,080,956	4,996,262	0	745,559	2,227,198	1,688,018	2,063,133
July-00	2,536,199	2,091,640	348,174	291,896	4,811,215	0	64,150	1,090,142	1,358,507	1,660,398
August-00	1,314,444	1,070,876	105,047	115,738	4,564,486	0	20,972	873,556	949,221	1,160,159
September-00	1,001,212	924,912	0	20,823	4,317,757	0	4,071	637,182	730,704	893,082
October-00	98,709,050	37,986,089	6,465,855	10,636,809	5,785,794	0	3,545,420	1,795,782	1,290,293	1,577,025
November-00	144,573,669	62,389,651	22,748,241	45,083,184	7,310,579	20,793,331	37,036,127	22,000,458	2,747,076	3,357,537
December-00	15,900,646	21,108,690	7,234,918	8,520,574	7,151,439	10,752,751	15,448,965	3,713,977	3,082,367	3,767,337
January-01	7,563,057	19,103,695	8,933,703	22,049,663	7,278,505	12,321,082	27,667,425	13,149,913	3,344,985	4,088,315
February-01	10,778,119	17,146,472	9,975,088	14,655,916	7,895,327	16,144,433	28,916,416	8,435,487	3,221,268	3,937,105
March-01	9,622,916	19,596,636	11,855,628	26,396,742	8,758,879	19,130,769	41,789,230	14,966,137	3,627,106	4,433,130
April-01	5,285,868	11,359,214	8,178,627	11,414,995	10,732,710	12,162,446	18,916,484	4,772,110	3,566,982	4,359,644
May-01	44,303,070	23,325,397	10,781,344	26,862,121	11,317,458	10,095,747	19,747,380	7,185,585	3,682,605	4,500,962
June-01	3,695,930	5,861,876	3,717,628	6,232,285	8,882,243	2,066,055	6,594,393	3,704,480	3,319,548	4,057,225
July-01	12,975,348	3,409,048	2,884,248	3,512,334	8,082,841	1,727,872	1,424,355	2,859,523	3,156,519	3,857,967
August-01	14,226,194	8,757,100	2,259,657	5,317,368	7,158,841	0	1,173,196	4,194,492	2,714,837	3,318,135
September-01	5,442,796	15,214,727	4,909,774	8,392,232	10,177,570	9,334,879	8,602,380	6,388,982	2,674,369	3,268,673
October-01	5,150,615	4,701,557	2,328,823	3,516,039	7,895,327	10,162,679	12,313,573	5,141,441	2,426,935	2,966,254
November-01	217,713,043	20,814,424	12,788,212	21,031,773	11,164,486	16,064,404	18,890,449	29,205,818	2,773,805	3,390,207
December-01	30,226,533	7,008,897	3,026,228	3,756,792	11,624,636	16,029,961	28,235,130	10,662,579	3,787,823	4,629,561

Table 3.4. Estimated recharge rates, by recharge subzone, in the rediscretized regional Edwards aquifer models area, 2000—2003, San Antonio region, Texas.—Continued

[Monthly recharge rates have been estimated by the U.S. Geological Survey for the San Antonio segment of the Edwards aquifer since 1934. For the Guadalupe River Basin, recharge is assumed to be negligible and is not estimated by the U.S. Geological Survey. Monthly recharge rates for the Barton Springs segment of the Edwards aquifer for 2000-2003 were estimated using the methods described by Barrett and Charbeneau (1996) and Scanlon and others (2002). The Barton Springs segment other than Onion Creek includes the Little Bear Creek, Bear Creek, Slaughter Creek, Williamson Creek, and Barton Creek recharge basins]

Month-Year	Estimated recharge rate (cubic meters per month)									
	Recharge subzone									
	San Antonio segment								Barton Springs segment	
	Nueces-West Nueces River	Frio-Dry Frio River	Sabinal River	Area between Sabinal and Medina River	Medina River	Area between Medina River and Cibolo Creek	Cibolo Creek and Dry Comal Creek	Blanco River	Onion Creek	Barton Springs segment other than Onion Creek
January-02	11,806,244	5,423,141	4,233,931	5,071,488	9,054,953	9,755,560	13,715,385	3,129,298	4,006,351	4,896,651
February-02	5,224,695	4,221,452	2,813,975	2,435,091	8,943,925	5,626,580	5,484,832	2,013,671	3,513,795	4,294,638
March-02	3,345,938	3,567,386	2,286,660	1,585,642	8,709,533	4,321,384	4,166,771	3,339,609	3,642,137	4,451,501
April-02	3,574,604	3,807,186	2,472,872	1,532,867	8,487,477	655,241	3,349,558	3,790,173	3,398,172	4,153,321
May-02	3,241,283	4,866,987	2,625,515	1,555,020	7,957,009	1,767,118	1,544,823	3,298,125	3,245,549	3,966,782
June-02	6,142,292	2,747,478	1,628,680	1,173,494	7,266,168	0	6,803,089	8,704,268	2,765,712	3,380,314
July-02	22,397,820	173,499,971	28,719,089	274,569,715	12,953,271	146,651,517	270,495,169	56,132,948	3,466,390	4,236,698
August-02	3,364,633	6,116,427	2,755,490	7,309,614	9,091,963	16,379,860	97,549,416	22,009,741	3,608,606	4,410,519
September-02	2,271,343	11,368,225	11,229,759	44,847,685	12,459,813	5,463,426	90,383,767	22,984,136	3,190,050	3,898,949
October-02	37,244,749	22,500,865	14,651,846	54,988,343	12,459,813	3,244,664	8,584,846	14,170,155	3,076,739	3,760,458
November-02	3,556,296	9,649,260	6,954,286	20,185,646	9,128,972	12,332,298	34,378,942	27,218,324	3,406,265	4,163,213
December-02	1,024,018	7,935,409	6,688,451	10,660,362	9,116,636	10,260,587	15,927,800	18,277,137	3,816,728	4,664,890
January-03	3,737,497	11,711,029	5,324,285	6,023,293	9,496,598	9,888,058	22,141,792	7,770,641	3,901,133	4,768,052
February-03	3,297,489	8,571,612	3,574,971	5,715,180	9,496,598	12,193,561	22,394,062	22,727,332	3,683,761	4,502,375
March-03	3,327,317	8,116,482	3,124,246	7,942,040	9,957,981	13,966,733	14,555,354	3,178,416	4,134,693	5,053,513
April-03	3,168,071	6,508,846	2,544,323	5,008,101	9,227,664	8,145,198	16,793,872	4,546,807	3,720,761	4,547,597
May-03	2,182,029	5,186,767	1,753,718	2,874,761	8,758,879	5,783,097	9,875,477	4,252,251	3,591,263	4,389,321
June-03	17,290,343	19,368,633	6,593,602	12,569,792	9,816,112	7,332,075	13,138,732	6,455,332	3,324,173	4,062,878
July-03	5,144,288	10,331,499	5,809,213	29,623,078	9,816,112	2,260,968	9,800,558	6,322,755	3,196,987	3,907,429
August-03	3,250,875	6,314,498	2,168,718	3,768,349	8,450,467	2,160,599	5,428,349	5,446,454	2,936,834	3,589,464
September-03	57,392,439	21,652,124	2,171,165	2,787,663	8,475,140	1,009,528	5,156,996	3,884,392	2,445,435	2,988,865
October-03	77,559,058	21,482,481	2,801,281	2,822,970	8,276,523	1,883,196	1,346,406	2,913,304	2,030,347	2,481,535
November-03	4,476,422	11,735,280	1,737,813	2,231,154	7,833,645	2,454,163	1,962,918	2,801,731	1,492,698	1,824,409
December-03	3,919,304	7,482,726	1,501,219	1,778,986	7,414,206	2,277,308	6,880,718	3,653,293	1,431,418	1,749,510

Model Calibration and Sensitivity

The rediscretized regional Edwards aquifer models (conduit-flow and diffuse-flow models) were calibrated for steady-state and transient conditions. Average stresses (recharge and pumpage) during 2001, a representative year for the recent time period (2000–03), were used to simulate steady-state conditions. The transient simulation period for the rediscretized regional Edwards aquifer models was 2000–2003, including 48 monthly stress periods. The calibrated parameter values from the conduit-flow and diffuse-flow Edwards aquifer models were used as the initial parameter values for the conduit-flow and diffuse-flow rediscretized regional Edwards aquifer models, respectively. The interested reader is referred to Lindgren and others (2004) and Lindgren (2006) for further discussion of the calibration of the original Edwards aquifer models.

The steady-state and transient simulations for the rediscretized regional Edwards aquifer models were calibrated to 2000–2003 conditions, primarily using a trial-and-error approach, by varying the simulated recharge rates and hydraulic conductivities. The use of parameter estimation to determine optimized parameters for the steady-state simulation was investigated, but it was of limited usefulness due to correlation between the parameters. The initial average recharge rates for year 2001 and the initial monthly recharge rates for 2000–03 for the recharge subzones were adjusted during model calibration for the rediscretized regional Edwards aquifer models until the differences between model-computed and measured hydraulic heads and springflows were minimized. As a result of the calibration, the calibrated recharge rates were reduced by 10 percent for most of the recharge subzones and as much as 50 percent for the Cibolo Creek and Dry Comal Creek subzone, compared to the simulated initial rates. In addition, the hydraulic conductivities for some zones were adjusted for both the conduit-flow and diffuse-flow models, and the drain conductance for Leona Springs was reduced from 18,580 m^2/d to 9,290 m^2/d. The final calibrated distribution of horizontal hydraulic conductivity for the conduit-flow and diffuse-flow rediscretized regional Edwards aquifer models is shown in figures 3.9*A* and 3.9*B*, respectively. The distribution of storativity for the calibrated rediscretized regional Edwards aquifer models is the same as for the original Edwards aquifer models (Lindgren and others, 2004; Lindgren, 2006) and is shown in figure 3.10.

A series of sensitivity tests was made for the conduit-flow Edwards aquifer model (Lindgren and others, 2004) to ascertain how the model results were affected by variations greater than and less than the calibrated values of input data. Simulated hydraulic heads and springflows in the model were most sensitive to recharge, withdrawals, hydraulic conductivity of the conduit segments, and specific yield and relatively insensitive to spring-orifice conductance, northern boundary inflow, and specific storage (Lindgren and others, 2004). Larger values of hydraulic conductivity result in increased springflow if the reduced recharge, due to model cells going dry, is accounted for. Moving the simulated southern no-flow model boundary northward from the 10,000-mg/L dissolved-solids concentration line to the 1,000-mg/L dissolved-solids concentration line resulted in minimal changes in simulated hydraulic heads and springflows. The effect of lowering the simulated spring-orifice altitudes for Comal and San Marcos Springs was to appreciably lower hydraulic heads in the aquifer, because the spring-orifice altitudes serve as a controlling base level for hydraulic heads in the aquifer.

The overall goodness of fit of the original and rediscretized regional Edwards aquifer models to the observation data was evaluated using summary statistics and graphical analyses. The goodness of fit between simulated and measured hydraulic heads and springflows was quantified using the mean absolute difference, mean algebraic difference, and root mean square (RMS) error. If the ratio of the RMS error to the total head change in the modeled area is small, then the error in the head calculations is a small part of the overall model response (Anderson and Woessner, 1992).

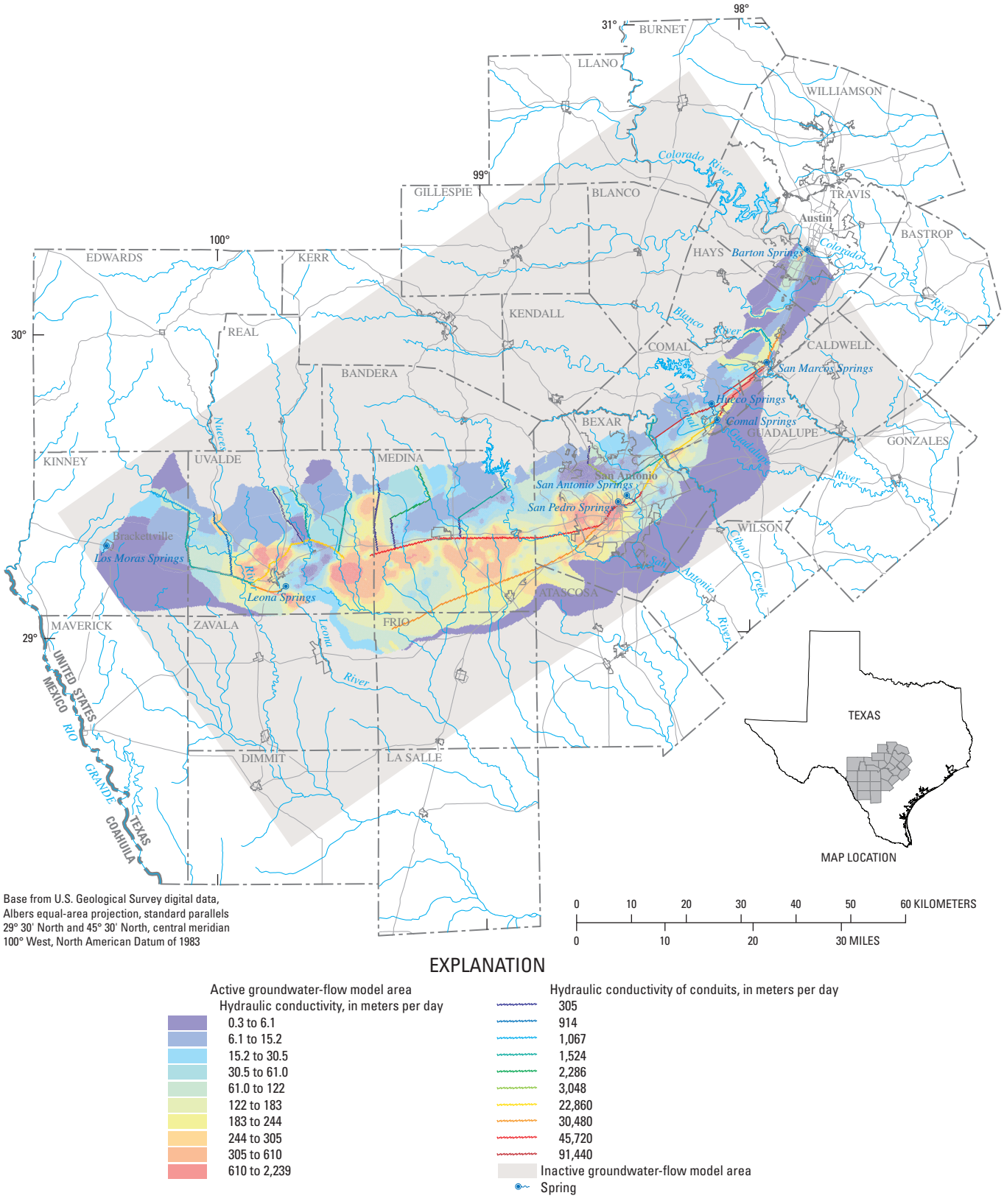

Figure 3.9*A*. Simulated distribution of horizontal hydraulic conductivity for the calibrated conduit-flow rediscretized regional Edwards aquifer model, San Antonio region, Texas.

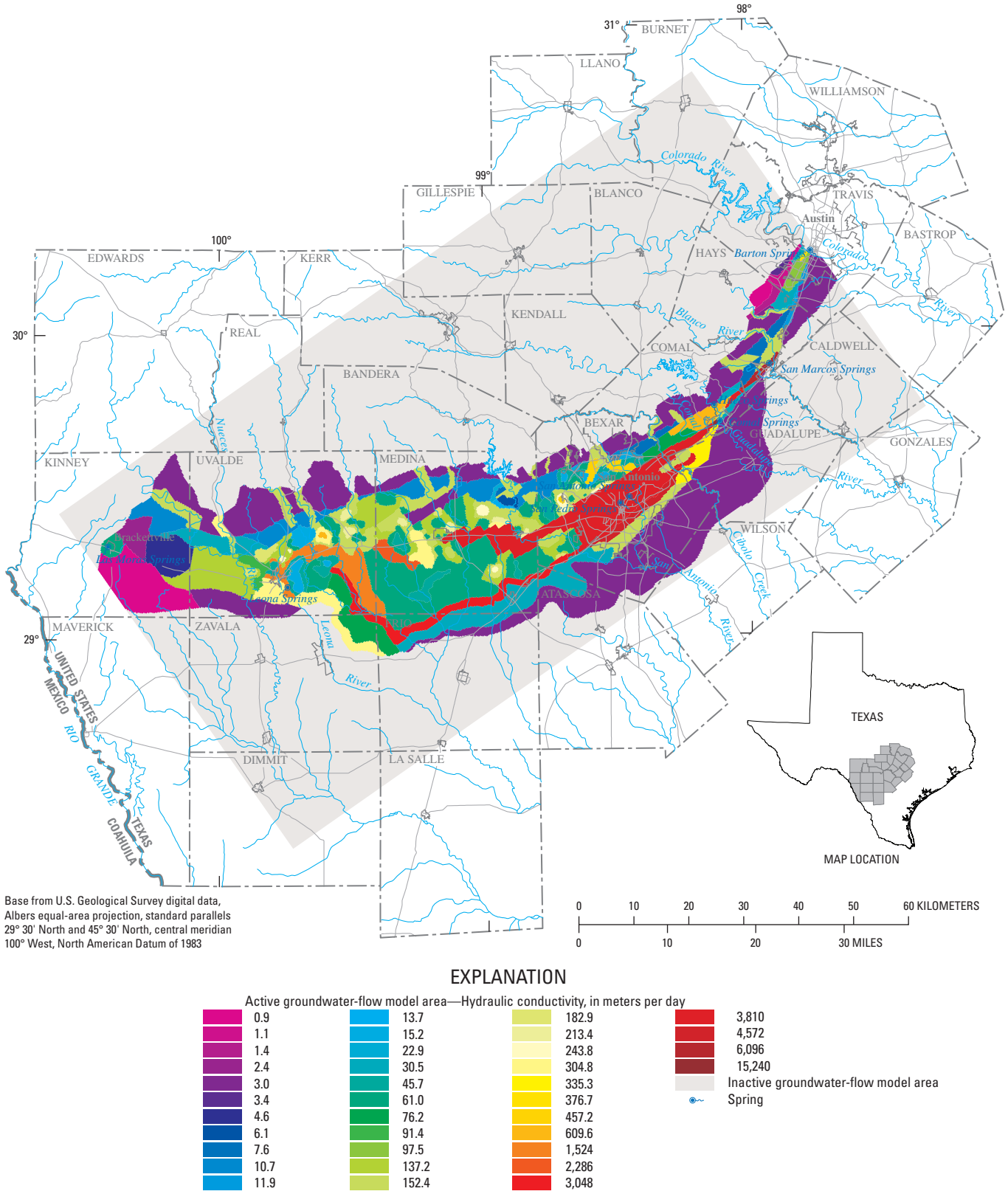

Figure 3.9*B*. Simulated distribution of horizontal hydraulic conductivity for the calibrated diffuse-flow rediscretized regional Edwards aquifer model, San Antonio region, Texas.

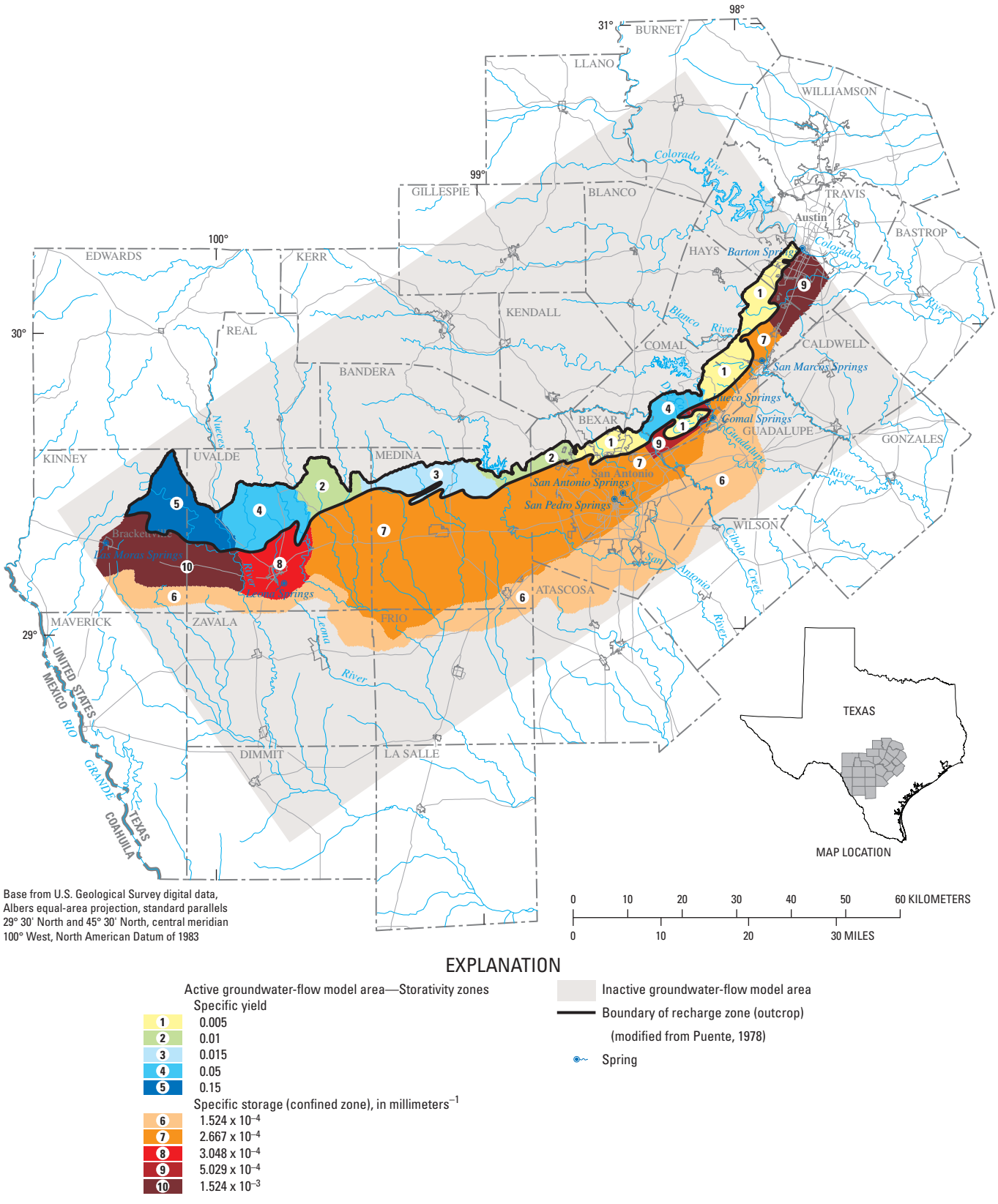

Figure 3.10. Simulated storativity zones for the calibrated rediscretized regional Edwards aquifer models, San Antonio region, Texas.

Model-Computed Hydraulic Heads

The steady-state simulation calibration results for the rediscretized regional Edwards aquifer models (conduit-flow and diffuse-flow models) include a comparison of simulated hydraulic heads to average measured water levels for 2001. Simulated hydraulic heads were within 9.0 m of measured water levels at 177 of the 229 wells used as targets for the conduit-flow rediscretized regional Edwards aquifer model for the calibrated steady-state simulation (fig. 3.11*A*). The difference was less than 6.0 m at 129 of the 229 wells. The mean absolute difference between simulated and measured hydraulic heads is 7.4 m (table 3.5). The RMS error is 10.5 m, which represents about 5 percent of the total head difference across the model area. For the diffuse-flow rediscretized regional Edwards aquifer model, simulated hydraulic heads were within 9.0 m of measured water levels at 185 of the 229 wells used as calibration targets for the steady-state simulation (fig. 3.11*B*). The difference was less than 6.0 m at 159 of the 229 wells. The mean absolute difference between simulated and measured hydraulic heads is 6.3 m (table 3.5). The RMS error is 11.0 m, which represents about 5 percent of the total head difference across the model area. The graphs of simulated relative to measured hydraulic heads indicate little spatial bias in the steady-state simulation results for the conduit-flow and diffuse-flow models (fig. 3.12*A*).

The transient simulation results for the rediscretized regional Edwards aquifer models (conduit-flow and diffuse-flow models) include a comparison of simulated hydraulic heads with synoptic sets of water levels in multiple wells during 2000–03. Eight synoptic sets of water-level measurements during January or February and July of each year were used for model calibration, (table 3.5). The mean absolute difference between simulated and measured hydraulic heads for the calibrated transient simulation for the conduit-flow rediscretized regional Edwards aquifer model ranged from 6.4 to 8.7 m for the eight time periods (table 3.5). The RMS error ranged from 9.8 to 10.6 m for seven of the eight time periods, but it was comparatively large (15.6 m) for July 2002, coincident with the large recharge to the Edwards aquifer that occurred during July 2002 (871.5 hm^3). These errors represent 4.4 to 4.8 percent of the total head difference across the model for seven of the eight time periods, compared with 7.0 percent for July 2002.

The mean absolute difference between simulated and measured hydraulic heads for the calibrated transient simulation for the diffuse-flow rediscretized regional Edwards aquifer model ranged from 6.0 to 8.7 m for the eight time periods (table 3.5), with the largest difference being for July 2002, as for the conduit-flow model. The RMS error ranged from 9.7 to 11.9 m for seven of the eight time periods, but it was somewhat larger (13.4 m) for July 2002. These errors represent 4.3 to 4.8 percent of the total measured head difference across the model area for the first five time periods (January 2000 through January 2002), compared to 5.2 to 6.0 percent for the last three time periods (July 2002 through July 2003). The graphs of simulated relative to measured hydraulic heads indicate little spatial bias in the transient simulation results for the conduit-flow and diffuse-flow models (figs. 3.12*B* and 3.12*C*).

Model-Computed Springflow

The steady-state simulation calibration results for the rediscretized regional Edwards aquifer models (conduit-flow and diffuse-flow models) include a comparison of simulated springflows with median springflows for 2001. The simulated springflows for Comal and San Marcos Springs for the calibrated steady-state simulation for the conduit-flow rediscretized regional Edwards aquifer model were within 1.3 and 0.3 percent of the median springflows for the two springs, respectively (table 3.5). The simulated springflows for San Antonio and San Pedro Springs were 17.6 and 37.5 percent greater than the median measured springflows, respectively. However, their discharges probably reflect local hydrogeologic conditions. The simulated springflow for Leona Springs was 63.6 percent greater than the median measured springflow. However, this discrepancy probably is reasonable because the reported discharge for Leona Springs might not account for all of the discharge from the Edwards aquifer to the Leona gravels (Green, 2004). The simulated springflows for Comal, San Marcos, and San Pedro Springs for the calibrated steady-state simulation for the diffuse-flow rediscretized regional Edwards aquifer model were within 1.2 percent of the median measured springflows for the three springs (table 3.5).

The transient calibration results for the rediscretized regional Edwards aquifer models (conduit-flow and diffuse-flow models) include a comparison of simulated springflows with a series of measurements of springflow during the 2000–03 period. The RMS errors for the conduit-flow rediscretized regional Edwards aquifer model for Comal, San Marcos, Leona, San Antonio, and San Pedro Springs ranged from 0.11 cubic meters per second (m^3/s) for San Pedro Springs to 1.44 m^3/s for Comal Springs (table 3.5). The RMS errors for the five springs, as a percentage of the range of springflow fluctuations measured at the springs, varied from 15.5 percent for San Antonio Springs to 27.0 percent for Leona Springs and were 17.7 percent or less for all but Leona Springs. The RMS errors for the diffuse-flow rediscretized regional Edwards aquifer model for Comal, San Marcos, Leona, San Antonio, and San Pedro Springs ranged from 0.17 m^3/s for San Pedro Springs to 2.47 m^3/s for San Antonio Springs (table 3.5). The RMS errors for the five springs, as a percentage of the range of discharge fluctuations measured at the springs, varied from 9.3 percent for Comal Springs and 16.7 percent for San Marcos Springs to 49.3 percent for San Antonio Springs.

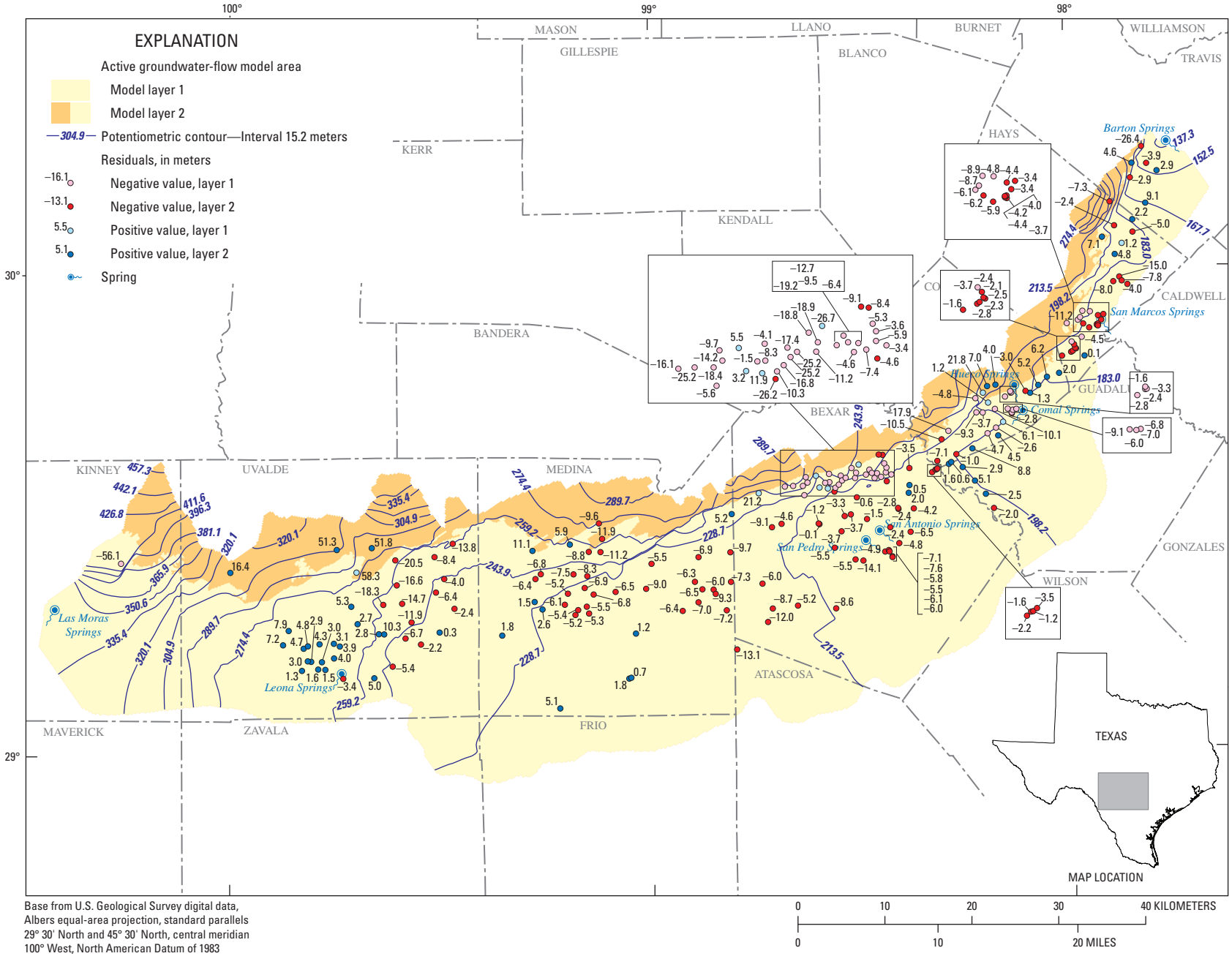

Figure 3.11*A*. Simulated potentiometric surface in model layer 2 and hydraulic head residuals in model layers 1 and 2 for the conduit-flow rediscretized regional Edwards aquifer model, steady-state simulation, San Antonio region, Texas.

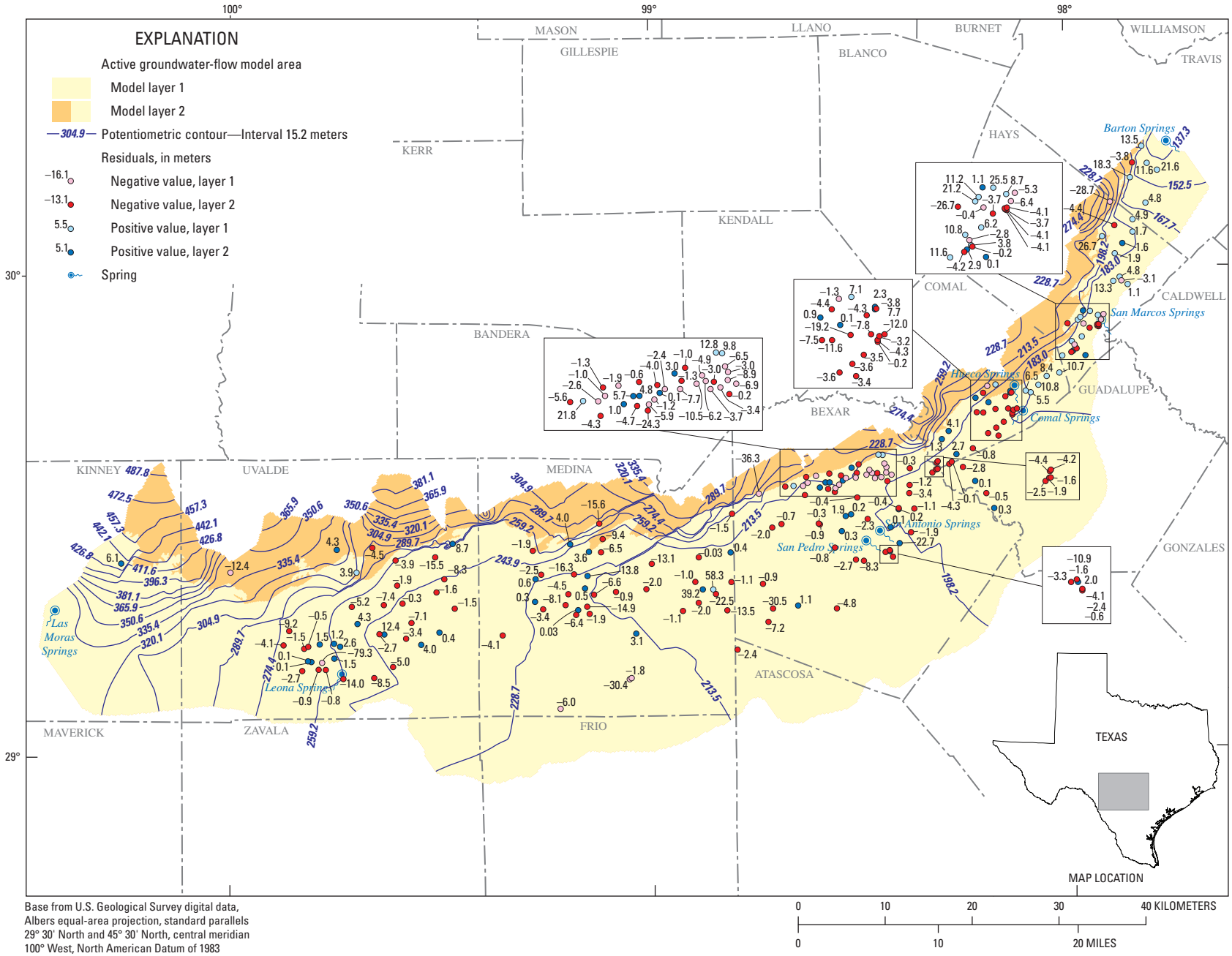

Figure 3.11*B*. Simulated potentiometric surface in model layer 2 and hydraulic head residuals in model layers 1 and 2 for the diffuse-flow rediscretized regional Edwards aquifer model, steady-state simulation, San Antonio region, Texas.

Table 3.5. Comparison of residuals for hydraulic heads and springflows for the conduit-flow and diffuse-flow rediscretized regional Edwards aquifer models, San Antonio region, Texas.

[Mean algebraic difference is the algebraic sum of the residuals, which is simulated water level or springflow minus the measured water level or springflow, divided by the number of wells. Mean absolute difference is the sum of the absolute values of the residuals divided by the number of measurements. m^3/s, cubic meters per second; NA, not applicable]

Time of measurements	Stress period	Number of wells	Hydraulic head residuals (meters)					
			Conduit-flow rediscretized regional Edwards aquifer model			Diffuse-flow rediscretized regional Edwards aquifer model		
			Mean algebraic difference	Mean absolute difference	Root mean square	Mean algebraic difference	Mean absolute difference	Root mean square
Steady-state	NA	229	3.4	7.6	11.2	1.4	6.3	11.0
January-00	1	235	1.8	6.8	10.3	0.0	6.0	9.7
July-00	7	221	0.7	6.7	10.5	0.0	6.9	10.6
February-01	14	218	-0.1	6.6	10.5	-0.5	6.7	10.5
July-01	19	221	1.9	6.8	9.9	0.5	6.4	10.1
January-02	25	222	1.1	6.4	9.8	-0.8	6.5	10.4
July-02	31	205	3.5	8.7	15.6	1.6	8.7	13.4
February-03	38	207	4.5	7.9	10.5	-0.8	7.2	11.9
July-03	43	229	2.8	7.0	10.1	-0.9	7.7	11.5

Spring name	Median 2001 springflow (m^3/s)	Period of measurements	County	Springflow residuals (cubic meters per second)							
				Conduit-flow rediscretized regional Edwards aquifer model				Diffuse-flow rediscretized regional Edwards aquifer model			
				Steady-state residual	Mean algebraic difference	Mean absolute difference	Root mean square	Steady-state residual	Mean algebraic difference	Mean absolute difference	Root mean square
Comal	9.69	Steady-state	Comal	0.15				0.08			
		2000–03			0.17	1.15	1.44		-0.16	0.64	0.76
San Marcos	6.57	Steady-state	Hays	0.03				-0.07			
		2000–03			-0.07	0.84	0.99		-0.14	0.83	1.03
Leona	0.33	Steady-state	Uvalde	0.21				0.21			
		2000–03			0.15	0.32	0.40		0.07	0.29	0.34
San Antonio	0.91	Steady-state	Bexar	0.14				0.01			
		2000–03			-0.26	0.56	0.78		1.45	1.60	2.47
San Pedro	0.24	Steady-state	Bexar	0.09				-0.09			
		2000–03			0.07	0.08	0.11		-0.12	0.13	0.17

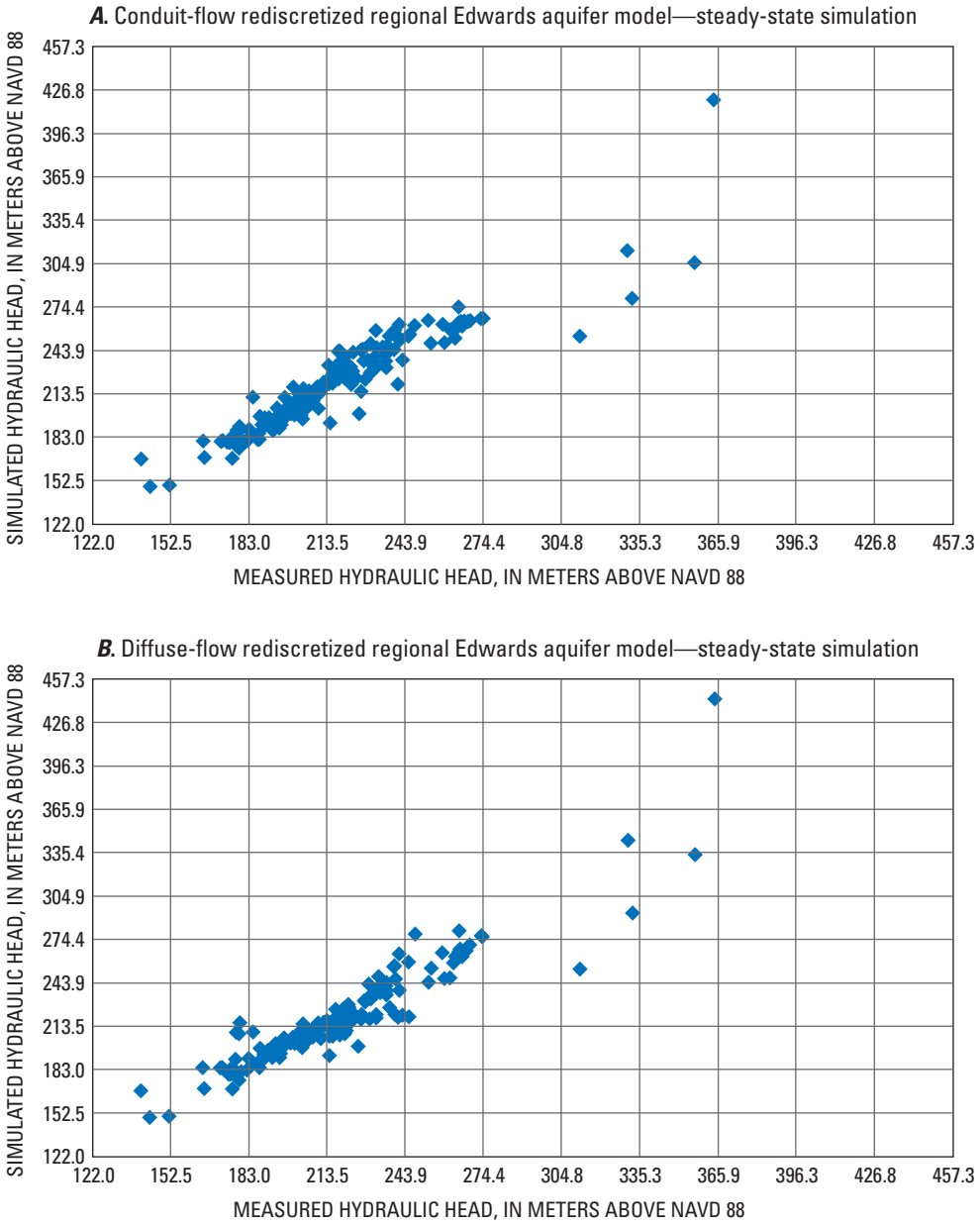

Figure 3.12*A*. Simulated relative to measured hydraulic heads for (*A*) conduit-flow and (*B*) diffuse-flow rediscretized regional Edwards aquifer models, steady-state simulation, San Antonio region, Texas.

A. Conduit-flow rediscretized regional Edwards aquifer model—February 2003

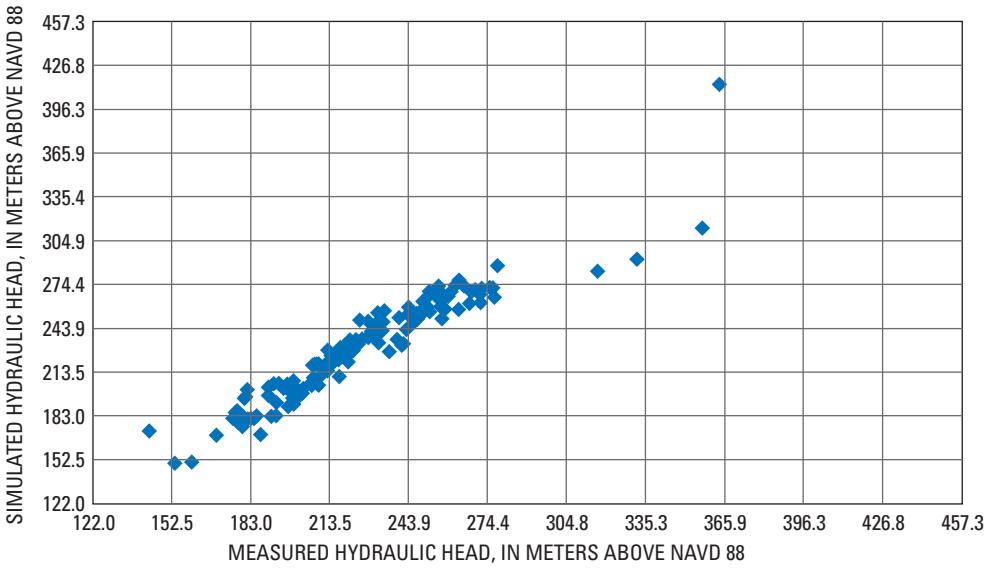

B. Diffuse-flow rediscretized regional Edwards aquifer model—February 2003

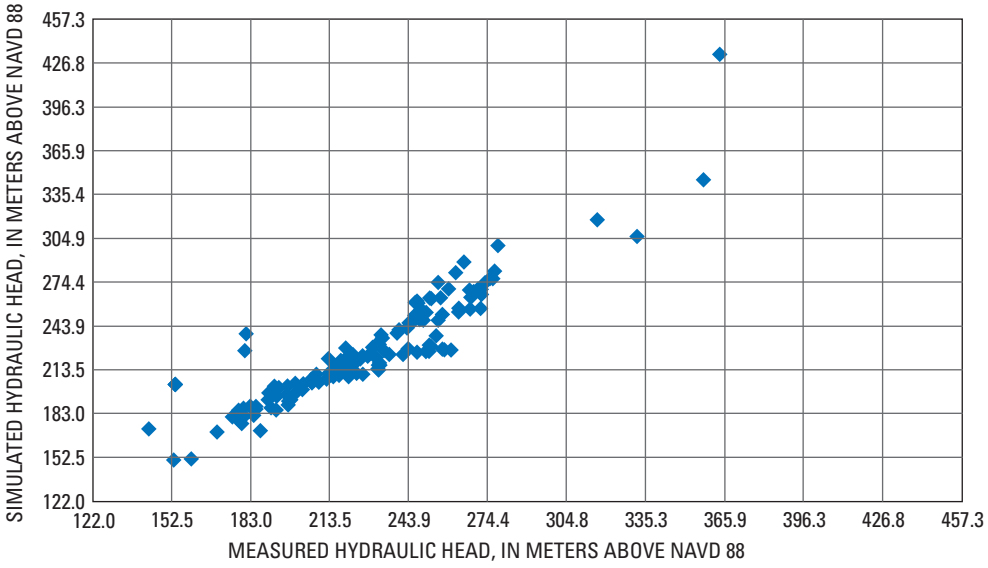

Figure 3.12*B*. Simulated relative to measured hydraulic heads for (*A*) conduit-flow and (B) diffuse-flow rediscretized regional Edwards aquifer models for February 2003, which was a period of average recharge and comparatively small groundwater withdrawals by wells, San Antonio region, Texas.

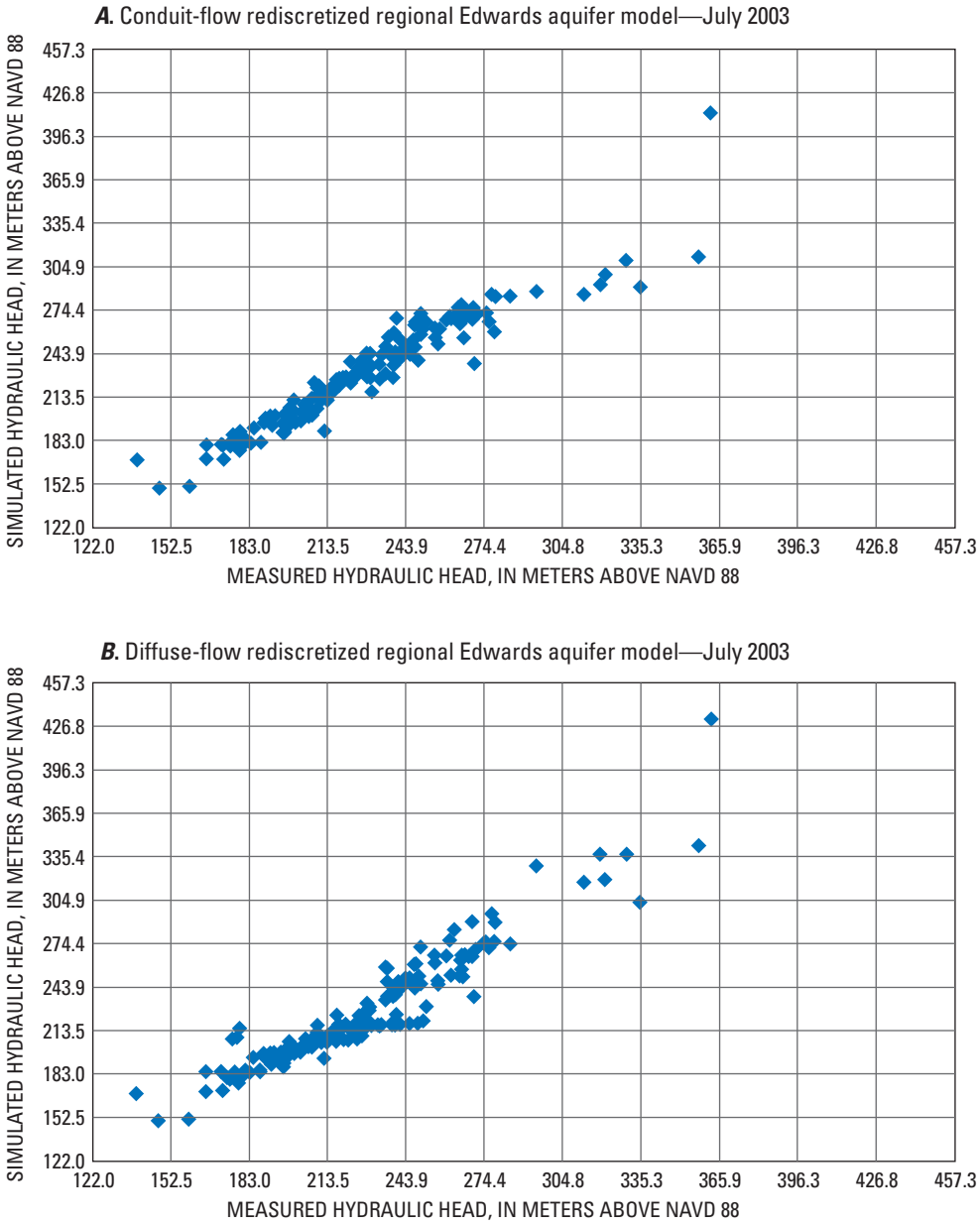

Figure 3.12*C*. Simulated relative to measured hydraulic heads for (*A*) conduit-flow and (*B*) diffuse-flow rediscretized regional Edwards aquifer models for July 2003,which was a period of average recharge and comparatively large groundwater withdrawals by wells, San Antonio region, Texas.

Model-Computed Water Budget

The water budgets for the rediscretized regional Edwards aquifer models (conduit-flow and diffuse-flow models) for the steady-state simulation and for year 2003 of thetransient simulation are shown in figure 3.13 and table 3.6. The steady-state simulation water budget for the conduit-flow rediscretized regional Edwards aquifer model indicates that recharge accounts for 95.9 percent of the sources of water to the Edwards aquifer and inflow through the northern and northwestern model boundaries contributes 4.1 percent (fig. 3.13*A*; table 3.6). Most of the simulated recharge, 91.3 percent, is applied in layer 2, because layer 1 is absent for much of the recharge zone (fig. 3.7). The largest discharges from the Edwards aquifer in the steady-state simulation water budget are springflow, 54.2 percent, and withdrawals by wells, 45.8 percent (fig. 3.13*A*; table 3.6). The groundwater withdrawals are greater for layer 1,which accounts for 63.9 percent of total withdrawals, than for layer 2,which accounts for 36.1 percent of total withdrawals. The steady-state simulation water budget for the diffuse-flow rediscretized regional Edwards aquifer model (fig. 3.13*B*; table 3.6) is similar to the simulated water budget for the conduit-flow rediscretized regional Edwards aquifer model.

The principal source of water to the Edwards aquifer, excluding change in storage, for the conduit-flow rediscretized regional Edwards aquifer model for the transient simulation is recharge, constituting 94.2 percent of the sources of water to the Edwards aquifer during 2003 (fig. 3.13*A*; table 3.6). Inflow through the northern and northwestern model boundaries contributed a relatively small amount of water, 5.8 percent. During 2003, recharge constituted 64.8 percent of the total sources to the aquifer, including change in storage, compared to 31.2 percent for the net annual change in storage, expressed as net release of water from storage or net gain of water to the aquifer (fig. 3.13*A*; table 3.6). Most of the net release of water from storage (83.3 percent) was derived from layer 2. The aquifer was being depleted of water—water was released from storage—for 10 of the 12 months during 2003. The principal discharges from the Edwards aquifer for the conduit-flow rediscretized regional Edwards aquifer model for the transient simulation during 2003 are springflow, 65.7 percent, and withdrawals by wells, 34.3 percent (fig. 3.13*A*; table 3.6). Net addition to storage,or discharge from the aquifer, occurred in September and October during 2003. The transient simulation water budget for the diffuse-flow rediscretized regional Edwards aquifer model (fig. 3.13*B*; table 3.6) is similar to the simulated water budget for the conduit-flow rediscretized regional Edwards aquifer model.

Simulation of Areas Contributing Recharge to Public-Supply Wells

The calibrated steady-state rediscretized regional Edwards aquifer models (conduit-flow and diffuse-flow models) were used to estimate water particle traveltimes and areas contributing recharge for 68 public-supply wells from the four quartiles of pumping rates using the MODPATH (Pollock, 1994) particle-tracking post processor and methods outlined in Chapter A, Section 1 of this Professional Paper. Use of the steady-state simulations, rather than the transient simulations, simplified and facilitated the simulation of areas contributing recharge and traveltimes to public-supply wells, especially with respect to dealing with weak sinks (Leon Kauffman, U.S. Geological Survey, written commun., 2008). Reilly and Pollack (1995) showed that when the mean traveltime is much greater than the cyclical nature of the stresses on a system, the steady-state results do not differ appreciably from a transient analysis. This conclusion can be expected to hold true for the steady-state results presented here. However, there are likely fast flow paths that are not represented in the models, and this can cause more variation in the traveltime distributions and locations of areas contributing recharge than would be computed by either the transient simulations or the steady-state simulations. The effects of storage, not accounted for in steady-state simulations, on traveltimes are likely to be minimal because the water released from storage is ultimately derived from recharge and is not a different source of water (Leon Kauffman, U.S. Geological Survey, written commun., 2008). The water released from storage is derived from recharge, is of an age corresponding to the time that recharge occurred, and is not a new source of water that would have a different age. The model-computed areas contributing recharge represent advective groundwater flow and do not account for mechanical dispersion. Advection-dispersion transport simulations would likely yield larger areas contributing recharge than advective particle-tracking simulations, because the effects of dispersion caused by aquifer heterogeneity would be included.

In addition to output from the groundwater-flow models, the MODPATH simulations require effective porosity values to calculate groundwater-flow velocities. For the rediscretized regional Edwards aquifer models (conduit-flow and diffuse-flow models), porosity values were assumed uniform within each layer based on typical regional values. A porosity of 0.18,the average for the Edwards aquifer reported by Hovorka and others (1996), was used for both layers (model layers 1 and 2) in the models. Because of the karst nature of groundwater flow in the study area, the porosity values used for this regional simulation would not be applicable to local karst conditions.

A.

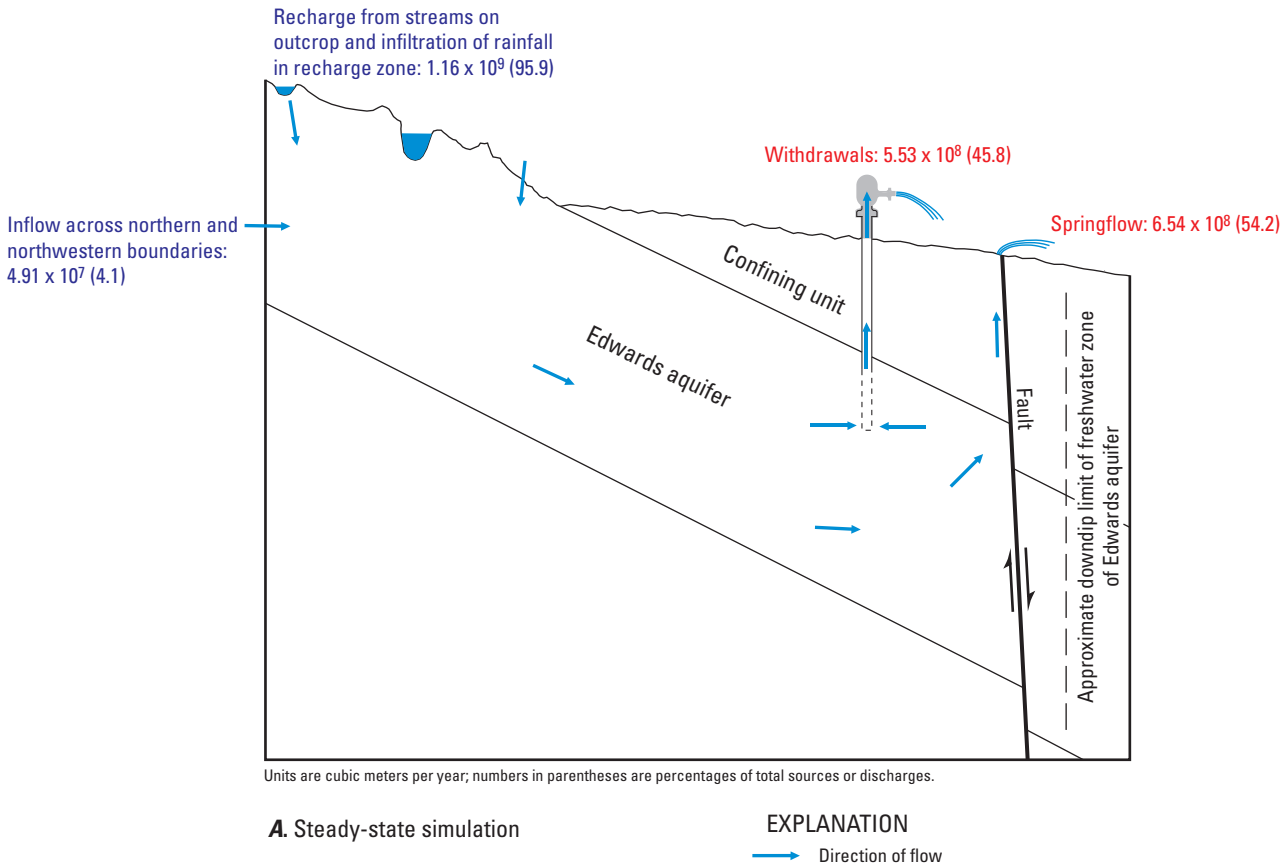

	2003
Recharge	+7.98 x 10^8 (64.8)
Boundary inflow	+4.89 x 10^7 (4.0)
Springflow	–8.10 x 10^8 (65.7)
Withdrawals	–4.22 x 10^8 (34.3)
Net change in storage	+3.85 x 10^8 (31.2)

Units are cubic meters; + is source of water to aquifer, including release of water from storage; – is discharge of water from aquifer, including addition of water to storage; numbers in parentheses are percentages of total sources or discharges.

Figure 3.13*A*. Schematic diagram showing simulated water-budget components for (*A*) steady-state simulation and (*B*) year 2003 of the transient simulation for the conduit-flow rediscretized regional Edwards aquifer model, San Antonio region, Texas..

B.

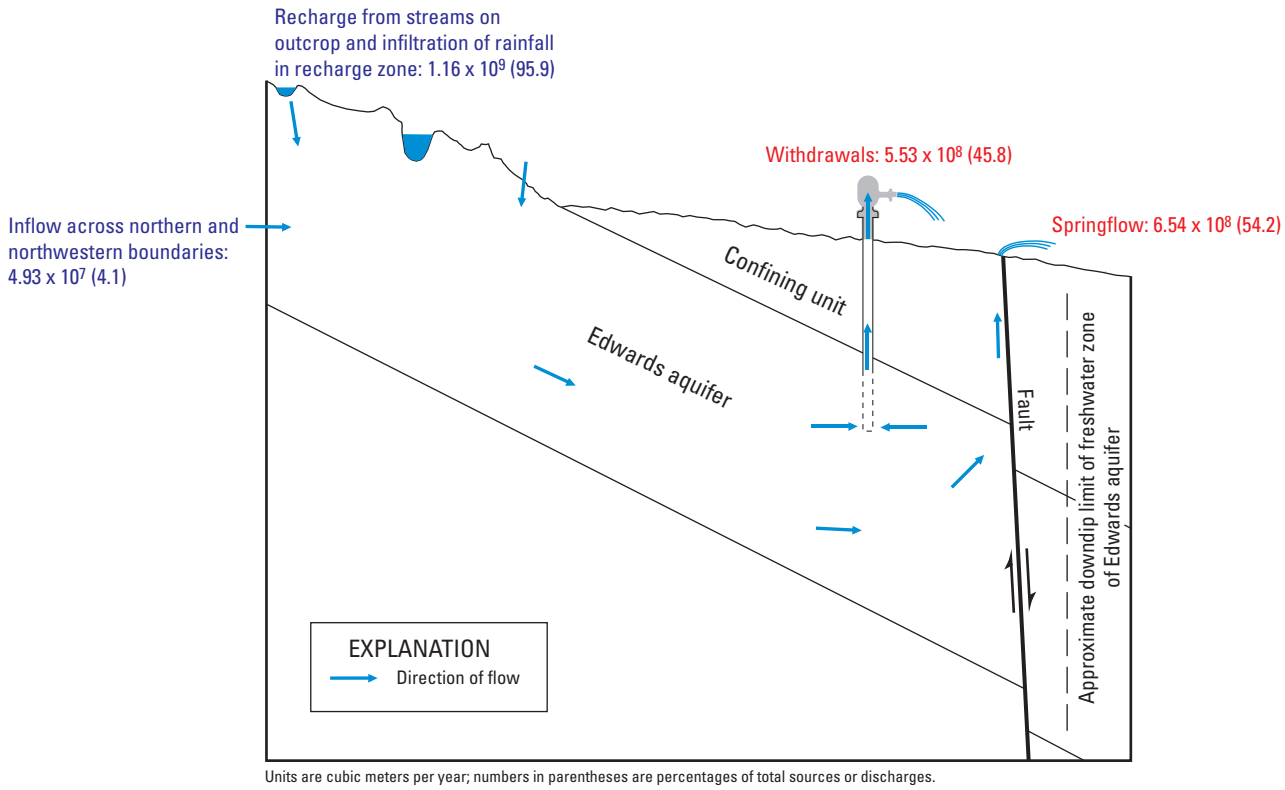

Units are cubic meters per year; numbers in parentheses are percentages of total sources or discharges.

A. Steady-state simulation

	2003
Recharge	+7.98 x 10^8 (62.8)
Boundary inflow	+4.93 x 10^7 (3.9)
Springflow	–8.48 x 10^8 (66.7)
Withdrawals	–4.23 x 10^8 (33.3)
Net change in storage	+4.22 x 10^8 (33.3)

Units are cubic meters; + is source of water to aquifer, including release of water from storage; – is discharge of water from aquifer, including addition of water to storage; numbers in parentheses are percentages of total sources or discharges.

B. Transient simulation

Figure 3.13*B*. Schematic diagram showing simulated water-budget components for (*A*) steady-state simulation and (*B*) year 2003 of the transient simulation for the diffuse-flow rediscretized regional Edwards aquifer model, San Antonio region, Texas.

Table 3.6. Simulated annual water budget for steady-state simulation and for year 2003 of the transient simulation for the conduit-flow and diffuse-flow rediscretized regional Edwards aquifer models, San Antonio region, Texas.

[Recharge includes leakage from streams through streambeds and infiltration of precipitation in interstream areas. Boundary inflow includes inflow through specified-flow boundary condition cells at the northern and northwestern model boundaries. Subtotal includes source or discharge components exclusive of changes in storage. Total includes changes in storage. Negative net change in storage indicates a net loss of water from storage (storage is included as a source). hm^3/yr, cubic hectometers per year; NA, not applicable]

	Source								
	Conduit-flow rediscretized regional Edwards aquifer model				Diffuse-flow rediscretized regional Edwards aquifer model				
Budget component and time period	Flow rate (hm^3/yr)	Percent of budget component	Percent of subtotal for sources or discharges	Percent of total sources or discharges	Flow rate (hm^3/yr)	Percent of budget component	Percent of subtotal for sources or discharges	Percent of total sources or discharges	Change in percent of total sources
Recharge									
Steady-state									
Layer 1	101	8.7	NA	8.3	101	8.7	NA	8.3	0.0
Layer 2	1,058	91.3	NA	87.6	1,058	91.3	NA	87.6	0.0
Subtotal	1,158	100.0	NA	95.9	1,158	100.0	NA	95.9	0.0
2003									
Layer 1	80	10.0	9.4	6.5	80	10.0	9.5	6.3	0.2
Layer2	719	90.0	84.8	58.3	719	90.0	84.7	56.5	1.8
Subtotal	799	100.0	94.2	64.8	799	100.0	94.2	62.8	2.0
Boundary inflow (layer 2)									
Steady-state	49	NA	NA	4.1	49	NA	NA	4.1	0.0
2003	49	NA	5.8	4.0	49	NA	5.8	3.9	0.1
Subtotal									
2003	848	NA	100.0	68.8	848	NA	100.0	66.7	2.1
Total sources									
Steady-state	1,207	NA	NA	100.0	1,208	NA	NA	100.0	0.0
2003	1,233	NA	NA	100.0	1,271	NA	NA	100.0	0.0
Discharge									
Withdrawals (pumpage)									
Steady-state									
Layer 1	353	63.9	NA	29.3	353	63.9	NA	29.3	0.0
Layer2	200	36.1	NA	16.5	200	36.1	NA	16.5	0.0
Subtotal	553	100.0	NA	45.8	553	100.0	NA	45.8	0.0
2003									
Layer 1	262	62.0	21.2	21.2	262	62.0	20.6	20.6	0.6
Layer2	161	38.0	13.1	13.1	161	38.0	12.7	12.7	0.4
Subtotal	423	100.0	34.3	34.3	423	100.0	33.3	33.3	1.0

Table 3.6. Simulated annual water budget for steady-state simulation and for year 2003 of the transient simulation for the conduit-flow and diffuse-flow rediscretized regional Edwards aquifer models, San Antonio region, Texas.—Continued

[Recharge includes leakage from streams through streambeds and infiltration of precipitation in interstream areas. Boundary inflow includes inflow through specified-flow boundary condition cells at the northern and northwestern model boundaries. Subtotal includes source or discharge components exclusive of changes in storage. Total includes changes in storage. Negative net change in storage indicates a net loss of water from storage (storage is included as a source). hm^3/yr, cubic hectometers per year; NA, not applicable]

Budget component and time period	Source								
	Conduit-flow rediscretized regional Edwards aquifer model				Diffuse-flow rediscretized regional Edwards aquifer model				
	Flow rate (hm^3/yr)	Percent of budget component	Percent of subtotal for sources or discharges	Percent of total sources or discharges	Flow rate (hm^3/yr)	Percent of budget component	Percent of subtotal for sources or discharges	Percent of total sources or discharges	Change in percent of total sources
Discharge—Continued									
Springflow (layer 1)									
Steady-state	654	NA	NA	54.2	655	NA	NA	54.2	0.0
2003	810	NA	65.7	65.7	848	NA	66.7	66.7	1.0
Subtotal									
2003	1,233	NA	100.0	100.0	1,271	NA	100.0	100.0	0.0
Total discharges									
Steady-state	1,207	NA	NA	100.0	1,208	NA	NA	100.0	0.0
2003	1,233	NA	100.0	100.0	1,271	NA	100.0	100.0	0.0
Net change in storage									
2003									
Layer 1	-64	16.7	NA	5.2	-89	21.1	NA	7.0	1.8
Layer 2	-321	83.3	NA	26.0	-333	78.9	NA	26.3	0.3
Subtotal	-385	100.0	NA	31.2	-423	100.0	NA	33.3	2.1

The MODPATH simulations were used to delineate areas contributing recharge to 68 public-supply wells. The contributing areas and pathlines for selected wells are shown on figures 3.14 and 3.15. Although only selected contributing areas and pathlines are presented on the figures in this report, contributing area statistics, as described in the database data dictionary in Appendix 1 of Chapter A, have been stored for all 65 public-supply wells to support further analysis, including comparison with other regional aquifer systems described elsewhere in this Professional Paper. In general, the pathlines outlining zones of contribution to public-supply wells extend upgradient to the north and northwest toward the recharge zone. For some wells, these pathlines initially trend upgradient to the west before extending to the north and northwest toward the recharge zone. The areas contributing recharge to the public-supply wells are restricted to the recharge zone because, as discussed previously in this report, no recharge occurs in the confined part of the aquifer. Figures 3.14 and 3.15 indicate that the areas contributing recharge and the pathlines outlining the zones of contribution computed by the rediscretized regional Edwards aquifer models (conduit-flow and diffuse-flow models)differ appreciably for many of the wells. The differences in the contributing areas and pathlines are because of differences in the hydraulic-conductivity distributions of the conduit-flow and diffuse-flow models (fig. 3.9). The computed pathlines outlining zones of contribution to selected public-supply wells tend to be aligned with the simulated zones of high hydraulic conductivity, representing a continuously connected network of conduits in the conduit-flow model (fig. 3.9*A*) and generally wider zones in the diffuse-flow model (fig. 3.9*B*). The distribution and extents of the high hydraulic conductivity zones differ

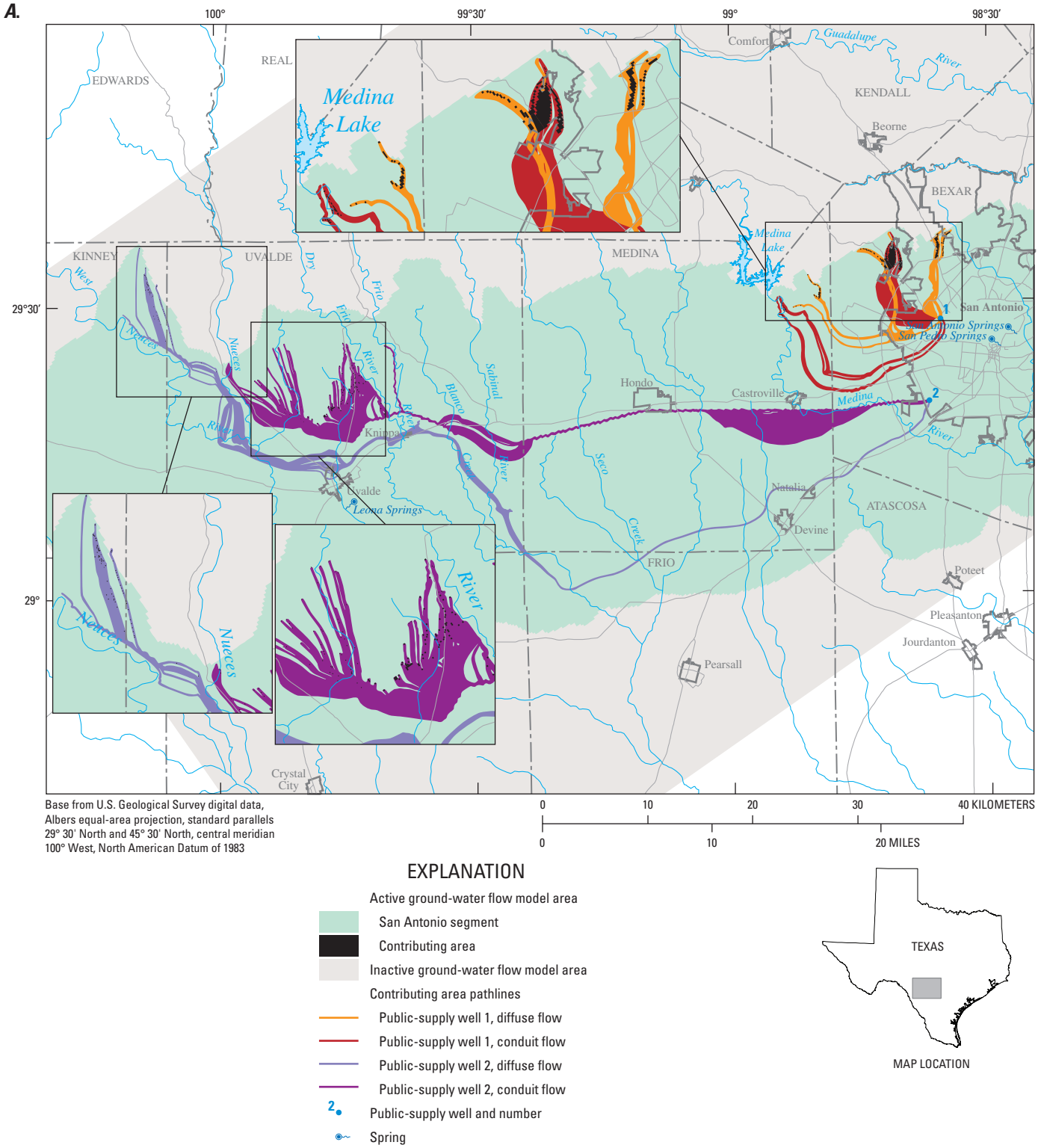

Figure 3.14*A*. Areas contributing recharge and zones of contribution for selected public-supply wells in Bexar County in the South-Central Texas regional study area simulated by the conduit-flow and diffuse-flow rediscretized regional Edwards aquifer models, San Antonio region, Texas.

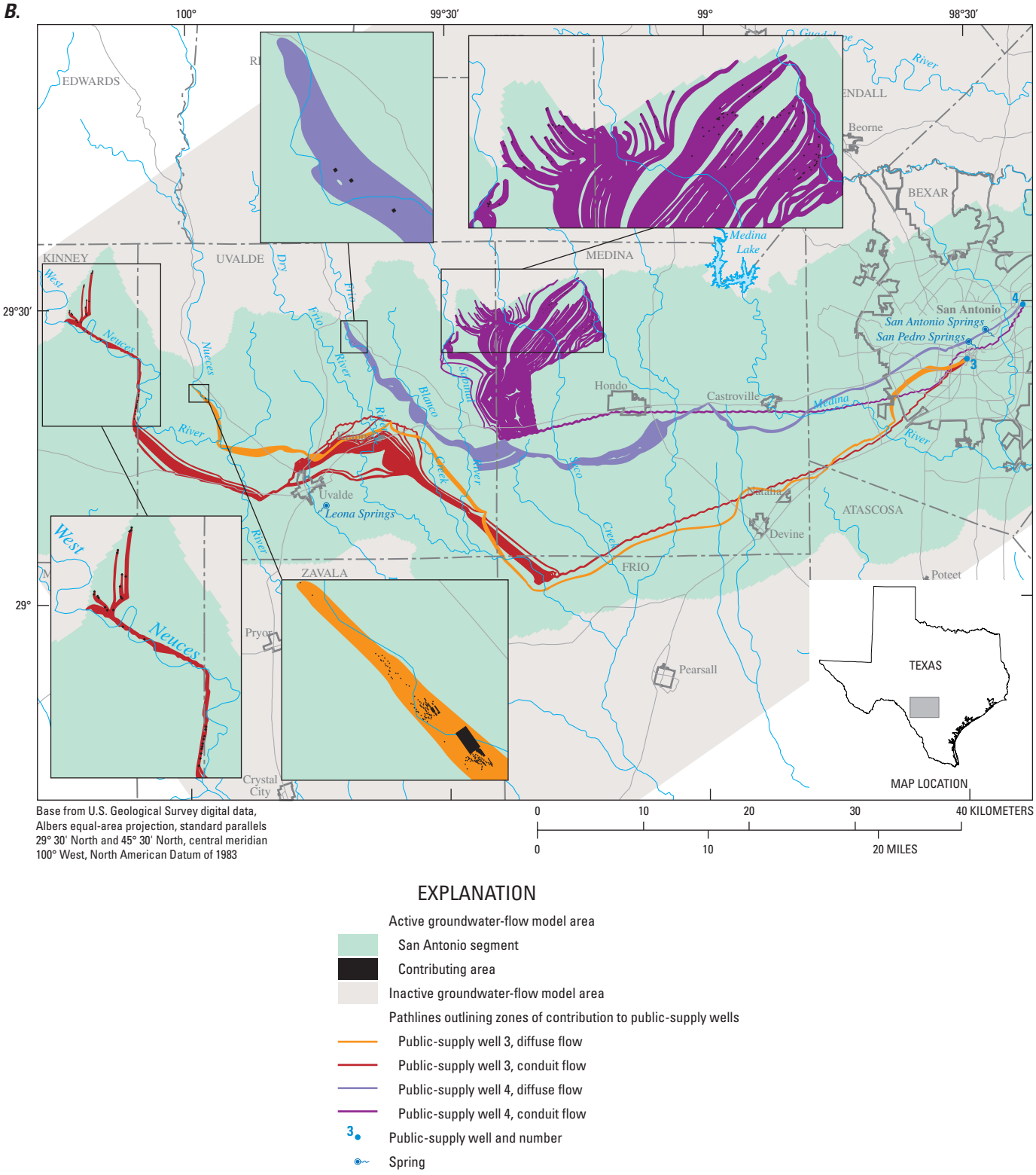

Figure 3.14*B*. Areas contributing recharge and zones of contribution for selected public-supply wells in Bexar County in the South-Central Texas regional study area simulated by the conduit-flow and diffuse-flow rediscretized regional Edwards aquifer models, San Antonio region, Texas.

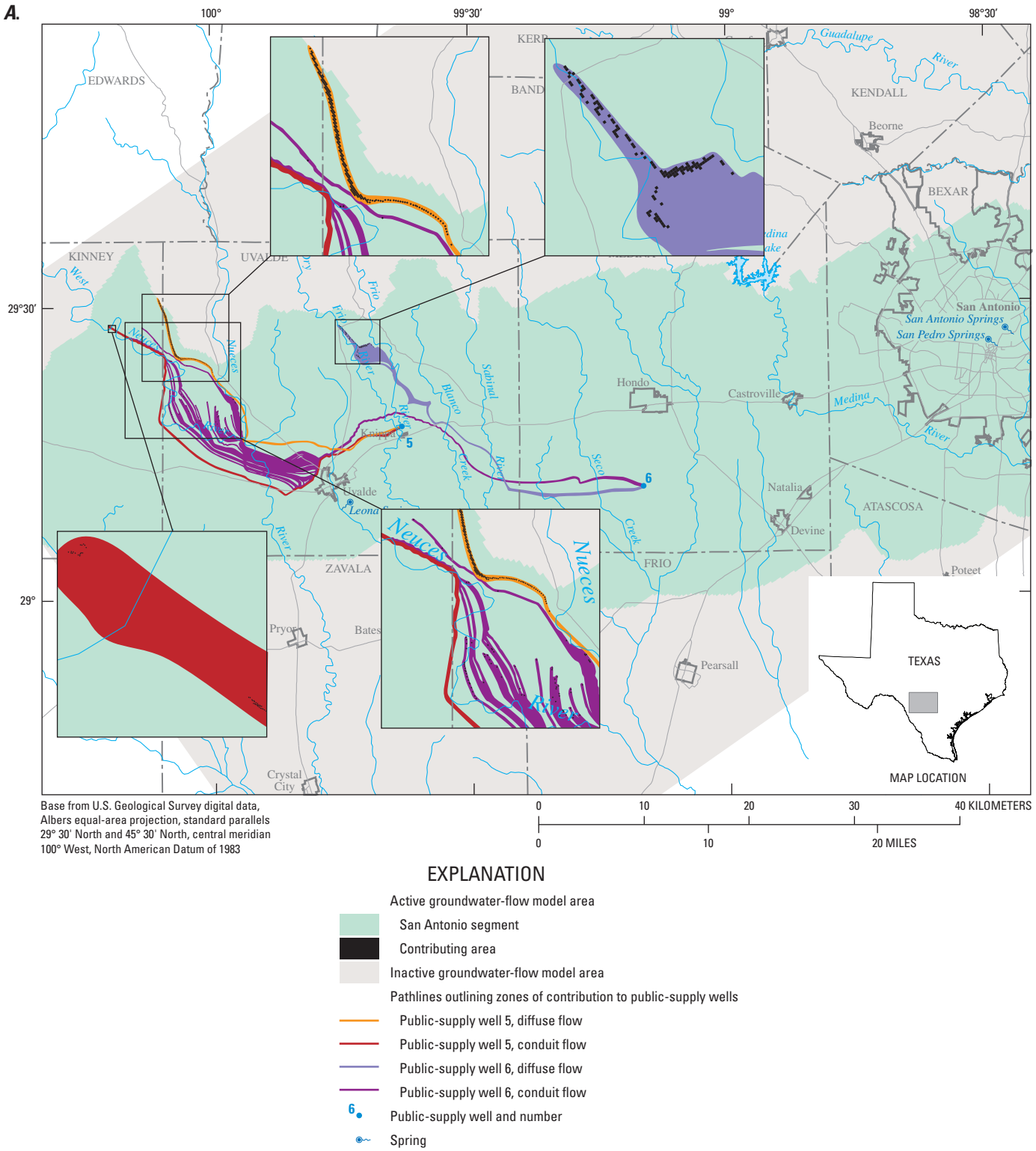

Figure 3.15*A*. Areas contributing recharge and zones of contribution for selected public-supply wells in Medina and Uvalde Counties in the South-Central Texas regional study area simulated by the conduit-flow and diffuse-flow rediscretized regional Edwards aquifer models, San Antonio region, Texas.

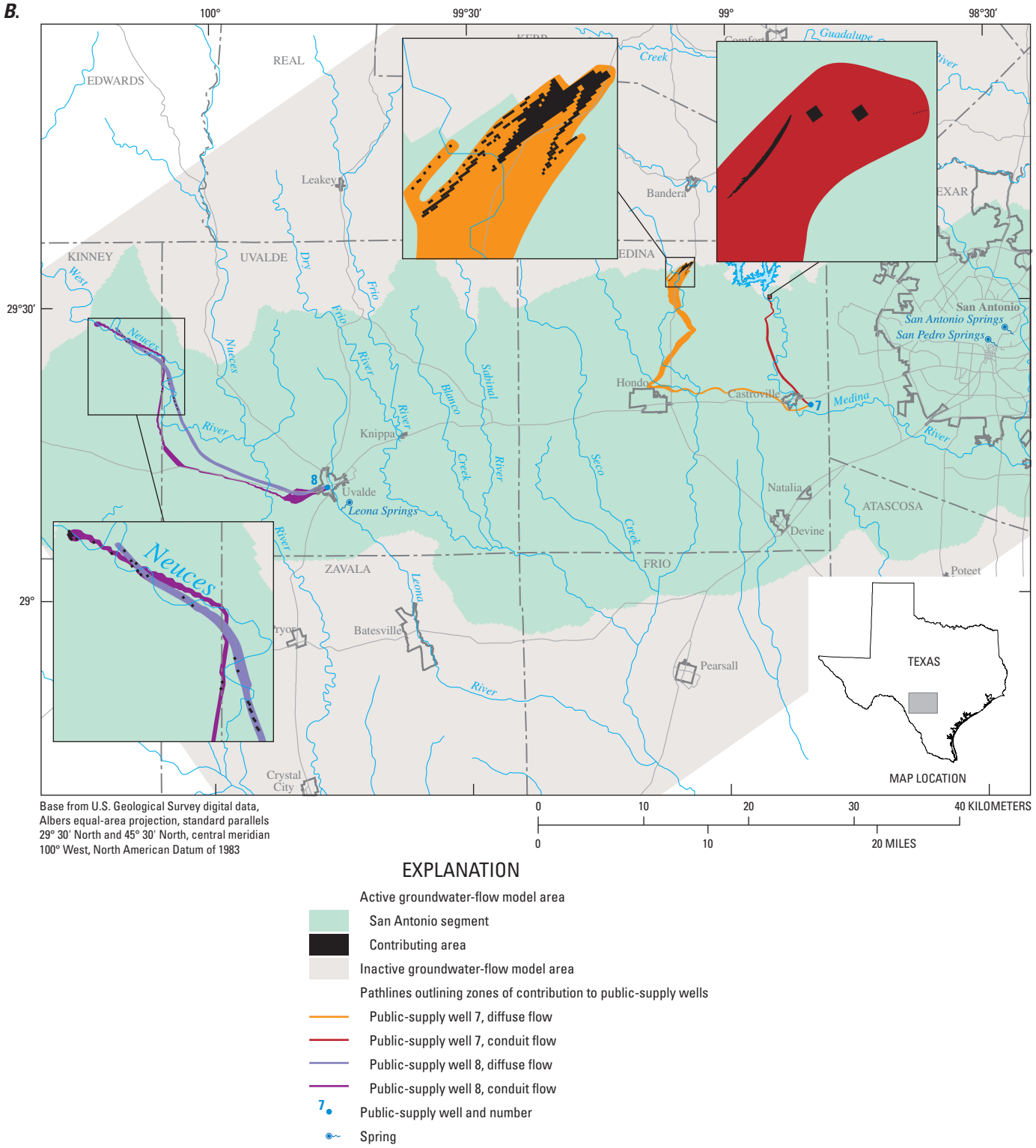

Figure 3.15*B*. Areas contributing recharge and zones of contribution for selected public-supply wells in Medina and Uvalde Counties in the South-Central Texas regional study area simulated by the conduit-flow and diffuse-flow rediscretized regional Edwards aquifer models, San Antonio region, Texas.

between the two models, resulting in the observed differences in the computed contributing areas and pathlines.

Summary statistics for computed particle traveltimes and flow and the size of areas contributing recharge to the public-supply wells are shown in table 3.7. The average area contributing recharge to the public-supply wells was approximately 340 and 230 hectares for the conduit-flow and diffuse-flow rediscretized regional Edwards aquifer models, respectively. The minimum area contributing recharge to the public-supply wells was less than 0.02 hectare for both models, but the maximum for the diffuse-flow rediscretized regional Edwards aquifer model (3,459 hectares) was about 1.4 times that for the conduit-flow rediscretized regional Edwards aquifer model (2,503 hectares).

Minimum computed traveltimes for the public-supply wells for the conduit-flow rediscretized regional Edwards aquifer model ranged from less than one to 817 years and for the diffuse-flow rediscretized regional Edwards aquifer model ranged from 5 to 987 years. Maximum computed traveltimes for the public-supply wells for the conduit-flow rediscretized regional Edwards aquifer model ranged from 13 to 5,263 years and for the diffuse-flow rediscretized regional Edwards aquifer model ranged from 9 to 1,491 years. The average computed traveltime to public-supply wells was greater for the conduit-flow rediscretized regional Edwards aquifer model (276 years) than for the diffuse-flow rediscretized regional Edwards aquifer model (191 years) (table 3.7). For the conduit-flow rediscretized regional Edwards aquifer model, on average, only about 1.3 percent of the flow to a public-supply well was less than 10 years old, about 17 percent of the flow to a public-supply well was less than 50 years old, and about 52 percent of the flow to a public-supply well was less than 200 years old (table 3.7). The corresponding percentages for the diffuse-flow rediscretized regional Edwards aquifer model were greater (1.9, 24, and 67 percent, respectively) (table 3.7) and are consistent with the lower average computed traveltime. Conversely, the percentage of the flow to a public-supply well that was greater than 500 years old was greater for the conduit-flow rediscretized regional Edwards aquifer model, about 11 percent,than for the diffuse-flow rediscretized regional Edwards aquifer model, about 8 percent. As for the model-computed contributing areas and pathlines, the model-computed traveltimes differ for the conduit-flow and diffuse-flow rediscretized regional Edwards aquifer models because of the differences in the hydraulic-conductivity distributions of the two models.

The computed traveltimes are probably much longer than actual traveltimes in the aquifer because (1) an average porosity value for the Edwards aquifer of 0.18 was used for the simulations, and (2) the regional groundwater-flow models do not accurately represent flow through local karst dissolution features. An analysis was done for this study comparing available data for groundwater-age tracers with estimates for groundwater-age tracers derived from simulations using the rediscretized regional Edwards aquifer models (Leon Kauffman, U.S. Geological Survey, written commun., 2008). The measured concentrations for the tracers tritium (^3H) and sulfur hexafluoride (SF_6) were compared to concentrations computed

Table 3.7. Summary statistics for computed particle traveltimes and flow and size of areas contributing recharge to public-supply wells in the South-Central Texas regional study area for the conduit-flow and diffuse-flow rediscretized regional Edwards aquifer models, San Antonio region, Texas.

[Average, average minimum, and average maximum of particle travel time to public-supply wells are the sum of the average values for the public-supply wells divided by the number of public-supply wells. Average percentage of flow to public-supply wells is based on the average flow-weighted age of water particles contributing recharge to the simulated public-supply wells. <, less than; >, greater than]

Particle travel time and flow to public-supply wells								
	Particle travel time to public-supply wells (years)			Average percentage of flow to public-supply wells				
Model	Average	Average minimum	Average maximum	<10 years old	<50 years old	<100 years old	<200 years old	<500 years old
Conduit-flow	219	151	497	0.3	17	35	56	91
Diffuse-flow	181	133	328	1.5	22	36	66	94

Area contributing recharge to public-supply wells									
	Size of area contributing recharge to public-supply wells (hectares)			Percentage of public-supply wells with contributing area of specified extent					
Model	Average	Minimum	Maximum	<4.0 hectares	<20.2 hectares	<40.5 hectares	<202.4 hectares	<404.7 hectares	>404.7 hectares
Conduit-flow	204	0.07	1,758	21.1	40.4	49.1	75.4	87.7	12.3
Diffuse-flow	277	0.03	3,452	44.1	54.2	61.0	71.2	79.7	20.3

using output from the conduit-flow and diffuse-flow rediscretized regional Edwards aquifer models. The median ^3H concentration for 154 groundwater samples was 3.3 tritium units (TU), whereas median ^3H concentrations derived from the model simulations were 1.2 TU for the conduit-flow rediscretized regional Edwards aquifer model and 0.1 TU for the diffuse-flow rediscretized regional Edwards aquifer model. The median SF_6 concentration for 43 groundwater samples was 4.1 parts per trillion by volume (pptv), whereas median SF_6 concentrations derived from the model simulations were 2.4 pptv for both rediscretized regional Edwards aquifer models. The lower median ^3H and SF_6 concentrations derived from the rediscretized regional Edwards aquifer models compared to the measured concentrations indicate that the model-derived groundwater ages tend to be older and the model-derived particle traveltimes tend to be longer than the actual groundwater ages and traveltimes in the aquifer. However, the model-derived concentrations for ^3H were greater than the measured concentrations, indicating a younger groundwater age and shorter traveltimes, for 14.8 and 29.2 percent of the model-derived concentrations for the conduit-flow and diffuse-flow rediscretized regional Edwards aquifer models, respectively. Similarly, the model-derived concentrations for SF_6 were greater than the measured concentrations, indicating a younger groundwater age and shorter traveltimes, for 34.2 and 23.7 percent of the model-derived concentrations for the conduit-flow and diffuse-flow rediscretized regional Edwards aquifer models, respectively.

Limitations and Appropriate Use of the Model

All numerical groundwater-flow models are simplifications of the real system and, therefore, have limitations. Limitations generally result from assumptions used to develop the conceptual and numerical models, limitations in the quality and quantity of the input data, and the scale at which the model can be applied. Use of a distributed, porous media model to simulate flow in a karst system is a simplification, and the original and rediscretized regional Edwards aquifer models will not be able to simulate some aspects of flow accurately in this system, particularly the effects of rapid and potentially turbulent flow in conduits. Further model limitations include the discretization of the model grid and the temporal discretization for the transient simulations. In addition, a combination of input to the models different from that used in the calibrated simulations could produce the same result; the solution is nonunique.

Model limitations also are associated with input data. The input datasets for the original and rediscretized regional Edwards aquifer models are based on scanty information in some areas and for some parameters, in particular the storativity distribution. Hydrogeologic data is relatively meager for the recharge zone, for the Kinney County area, and for areas south of the 1,000-mg/L dissolved-solids concentration line. Secondary porosity created by karst dissolution features contributes to uncertainty in values of hydraulic conductivity, which can vary by up to eight orders of magnitude ($3.05x10^{-4}$ to $3.05x10^4$m/d) in the Edwards aquifer (Hovorka and others, 1998). A fully accurate representation of groundwater flow in the models also is constrained by lack of knowledge of the location and characteristics of high-permeability zones or conduits. Conduit locations, as well as the physical dimensions, connectivity, and hydraulic properties of conduits, are subject to considerable uncertainty. The original and rediscretized regional Edwards aquifer models are regional in nature and, therefore, best suited for the evaluation of variations in spring discharge, regional water-level changes, and the relative comparison of regional water-management scenarios. Accuracy and applicability of the models decrease when changing from the regional to the local scale.

Computed areas contributing recharge and groundwater traveltimes to public-supply wells for this study are based on calibrated steady-state models and an estimated average effective porosity value of 0.18. In a steady-state model, changes to input porosity values do not change the area contributing recharge to a given well. Changes to input porosity values, however, will change computed traveltimes from recharge areas to discharge areas (public-supply wells) in direct proportion to changes of effective porosity, because there is an inverse linear relation between groundwater flow velocity and effective porosity and a direct linear relation between traveltime and effective porosity. For example, a 1-percent decrease in porosity will result in a 1-percent increase in velocity and a 1-percent decrease in particle traveltime.

The rediscretized regional Edwards aquifer models were designed to delineate areas contributing recharge to public-supply wells, to help guide data collection, and to support future local modeling efforts. For karst terrains, where an appreciable amount of flow occurs through a series of discrete openings, conduits, and fractures, a porous-media approach at a regional scale cannot accurately predict zones of contribution, areas contributing recharge, and traveltimes to public-supply wells. Kuniansky and others (2001) found that an effective porosity of 1 to 3 percent was needed for the karst Edwards aquifer system in Texas to match estimated traveltimes derived from geochemical mixing models. Therefore, the computed areas contributing recharge and traveltimes to public-supply wells presented in this report, using an average porosity for the Edwards aquifer of 0.18 (Hovorka and other, 1996), are only one possible scenario of groundwater transport to public-supply wells. A detailed sensitivity analysis of porosity distributions was beyond the scope of this study, although comparisons of simulated groundwater traveltimes to groundwater ages would provide a more thorough evaluation of effective porosity values, and, thus, refine the conceptual model. Future work in the study area will include development of a local model and simulation of discrete karst features.

References Cited

Abbott, P.L., and Woodruff, C.M., Jr., 1986, eds., The Balcones escarpment—Geology, hydrology, ecology and social development in central Texas: Geological Society of America.

Anderson, M.P., and Woessner, W.W., 1992, Applied groundwater modeling: Academic Press, Inc., New York, 381 p.

Baker, E.T., Jr., Slade, R.M., Jr., Dorsey, M.E., Ruiz, L.M., and Duffin, G.L., 1986, Geohydrology of the Edwards aquifer in the Austin area, Texas: Austin, Texas Water Development Board Report 293, 215 p.

Barrett, M.E., and Charbeneau, R.J., 1996, A parsimonious model for simulation of flow and transport in a karst aquifer: Technical Report Center for Research in Water Resources, Report 269, 149 p.

Bomar, G.W., 1994, Texas Weather: Austin, University of Texas Press, 287 p.

Brune, Gunnar, 1975, Major and historical springs of Texas: Austin, Texas Water Board Report 189, 103 p. [Available from National Technical Information Service, Springfield, Va., 22161 as NTIS report PB–296 524/2.]

Brune, Gunnar, and Duffin, G.L., 1983, Occurrence, availability and quality of ground water in Travis County, Texas: Texas Department of Water Resources Report 276, 219 p.

Bush, P.W., Ardis, A.F., Fahlquist, Lynne, Ging, P.B., Hornig, C.E., and Lanning-Rush, Jennifer, 2000, Water quality in south-central Texas, Texas, 1996–98: U.S. Geological Survey Circular 1212, 32 p.

Clement, T.J., 1989, Hydrochemical facies in the badwater zone of the Edwards aquifer, central Texas: Austin, University of Texas, Masters thesis, 168 p.

Elliott, W.R., and Veni, George, eds., 1994, The caves and karst of Texas—Guidebook for the 1994 convention of the National Speleological Society *with emphasis on* the southwestern Edwards Plateau: Huntsville, Ala., National Speleological Society, 342 p.

Fahlquist, Lynne, and Ardis, A.F., 2004, Quality of water in the Edwards and Trinity aquifers, south-central Texas, 1996–98: U.S. Geological Survey Scientific Investigations Report 2004–5201, 17 p.

George, W.O., 1952, Geology and ground-water resources of Comal County, Texas: U.S. Geological Survey Water-Supply Paper 1138, 126 p.

Green, R.T., 2004, Geophysical survey to determine the depth and lateral extent of the Leona aquifer and evaluation of discharge through the Leona River floodplain, south of Uvalde, Texas: San Antonio,contract report to Edwards Aquifer Authority, 17 p.

Groschen, G.E., 1996, Hydrogeologic factors that affect the flowpath of water in selected zones of the Edwards aquifer, San Antonio region, Texas: U.S. Geological Survey Water Resources Investigations Report 96–4046, 73 p.

Hamilton, J.M., Johnson, S., Esquilin, R., Thompson, E.L., Luevano, G., Wiatrek, A., Mireles, J., Gloyd, T., Sterzenback, J., Hoyt, J.R., and Schindel, G., 2003, Edwards Aquifer Authority hydrogeological data report for 2002: San Antonio, Edwards Aquifer Authority, 134 p. [Available online at *http://www.edwardsaquifer.org*.]

Harbaugh, A.W., Banta, E.R., Hill, M.C., and McDonald, M.G., 2000, MODFLOW-2000, the U.S. Geological Survey modular ground-water model—User guide to modularization concepts and the ground-water flow process: U.S. Geological Survey Open-File Report 00–92, 121 p.

Holt, C.L.R., Jr., 1959, Geology and ground-water resources of Medina County, Texas: U.S. Geological Survey Water-Supply Paper 1422, 213 p. [Also published as Texas Board of Water Engineers Bulletin 5601, 278 p., 1956.]

Homer, C.C., Huang, L., Yang, B., Wylie and Coan, M., 2004, Development of a 2001 National Landcover Database for the United States: Photogrammetric Engineering and Remote Sensing, v. 70, no. 7, July 2004, p. 829–840.

Hovorka, S.D., Dutton, A.R., Ruppel, S.C., and Yeh, J.S., 1996, Edwards aquifer ground-water resources—Geologic controls on porosity development in platform carbonates, South Texas: Austin, University of Texas, Bureau of Economic Geology Report of Investigations 238, 75 p.

Hovorka, S.D., Mace, R.E., and Collins, E.W., 1998, Permeability structure of the Edwards aquifer, south Texas—Implications for aquifer management: Austin, University of Texas, Bureau of Economic Geology Report of Investigations 250, 55 p.

Hovorka, S.D., Phu, T., Nicot, J.P., and Lindley, A., 2004, Refining the conceptual model for flow in the Edwards aquifer—Characterizing the role of fractures and conduits in the Balcones fault zone segment: San Antonio, contract report toEdwards Aquifer Authority, 53 p.

Hovorka, S.D., Ruppel, S.C., Dutton, A.R., and Yeh, J.S., 1993, Edwards aquifer storage assessment, Kinney County to Hays County, Texas: San Antonio, Edwards Underground Water District, 109 p.

Johnson, S.B., Schindel, G.M., and Hoyt, J.R., 2002, Groundwater chemistry changes during a recharge event in the karstic Edwards aquifer, San Antonio, Texas: Geological Society of America, pnline abstract 186–8. [Available at *http://gsa.confex.com/gsa/2002AM/finalprogram/abstract_45931.htm*.]

Kier, R.S., Garner, L.E., and Brown, L.F., Jr., 1977, Land resources of Texas: Austin, University of Texas, Bureau of Economic Geology Land Resources Laboratory Series 1977, 42 p.

Klemt, W.B., Knowles, T.R., Edler, G.R., and. Sieh, T.W., 1979, Ground-water resources and model applications for the Edwards (Balcones fault zone) aquifer in the San Antonio region: Austin, Texas Water Development Board Report 239, 88 p.

Kuniansky, E.L., Fahlquist, Lynne, and Ardis, A.F., 2001, Travel times along selected flow paths of the Edwards Aquifer, Central Texas, *in* Kuniansky, E.L. ed., 2001, U.S. Geological Survey Karst Interest Group Proceedings, St. Petersburg, Florida, February 13–16, 2001: U.S. Geological Survey Water-Resources Investigations Report 01–4011, p. 69–77.

Larkin, T. J., and Bomar, G. W., 1983, Climatic atlas of Texas: Austin, Texas Department of Water Resources, LP–192, 151 p.

LBG-Guyton Associates, 1995, Edwards Aquifer groundwater divides assessment, San Antonio region, Texas: Austin, Texas: LBG-Guyton Associates, Report prepared for theEdwards Underground Water District, Report 95–01, 35 p.

Lindgren, R.J., 2006, Diffuse-flow conceptualization and simulation of the Edwards aquifer, San Antonio region, Texas: U.S. Geological Survey Scientific Investigations Report 2006–5319, 47 p.

Lindgren, R.J., Dutton, A.R., Hovorka, S.D., Worthington, S.R.H., and Painter, Scott, 2004, Conceptualization and simulation of the Edwards aquifer, San Antonio region, Texas: U.S. Geological Survey Scientific Investigations Report 2004–5277, 143 p.

Lozo, F.E., and Smith, C.I., 1964, Revision of Comanche Cretaceous stratigraphic nomenclature, southern Edwards Plateau, southwest Texas: Gulf Coast Association of Geological Societies Transactions, v. 14, p. 285–307.

Mace, R.E., Chowdhury, A.H., Anaya, Roberto, and Way, S.C., 2000, Groundwater availability of the Trinity aquifer, Hill Country area, Texas—Numerical simulations through 2050: Austin, Texas Water Development Board Report 353, 169 p.

Maclay, R.W., 1989, Edwards aquifer in the San Antonio region—Its hydrogeology and management: South Texas Geological Society Bulletin, v. 30, no. 4, p. 11–28.

Maclay, R.W., 1995, Geology and hydrology of the Edwards aquifer in the San Antonio area, Texas: U.S. Geological Survey Water-Resources Investigations Report 95–4186, 64 p.

Maclay, R.W., and Land, L.F., 1988, Simulation of flow in the Edwards aquifer, San Antonio region, Texas, and refinements of storage and flow concepts: U.S. Geological Survey Report Water-Supply Paper 2336–A, 48 p.

Maclay, R.W., and Rettman, P.L., 1973, Regional specific yield of the Edwards aquifer and associated limestones in the San Antonio, Texas, area: U.S. Geological Survey Open-File Report 73–172, 14 p. [Also published as Edwards Underground Water District Report, 10 p., 1973.]

Maclay, R.W., and Small, T.A., 1976, Progress report on geology of the Edwards aquifer, San Antonio area, Texas, and preliminary interpretation of borehole geophysical and laboratory data on carbonate rocks: U.S. Geological Survey Open-File Report 76–627, 65 p.

Maclay, R.W., and Small, T.A., 1983, Hydrostratigraphic subdivisions and fault barriers of the Edwards aquifer, south central Texas: Journal of Hydrology, v. 61, no. 1–3, p. 127–146.

Maclay, R.W., and Small, T.A., 1984, Carbonate geology and hydrology of the Edwards aquifer in the San Antonio area, Texas: U.S. Geological Survey Open-File Report 83–537, 72 p. [Also published as Texas Water Development Board Report 296, 90 p., 1986.]

Maupin, M.A., and Barber, N.L., 2005, Estimated withdrawals from principal aquifers in the United States, 2000: U.S. Geological Survey Circular 1279, 46 p.

Moran, M.J., Lapham, W.W., Rowe, B.L., and Zogorski, J.S., 2002, Occurrence and status of volatile organic compounds in ground water from rural, untreated, self-supplied domestic wells in the United States, 1986–99: U.S. Geological Survey Water-Resources Investigations Report 02–4085, 50 p.

Musgrove, M., Fahlquist, L., Houston, N.A., Lindgren, R.J., and Ging, P.B., 2010, Geochemical evolution processes and water-quality observations based on results of the National Water-Quality Assessment Program in the San Antonio segment of the Edwards aquifer, 1996–2006: U.S. Geological Survey Scientific Investigations Report 2010−5129, 93 p. (Available at *http://pubs.usgs.gov/sir/2010/5129/*.)

National Hydrography Dataset Plus, 2007: accessed July 2007 at *http://www.horizon-systems.com/nhdplus/data.php*.

Oetting, G.C., 1995, Evolution of fresh and saline groundwaters in the Edwards aquifer, central Texas—Geochemical and isotopic constraints on processes of fluid-rock interaction and fluid mixing: Austin, University of Texas, Masters thesis, 203 p.

Ogden, A.E., Quick, R.A., Rothermel, S.R., and Lundsford, D.L., 1986, Hydrological and hydrochemical investigation of the Edwards aquifer in the San Marcos area, Hays County, Texas: San Marcos, Tex., Edwards Aquifer Research and Data Center, 364 p.

Painter, Scott, Jiang, Yefang, and Woodbury, Allan, 2002, Edwards aquifer parameter estimation project final report: San Antonio, Tex., Southwest Research Institute [variously paged].

Peacock, D.C.P., and Sanderson, D.J., 1994, Geometry and development of relay ramps in normal fault systems: American Association of Petroleum Geologists Bulletin, v. 78, no. 2, p. 147–165.

Pollock, D.W., 1994, Source code and ancillary data files for the MODPATH particle tracking package of the groundwater flow model MODFLOW; version 3, release 1: U.S. Geological Survey Open-File Report 94–0463, 6 p., 2 diskettes.

Puente, Celso, 1978, Method of estimating natural recharge to the Edwards aquifer in the San Antonio area, Texas: U.S. Geological Survey Water-Resources Investigations Report 78–10, 34 p.

Reilly, T.E., and Pollock, D.W., 1995, Effects of seasonal and long-term changes in stress on sources of water to wells: U.S. Geological Survey Water-Supply Paper 2445, 25 p.

Renken, R.A., 1998, Ground water atlas of the United States, Segment 5—Arkansas, Louisiana, and Mississippi: U.S. Geological Survey Hydrologic Investigations Atlas 730–F, p. F19–F25. (Also available at *http://pubs.usgs.gov/ha/ha730/ch_f/index.html*.)

Rose, P.R, 1972, Edwards Group, surface and subsurface, central Texas: Austin, University of Texas, Bureau of Economic Geology Report of Investigations 74, 198 p.

Rothermel, S.R., Ogden, A.E., and Snider, C.C., 1987, Hydrochemical investigation of the Comal and Hueco Spring systems, Comal County, Texas: San Marcos, Tex., Edwards Aquifer Research and Data Center Report R1–87, 182 p.

Ryder, P.D., 1996, Ground water atlas of the United States, Segment 4—Oklahoma and Texas: U.S. Geological Survey Hydrologic Investigations Atlas 730–E, p. E19–E25. (Also available at *http://pubs.usgs.gov/ha/ha730/ch_e/index.html*.)

Scanlon, B.R., Mace, R.E., Smith, Brian, Hovorka, S.D., Dutton, A.R., and Reedy, R.C., 2002, Groundwater availability of the Barton Springs segment of the Edwards aquifer, Texas—Numerical simulations through 2050: Austin, University of Texas, Bureau of Economic Geology, 36 p. [Prepared for Lower Colorado River Authority.]

Schindel, G.M., Johnson, S.B., Worthington, S.R.H., Alexander, E.C., Jr., Alexander, Scott, and Schnitz, Lewis, 2002, Groundwater flow velocities for the deep artesian portion of the Edwards aquifer, near Comal Springs, Texas, *in* Annual Meeting of the Geological Society of America, Denver, Colo., October 27–30, 2002: Geological Society of America Abstracts with Programs, v. 34, no. 6, p. 347.

Schultz, A.L., 1992, Using geophysical logs in the Edwards aquifer to estimate water quality along the freshwater/saline-water interface (Uvalde to San Antonio, Texas): San Antonio, Edwards Underground Water District Report 92–03, 47 p.

Senger, R.K., and Kreitler, C.W., 1984, Hydrogeology of the Edwards aquifer, Austin area, Central Texas: Austin, University of Texas, Bureau of Economic Geology Report of Investigations 141, 35 p.

Sieh, T.H., 1975, Edwards (Balcones fault zone) aquifer test well drilling investigation: Austin, Texas Water Development Board Report, 117 p.

Slade, R.M., Jr., and Persky, Kristie, 1999, Floods in the Guadalupe and San Antonio River Basin in Texas, October 1998: U.S. Geological Survey Fact Sheet 147–99, 4 p.

Slade, R.M., Jr., Ruiz, Linda, and Slagle, Diana, 1985, Simulation of the flow system of Barton Springs and associated Edwards aquifer in the Austin area, Texas: U.S. Geological Survey Water-Resources Investigations Report 85–4299, 49 p.

Slattery, R.N., 2004, Recharge to the Edwards aquifer in the San Antonio area, Texas, 2003: U.S. Geological Survey, accessed July 12, 2004, at *http://tx.usgs.gov/reports/dist/dist-2004-01*.

Texas Water Development Board, 2008, Historical Water Use Information: accessed February 28,2007, at *http://www.twdb.state.tx.us/wushistorical/*.

Thorkildsen, D.F., and McElhaney, P.D., 1992, Model refinement and applications for the Edwards (Balcones fault zone) aquifer in the San Antonio region, Texas: Austin, Texas Water Development Board Report 340, 33 p.

Tomasko, David, Fisher, Ann-Marie, Williams, G.P., and Pentecost, E.D., 2001, A statistical study of the hydrologic characteristics of the Edwards aquifer: Chicago, Argonne National Laboratory, 38 p.

U.S. Department of Agriculture, 2007, Geospatial Data Gateway: accessed July 2007 at *http://datagateway.nrcs.usda.gov/*.

U.S. Environmental Protection Agency, 2006, 2006 edition of the drinking water standards and health advisories: accessed January 30, 2008, at *http://www.epa.gov/waterscience/criteria/drinking/dwstandards.pdf*.

U.S. Geological Survey, 1999, The quality of our Nation's waters—Nutrients and pesticides: U.S. Geological Survey Circular 1225, 82 p.

Vauter, B.K., 1992, Geology and its influence on cavern development in an area surrounding Natural Bridge Caverns, Comal County, Texas: Geological Society of America Abstracts with Programs, v. 24, no. 1, p. 49.

Veni, George, 1988, The caves of Bexar County (2d ed.): Austin, University of Texas, Texas Memorial Museum Speleological Monograph 2, 300 p.

Woodbury, A.D., and Ulrych, T.J., 1998, Minimum relative entropy and probabilistic inversion in groundwater hydrology: Stochastic Hydrology and Hydraulics, v. 12, p. 317–358.

Woodbury, A.D., and Ulrych, T.J., 2000, A full-Bayesian approach to the groundwater inverse problem for steady state flow: Water Resources Research, v. 36, no. 8, p. 2,081–2,093.

Woodruff, C.M., Jr., and Abbott, P.L., 1986, Stream piracy and evolution of the Edwards aquifer along the Balcones Escarpment, Central Texas, *in* Abbot, P.L., and Woodruff, C.M., Jr. eds., The Balcones escarpment—geology, hydrology, ecology and social development in central Texas: Geological Society of America, p. 77–100.

Worthington, S.R.H., 2004, Conduits and turbulent flow in the Edwards aquifer: Worthington Groundwater, contract report to Edwards Aquifer Authority, San Antonio, 41 p.

Appendix 1. Updates to the Particle-Tracking Program MODPATH to Improve Efficiency for Use in Computing Transient-State Contributing Areas for Wells that Act as Weak Sinks

Updates to the Particle-Tracking Program MODPATH to Improve Efficiency for Use in Computing Transient-State Contributing Areas for Wells that Act as Weak Sinks

The following 11 changes were made to version 5.0 of the particle-tracking program, MODPATH (Pollock, 1994), so that the weak sink program would run correctly and efficiently for the transient case:

1. The checking process for IFACE was changed, because some compilers treat the empty spaces differently. A character variable with length 5 is used to do the check rather than CTMP, which is length 16.

   In file BUDGETRD.FOR:
   After line 131 in subroutine RDBDNM, add variable declaration.

```
      CHARACTER*16 TXTSAV
C added to improve IFACE check
      character*5 ifchk
      SAVE IOLD,KS,KP,TXTSV,NC,NR,NLCODE
```

   At line 177 in subroutine RDBDNM, change the check for IFACE.

```
                DO 10 I=1,NVAL-1
                ifchk = ctmp(i)
C original      IF(CTMP(I).EQ.'IFACE') NIFACE=I+1
                IF(ifchk.EQ.'IFACE') NIFACE=I+1
10              CONTINUE
```

2. A loop was added to the particle-tracking code to determine which particles already have been released at the beginning of each time step. This limits the number of times that hydraulic-head values are read from the MODPATH CBF file. In the modified code it is assumed that the particles are sorted by release time in the starting locations file. The sorting is done in the weak sink program.

   In file MPDRIVE.FOR:
   In subroutine DRIVER, change line 265

```
C original GO TO 69
         GO TO 701
```

   In subroutine DRIVER, add a line number at line 339

```
701       if(mode.eq.2 .and. iend.eq.0 .and. iunit(18).gt.0) then
```

3. The code was changed to allow for particles to be released at multiple times for backward tracking.

   In file MPDATIN.FOR:
   In subroutine DATIN, comment out line 537

```
C original IF(TRLEAS.NE.0.0 .AND. IREV.EQ.1) GO TO 150
```

   In Subroutine DATIN, add after line 585

```
C add code to allow multiple release times in backward tracking
      if (irev.eq.1) trleas = -1*trleas
C keep track of minimum release time
```

```
          if((trleas.lt.trmin).or.(n.eq.1)) then
            trmin = trleas
          end if
```

In file MPDRIVE.FOR:
In subroutine DRIVER, change line 48

```
   C original5TIMX,IBSTRT,ZLC,HDRY,HNOFLO,TOT,ICMPCT,TBGABS,LAYCBD,ISSFLG)
         5TIMX,IBSTRT,ZLC,HDRY,HNOFLO,TOT,ICMPCT,TBGABS,LAYCBD,ISSFLG
         +stlcomment,trmin,tbegin)
```

In subroutine DRIVER, add after line 138

```
          if(irev.eq.1) then
            timrel = tbgabs-trmin
          else
            timrel = trmin + tbgabs
          end if
          told = trmin
          call getps(PERLEN,NUMTS,TIMX,NPER,TIMREL,TBEGIN,KKPER,
         1                 KKSTP,IERR)
```

In subroutine DRIVER, add after line 161

```
          if(irev.eq.1) then
            told = told-(1.0-TIMREL)*DTSTP
          else
            told = told - TIMREL*DTSTP
          end if
          timstp = dtstp + told
```

In subroutine DRIVER, comment out lines 245 and 252

```
   C original  IF(IREV.EQ.0) THEN
   C original  END IF
```

4. The code was compiled in double precision to allow for more accuracy in computing times and position coordinates.

In file FLOWDATA.FOR:
In subroutine HQDATA, change line 103

```
   C original LREC= 4*(NCOL+1)
          LREC= 8*(NCOL+1)
```

In subroutine MAKEHQ, change line 279

```
C original       DBYTES=4.D0*(DBLE(NCOL)+1.D0)*DBLE(NCHECK)
      DBYTES=8.D0*(DBLE(NCOL)+1.D0)*DBLE(NCHECK)
```

In subroutine CBFSIZ, change line 932

```
C original DBYTES= 4.D0*(DBLE(NCOL)+1.D0)*DBLE(NREC)
      DBYTES= 8.D0*(DBLE(NCOL)+1.D0)*DBLE(NREC)
```

5. The code was changed to allow for the IEVTTP variable to be used for ET SEGMENTS package and for the Stream Leakage to be assigned to Face 6 because there is no allowance for setting IFACE.

In file FLOWDATA.FOR

In subroutine FLOWS, add new lines after line 599.

```
IF(TEXT.EQ.'     ET SEGMENTS') ITOP=IEVTTP
IF(TEXT.EQ.'  STREAM LEAKAGE') ITOP=1
```

6. The code was changed to allow a comment to be added to the starting locations files that would be added to the endpoint file.

In File MPATH5.FOR:
In the Main Program, add after line 75

```
      character*256,dimension(:), allocatable:: STLCOMMENT
```

In the Main Program, add after line 247

```
      allocate (stlcomment(MAXPTS))
```

In file MPDATIN.FOR:
In Subroutine DATIN, change line 18

```
     5TIMX,IBSTRT,ZLC,HDRY,HNOFLO,TOT,ICMPCT,TBGABS,LAYCBD,ISSFLG,

    6  stlcomment,trmin,tbegin)
```

In Subroutine DATIN, add after line 25

```
      character*256 STLCOMMENT,comment
```

In Subroutine DATIN, add after line 40

```
     +,STLCOMMENT(NPART)
```

In file WRITEPTS.FOR:
In subroutine WRITEP, add after line 46

```
      character*256 stlcomment
     1
```

In subroutine WRITEP, change line 54

```
C original     1         1X,E12.5,a256)
     1         1X,E12.5,a256)
```

7. The code was changed to allow for the maximum line length in the starting locations file to be more than 81.

In file MPDATIN.FOR:
In subroutine DATIN, change line 25

```
C original  CHARACTER*81 LINE2

      CHARACTER*256 LINE2
```

In subroutine DATIN, add after line 536

```
          comment = line2(iwlast+1:256)
```

In subroutine DATIN, add after line 569

```
       stlcomment(n) = comment
```

In file MPDRIVE.FOR:
In subroutine DRIVER, change line 16

```
C original  5HNOFLO,VER,LAYCBD,ISSFLG)

      5HNOFLO,VER,LAYCBD,ISSFLG,STLCOMMENT)
```

In subroutine DRIVER, add after line 21

```
character*256 STLCOMMENT
```

In subroutine DRIVER, add after line 33

```
+,STLCOMMENT(NPART)
```

In subroutine DRIVER, change line 48

```
C original 5TIMX,IBSTRT,ZLC,HDRY,HNOFLO,TOT,ICMPCT,TBGABS,LAYCBD,ISSFLG)

      5TIMX,IBSTRT,ZLC,HDRY,HNOFLO,TOT,ICMPCT,TBGABS,LAYCBD,ISSFLG

      +stlcomment,trmin,tbegin)
```

In subroutine DRIVER, changes lines 522 and 537

```
C original 2 KFRST,IZONE2,NSFRST,IPCODE,TRLEAS,NROW,NCOL,stlcomment(N))

      2   KFRST,IZONE2,NSFRST,IPCODE,TRLEAS,NROW,NCOL,stlcomment(N))


C original 2 KFRST,IZONE2,NSFRST,IPCODE,TRLEAS,NROW,NCOL,stlcomment(N))

      2   KFRST,IZONE2,NSFRST,IPCODE,TRLEAS,NROW,NCOL,stlcomment(N))
```

In file WRITEPTS.FOR
In subroutine WRITEP, change line 46

```
C original 2 NROW,NCOL)

      2 NROW,NCOL,stlcomment)
```

In subroutine WRITEP, change line 52

```
C original 1                  NDFRST,IZONE2,NSFRST,IPCODE,TRLEAS

      1                 NDFRST,IZONE2,NSFRST,IPCODE,TRLEAS, stlcomment


      2
```

In subroutine WRITEP, change line 54

```
C original     1         1X,E12.5,a256)

      1         1X,E12.5,a256)
```

In subroutine WRITEP, change line 65

```
C original 1     JFRST,IFRST,KFRST,IZONE2,NSFRST,IPCODE,TRLEAS

      1     JFRST,IFRST,KFRST,IZONE2,NSFRST,IPCODE,TRLEAS, stlcomment
```

In subroutine WRITEP, change line 67

```
C original 1    1X,I6,1X,E12.5,a256)

      1    1X,I6,1X,E12.5,a256)
```

8. The code was changed to allow the endpoint file to be written with free format.

In file MPDATIN.FOR:

```
In Subroutine DATIN, add after line 320

      IF(INDEX(LINE,'FREE').ne.0) ICMPCT = ICMPCT - 2
```

In file WRITEPTS.FOR:
In subroutine WRITEP, add after line 55

```
      ELSE IF(ICMPCT.EQ.-1) THEN

        ND= (K-1)*NROW*NCOL + (I-1)*NCOL + J

        NDFRST= (KFRST-1)*NROW*NCOL + (IFRST-1)*NCOL + JFRST

        WRITE(IU,*) IZONE,ND,X,Y,ZL,TOT,XSTRT,YSTRT,ZLSTRT,

      1     NDFRST,IZONE2,NSFRST,IPCODE,TRLEAS,stlcomment
```

In subroutine WRITEP, add after line 60

```
      ELSE IF(ICMPCT.EQ.-2) THEN

        inquire (iu, recl=ir)

        WRITE(IU,*) IZONE,J,I,K,X,Y,Z,ZL,TOT,XSTRT,YSTRT,ZLSTRT,

     1     JFRST,IFRST,KFRST,IZONE2,NSFRST,IPCODE,TRLEAS, stlcomment
```

9. The code was changed to use the zone codes specified in the MODPATH input for determining whether or not a particle stops.

In file MPDRIVE.FOR:
In subroutine DRIVER, change lines 500 and 503

```
C original      IZONE=IBOUND(JLC(N),ILC(N),KLC(N))

       IZONE=IBSTRT(JLC(N),ILC(N),KLC(N))

C original      IZONE2=IBOUND(JFRST,IFRST,KFRST)

       IZONE2=IBSTRT(JFRST,IFRST,KFRST)
```

10. The code was changed to allow the layer index to be specified as 0, which is specified in the MODPATH documentation when a particle is to be placed in the top active layer.

In file STARTLOC.FOR:
In Subroutine GETIJK, change line 152

```
C original  IF(K.LT.1 .OR. K.GT.NLAY) THEN

        IF(K.LT.0 .OR. K.GT.NLAY) THEN
```

11. The code was changed to increase the default record length.

In file UTILMP.FOR:
In subroutine OPNFIL, change lines 311 and 320

```
C original OPEN (IU,FILE=FNAME,STATUS='OLD',FORM=FMT,ACCESS=ACS,IOSTAT=IERR)

       OPEN (IU,FILE=FNAME,STATUS='OLD',FORM=FMT,ACCESS=ACS,IOSTAT=IERR,

      + recl=5000)


C original OPEN (IU,FILE=FNAME,STATUS='NEW',FORM=FMT,ACCESS=ACS,IOSTAT=IERR)

       OPEN (IU,FILE=FNAME,STATUS='NEW',FORM=FMT,ACCESS=ACS,IOSTAT=IERR,

      + recl=5000)
```

References Cited

Pollock, D.W., 1994, User's guide for MODPATH/MODPATH-PLOT, version 3: A particle tracking post-processing package for MODFLOW, the U.S. Geological Survey finite-difference ground-water flow model: U.S. Geological Survey Open-File Report 94–464 [variously paged]. (Also available at *http://pubs.er.usgs.gov/publication/ofr94464*.)

Prepared by the Columbus Publishing Service Centers.

Edited by Elizabeth A Ciganovich.

Illustrations by Allan C. Long and Rosemary S. Stenback.

Design and layout by Rosemary S. Stenback.

For more information concerning this report, please contact
Eberts, Sandra M., U.S. Geological Survey, 6480 Doubletree Avenue,
Columbus, OH 43229, smeberts@usgs.gov

Eberts, Sandra M., ed.—**Hydrogeologic Settings and Groundwater-Flow Simulations for Regional Investigations of the Transport of Anthropogenic and Natural Contaminants to Public-Supply Wells—Investigations Begun in 2004**—Professional Paper 1737–B